cAMP signaling reverses platelet spreading via inhibition of RhoA

Muhammad Zuhair Yusuf

A thesis submitted for the degree of
Doctor of Philosophy in Medical Sciences

The University of Hull and
The University of York

Hull York Medical School (HYMS)

October, 2016

Abstract

Prostacyclin (PGI_2) is a key regulator of platelet function. There is a significant field of research which outlines the role of PGI_2 in inhibiting platelets in circulation, and therefore playing a major role in the prevention of excessive thrombus formation. PGI_2 signalling is countered by strong activatory stimuli leading to platelet spreading and thrombus formation. However little is known if PGI_2 plays a role after platelet activation. Therefore, the aim of this study was to identify the effect of PGI_2 on already activated platelets. Therefore, thrombi were formed on fibrinogen and/or collagen, and then PGI_2 was flowed over the top. This revealed a significant reduction in thrombus surface area on fibrinogen, and both surface area coverage, and thrombus height on collagen, demonstrating the ability of PGI_2 to modulate a pre-formed thrombus. To understand the mechanism behind this event it was postulated that PGI_2 was modulating the actin cytoskeleton of an activated platelet, leading to thrombus instability.

To identify if cytoskeletal changes were induced by PGI_2, platelet spreading was monitored. Platelet spreading follows a defined sequence of events, with the formation of filopodia, actin nodules, lamellipodia and finally stress fibres. By understanding the percentage of platelets containing each structure, it would be possible to identify the role of PGI_2 within platelet spreading. Therefore, platelets were allowed to spread, before stimulation with PGI_2. This identified that PGI_2 induced a significant reduction in stress fibre formation whilst inducing actin nodule formation. Alongside this there was a reduction in the surface area of the platelet. Further to this PGI_2 was shown to induce a strong elevation of cAMP within fully spread platelets. This reversal of stress fibre formation occurred in a PKA dependent manner as inhibition of PKA induced an inhibition of the stress fibre reversal induced by PGI_2.

Stress fibre formation is linked to RhoA activity. Inorder to understand if PKA was modulating RhoA, the phosphorylation and activity status of RhoA was monitored. We showed clearly that PKA both induced the phosphorylation, but also significantly reduced the activity of RhoA in spread platelets. Further to this, there was a reduction in the phosphorylation of the light chains of Myosin II.

Thus, PGI_2 modulates the actin cytoskeleton via a PKA dependent inactivation of RhoA, leading to stress fibre reversal and thrombus instability.

Publication from the thesis

Yusuf M.Z., Raslan Z., Atkinson L., Aburima A., Thomas S.G., Naseem K.M. and Calaminus S.D.J. Prostacyclin reverses platelet spreading leading to instability of thrombus formation via cAMP mediated regulation of RhoA activity. 2016.

Submitted to Journal of Thrombosis and Haematology (JTH)

Presentations

Oral:

- cAMP signaling reverses platelet activation via inhibition of RhoA. HYMS 5th postgraduate research conference, York, UK (2016). (Winner of best 3-minute thesis presentation award).
- cAMP signaling reverses platelet spreading via inhibition of RhoA. The Allam Lecture, Hull, UK (2016).

Poster(s):

- Yusuf M.Z., Raslan Z., Atkinson L., Aburima A., Naseem K.M. and Calaminus S.D.J. cAMP signaling reverses platelet activation via inhibition of RhoA. Northern Vascular Biology Forum, Hull, UK (2016).
- Yusuf M.Z., Raslan Z., Atkinson L., Aburima A., Naseem K.M. and Calaminus S.D.J. cAMP signaling reverses platelet activation via inhibition of RhoA. HYMS 5th postgraduate research conference, York, UK (2016).
- Yusuf M.Z., Raslan Z., Atkinson L., Aburima A., Naseem K.M. and Calaminus S.D.J. cAMP signaling reverses platelet spreading via inhibition of RhoA. The Allam Lecture, Hull, UK (2016).
- Yusuf M.Z., Naseem K.M. and Calaminus S.D.J. Prostacyclin regulates platelet actin dynamics via Protein Kinase A activation. The UK Platelet Conference, Leicester, UK (2015).

List of Illustrations

CHAPTER 1

CHAPTER 2

CHAPTER 3

CHAPTER 4

CHAPTER 5

Chapter 6

List of Tables

Table of Contents

List of videos

Supplementary Video 1: Formation of thrombi over fibrinogen coated flow chambers. Whole blood, stained with 10μM $DiOC_6$ was flown over fibrinogen (300μg/ml) coated slides for 2 minutes at a shear rate of $1000s^{-1}$, to enable the formation of thrombi. Videos are representative of three experiments.

Supplementary Video 2: Post perfusion of 100nM PGI_2 induces embolisation of preformed thrombi on fibrinogen. After 2 minutes of flowing whole blood and formation of thrombi, PBS containing 100nM PGI_2 was perfused over these preformed thrombi for 10 minutes at $1000s^{-1}$ and the effect on thrombi was observed. Videos are representative of three experiments.

Supplementary Video 3: Post perfusion of PBS does not affect thrombus embolization on fibrinogen. After 2 minutes of flowing whole blood and formation of thrombi, PBS was perfused over these preformed thrombi for 10 minutes at $1000s^{-1}$ and the effect on thrombi was observed. Videos are representative of three experiments.

Supplementary Video 4: Formation of thrombi in the presence of PKA inhibitors over fibrinogen coated flow chambers. Whole blood was treated with PKA inhibitors - 500μM RP-8-CPT-cAMP (RP) and 10μM KT5720 (KT) for 20 minutes. It was stained with 10μM $DiOC_6$ was flown over fibrinogen (300μg/ml) coated slides for 2 minutes at a shear rate of $1000s^{-1}$, to enable the formation of thrombi. Videos are representative of three experiments.

Supplementary Video 5: Post perfusion of 100nM PGI_2 in the presence of PKA inhibitors does not induce embolisation of preformed thrombi on fibrinogen. After 2 minutes of flowing whole blood (in the presence of 500μM RP-8-CPT-cAMP and 10μM KT5720) and formation of thrombi, PBS containing 100nM PGI_2 in the presence of 500μM RP-8-CPT-cAMP and 10μM KT5720 was perfused over the preformed thrombi

for 10 minutes at $1000s^{-1}$ and the effect on thrombi was observed. Videos are representative of three experiments.

Supplementary Video 6: Post perfusion of PBS in the presence of PKA inhibitors does not induce embolisation of preformed thrombi on fibrinogen. After 2 minutes of flowing whole blood (in the presence of 500μM RP-8-CPT-cAMP and 10μM KT5720) and formation of thrombi, PBS containing 100nM PGI_2 in the presence of 500μM RP-8-CPT-cAMP and 10μM KT5720 was perfused over the preformed thrombi for 10 minutes at $1000s^{-1}$ and the effect on thrombi was observed. Videos are representative of three experiments.

Supplementary Video 7: Formation of thrombi over collagen coated flow chambers. Whole blood, stained with 10μM $DiOC_6$ was flown over collagen (25μg/ml) coated slides for 2 minutes at a shear rate of $1000s^{-1}$, to enable the formation of thrombi. Videos are representative of three experiments.

Supplementary Video 8: Post perfusion of 100nM PGI_2 induces embolisation of preformed thrombi on collagen. After 2 minutes of flowing whole blood and formation of thrombi, Tyrodes containing 100nM PGI_2 was perfused over these preformed thrombi for 10 minutes at $1000s^{-1}$ and the effect on thrombi was observed. Videos are representative of three experiments.

Supplementary Video 9: Post perfusion of PBS does not affect thrombus embolization on collagen. After 2 minutes of flowing whole blood and formation of thrombi, Tyrodes was perfused over these preformed thrombi for 10 minutes at $1000s^{-1}$ and the effect on thrombi was observed. Videos are representative of three experiments.

Supplementary Video 10: Formation of thrombi in the presence of PKA inhibitors over collagen coated flow chambers. Whole blood was treated with PKA inhibitors - 100μM RP-8-CPT-cAMP (RP) and 2μM KT5720 (KT) for 20 minutes. It was stained with 10μM $DiOC_6$ was flown over collagen (25μg/ml) coated slides for 2 minutes at a shear rate of $1000s^{-1}$, to enable the formation of thrombi. Videos are representative of three experiments.

Supplementary Video 11: Post perfusion of 100nM PGI_2 in the presence of PKA inhibitors does not induce embolisation of preformed thrombi on collagen. After 2 minutes of flowing whole blood (in the presence of 100μM RP-8-CPT-cAMP and 2μM KT5720) and formation of thrombi, PBS containing 100nM PGI_2 in the presence of 100μM RP-8-CPT-cAMP and 2μM KT5720 was perfused over the preformed thrombi for 10 minutes at $1000s^{-1}$ and the effect on thrombi was observed. Videos are representative of three experiments.

Supplementary Video 12: Post perfusion of PBS in the presence of PKA inhibitors does not induce embolisation of preformed thrombi on collagen. After 2 minutes of flowing whole blood (in the presence of 100μM RP-8-CPT-cAMP and 2μM KT5720) and formation of thrombi, PBS containing 100nM PGI_2 in the presence of 100μM RP-8-CPT-cAMP and 2μM KT5720 was perfused over the preformed thrombi for 10 minutes at $1000s^{-1}$ and the effect on thrombi was observed. Videos are representative of three experiments.

Abbreviations

5-HT	Serotonin
βTD	β tail domain
AC	Adenylyl cyclase
ADAP	Adhesion- and Degranulation-promoting Adapter Protein
ADP	Adhenosine Diphosphate
AKAP	A Kinase Anchoring Protein
Akt1/2 / PKB	Protein Kinase B
Arp2/3	Actin related protein 2/3
ATP	Adenosine Triphosphate
ATPase	Adenosine 5'-Triphospatase
BSA	Bovine Serum Albumin
Ca^{2+}	Calcium
cAMP	Cyclic Adenosine Monophosphate
cGMP	Cyclic Guanosine Monophosphate
C-terminal	Carboxyl terminal
CD36	Cluster of differentiation 36
CD63	Cluster of differentiation 63
Cdc42	Cell division control protein 42
COX-1	Cyclooxygenase 1
COX-2	Cyclooxygenase 2
CRIB	Cdc42/Rac1 Binding Domain
Crk	Proto-oncogene (c-Crk)
CVD	Cardiovascular Diseases
CXCR4	Chemokine receptor type 4
DAG	Diacylglycerol
DiOC6	3,3'-Dihexyloxacarbocyanine Iodine
ECM	Extracellular matrix
ELMO	Engulfment and Cell Motility
F-actin	Filamentous actin
FAK	Focal Adhesion Kinase
FcRγ	Fragment crystallizable receptor gamma subunit

FDA	Food and Drug Administration
FSK (Fsk)	Forskolin
GAPDH	Glyceraldehyde 3-phosphate dehydrogenase
G-actin	Globular actin
GPCR	G-Protein Coupled Receptor
GAF	cyclic nucleotide (cGMP) binding domain on PDE2 and PDE5
GAP	GTPase activating proteins
GDI	Guanine-nucleotide dissociation inhibitor
GDP	Guanosine diphosphate
GEF	Guanine-nucleotide exchange factor
GFOGER	Gly-Phe-Hyp-Gly-Glu-Arg (Collagen recognition sequence)
GSK3α/β	Glycogen synthase kinase 3α/β
GTP	Guanosine Triphosphate
GPIb-V-IX	Glycoprotein Ib-IX-V
GPIIb/IIIa	Glycoprotein IIb/IIIa
GPO	Gly-Pro-Hyp (repeat present on collagen)
GPVI	Glycoprotein VI
I-EGF1	Integrin β-chain region
ILK	Integrin-linked kinase
IP_3	Inositol trisphosphate
ITAM	Immuno-receptor Tyrosine-based Activation Motif
kDa	kiloDalton
LASP	LIM and SH_3 domain proteins
LIMK	LIM Kinase (Lin11, Isl-1 and Mec-3)
MMP-9	Matrix metalloproteinase -9
Mg^{2+}	Magnesium
MLC	Myosin Light Chain
MLCK	Myosin Light Chain Kinase
MLCP	Myosin Light Chain Phosphatase
NH_2	Amino group
NO	Nitric oxide
NOS	Nitric oxide synthase

NPFs	Nucleation promoting factors
N-terminal	Amino terminal
$P2Y_1$	Purigenic class of G-protein-coupled receptor 1
$P2Y_{12}$	Purigenic class of G-protein-coupled receptor 12
PAH	Pulmonary arterial hypertension
PAR	Protease activated receptor
PBS	Phosphate Buffer Saline
PDE	Phosphodiesterase
PGI_2	Prostaglandin I_2 (Prostacyclin)
PGG_2	Prostaglandin G_2
PGH_2	Prostaglandin H_2
PGE_2	Prostaglandin E_2
PGF_2	Prostaglandin E_2
PI3K	Phosphatidylinositol 3-kinase
PIP_2	Phosphoinositol Bis (2) Phosphate
PIP_3	Phosphoinositol Tri (3) Phosphate
PINCH	Particularly Interesting Cys-His-rich protein
PLCβ	Phospholipase Cβ
PLCγ2	Phospholipase Cγ2
PKA	Protein Kinase A
PKC	Protein Kinase C
PKG	Protein Kinase G
PLA2	Phospholipase A_2
PPACK	Phenylalanyl-Prolyl-Arginyl Chloromethyl Ketone
PS	Phosphatidylserine
PSI	Plexin/semaphoring/integrin
Rac1	Ras-related C3 botulinum toxin substrate 1
RGD	Arginine(R) – Glycine(G) – Aspartate(D)
RhoA	Ras homologous A
Rif	Rho in filopodia
ROCK	Rho-associated coiled-coil kinase
ROS	Reactive Oxygen Species

RP-8CPT-cAMPS	RP-8-(4-Chlorophenylthio) adenosine-3',5'-cyclic AMPS
SCF	Stem Cell Factor
SDF1	Stromal-cell Derived Factor 1
SEM	Standard Error of Mean
sGC	soluble guanylate cyclase
SFK	Src- Family Kinase
SH3 domain	Src Homology 3 domain
TC10	Ras related GTPase
TNF	Tumour necrosis factor
TPa	Thromboxane receptor 'a'
TPb	Thromboxane receptor 'b'
TPO	Thrombopoietin
TXA_2	Thromboxane A_2
VASP	Vasodilator Simulated Protein
VCA	Verprolin, cofilin, acidic domain
vWF	von Willebrand Factor
WAS	Wiskott-Aldrich Syndrome
WASp	Wiskott-Aldrich Syndrome protein
WAVE	WASp-family verprolin-homologous protein
WHO	World Health Organization

Acknowledgement

Happy to have achieved this far,
Happy to have put all my efforts in,
Happy to have tried and not lost hope,
Happy to have built and not criticised.

Happy to have written this myself, I would like to thank The Almighty ALLAH to have provided me the opportunity to stay firm and to have belief in myself to endeavour this ever challenging task of opting for a PhD and completing it. I entrust myself with all the future endeavours with His will.

I would like to thank my parents for all the sacrifices they had made for me, as I know with tears in my eyes what they have stood by me for. Thankyou is a small word to express myself but it encompasses my gratitude for you both. I hope I could express this to you in person at some time.

Simon Calaminus, my supervisor, my mentor, my idealist and my optimist. What a person he is…! A caring gentleman who speaks gently and convinces you instantly. He took care of me like a child, encouraged me with passion in his eyes, made me see the light at the end of the tunnel while I worked endlessly in the lab (or was it the tunnel) and I am happy he stood by me through all of my frenzy moments. I owe you Simon, Thank you.

Khalid Naseem, an aura of knowledge, power and passion and quite contrary to the other qualities he is a friendly person who would make you think on your heels. He has been a great inspiration to my life. Something to look up to and every time when one thinks they have the answer to his riddle he raises his standards, so anyone can imagine how hard it becomes to catch up with him. Thank you Khalid for all the advice, all the support and all the eye-wink situations.

Hafsa, my beautiful wife, I believe there is a lot that we may have missed and a lot that we have achieved in our lives together; all down to the memories that we stood for each other. I owe you for the sacrifices you made for me and I thank you for your enduring patience. I pray our life is long enough to let us continue gathering happy moments and live through the thick and thins of life by supporting one another. Shukria!

Junaid, my brother, my best friend, my secret keeper and the only person who could beat me during swimming sessions (as we were the only two competing). Thank you bhai for keeping me composed and looking out for me. Danke Freund!

I think I was too busy working that I do remember seeing daylight turning into night too quickly. I would like to thank all my colleagues for cheering me up at this opportunity, they stood by my side as they too were obviously working very hard. Good constructive discussions with Lloyd, Zaher, Jawad, Martin and Ahmed. Nice tea and coffee breaks with Jawad and Jiwei. Enjoyed my passive smoking with Libyan, Syrian, Pakistani and Chinese colleagues. Enjoyed your company; Mihray, Martin, Katie, Pooja and Kochar. I hope I have not missed out anyone. Thank you for all the support. As the saying goes 'To put a comma to the friendship and never a full stop', Meet You Again Fellas!

Studying for becoming a medic and opting for incorporating research with it, made me come at a crossroads. I made my choice and I stick to it, not many medics would like to dwell this path. I want to be the beam of light for them, I want to travel the road which was less travelled by. I would like to quote from the poem "The road not taken" by Robert Frost:

"I shall be telling this with a sigh,
Somewhere ages and ages hence:
Two roads diverged in a wood, and I __
I took the one less travelled by,
And that has made all the difference."

Author’s declaration

‘I confirm that this work is original and that if any passage(s) or diagram(s) have been copied from academic papers, books, the internet or any other sources these are clearly identified by the use of quotation marks and the reference(s) is fully cited. I certify that, other than where indicated, this is my own work and does not breach the regulations of HYMS, the University of Hull or the University of York regarding plagiarism or academic conduct in examinations. I have read the HYMS Code of Practice on Academic Misconduct, and state that this piece of work is my own and does not contain any unacknowledged work from any other sources’.

CHAPTER 1:

General Introduction

1.1 Introduction

Platelets are blood constituents that are characterized by their small size and anucleate presence (Harker et al., 2000). They are produced by pinching-off of megakaryocyte cytoplasmic extensions in the vessels of the bone marrow (Harker et al., 2000). The platelet circulates in the blood for approximately ten days and is removed from circulation by the spleen (Harker et al., 2000). The main function of the platelet is to arrest bleeding after injury, through the formation of a thrombus. In addition to preventing blood loss, these cells are also thought to be involved in pro-inflammatory responses via crosstalk with neutrophils; produce antimicrobial peptides to counter infection during trauma; and play a pathological role during cancer metastasis (Gawaz et al., 2005, Semple et al., 2011).

To ensure haemostasis, platelets rapidly respond to the denuding of the vascular basement membrane, resulting from an injury. The platelet response is initiated by their adherence to the exposed collagen and von Willibrand factors (vWF) via its glycoprotein receptors, GPVI and GPIb-IX-V, respectively. Once the platelets start rolling and adhering to the exposed matrix proteins, it leads to their activation. This is followed by secretion from specific cytoplasmic granules, alpha and dense granules which are present within the platelets. These granules have various mediators such as ADP, ATP, serotonin (5-HT), TXA_2 and fibrinogen (Petersen et al., 2002, Wei et al., 2009). These released substances further increase platelet activation and cause firmer platelet adhesion, platelet spreading and the aggregation culminates in the formation of a haemostatic plug (Wei et al., 2009).

1.2 Production and structure of platelets:

1.2.1 Megakaryocyte

Megakaryocytes are haematopoietic cells which reside primarily in the bone marrow (Ogawa, 1993), but can also be found in the lungs, spleen and liver. They are large cells ranging from 50 to 100 μm in diameter (Machlus and Italiano, 2013) and comprise of approximately 0.01% of all the nucleated cells present in the bone marrow (Nakeff and Maat, 1974). Signalling by cytokines such as Stem Cell Factor (SCF) and Thrombopoietin (TPO), commits haematopoietic stem cells to develop into megakaryocytes (Kaushansky, 2009). Their development involves the maturation of the cytoplasm, an increase in the nuclear content (Zimmet and Ravid, 2000), elaboration of the limiting cytoplasmic membrane and formation of proplatelets (Machlus and Italiano, 2013). The final stage of

proplatelet formation is the release of immature dumbbell-shaped platelets directly into the bloodstream where they finalize their stage of maturation and circulate within the blood (Machlus and Italiano, 2013).

The development of the haematopoietic stem cell up to the stage of megakaryocyte formation and release of platelets in the circulation requires migration of the cell. The stem cell resides within a hypoxic collagen I rich environment, called the osteoblastic niche. During megakaryocyte development the cell moves to a normoxic, fibrinogen, fibronectin and collagen IV rich environment next to blood vessels, called the vascular niche. This migratory response is driven by stromal-cell derived factor 1 (SDF1). The mature megakaryocytes express CXCR4, an SDF1 receptor, which induces the production of Matrix Metalloproteinase-9 (MMP-9). The MMP-9 helps the megakaryocyte for its migration towards an increasing concentration of SDF1 (Lane et al., 2000). The migration response involves the reorganization of the actin within the cell. Actin polymerisation allows the formation of long actin filaments, which can be organised into particular structures, therefore giving the cell structural integrity and the ability to push and pull on its environment.

1.2.2 Platelets

The platelets are anucleate structures which receive all of its constituents from the megakaryocytes. Structurally a platelet has a discoid shaped resting state which could be divided into three regions; peripheral, structural and organelle zones.

1) The peripheral zone is involved in adhesion and aggregation of platelets. It consists of an exterior glycocalyx having coagulation factors (I, II, VII, IX, X) and the major platelet receptors; GPIb (for vWF), GPIIb/IIIa (for fibrinogen) and GPVI (for collagen).

2) The structural zone is involved in providing an arrangement and support to the platelet through microtubules and microfilaments. The microtubule encases the platelet, hence, maintaining its discoid appearance; while microfilaments (actin and myosin) which are present in the cytoplasm help in cellular contraction (Root and Hofmann, 1963).

3) The organelle zone is responsible for metabolic activities. It has:

i) Mitochondria which provide energy for the platelet functioning required during their activation or granule release. In addition it is also involved in the production of reactive

oxygen species (ROS) that act as signalling molecules on interaction with collagen and ultimately the release of cytochrome c that results in platelet apoptosis (Ivanciu et al., 2014).

ii) Dense granules (around 7 per platelet) that contain, calcium (Ca^{2+}), serotonin (5-HT), adenosine triphosphate (ATP), adenosine diphosphate (ADP), magnesium (Mg^{2+}), guanosine triphosphate (GTP) and guanosine diphosphate (GDP) (Kahr, 2009).

iii) Alpha granules which are larger in size and most abundant in number (40 – 80 per platelet) than dense granules. Alpha granules contain adhesion molecules such as vWF / fibrinogen / P-selectin, chemokines, cytokines, fibrinolytic regulators, immunologic modulators, coagulation factors, complement proteins, growth factors, and pro- and anti-angiogenic factors (Kahr, 2009, Blair and Flaumenhaft, 2009).

iv) Lysosomal granules which contain microbicidal enzymes, and acid hydrolases.

v) Peroxisomes.

vi) Glycogen granules.

Apart from these zones, an elaborate membrane system exists in the platelet (White and Clawson, 1980). It is composed of a dense tubular system which provides space for synthesis (ATPase/Prostaglandin) and storage (Ca^{2+}/Mg^{2+}). In addition there is an open canalicular system which along with helping to transport substances across, also acts as a reservoir of membrane which is utilized during platelet spreading (Blair and Flaumenhaft, 2009).

1.3 Platelet receptors and their ligands:

The circulating platelets are separated from interacting with the activatory extracellular matrixes (ECM) in the vessel wall by the layer of endothelial cells acting as a barrier between them. The ECM proteins have a major role, in the body, in providing structural and organizational stability to the surrounding cells. Upon endothelial damage, it acts as a strong prothrombotic surface for platelets. Fibrinogen (present in the plasma and vessel wall) and collagen (present in the vessel wall), form the major ligands for the platelet receptors that are involved with activation of platelets and formation of a thrombus.

Alongside these ECM proteins, there are a series of additional agonists which modulate platelet function in an inhibitory and activatory manner. To enable the platelets to interact

with these ligands, they have a wide variety of receptors that includes; integrins ($\alpha_{IIb}\beta_3$, $\alpha_2\beta_1$), leucine-rich-repeated receptors (GP Ib/IX/V, Toll like receptors), G-protein coupled receptors (Thrombin receptors-PAR1 - PAR4), ADP receptors-$P2Y_1$ and $P2Y_{12}$, thromboxane receptors-TPα and TPβ, proteins from the immunoglobulin superfamily (GPVI), C-type lectin receptors (P-selectin), tyrosine kinase receptors (thrombopoietin receptor, Gas-6, Ephrin and Eph kinases) and many other types as well (CD63, CD36, TNF receptor) (Rivera et al., 2009, Murugappan et al., 2004).

The expression of these receptors, on the surface of the platelets, enables them to respond to any stimuli in a swift manner.

1.3a Integrin family

Integrins are heterodimeric structures, composed of α and β subunits. There are 18α and 8β subunits which form at least 24 distinct integrin receptors (Hynes, 2002). Each of these subunits themselves has an extracellular, transmembrane and intracellular domain. These domains help the transmission of signals in either direction, connecting the outside of the cell to its inside machinery.

In general, the extracellular domain of the integrin is large (approximately 80-150 kDa) (Zent and Pozzi, 2010). It is subdivided into globular N-terminal sequences for ligand binding which are supported by extended leg regions that link the extracellular domain to the transmembrane and the cytoplasmic tail of each subunit (Nermut et al., 1988), as shown in figure 1.1.

However the structures of α and β subunits of the integrins have different sections. The insert in figure 1.1 shows globular α subunit which has a β-propeller head, a thigh domain, a knee and two calf domains (Zent and Pozzi, 2010). Within half the population of α subunits of the integrin is an inserted I-domain in β-propeller region. This I-domain serves as the binding site for extracellular ligands and divalent metal ions (Zent and Pozzi, 2010). Similarly the insert in figure 1.1 shows the extracellular region of the β subunit also has an I-like domain (similar in structure to I domain of the α subunit), a PSI (plexin/semaphoring/integrin), hybrid domain, 4 I-EGF domains and a βTD (β tail domain).

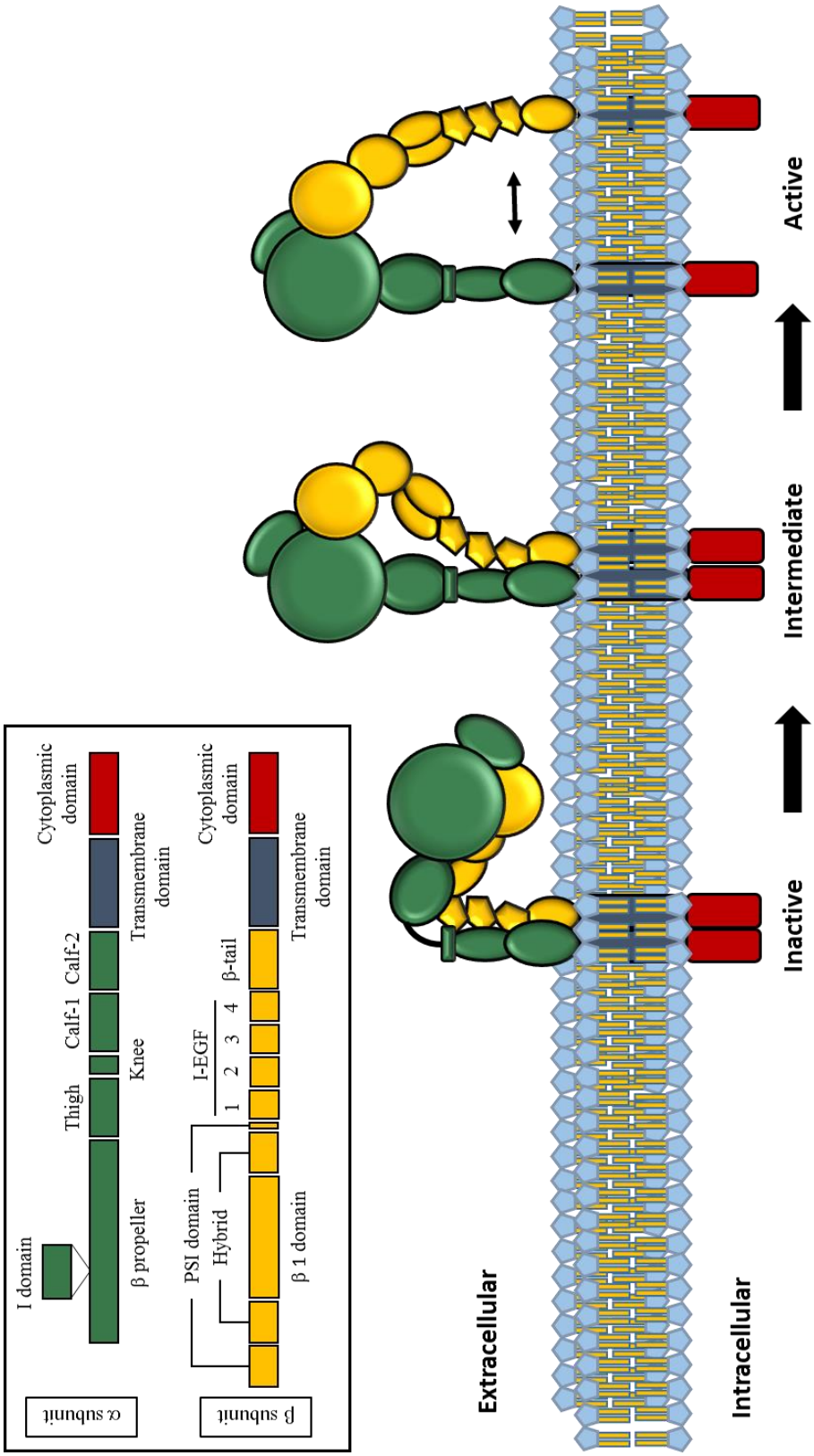

Figure 1. 1: Structure of the integrin receptor in platelets. Integrins are hetrodimeric structures composed of alpha and beta subunits. There are three domains for each subunit; extracellular domain [α- subunit (green) and β–subunit (yellow)], transmembrane domain (blue) and cytoplasmic domain (red). The inactive state of the integrins is in a bent state which becomes upright in an intermediate state and upon detachment of the transmembrane and cytoplasmic domain of αand β subunits becomes active. The insert shows the structural division of α-subunit (green) and β–subunit (yellow). Adapted from (Luo and Springer, 2006).

The transmembrane domain of the integrin is an alpha helix coil which has a membrane spanning length of approximately 24-29 amino acids (Zent and Pozzi, 2010). It links the extracellular domain to the cytoplasmic domain of the receptor. The cytoplasmic domain is short (with the exception of β4) and plays key roles in signalling by recruiting intracellular proteins such as talin, kindlin, filamin, FAK, ILK and $G\alpha_{13}$ (Shattil and Newman, 2004, Zent and Pozzi, 2010, Liu et al., 2000, Wegener et al., 2007, Gong et al., 2010). The β subunit has conserved cytoplasmic phosphotyrosine-binding motifs for interacting with multiple proteins, including talin, filamin and kindlin. The heterodimeric state of the integrin in the resting platelets is maintained by the interactions between the glycine residues of the α and β subunits within the transmembrane domain and between arginine from α subunit and aspartic acid from β subunit (Gottschalk, 2005, Adair and Yeager, 2002, Vinogradova et al., 2002, Zent and Pozzi, 2010).

The integrins can exist as either basally active or basally inactive, depending on the cell types under consideration. These states of integrin activity cycle between one another depending on the activatory status of the cell. Adherent cells attached to the basement membrane have an active basal integrin conformation while platelets in circulation have an inactive conformation of the integrins. In platelets, the involvement of the metal ion aids the interaction of the ligand to its receptor. It helps in changing the conformation of the integrin from its closed inactive form to an active state (Liddington and Ginsberg, 2002). The inactive form of the integrin exists in a bent position, with the bend occurring in the knee region for the α subunit and I-EGF1 region of the β subunit. In the intermediary position the bend straightens but the transmembrane and cytoplasmic regions remian close together. The fully active form of the integrin exists with the legs, one for each of α and β subunits, separating from each other. Once the integrin has bound to its receptor, complexes are recruited at the cytoplasmic domain and hence downstream signalling ensues (Figure 1.1).

There are several integrin receptors in platelets. My focus will be on $\alpha_{IIb}\beta_3$ and $\alpha_2\beta_1$, as they are receptors for fibrinogen and collagen, respectively.

1.3.1 Fibrinogen and its receptor

Fibrinogen is the main ligand binding to the integrin $\alpha_{IIb}\beta_3$ (glycoprotein IIb/IIIa) (Zucker and Masiello, 1984, Lyman et al., 1997). It is a large glycoprotein molecule which exists as

a dimer. Each of the monomers is composed of 3 non-identical polypeptide chains of Aα, Bβ and γ, which coil around each other. These monomers are arranged in an anti-parallel manner and are held together by means of disulphide bonds. At the carboxyl terminal of these chains lies the D domain. Between the two D domains is the E domain (Figure 1.2). The E-domain contains the N-terminals of the 6 chains (2Aα, 2Bβ and 2γ) from the D domains. Within this E domain, lie the thrombin cleavage sites, present on the 2Aα and 2Bβ chains. Once cleaved by thrombin, 4 active sites are generated on each E-domain that binds to individual D-domains of other fibrinogen molecules (Figure 1.2), resulting in the formation of a fibrin meshwork. Between the D and E domains is the coiled coil region which contains the plasmin cleavage site. Once the thrombin activates fibrinogen, it also causes activation of the negative regulatory mechanism by converting plasminogen to plasmin. Plasmin then cleaves the fibrinogen molecule, thereby limiting the extent of the formation of a fibrin meshwork.

Fibrinogen contains three integrin binding sites, two RGD (Arginine-Glycine-Aspartate) sites one on each of the carboxyl ends of the Aα chains, along with another integrin binding site at the γ-chain (Rooney et al., 1996, Kloczewiak et al., 1984). Binding of integrin $\alpha_{IIb}\beta_3$ involves interactions with the RGD sequence along with the γ-chain sequence of fibrinogen (Salsmann et al., 2005). It has been noted in the literature, by using terminal deletion of γ-chain *in vitro* (Holmback et al., 1996) and transgenic mice *in vivo* (Rooney et al., 1996), the primary site of interaction is the γ-chain sequence of fibrinogen with the β-propeller region of α_{IIb} subunit of the integrin receptor (Smith et al., 1990, Kloczewiak et al., 1984, Farrell and Thiagarajan, 1994, Farrell et al., 1992). This communication facilitates changes in the β_3 subunit of integrins and enables interaction with the RGD sequence of fibrinogen. Engagement of the two fibrinogen recognition sites is followed by full activation of integrin $\alpha_{IIb}\beta_3$ resulting in downstream signalling (Rooney et al., 1996).

1.3.1.1 Integrin $\alpha_{IIb}\beta_3$

The integrin $\alpha_{IIb}\beta_3$ is a major platelet receptor which is highly expressed on the surface, with approximately 40,000 - 80,000 $\alpha_{IIb}\beta_3$ receptors present on each platelet (Wagner et al., 1996). It can interact with various adhesive proteins including fibrinogen, fibronectin, vWF and vitronectin (Mekrache et al., 2002).

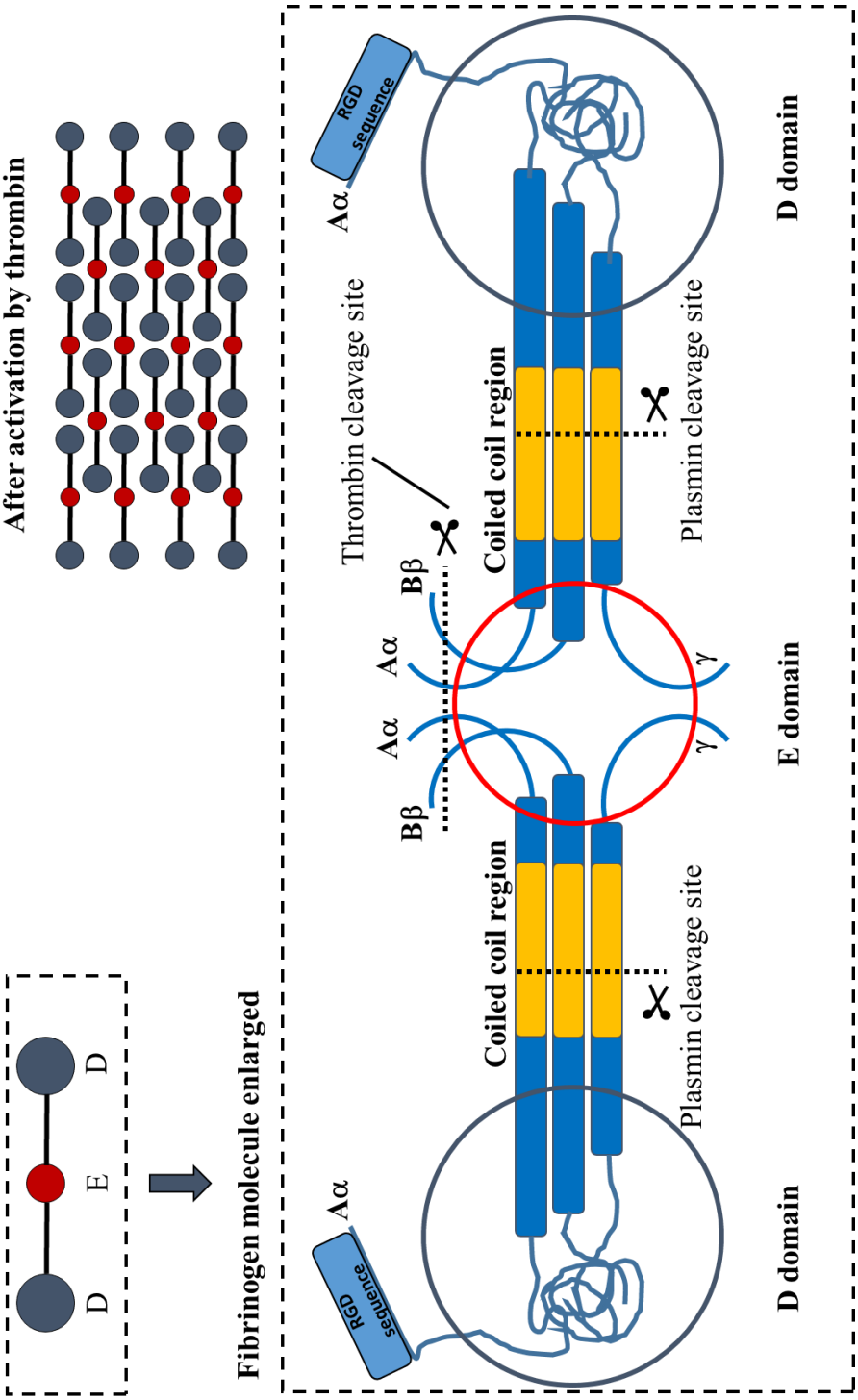

Figure 1. 2: Structure of fibrinogen. Fibrinogen is a dimer. Each of the monomer has 3 non-identical polypeptide chains; Aα, Bβ and γ. Structurally the two monomers are arranged facing each other with the centrally located E-domain and the peripherally located two D-domains. Thrombin cleavage at E-domain exposes active sites for binding of D-domains of other fibrinogen molecules and thus forms fibrin meshwork. The RGD sequence present on the Aα chain helps fibrinogen binding to integrin receptor. Adapted from (McDowall, 2006).

The integrin, $\alpha_{IIb}\beta_3$, exists in an inactive and an active conformational state (Litvinov et al., 2012). Resting platelets have an inactive $\alpha_{IIb}\beta_3$, therefore a low affinity for its ligand (Kieffer et al., 1991). Once triggered by agonists, a conformational change in the $\alpha_{IIb}\beta_3$ complex occurs, which activates the fibrinogen receptor increasing the affinity for fibrinogen binding. Activation does lead to an increased expression of the receptor on the platelet surface, as the number of surface receptors does not change (Litvinov et al., 2012). Presence of divalent ions such as Mn^{2+} implies faster binding of integrin $\alpha_{IIb}\beta_3$ to fibrinogen, as it is an integrin activator. Its presence thereby increases the active state of the receptor while reducing its inactive state (Litvinov et al., 2012).

Absence of agonist does not cease but only reduces the rate of fibrinogen binding to its receptors (Shattil et al., 1985). Depending upon the level of platelet activation, the fibrinogen may bind to its receptor, $\alpha_{IIb}\beta_3$ complex in two ways (Mekrache et al., 2002).

- In an active state of the platelet the extracellular domain of $\alpha_{IIb}\beta_3$ recognizes the RGD motif on adhesive ligands (Hynes, 2002, Ruoslahti and Pierschbacher, 1986). The RGD sequences of fibrinogen is located on the 95-97 and 572-574 on its Aα chain which interacts with the integrin $\alpha_{IIb}\beta_3$ 109-171 amino acids sequence present on β–chain, generates a signal (Mekrache et al., 2002).
- In an inactive platelet (as on addition of platelets to immobilized fibrinogen) the presence of dodecapeptide (12 amino acids) sequence at the C-terminus (400-411) of its γ-chain interacts with integrin $\alpha_{IIb}\beta_3$ (294-314) at its α_{IIb} subunit (Gartner et al., 1993, Zaidi et al., 1996, Farrell and Thiagarajan, 1994). Stable bonding of fibrinogen to $\alpha_{IIb}\beta_3$ depends upon the contact duration (Litvinov et al., 2012). Attachment of dodecapeptide provides an enabling environment for the RGD sequence on fibrinogen to interact with the β_3 subunit of the integrin, thus activating the downstream signalling (Rooney et al., 1996).

Binding of integrins to its ligand, enables the cell to interact with its surrounding or for the surrounding to modify the cell. These instances identify the bidirectional role played by integrins in general and more so specifically the role played by $\alpha_{IIb}\beta_3$ in platelets. The agonists which are released by activated platelets prime the receptor and lead to the 'Inside-out' activation of $\alpha_{IIb}\beta_3$. Direct stimulation of the receptor by its ligand is termed as

'Outside-in' activation. Both of these cases of receptor activation lead to the involvement of the downstream signalling complexes.

1.3.1.1a Outside-in

Ligand binding directly onto the receptor initiates outside-in signalling that regulate many cellular functions such as cell spreading and migration (Ruoslahti and Pierschbacher, 1986, Kim et al., 2003, Ginsberg et al., 2005). Integrin $\alpha_{IIb}\beta_3$ has multiple ligands (fibrinogen, vWF, fibronectin) and mediates platelet spreading and aggregation on vascular surfaces (Ruggeri, 2002, Shattil and Newman, 2004, Jackson, 2007, Phillips et al., 2005). Bidirectional signalling of integrins is impaired if either α_{IIb} (Tronik-Le Roux et al., 2000) or β_3 (Hodivala-Dilke et al., 1999) is affected in humans, identifying the importance of the heterodimerisation of the receptor. Defective downstream signalling also arises if the interaction of β_3 subunit is hampered with its regulatory proteins, such as talin and SFK (Leisner et al., 2007, Shattil and Newman, 2004).

1.3.1.1b Inside-out

Inside-out signalling directs the availability of an appropriate stimulus to lead the activation of the receptor. This notion becomes important where the availability of the ligand is in close proximity to that of its receptor. In platelets, an injury to the blood vessel wall leads to release of agonists such as ADP and thrombin. The activation by the agonist induces conformational changes in the extracellular domain of the $\alpha_{IIb}\beta_3$ (Ma et al., 2006, Wegener et al., 2007, Luo et al., 2007) which leads to exposure of the extracellular ligand binding sites. Once the ligand such as fibrinogen binds to the $\alpha_{IIb}\beta_3$, it causes outside-in signalling, helping the formation of aggregates, which later culminates into the formation of a clot.

1.3.1.2 Downstream signalling via fibrinogen-integrin interaction

Fibrinogen binding to integrin $\alpha_{IIb}\beta_3$ induces downstream signalling events that lead to activation of further receptors, secretion and/or degranulation, stable adhesion, platelet spreading and recruitment of leukocytes to the site of injury and/or inflammation (figure 1.3). To mediate these effects, the activity of the integrin receptor is brought to its intermediate state via talin and kindlin binding at the cytoplasmic region of the β_3 subunit of the integrin. This induces a firmer and later full activation of the integrin $\alpha_{IIb}\beta_3$ receptor

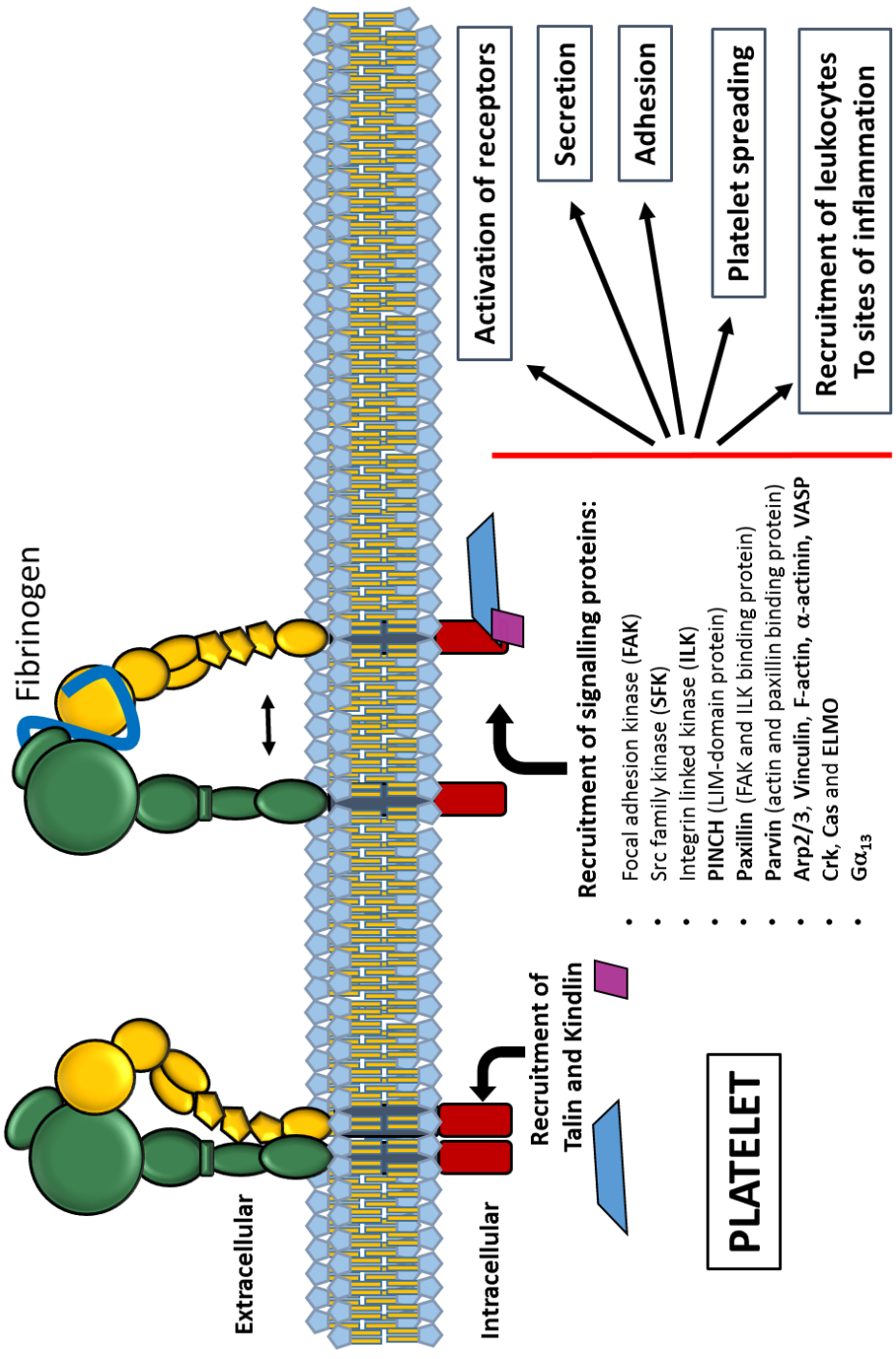

Figure 1. 3: Downstream effects of fibrinogen interaction with integrin, $\alpha_{IIb}\beta_3$. Fibrinogen binding to $\alpha_{IIb}\beta_3$ led to recruitment of multiple signalling proteins. These proteins formed multitude of interconnections that resulted in a complex output to produce activation of receptors, secretion or degranulation, adhesion, platelet spreading and recruitment of leukocytes to sites of injury and/or inflammation.

by binding to fibrinogen. Full activation recruits multiple signalling proteins, which forms an 'Adhesome' as had been identified by Zaidel-Bar et al (2007). The adhesome consists of an expanding list of 156 components with multitudes of interconnections (Geiger et al., 2001). Of that list some of the proteins involved with the remodelling of actin cytoskeleton includes focal adhesion kinase (FAK), Src family kinase (SFK), Arp2/3, Vinculin, filamentous actin, α-actinin, VASP, Crk, p130Cas, p190RhoGEF, ELMO, integrin linked kinase (ILK), LIM-domain protein (PINCH), Paxillin (FAK, Vinculin and ILK binding protein), Parvin (actin and paxillin binding protein) and $G\alpha_{13}$ (Figure 1.3).

Outside-in signalling via integrin $\alpha_{IIb}\beta_3$ leads to activation of Src and FAK. The presence of FAK recruits additional proteins such as ILK, Paxillin and Parvin. Together with FAK, Paxillin activates a small RhoGTPase molecule, Cdc42. Activation of Src in the presence of FAK leads to recruitment of p130Cas and Crk that activates another small RhoGTPase, Rac. Activation of Rac is also promoted by the activation of Cdc42. In the meantime, Src stimulation activates 190RhoGAP and deactivates p190RhoGEF; that modulates the levels of yet another downstream RhoGTPase, RhoA. The interplay of the activity levels of these small RhoGTPases accounts for the spreading of the platelets that involves filamentous actin and actin related proteins such as Arp2/3.

1.3.2 Collagen and its receptors

Collagen is a highly abundant protein in the body, nearly 30% of the total protein by mass (Bergmeier and Hynes, 2012). It consists of large superfamily comprising of 28 members, of which collagen types I, II, III and IV are the most abundant (90% of the total) (Watson, 2009). It consists of three polypeptide chains (α chains) that twist in a right-handed manner to form a triple helix (Ricard-Blum, 2011). This helix is stabilized by the repetitive presence of glycine (G), proline (P) and hydro-oxyproline (O) along with hydrogen bonding and electrostatic interactions (Persikov et al., 2005).

Collagen types I, III and V are present in the deeper layers of the vascular wall while collagen type IV is present in the superficial layers (Bergmeier and Hynes, 2012). Thus depending on the depth of injury, the degree of response initiated is dependent on the type of collagen exposed as type I generates a stronger response than type IV (Jung et al., 2008). This generation of response is dependent on the activation of platelet surface receptors, GPVI and integrin $\alpha_2\beta_1$ (Moroi et al., 1989, Nieuwenhuis et al., 1985, Kehrel et al., 1988) by the repetitive GPO regions on collagen.

1.3.2.1 GPVI

GPVI is the main collagen binding receptor on platelets. It is an adhesion receptor which is an example of a type I transmembrane glycoprotein from the immunoglobulin superfamily (Clemetson et al., 1999, Clemetson and Clemetson, 2001). Structurally GPVI is divided into an extracellular, transmembrane and a short cytoplasmic domain. The extracellular domain is composed of two immunoglobulin-like domains (D1 and D2), which are connected to the transmembrane and cytoplasmic regions by a mucin-like stalk (Figure 1.4). The ligand binding region is located on the D1 domain while the D2 domain helps in the dimerization of the receptor (Horii et al., 2006). GPVI is non-covalently associated with the FcR γ-chain at the transmembrane domain owing to the presence of arginine and 6 other juxtaposed aminoacids (Nieswandt and Watson, 2003, Dutting et al., 2012). The cytoplasmic region of GPVI binds to the Src-homology 3 (SH3) domain of the tyrosine kinase family members, Fyn and Lyn (Nieswandt and Watson, 2003).

On activation of GPVI by collagen, the ITAM (Immuno-receptor Tyrosine-based Activation Motif) domain present in FcR γ-chain on platelet is phosphorylated at tyrosine residues by Fyn or Lyn (Figure 1.4) (Watson, 2009). This phosphorylation event of tyrosine, recruits Syk which generates the formation of a signalosome. The signalosome is composed of an adaptor protein - LAT, phospholipase C γ2 subunit (PLCγ2), PI3Kinase, Gads, Vav1/3 and Btk/Tec family kinase. The LAT-SLP76 signalosome, PI3Kinase and also directly via Syk, all lead to activation of PLCγ2 that culminates in platelet activation by release of Ca^{2+}, activation of Protein Kinase C (PKC), degranulation and inside-out activation of integrins (Figure 1.4) (Nieswandt and Watson, 2003, Watson, 2009, Chen and Kahn, 2003).

1.3.2.2 $\alpha_2\beta_1$

Apart from GPVI, the integrin receptor that binds to collagen is $\alpha_2\beta_1$. In comparison to the integrin $\alpha_{IIb}\beta_3$, it has significantly fewer receptors present on the platelet surface (2000 - 4000) (Watson, 2009). However, similar to $\alpha_{IIb}\beta_3$, it exists in an inactive form on the platelet surface (Nuyttens et al., 2011). On activation it provides firm attachment to the platelets at the site of vascular injury (Watson, 2009, Chen and Kahn, 2003). This attachment involves an interaction between I-domain in β-propeller region of the α_2-subunit of $\alpha_2\beta_1$ integrin with the GFOGER sequence in the collagen molecule (Emsley et al., 2000).

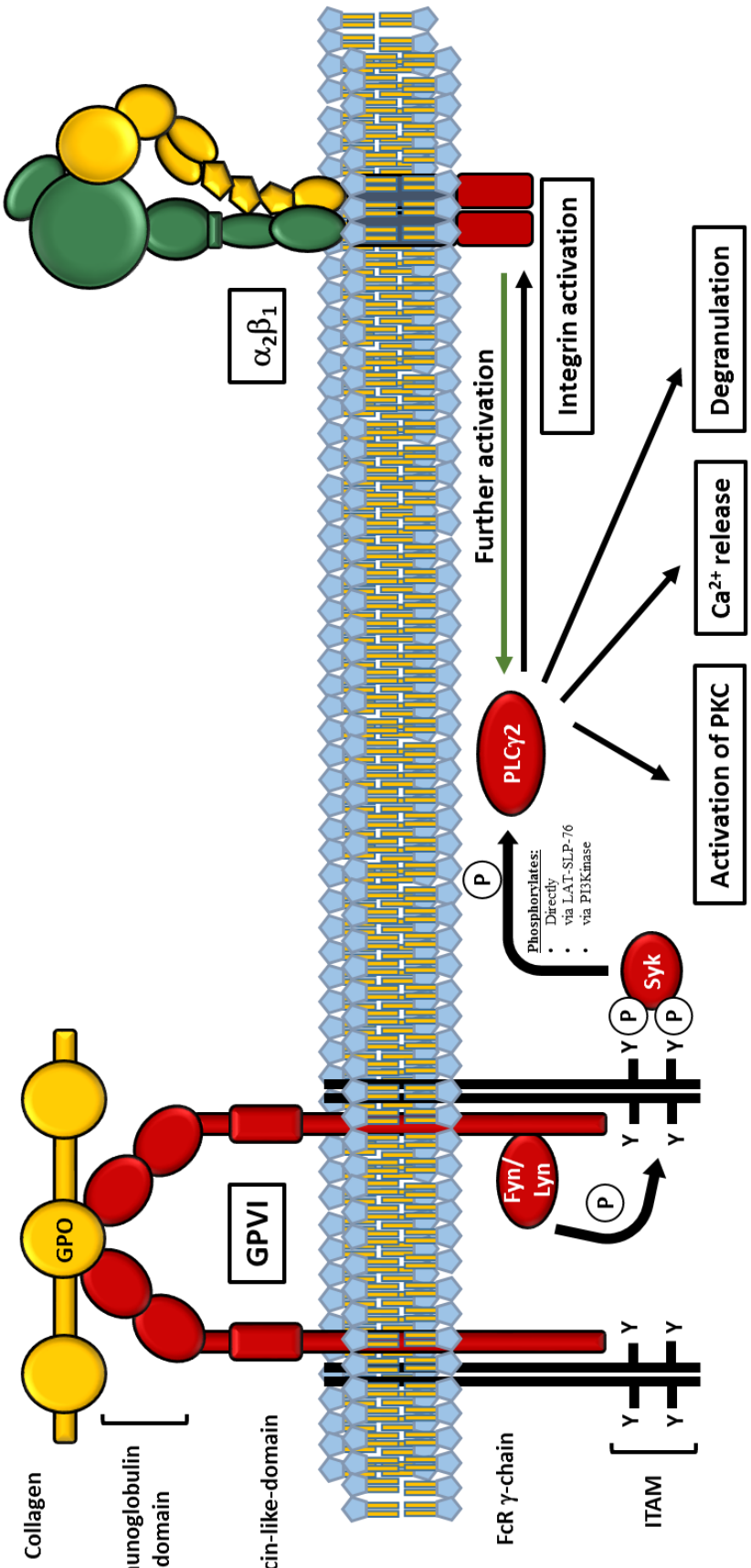

Figure 1. 4: Downstream effects of collagen signalling with GPVI and integrin - $\alpha_2\beta_1$ activation. Collagen binding to receptor GPVI leads to recruitment of SFK proteins, Fyn and Lyn. These proteins phosphorylate the ITAM residues that lead to recruitment of Syk. The Syk phosphorylates PLCγ2; directly, via LAT-SLP-76 or via PI3Kinase, thereby activating it. This leads to activation of PKC, release of Ca^{2+} from the stores, degranulation and integrin $\alpha_2\beta_1$ activation. Integrin activation amplified the activation of PLCγ2 that led to compounding the activation of platelets. Adapted from (Watson et al., 2001)

A two-receptor model for platelet activation on collagen had been suggested via GPVI and $\alpha_2\beta_1$ (Chen and Kahn, 2003). Previously it was conferred that $\alpha_2\beta_1$ was the main receptor for interaction with collagen (Barnes et al., 1998). Recent studies have identified that loss of GPVI abolishes the downstream signalling of interaction with collagen (Moroi et al., 1989, Nieswandt et al., 2000, Nieswandt et al., 2001). It has now been proven that GPVI activates the integrin receptor $\alpha_2\beta_1$, on binding to collagen (Chen and Kahn, 2003). Similar to GPVI, integrin $\alpha_2\beta_1$ also interacts with Src kinase that prompts further activation of PLCγ2 leading to an increase in the response generated by GPVI (Figure 1.4) (Inoue et al., 2003).

1.3.3 Additional important ECM proteins

Apart from fibrinogen and collagen, other platelet agonists that provoke activation of platelets include von Willebrand factor (vWF), laminin, fibronectin and vitronectin, among other ligands (Yurchenco, 2011, Hallmann et al., 2005, Voss and Rauterberg, 1986, Bergmeier and Hynes, 2012). The exposure of ECM in the blood vessel wall, directs the circulating vWF to be decorated on the exposed site of endothelial injury. The vWF interacts with the glycoprotein receptor complex, GPIb-IX-V, present on the surface of platelets that leads to tethering and rolling of platelets under flow. This interaction allows enough time for engagement of GPVI receptor with collagen, thereby activating platelets. In humans, lack of either the receptor, GPIb-IX-V, as had been seen in Bernard Soulier syndrome or the absence of vWF (Caen et al., 1976, Bernard and Soulier, 1948, Nurden, 1999), or in mice, depletion of either the receptor (Ware et al., 2000) or the ligand (Denis et al., 1998), resulted in severe bleeding diathesis. The interaction between vWF and GPIb-IX-V forms an important mediator of platelet activation. In the presence of raised cAMP levels, GPIb component is phosphorylated which inhibits the vWF interaction with GPIb-IX-V and hence inhibits platelet activation (Raslan et al., 2015b).

1.3.4 GPCR

G-protein coupled receptors (GPCRs) play an important role in platelet signal transmission. The GPCRs are composed of a 7 transmembrane serpentine structure. The C-terminus is located intracellularly while the N-terminus is exposed extracellularly (Dohlman et al., 1987, Kroeze et al., 2003, Nathans and Hogness, 1983, Peralta et al., 1987). A heterotrimeric G protein is composed of α, β and γ subunits, which bind at the intracellular region of the receptor (Kobilka et al., 1988, Wess et al., 1989, Wong et al., 1990). The γ

subunit is small and requires interaction with β subunit for it to fold on it, hence the formation of the βγ subunit (Hurowitz et al., 2000). Both, β and γ subunits, have not been identified to function independently of each other (Hurowitz et al., 2000). Binding of the βγ subunit to α subunit results in conformational changes to the α subunit, thereby restricting both, βγ and α subunits, from exerting their effects on the effector proteins (Clapham and Neer, 1997). Stimulation of the GPCR by an agonist leads to replacement of the GDP with a GTP on α subunit. This leads to dissociation of α subunit from the βγ subunit, while the β and γ subunits remain tightly associated to each other.

The downstream activity of the GPCR depends on the classification of the α subunit. It exists as $G\alpha_s$ (activates adenylyl cyclase which increases cAMP), $G\alpha_i$ (inhibits adenylyl cyclase which decreases cAMP), $G\alpha_q$ (activates phospholipase C and also activates PKC thereby increasing Ca^{2+} concentration intracellularly) and $G\alpha_{12/13}$ (activates Rho which leads to actin remodelling and shape change). The βγ subunit causes an increase in phosphoinositide-3-kinase (PI3K). The PI3K leads to an increase in integrin activation via Akt 1/2 and it also potentiates the release of α- and dense granules that amplifies platelet activation (Joo, 2012).

1.3.4.1 Agonist mediated

Many platelet agonists bind to GPCRs, for example thrombin binds to PAR1 and PAR4, ADP interacts with $P2Y_1$ and $P2Y_{12}$ and TXA_2 mainly binds to TPα. Thrombin and TXA_2 receptors, couple with $G\alpha_q$ and $G\alpha_{12/13,}$ to mediate an increase in Ca^{2+} concentration (Offermanns et al., 1997, Yamanishi et al., 1983) that results in the shape change of platelets (Moers et al., 2003). Thrombin is also involved with a reduction in cAMP levels (Lagarde and Dechavanne, 1977) thereby acting as a potent platelet activator. ADP acts by coupling to $G\alpha_q$ and $G\alpha_i$ causing an increase in cytosolic Ca^{2+} concentration and inhibiting levels of cAMP, respectively. However, ADP too causes change in shape of the platelet but it does not associate with the $G\alpha_{12/13}$ subunit, rather it does so by means of the $G\alpha_q$ subunit (Offermanns et al., 1997, Ohlmann et al., 2000).

The increase in Ca^{2+} concentration observed by thrombin, TXA_2 and ADP is mediated by an increase in the levels of phospholipase Cβ (PLCβ). Activation of PLC generates inositol (1,4,5) triphosphate (IP_3) and diacylglycerol (DAG). This leads to stimulation of PKC and an increase in intracellular Ca^{2+} levels that triggers the inside-out signalling of integrin,

αIIbβ3, via activation of RapIb (Franke et al., 1997, Franke et al., 2000, Jung et al., 2006, Prevost et al., 2004, Woulfe et al., 2002) along with release of alpha and dense granules from the platelets (Walker and Watson, 1993, Siess and Lapetina, 1988).

1.3.4.2 Antagonist mediated

PGI_2 is an antagonist to platelet activation. It signals through the IP receptor which is classed as a GPCR that is coupled to $G\alpha_s$ (Jantzen et al., 2001). PGI_2 keeps the platelets flowing in the blood in a quiescent state by binding to its receptor. This ligand interaction causes an increase in adenylyl cyclase activity, resulting in an intracellular rise in cAMP levels (Salzman et al., 1972, Yamanishi et al., 1983). This rise in cAMP levels causes downstream phosphorylation of proteins that culminates in inhibition of the platelets (Best et al., 1977).

1.4 Platelets in circulation

In a normal blood vessel, platelets are pushed towards the periphery of the flowing blood by red blood cells. This brings the platelets closer to the endothelial lining of the vessel. The endothelium produces prostacyclin (PGI_2) and nitric oxide (NO), which bathes the platelets in the circulation and keeps them in an inhibitory state (Furchgott et al., 1984, Moncada et al., 1976).

1.4.1 Prostacyclin

Eicosanoids is a group of 20 carbon containing fatty acids, which function as signalling molecules for a cell. Arachidonic acid (5, 8, 11, 14 eicosatetraenoic acid) is the precursor of these eicosanoids. The arachidonic acid is bound to the phospholipids of the plasma membrane. It is released from its bound state by hydrolysis, by phospholipase A_2 (PLA_2) or phospholipase C (PLC). Upon release, oxidation by the cyclo-oxygenase enzyme, at carbon positions 9, 11 and 15 enables the formation of prostaglandin G_2 (PGG_2) and Prostaglandin H_2 (PGH_2). These prostaglandins are intermediary to their conversion to the classical prostaglandins; PGE_2, PGF_2, TXA_2 and PGI_2.

PGI_2 (9-deoxy 6, 9 alpha-epoxy-Δ5-$PGF_{1\alpha}$), is formed from PGH_2 by the enzyme, prostacyclin synthase (Figure 1.5). It contains a 20 carbon (C_{20}) molecular structure with a cyclopentane ring. This ring is formed between the carbon positions, C_8 to C_{12}. In PGI_2 there is an attachment of oxygen between C_6 and C_9, thereby forming another ring. The remaining structure is composed of two side chains, R_1 (C_1 to C_5) which contains a double

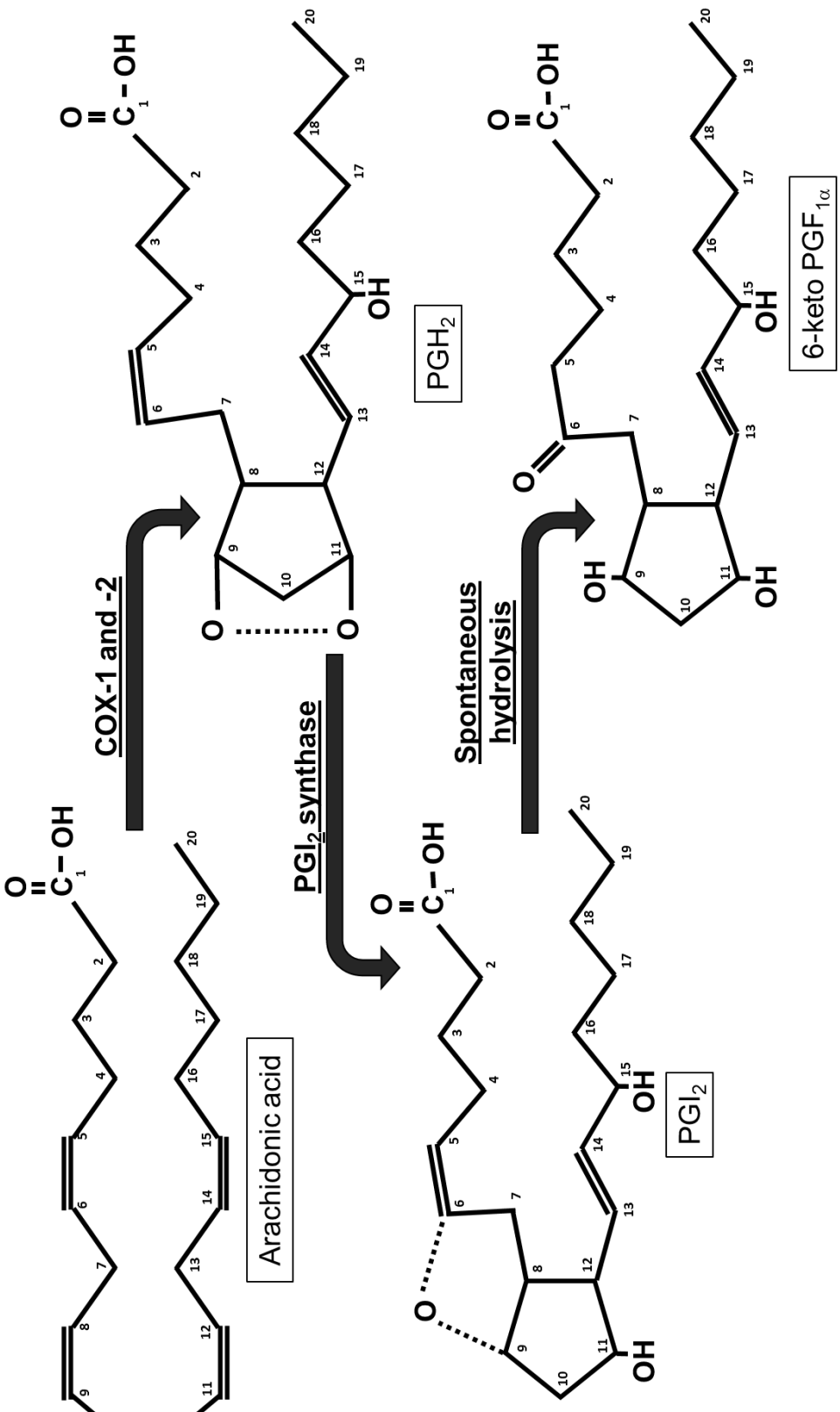

Figure 1. 5: Biochemical pathway to prostacyclin (PGI_2) formation. Arachidonic acid is the precursor to the formation of PGI_2. Arachidonic acid is converted to PGH_2 by the activity of the cyclo-oxygenase enzyme (COX-1 and COX-2). The PGH_2 is converted to PGI_2 by the enzyme PGI_2 synthase. The formed PGI_2 is spontaneously hydrolysed to 6-keto $PGF_{2\alpha}$.

bond at C_5, and R_2 (C_{13} to C_{20}) which contains a double bond at C_{13} (Whittaker et al., 1976).

PGI_2 is an unstable compound having a half-life of about 3 minutes (Wild, 2005). Due to its short half-life, once synthesised by the healthy vascular endothelium it can act in its local vicinity, by inhibiting platelet activation and acting as a vasodilator to the walls of the vasculature (Wild, 2005). It produces these effects by binding to its receptor and leading to downstream activation of adenylyl cyclase (Figure 1.6) (Bergmeier and Hynes, 2012). This activation leads to conversion of adenosine triphosphate (ATP) to cyclic adenosine monophosphate (cAMP) (Best et al., 1977). The cAMP further activates Protein Kinase A (PKA) causing the phosphorylation of its downstream substrates (Figure 1.6). The effect of the released PGI_2 is removed as it is spontaneously hydrolysed to its less active form of 6-keto-$PGF_{1\alpha}$ (Figure 1.5).

1.4.1.1 Adenylyl cyclase and Phosphodiesterase

The levels of cAMP in the cell are dependent on the enzyme activity of adenylyl cyclase (generation) and phosphodiesterase (degradation) (Figure 1.6) (Soderling and Beavo, 2000, Sunahara et al., 1996).

In mammals, 9 membrane bound isoforms of adenylyl cyclases (AC) have been identified (Hanoune and Defer, 2001). These enzymes convert ATP to cAMP. In platelets, AC isoform 3 (AC3), isoform 6 (AC6) and isoform 7 (AC7) have been identified (Dittrich et al., 2008, Katsel et al., 2003). They possess an intrinsic activity that could either be enhanced or reduced depending on the type of stimulus perceived by the platelets (Tasken and Aandahl, 2004). Structurally AC is composed of a small cytoplasmic domain at its N-terminal, two transmembrane domains and two large cytoplasmic domains. The large cytoplasmic domains are further divided into C1a and b and C2a and b (Tasken and Aandahl, 2004), providing sites for attachment of different proteins such as $G\alpha_s$, $G\alpha_i$, $\beta\gamma$-subunits and PKC (Sunahara et al., 1996). On binding to its receptor, PGI_2 releases $G\alpha_s$ that binds to the C2a unit of the AC cytoplasmic domain, leading to an increase in AC activity and thereby a rise in cAMP levels.

The phosphodiesterases (PDEs), on the other hand, are enzymes that degrade the cyclic nucleotides to their respective nucleosides monophosphate. It has been identified that platelets express PDE2A, PDE3A and PDE5A (Haslam et al., 1999). In platelets, the

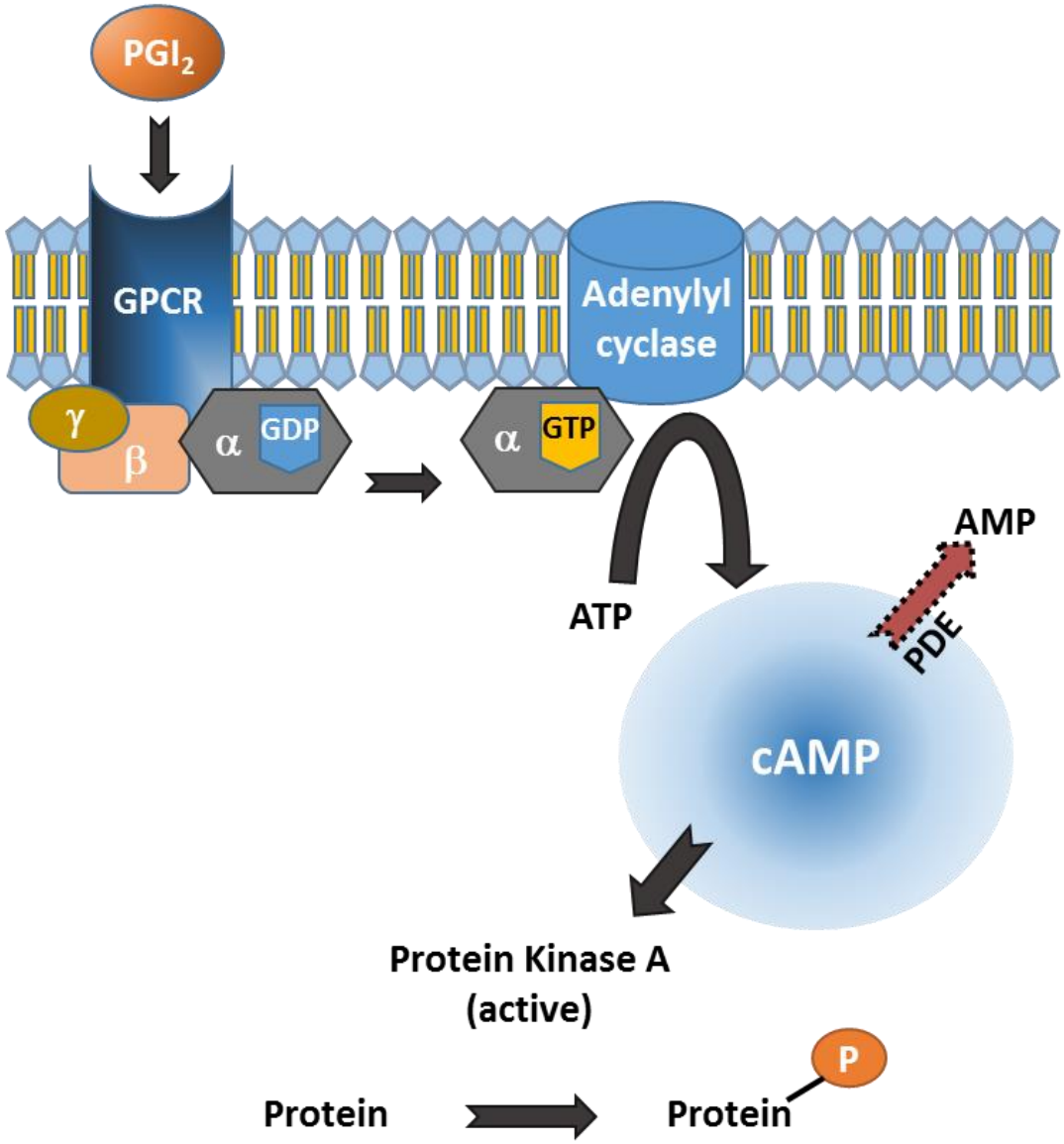

Figure 1. 6: Downstream signalling pathway to prostacyclin (PGI_2) stimulation. Platelets are exposed to PGI_2, which binds to its G-protein coupled receptor (GPCR) on the surface. The GPCR is bound intracellularly to the heterotrimeric G proteins (α, β, γ). On binding of PGI_2 the Gα subunit is relieved from the βγ subunit by replacing its GDP with GTP. The GTP bound form of Gα subunit binds to adenylyl cyclase, increasing its activation elevating the concentration of cAMP. An increase in the intracellular pool of cAMP activates Protein Kinase A (PKA). PKA mediates its downstream effects via phosphorylation of substrate proteins. The amount of cAMP is kept in check by the phosphodiesterase enzyme(s) that converts cAMP to adenosine monophosphate (AMP).

interplay between PDE2 and PDE3 regulate the levels of cAMP while PDE5 individually regulates cGMP levels. Upon encountering PGI_2, intracellular cAMP levels increase. Importantly however cAMP via PKA stimulation additionally increases PDE3 activity, hence providing a negative feedback control for its' levels (Macphee et al., 1988) allowing platelets exposed to PGI_2 in circulation to maintain low levels of intracellular cAMP (Sim et al., 2004). cGMP also can stimulate PDE2 and PDE5 activity by binding to a cyclic nucleotide binding domain (called GAF), while it inhibits PDE3 activity levels by competing for the cAMP binding domain at the catalytic site of the adenylyl cyclase (Dunkern and Hatzelmann, 2005, Feijge et al., 2004, Macphee et al., 1988).

On the other hand, Thrombin and ADP aide their activation of platelets, by inhibiting the levels of cAMP intracellularly. They act via $G\alpha_i$ and $G\alpha_q$ coupled receptors present on the platelet surface. Working downstream of $G\alpha_i$ the level of adenylyl cyclase activity is reduced which brings down the level of cAMP in the platelet. Similarly, acting via $G\alpha_q$, the levels of cAMP are controlled via phosphorylation of PDE3 that increases its activity.

1.4.1.2 Protein Kinase A (PKA)

PKA is a holoenzyme that is activated by an increase in the levels of cAMP in the platelets (figure 1.6). It is composed of two regulatory and two catalytic domains. On each regulatory domain there are two cAMP attachment sites. On binding of cAMP to these sites on the regulatory subunit, the catalytic domain becomes unbound and active.

The PKA enzyme forms a tetramer, from a combination of 2 regulatory subunits (RIα, RIβ, RIIα and RIIβ) and 2 catalytic subunits (Cα, Cβ and Cγ) (Skalhegg and Tasken, 2000, Tasken et al., 1997). Platelet have been identified to express all these subtypes of regulatory and catalytic domains (Burkhart et al., 2012, Pidoux and Tasken, 2010). This provides a large number of combinations in platelets that would have differing affinities of binding to cAMP and being activated.

On activation via cAMP, the PKA phosphorylates a multitude of downstream proteins that are involved with inhibition of platelet activation. It inhibits Phospholipase C activation which thereby reduces: 1) PKC activation, 2) Ca^{2+} mobilisation, 3) integrin expression, 4) myosin light chain phosphorylation, 5) actin polymerisation, 6) granule release and 7) the adhesion and aggregation of platelets via targeting the RapI protein (Siess and Lapetina,

1990), (Cavallini et al., 1996, Quinton and Dean, 1992), (Feinstein and Fraser, 1975), (Franke et al., 1997, Hoffmeister et al., 2008, Kawata et al., 1989).

1.4.2 Nitric Oxide

In addition to PGI_2 another important molecule that can inhibit platelets, nitric oxide (NO), is released by the vascular endothelium (Palmer et al., 1988). NO has a very short half-life of 6-30 seconds and so is continually synthesized from the endothelial cells (Palmer et al., 1988). The enzyme nitric oxide synthase (NOS) converts the aminoacid arginine to citrulline in the presence of oxygen and various cofactors to generate nitric oxide (Forstermann et al., 1991).

The release of NO in the circulation allows for it to freely diffuse across the plasma membrane and directly activate soluble guanylate cyclase (sGC). This activation leads to conversion of guanosine triphosphate (GTP) to cGMP. The cGMP activates Protein Kinase G (PKG) that affects the phosphorylation status of multiple cellular targets. There is an extensive list of the effects of these phosphorylation events of which a few include, inhibition of platelet activation (Moncada et al., 1991), action as a vasodilator by reducing the tone of the blood vasculature (Strijdom et al., 2009) and inhibition of leukocyte adhesion to the endothelium (Bath et al., 1991, De Caterina et al., 1995).

1.5 Platelets on activation (Thrombus formation):

The platelet responds to the denuding of the vascular basement membrane, and the exposure of collagen, vWF and other ECM proteins, and causes the formation of a thrombus. This process is highly regulated and undergoes a series of distinct steps.

1.5.1 Steps of thrombus formation

Blood is carried, throughout the body, in the vasculature which is lined internally by nonthrombogenic endothelial cells. They release PGI_2 and NO which keep the circulating platelets in the blood in a quiescent state. Due to their small size platelets are shifted to the periphery of the vessels in the circulating blood. This peripheral shifting is provided by the red blood cells and hence places the platelet in close vicinity both to the natural inhibitory chemicals, and to possible damage to the endothelial layer. Once the endothelial layer is damaged by trauma, ECM proteins are exposed, which are highly thrombogenic. Platelets which have multiple external receptors and various signalling pathways are highly sensitive to external stimuli and they act rapidly to the insult incurred, which results in its

haemostatic effect. The sequence of events after damage of endothelial layer in the vasculature, as shown in Figure 1.7, are detailed below:

1) Tethering: Under high shear rates such as that observed in arterial flow, platelets tether by binding to vWF, immobilized on collagen, via its receptor complex, GPIb-IX-V (Berndt, 2001). This transient association between vWF and GPIb-IX-V results in platelets rolling on the surface and provides time for GPVI to bind to collagen. Under low shear rate such as that observed in veins, GPVI binds to collagen directly and results in the activation of integrins.

2) Integrin activation and stable adhesion: The association between vWF and GPIb-IX-V allows time for the low affinity receptor GPVI to bind to collagen. This interaction results in the activation of integrin such as $\alpha_2\beta_1$ and $\alpha_{IIb}\beta_3$, which bind to collagen and vWF, respectively. These interactions provide stability for the platelet adhesion.

3) Spreading and Secretion: Following stable adhesion, massive reorganisation of the actin cytoskeleton of platelets occur which results in the formation of filopodia and lamellipodia. These structures increase the platelet surface area drastically and hence provide further stability to the adhesion of platelets to the matrix protein. Once the platelets are adhered and spread on the exposed ECM it causes them to release alpha and dense granules. Hence an increase in ADP, ATP, thrombin, serotonin, TXA_2 and fibrinogen along with other effectors in the vicinity of the platelets. These secondary mediators then allow for the activation of other platelets in the neighbourhood.

4) Aggregate formation: Activation of the platelets in the neighbourhood leads to the binding of fibrinogen and vWF to their activated integrin, $\alpha_{IIb}\beta_3$. This along with further activation by ADP and TXA_2 results in the formation of a platelet aggregate.

5) Clot retraction: Endothelial damage via generation of phospatidylserine (PS) and tenase complex (activated factors VIII and IX) recruitment results in the formation of prothrombinase complex (activated factors V and X). The prothrombinase

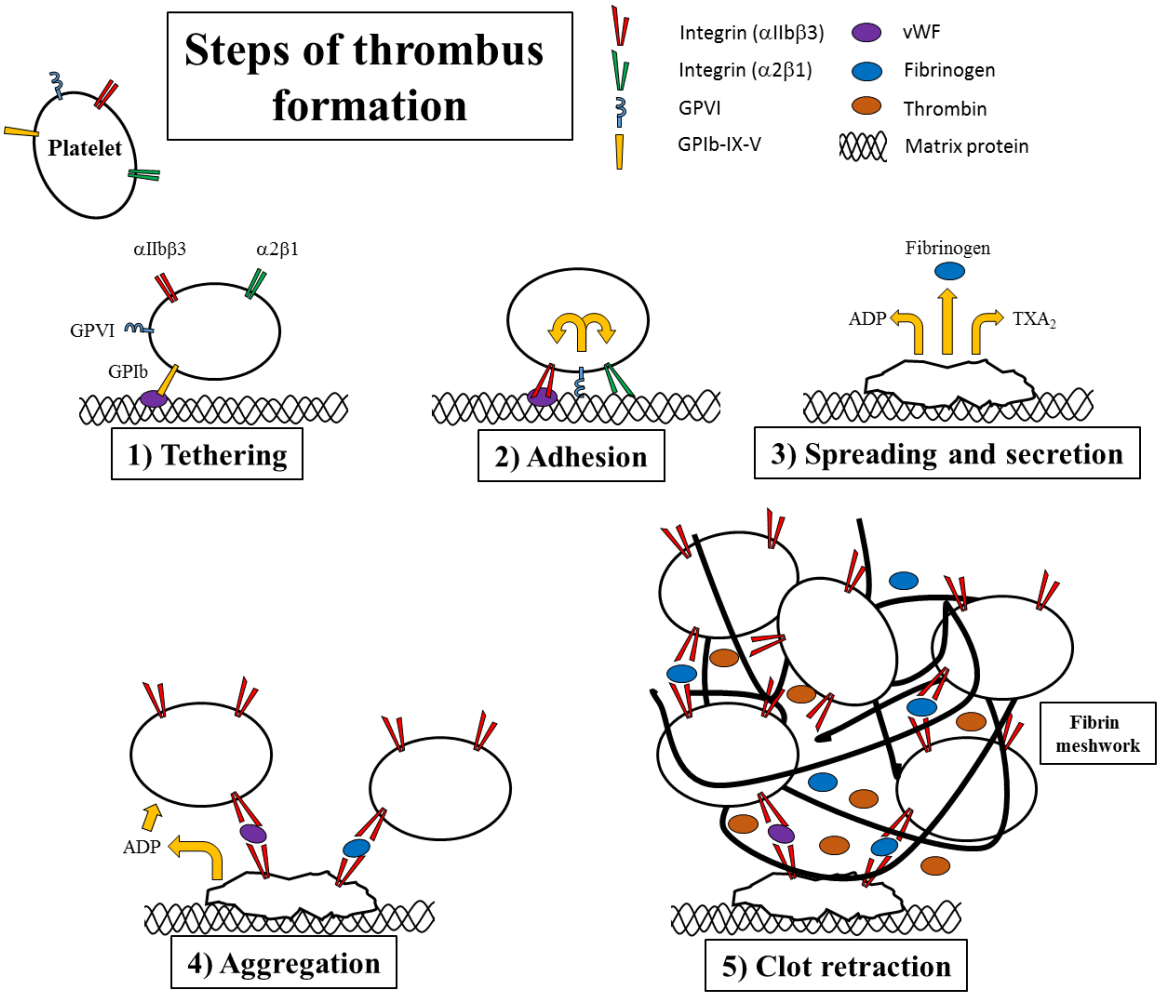

Figure 1. 7: Steps of thrombus formation. Formation of thrombus is a highly regulated process. On endothelial injury, the ECM proteins are exposed. The exposed ECM is bound by the circulating vWF. **1)** Attachment of vWF aids in the recruitment of platelets via GPIb-IX-V receptor. This enables the platelet to tether and roll on the site of injury. **2)** The tethering of platelets, slows their speed so as to provide chance to the GPVI receptor for interaction with collagen. On activation via GPVI the integrins are activated. **3)** Attachment via integrins provide stable adhesion that results in spreading of platelets and secretion (ADP, fibrinogen, TXA_2) to occur. **4)** Secretion is followed by formation of platelet aggregates, where platelets interact with each other via activated integrins. **5)** The conversion of prothrombin to thrombin leads to conversion of soluble fibrinogen to fibrin that forms a meshwork, which results in the retraction of the clot. Adapted from (Watson, 2009).

complex leads to the conversion of prothrombin to thrombin. The thrombin then further activates platelets, activates the coagulation cascade and cleaves the soluble fibrinogen into insoluble fibrin meshwork. The fibrin meshwork strengthens the thrombus and leads to retraction of the clot.

1.5.2 Recent insight to thrombus formation

Recent advances in the research conducted on thrombus formation has challenged the prior assumption of a thrombus to be a homogeneous clump of activated platelets that stems the loss of blood from the circulation. In late 1960s, electron microscopic images of platelets had hinted the differing levels of platelet activation in a thrombus (Stehbens and Biscoe, 1967). Publications from the group of Lawrence F. Brass based at The University of Pennsylvania have reaffirmed the variation in the level of platelet activity with reimaging a thrombus using a computational approach. They identified that the thrombus has distinct zones within its structure (Stalker et al., 2014, Tomaiuolo et al., 2014, Welsh et al., 2016, Welsh et al., 2014).

These zones have differing levels of platelet activity hence a heterogeneous pool of platelets are found within a thrombus. The inner zone of a thrombus is composed of compactly arranged platelets that form the core to the outer shell which is made up of loosely arranged platelets. The loose or compact arrangement of the platelets defines the porosity present in the different zones, with the inner zone being less porous in comparison to the outer zone. The porosity of the zone is mediated by the activity status of these platelets, which is directed by the presence of thrombin in the core and ADP and TXA_2 in the shell (Welsh et al., 2014). Thrombin formation occurs near the site of injury that leads to enhanced activation of platelets in its vicinity (Stalker et al., 2014). The enhanced platelet activation by thrombin enables them to spread better, to have a greater contact dependent signalling and therefore to decrease the porosity in this inner zone and restrict the molecular transport within the core. This traps the thrombin within the core that continues to activate the platelets, thus enabling secretion and release of ADP and TXA_2, identified by an increase in P-selectin (Stalker et al., 2014). The released mediators thereby modulate the activity in the shell of the thrombus. Interestingly the shell does not have an increased expression of P-selectin, signifying reduced activation, therefore loosely arranged platelets that leads to an increase in porosity and reduced contact dependent

signalling (Stalker et al., 2014). In between the outer and the inner zone is a transitional zone which overlaps the properties of the two zones (Stalker et al., 2014).

1.6 Platelet actin cytoskeleton

Actin is a highly conserved protein present in all eukaryotic cells. It constitutes 15-20% of the total proteins present in the platelet (Fox, 1993, Hartwig, 1999). It is made up of 374 aminoacid residues and has a molecular weight of 42kDa (Elzinga et al., 1973). In humans, three types of actin exist; α, β and γ. Of these only β and γ are found in the platelets (Pollard, 2001). The actin isoforms have a high level of sequence similarity that allows them to co-polymerise with each other, differing only in their rate of polymerisation (Khaitlina, 2001).

Within a platelet, actin exists in two forms, monomeric (globular: G-actin) and polymeric (filamentous: F-actin), and there is constant cycling between these two forms. Platelets maintain two pools of filamentous actin, one that is associated with the membrane skeleton while the other is maintained in the cytosol. Furthermore platelets also have a large pool of globular actin (Fox and Phillips, 1983, Hartwig and DeSisto, 1991).

Structurally actin is made up of two domains with an ATP/ADP binding site and a site for a divalent cation, both positioned in the cleft between the two domains (Kabsch et al., 1990). Binding of an ATP in the cleft of the G-actin monomer increases the rate of actin polymerisation while having an ADP decreases this rate. Each of these domains themselves consists of two subdomains; whilst a molecule of actin would comprise of 4 subdomains: labelled 1 – 4. Upon polymerisation of G-actin, the subdomains 3 and 4 are arranged closer to the axis of the F-actin thereby forming the inner, while subdomains 1 and 2 forms the outer region of the structure. On their transition from globular to filamentous form, the inner subdomains give a twist of 20^{o} on the outer subdomains, which provides a left-handed single-stranded helical structure for F-actin (Oda et al., 2009).

1.6.1 Actin polymerisation

Globular actin is polymerised to form filamentous actin. The process of actin polymerisation consists of an initial nucleation step, followed by elongation of the actin filament. In an inactivated platelet, the elongation reaches a treadmilling state (Mullins et al., 1998, Weber et al., 1992), where the rate of actin polymerisation is similar to the rate

of actin dissociation from the filament. Upon activation, the process of actin polymerisation continues to increase the length of the actin filament in a linear or a branched manner, while inhibiting the depolymerisation factors.

The initiation of actin polymerisation occurs by a *denovo* nucleation process in the presence or absence of nucleation factors (Figure 1.8). It is an energetically unfavourable option so it involves an initial lag phase during which oligomeric actin is formed (2-3 monomers of G-actin). The presence of nucleation promoting factors (NPFs), such as the Arp2/3 complex and the Wiskott Aldrich Syndrome Protein (WASp) family of proteins, facilitated the step of actin nucleation. The Arp2/3 complex is structurally composed of seven subunits (Bearer et al., 2002). The Arp2 and Arp3 structurally resemble actin and on combination they form a dimer similar to that formed by actin itself, thereby promoting attachment of other G-actin molecules, hence initiating actin polymerisation (Bearer et al., 2002). The Arp 2/3 complex is also involved with initiating the branching of actin filaments on already formed actin filaments (Svitkina and Borisy, 1999). The WASp family interacts with the Arp2/3 complex and lead to an increase in the polymerisation activity of Arp2/3 (Zalevsky et al., 2001). Therefore, Arp2/3 and WASp forms the core regulators for actin nucleation.

The actin oligomers formed, act as seeds on which a filament can undergo elongation. The actin filament has two ends; the fast growing barbed end and a slow growing pointed end (Korn et al., 1987). In the ATP bound form, the G-actin has a 10 fold increased affinity for the barbed end. This was confirmed by the use of cytochalasin, an actin filament stabiliser which inhibits recruitment of actin monomers to the barbed end (Fox and Phillips, 1981).

There are various strategies used by the cell to maintain or increase actin filament growth. It attains a level of filament treadmilling, whereby the rate of actin filament formation approximates the rate of dissociation. It may involve proteins that directly modulate the dissociation or polymerisation of actin filaments. It could also employ proteins that may cap the ends of the filament and thus limit the filament from growing. All these factors come into play when a cell is stimulated.

The proteins required to modulate the actin cytoskeleton includes a cytosolic actin sequestering protein, thymosin β4 (Tβ4) that inhibits actin assembly in platelets by binding

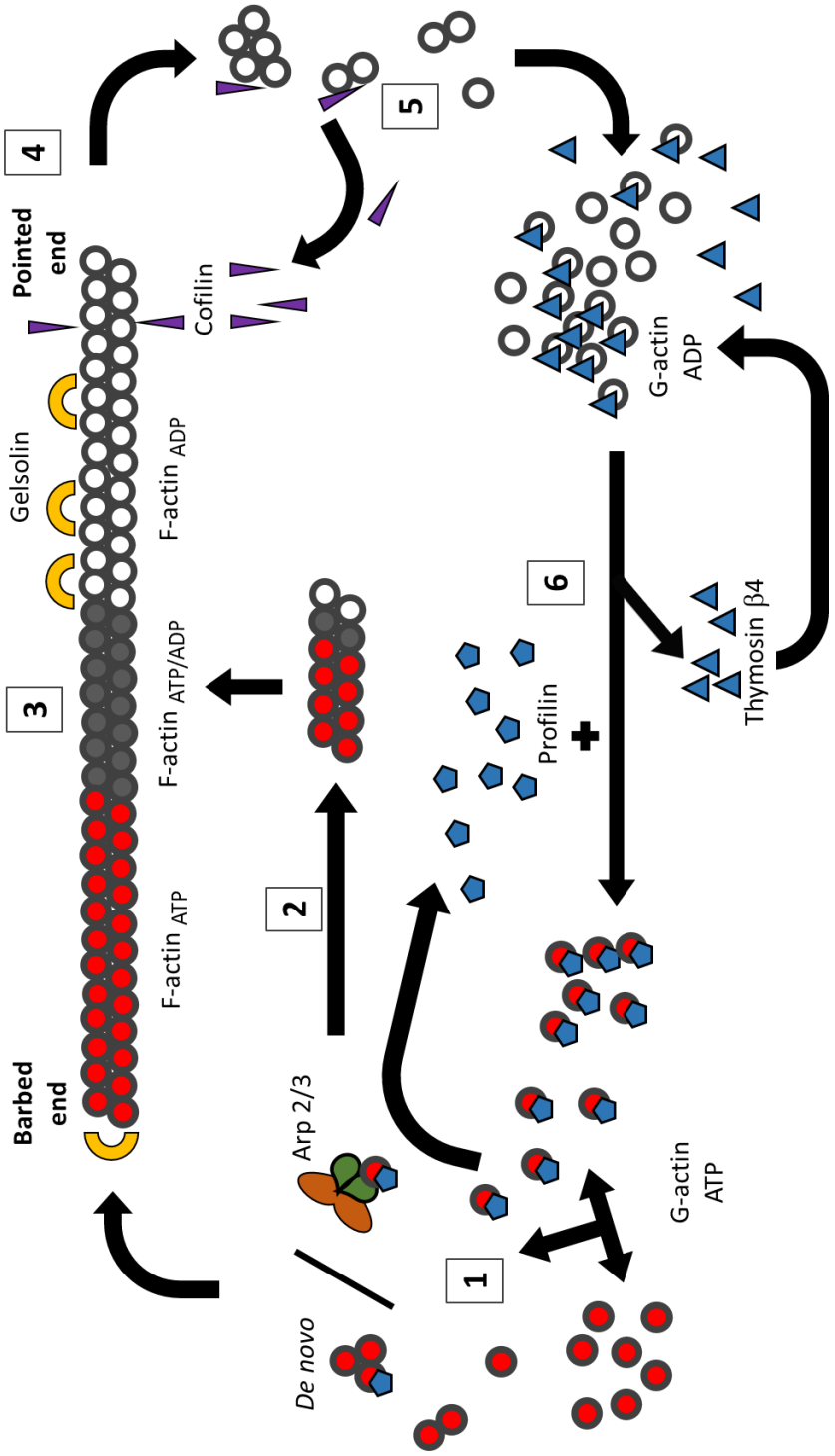

Figure 1. 8: Sequence of actin polymerisation and depolymerisation. 1) G-actin being bound to ATP, in the presence or absence of profilin, leads to nucleation. 2) The nucleation could either be de novo and/or Arp2/3 mediated and forms the seed for ATP-bound G-actin to bind and form an actin polymer. 3) Depending upon the stimulatory status of the cell, the actin continues to polymerise and form a filament. 4) The length of the filament is controlled by the hydrolysis of ATP on the F-actin. 5) This enables actin depolymerisation factors (such as Cofilin, Gelsolin) to bind to the filamentous actin and starts removing fragments of the F-actin. 6) These ADP bound F-actin filamenets depolymerise and return to the pool of ADP bound G-actin. The cycle continues when the GDP is replaced by ATP in the G-actin leading to the establishment of new actin filaments. Adapted from (Mullins et al., 1998)

to 60-65% of G-actin and not allowing for them to nucleate (Goldschmidt-Clermont et al., 1992, Pantaloni and Carlier, 1993). Upon stimulation of platelets profilin displaces Tβ4 and helps to exchange the ADP on actin monomers with ATP and therefore makes the actin monomers available for polymerisation.

Although actin polymerisation is key to the spreading response in platelets, actin depolymerisation and actin filament capping also play an important role. Actin depolymerisation will occur when the concentration of G-actin decreases and new monomers need to be made available in order to continue to make further actin filaments. Capping of filaments occurs so that these filaments are no longer extended as the cell wishes to respond in a different manner to its environment. There are a number of proteins which help to sever or cap actin filaments, thereby reducing the length of actin filament or hinder their elongation, respectively. These include cofilin, gelsolin, CapZ, gCAP39, tropomodulin severin and villin. These proteins have overlapping functions of severing and/or capping at either the pointed (-) or the barbed (+) end of actin filament (Table 1.1).

Cofilin is an actin depolymerizing factor (Davidson and Haslam, 1994). It binds to the ADP bound-actin at the pointed end of the filament and cleaves off the monomer (Carlier et al., 1997). The actin monomer is recycled by the nuclear exchange of ADP to ATP by profilin. This ATP-attached actin may then be incorporated to the barbed end of the growing filament.

Gelsolin and similar severing and capping proteins (shown in Table 1.1) such as CapZ, Severin, Villin, gCAP39 and tropomodulin either bind the barbed or the pointed end of the actin filament to limit the elongation of the filament (Barkalow et al., 1996), or promote breaking of the actin filament. Activation of platelets promotes gelsolin's activity that reduces already formed filamentous actin by severing the actin and increasing the pointed ends of these filaments and thereby facilitates formation of new filaments which are required by the cell to generate its response (Yin et al., 1981).

1.7 Mechanism of platelet actin cytoskeletal rearrangement

The actin cytoskeleton is key to the function of the platelet, with the ability to spread and form strong adhesions to the ECM critical to the thrombus formation process. The process of platelet spreading, and therefore the reorganisation of the actin cytoskeleton is well defined, with first the formation of filopodia - finger like projections that is followed by

.

Actin Binding Protein(s)	Function(s)
Arp2/3	- Actin cross-linking proteins
CapZ	- Filament-depolymerisation protein - F-actin end-binding protein at barbed-end (+)
Cofilin	- Filament-depolymerisation protein
DNase I	- Monomer-binding protein sequester G-actin - Prevents actin polymerisation
gCAP39	- F-actin end-binding protein at barbed-end (+)
Gelsolin	- Filament severing protein, - F-actin end-binding protein at barbed-end (+)
Severin	- Filament severing protein, - F-actin end-binding protein
Thymosin β4	- Monomer-binding protein sequester G-actin - Prevents actin polymerisation
Tropomodulin	- F-actin end-binding protein at pointed-end (-)
Tropomyosin	- Stabilising actin filament and preventdepolymerisation
Villin	- Filament severing protein, - F-actin end-binding protein - Helps in actin filament crosslinking

Table 1. 1: Proteins involved in binding to actin. These proteins bind to actin and control the effective length of the actin filament. The (+) refers to the binding preference for barbed end and (-) refers to the binding preference for pointed end of the actin filaments. Adapted from (Lodish et al., 2000, dos Remedios et al., 2003)

lamellipodia - a crosslinked actin rich structure which fills in the gaps between these filopodia. During lamellipod formation the actin cytoskeleton starts to rearrange into stress fibres, which act as both a brake on the extent of the lamellipodial extension and maintains the shape of the platelet (Zucker and Nachmias, 1985). Disruption of both lamellipodia and stress fibre formation can cause embolisation of thrombus formation, due to an inability of the thrombus to withstand high shear (Calaminus et al., 2007, Owen et al., 2005).

These structures are tightly regulated by signalling pathways which are influenced by the stimuli received by the cell from its environment. This is coordinated by the Rho family of small GTPases (Chang et al., 2005b).

1.7a Rho GTPases:

Ras homologus (Rho) GTPases constitute a sub-group of the Ras proto-oncogene family (Barbacid, 1987, Shields et al., 2000). Signalling through these proteins helps in mediating downstream effects in the cell. They cycle between binding either to a GTP or GDP, depending upon their level of activity. Once GTP-bound the RhoGTPase becomes active. Upon hydrolysis the GTP converts to GDP and leads the conformation to an inactive form. Conversion of the GDP/GTP-bound forms is tightly regulated by the presence of Rho Guanine Exchange Factor (GEF), Rho GTPase Activating Protein (GAP) and Rho Guanine Dissociation Inhibitor (GDI). The GEF is involved in the conversion of GDP-bound form to a GTP-bound form, while GAP activates the intrinsic GTPase activity of Rho protein and hydrolyses GTP to GDP (Moon and Zheng, 2003, Schmidt and Hall, 2002). The GDI hinders the dissociation of GDP from the Rho proteins in resting platelets, thereby blocking the conversion of the GDP-bound form to its GTP counterpart. Upon platelet stimulation this interaction with GDI dissociates and hence the Rho GTPases become available to modulate downstream effects (Olofsson, 1999, Sasaki and Takai, 1998).

The Rho GTPases comprises of 20 Rho family members that could be categorised into 8 subgroups, depending on their domain alignment into classical Rho GTPases (Rho, Rac, Cdc42 and Rif) and atypical Rho GTPases (Rnd, RhoUV, RhoH and RhoBTB) (Table 1.2) (Aspenstrom et al., 2004, Azzarelli et al., 2014, Heasman and Ridley, 2008, Infante and Ridley, 2013, Villalonga and Ridley, 2013). The members of classical Rho GTPases, RhoA, Rac1 and Cdc42, have been extensively researched in platelets and other cell types (Aslan and McCarty, 2013, Azzarelli et al., 2014, Heasman and Ridley, 2008, Infante and Ridley, 2013, Villalonga and Ridley, 2013). Many actin structures have been associated

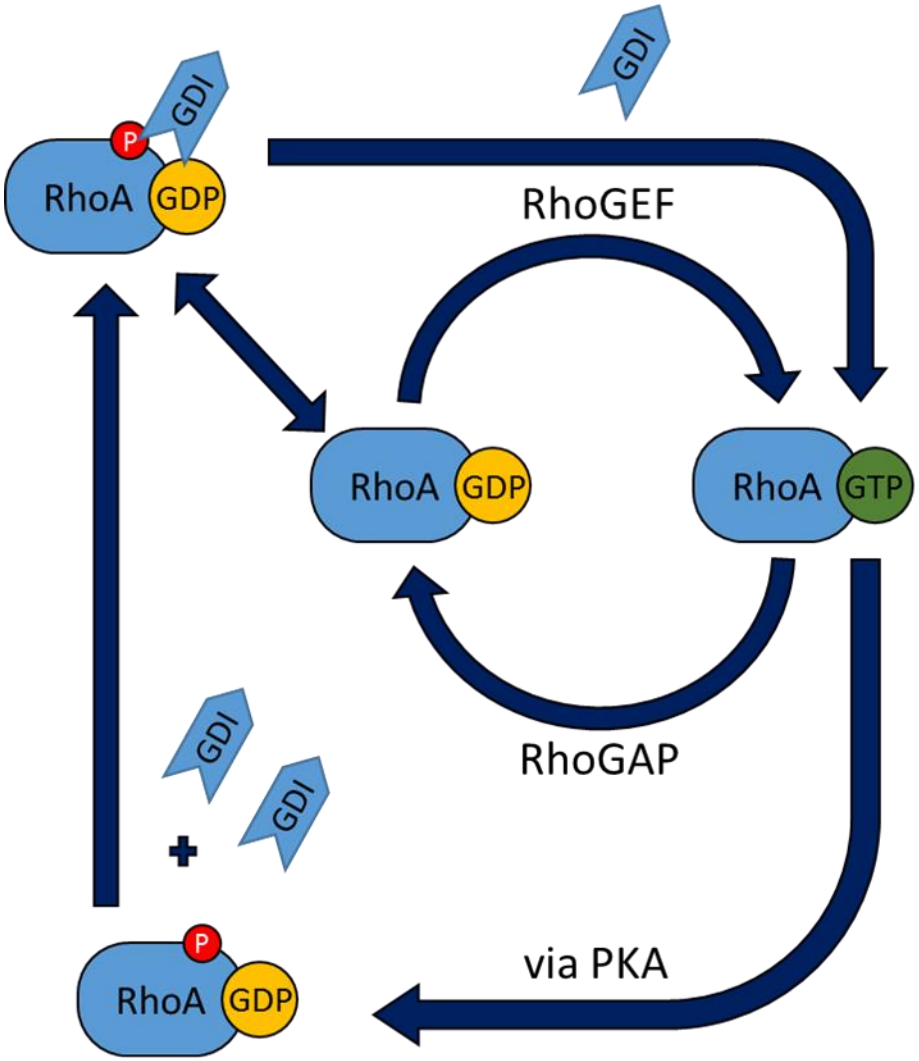

Figure 1. 9: RhoA activity level is mediated in a cyclic manner within a cell. RhoA cycles between its GDP and its GTP bound form via activity of the RhoGEF and RhoGAP. The RhoGEF converts Rho from its GDP to its GTP bound form. RhoA converts back from its GTP bound form to its GDP bound form. On exposure to an increase in cAMP via PKA, RhoA is phosphorylated which tags it to be bound to GDI. On attachment of GDI, RhoA is hindered to convert from its GDP bound form to GTP bound form of RhoA.

	Rho subfamilies	Rho members	% Similarity	Comments
Classical Rho GTPases	**Rho**	RhoA		-Involved in actomyosin contractility -Helps forming stress fibres and focal adhesions
		RhoB	84%	
		RhoC	92%	
	Rac	Rac1		-Induces formation of lamellipodia -Helps in focal adhesion turnover
		Rac2	92%	
		Rac3	93%	
		RhoG	72%	
	Cdc42	Cdc42		-Induces formation of filopodia and thick actin bundles -Involved in vesicle trafficking
		TC10 (RhoQ)	62%	
		TCL (RhoJ)	55%	
	Rif	Rif (RhoF)		-Very long and flexible filopodia, greater actin filament assembly and intracellular trafficking of endosomes
		RhoD	50%	
Atypical Rho GTPases	**Rnd**	Rnd1		-GTP-bound in the wild type state. -Formed dorsal microvilli, suggesting reorganisation of stress fibres to dorsal protrusions. -It also contain ezrin
		Rnd2	51%	
		Rnd3 (RhoE)	58%	
	RhoUV	RhoU (Wrch1, Chp2)		-Possess high intrinsic GDP/GTP exchange rate. -Possible involvement with filopodia and lamellipodia formation due to structural similarity with Cdc42 and Rac.
		RhoV (Wrch2, Chp)	54%	
	RhoH	RhoH (TTF)		-Inhibits Rac1 signaling
	RhoBTB	RhoBTB1		-Involved with vesicular structures in the cytoplasm -Aids transcriptional regulation
		RhoBTB2	66%	

Table 1. 2: List of RhoGTPases. The list of Rho GTPase family that has been categorised into groups and subgroups. Adapted from (Aspenstrom et al., 2004, Aslan and McCarty, 2013, Azzarelli et al., 2014, Heasman and Ridley, 2008, Infante and Ridley, 2013, Villalonga and Ridley, 2013)

with specific RhoGTPases; Cdc42 is thought to be involved in filopod formation, Rac is involved in lamellipod formation and RhoA in the formation of stress fibre (Calaminus et al., 2008, Aslan and McCarty, 2013).

For these actin cytoskeletal changes to take effect the Rho effectors need to be activated. Normally these effectors have their binding site blocked by the presence of the structural looping of the protein onto itself thereby providing a Rho GTPase autoinhibitory mechanism. Upon platelet activation, disruption of the intramolecular autoinhibitory interaction occurs which releases the binding sites for RhoGTPases resulting in their downstream effects.

1.7.1 Cdc42 and filopodia

Filopodia are slender projections of the cell membrane. They are used by the cell for sensing the surrounding extracellular matrix and identifying the presence of adhesion receptors to bind them (Wood and Martin, 2002). They are filled with actin filaments that extend the length of the structure with the barbed end directed towards the protrusion (Figure 1.10) (Small, 1988).

The formation of filopod is regulated by the small RhoGTPase, Cdc42 (Nobes and Hall, 1995). Cdc42 (cell division cycle 42) was discovered in the yeast while mediating its budding and managing their polarity. On stimulation, as shown in figure 1.9, the platelet GTP-bound form of Cdc42 binds to the GTP-binding domain (CRIB domain – Cdc42/Rac Interactive Binding) of the WASP protein. The WASP protein folds on itself, causing an autoinhibited state in which the CRIB domain is bound to the VCA domain (Actin and Arp2/3 binding region). In the presence of PIP_2, the interaction of Cdc42 with WASP protein is followed by interaction with the Apr2/3 complex that leads to actin recruitment and its polymerisation. Filopod form the finger-like projections via tight bundling of the actin filaments that are formed parallel to each other. This is achieved by the presence of regulatory protein, the formins (i.e. mDia2) (Schirenbeck et al., 2005, Yang et al., 2007). The formin associate with the growing end of the actin filament by encircling it and continues to recruit actin monomers while inhibiting the binding of the capping proteins, thereby a rapid and non-branched growth of the actin filament occurs (Figure 1.10).

Cdc42 has been regarded as a regulator of filopodia formation, secretion and exocytosis in various cell types (Hong-Geller and Cerione, 2000, Kozma et al., 1995, Nobes and Hall, 1995, Zhang et al., 2001). It is highly expressed in platelets (Burkhart et al., 2012). As with

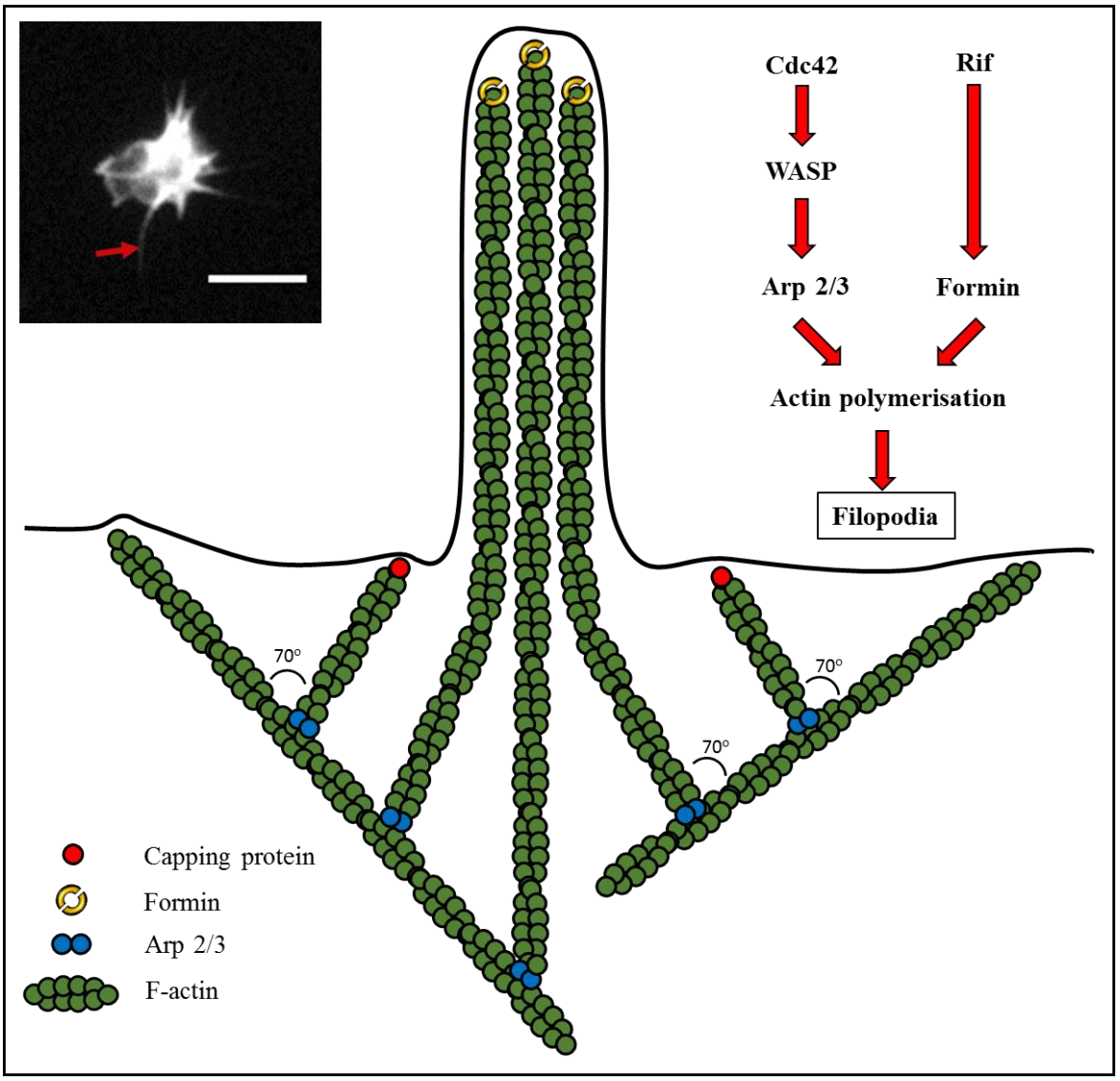

Figure 1. 10: Structure of filopod. A filopod is a slender finger-like projection form the platelet. The schematic shows a graphical appearance of filopod along with the signalling involved for its' formation. The insert on the upper left shows the filopod (identified by a red arrow) in a platelet. Scale bar is 5μm. Adapted from (Mellor, 2010).

other cell types it was presumed that its activation should result in platelet filopodia formation. With the current level of understanding, discrepancy exists as different studies identifying the role of Cdc42 in platelets have differing outcomes. A study on platelets using secramine, a Rho GTPase inhibitor which has been considered specific for Cdc42, identified the importance of Cdc42, as its absence by binding to the inhibitor rendered it unavailable for the formation of filopodia in the cell (Chang et al., 2005a, Pelish et al., 2006, Pula and Poole, 2008).

In agreement with this platelets from a Cdc42 knockout mouse model, with the gene targeted at the level of haematopoietic cells resulted in an impaired filopodia formation, reduced spreading, secretion and aggregation (Akbar et al., 2011). However gene deletion of Cdc42 in a megakaryocyte-platelets specific manner (Pleines et al., 2010), identified no change in filopodia formation in these platelets on fibrinogen but it hampered its formation on vWF (Pleines et al., 2010). This brought an insight that mechanisms independent of Cdc42 may exist for the formation of filopodia in platelets and secondly the formation of filopodia by Cdc42 could be GPIb linked (platelet receptor for vWF).

There are other Rho GTPases which mechanistically result in the filopodia formation, acting independent of the Cdc42 (Pellegrin and Mellor, 2005). The list includes Rif (Rho in filopodia), TC10, RhoT and Wrch-1 (a Cdc42-like protein) (Abe et al., 2003, Ellis and Mellor, 2000, Murphy et al., 1999, Ruusala and Aspenstrom, 2008). In an overexpression system, Rif has been identified to interact with formin and causes formation of longer filopod (Figure 1.10) (Ellis and Mellor, 2000). Although Rif has been found to form filopodia in other cell types; in platelets, it is dispensable (Goggs et al., 2013).

1.7.2 Rac and Lamellipodia

Lamellipod is a thin sheet-like structure formed in a cell. Initially on Swiss 3T3 fibroblasts, it was found that Rac caused polymerisation of actin and led to the formation of lamellipodia and membrane ruffles (Ridley et al., 1992). Upon stimulation, it starts to fill the gaps that are formed between the filopodia; via extension of the cytoplasmic front of the cell. This extension of the cytoplasmic front is composed of highly branched actin filaments (Svitkina and Borisy, 1999). This branching occurs in the presence of the Arp2/3 complex and forms a complex meshwork of actin filaments (Figure 1.11) (Nobes and Hall, 1995, Ridley, 1995). The Arp 2/3 complex nucleates actin polymerisation and binds to an already formed actin filament at an angle of 70^{o} (Svitkina and Borisy, 1999).

In platelets the formation of lamellipod is regulated by the small GTPase, Rac (Figure 1.11) (Ridley, 1995). On stimulation Rac1 binds to the WAVE complex (Figure 1.11) (Yamazaki et al., 2003). The WAVE complex is in a closed state, which on binding to PIP_3 and Rac-GTP opens its confirmation, enabling the VCA region to be exposed (Takenawa, 2010). The Arp2/3 complex binds to the VCA domain and initiates actin polymerisation (Figure 1.11). Absence of formin (mDia2), allows the branching of the actin filaments via the Arp2/3 complex on already formed actin filaments. Actin depolymerising agents, gelsolin or cofilin, play their part by cleaving-off actin oligomers from the filamentous actin. These oligomers are then incorporated to the expanding actin filaments either to increase its length or to enable branching to take place (Aslan et al., 2013, Falet et al., 2002).

Three isoforms for Rac exists - Rac1, Rac2 and Rac3. Using a serial analysis gene expression (SAGE) system, Rac3 was confirmed to be absent in platelets. The remaining Rac isoforms, Rac1 and Rac2, were identified to be present in the platelet, of which trace amounts of Rac2 was recognised (Burkhart et al., 2012, McCarty et al., 2005). Using murine platelets of Rac1/Rac2 double knockout its role in the platelets lamellipodial formation was confirmed (McCarty et al., 2005). Therefore, Rac1 is the most important isoform of Rac present in platelets that helps in the formation of lamellipod and is also known to maintain stability of a thrombus (McCarty et al., 2005).

1.7.3 Actin nodules

At present it is not clear which, or if any Rho GTPases is responsible for actin nodule formation. An actin nodule is a punctate area of actin which are present in the early stages of platelet spreading. These are highly dynamic structures and have been proposed to be the precursor to lamellipod and stress fibre formation in the platelet (Calaminus et al., 2008). As the platelet spreading proceeds into attaining a fully spread form, they disappear and stress fibres are formed (Calaminus et al., 2008, Kasirer-Friede et al., 2010). These nodules are filamentous actin structures as they had been stained by phalloidin (Calaminus et al., 2008), which has a high and irreversible binding affinity for filamentous actin (Faulstich et al., 1977). Since their first identification by Calaminus et al in 2008, their role is still unclear and further work needs to be completed to understand their true function.

However, actin nodules have been found to be co-localised with proteins that regulate the actin cytoskeletal structures. The list includes the Arp2/3 complex, Rac, β-integrins (β1

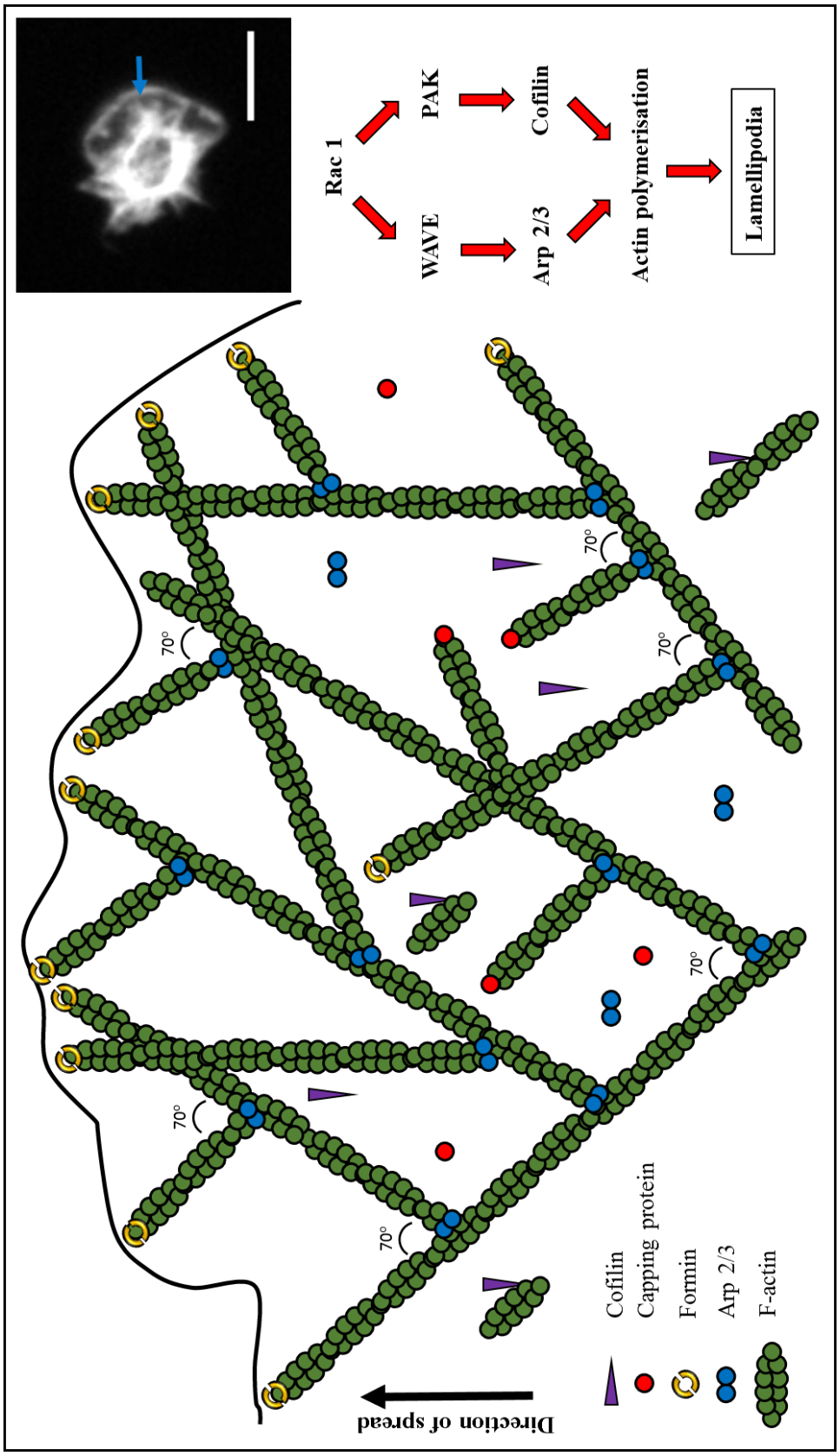

Figure 1. 11: Structure of lamellipod. A lamellipod is an extension of the cytoplasmic front which has been shown in the schematic as a graphical presence at the leading edge of a platelet. The Rac1 signalling involved in the formation of lamellipodia is also shown. The insert on the upper right shows the lamellipod (identified by a blue arrow) in a platelet. Scale is 5µm. Adapted from (Lai et al., 2008).

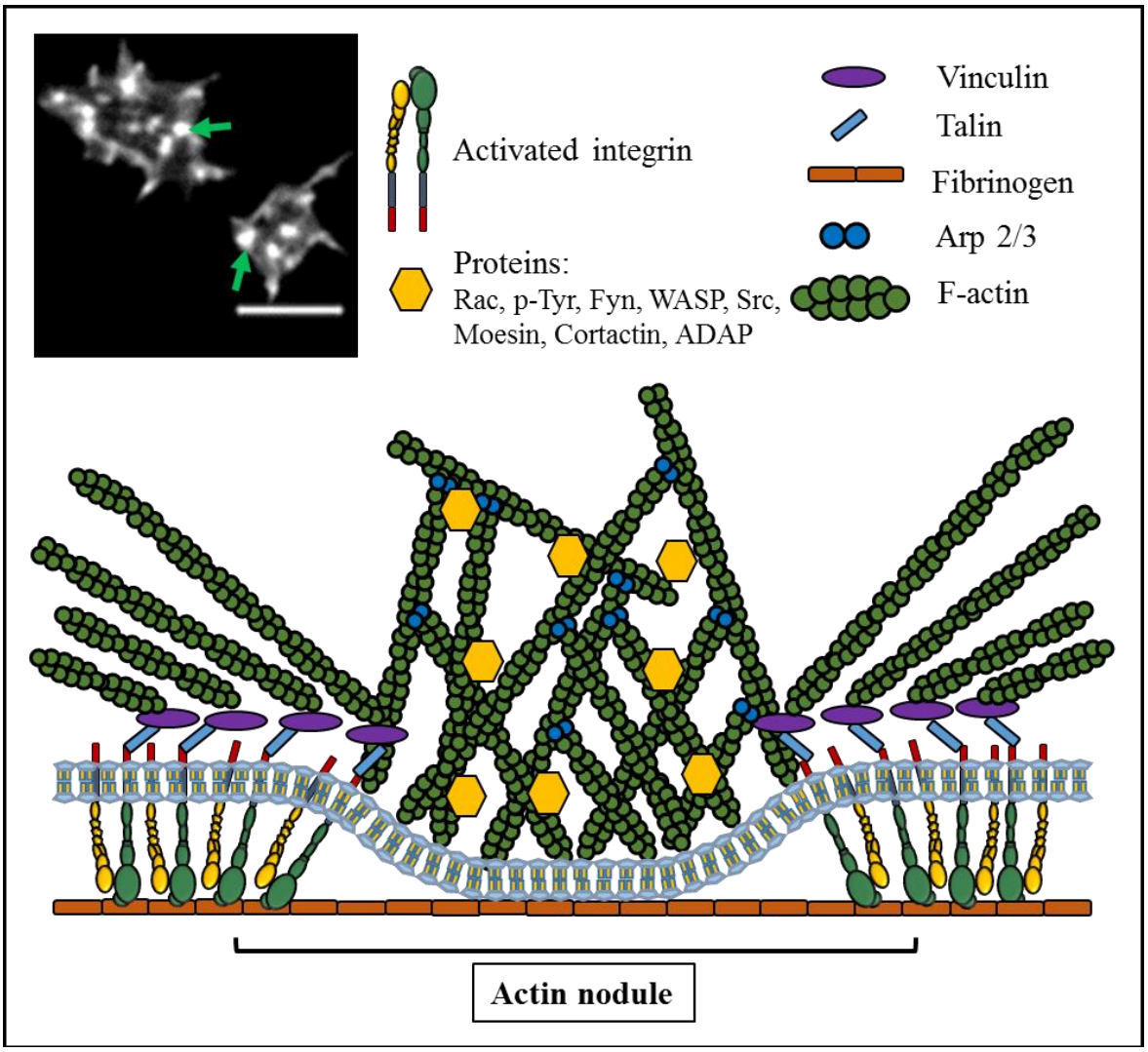

Figure 1. 12: Structure of actin nodule. An actin nodule is a filamentous actin structure which has been identified in the early stages of platelet spreading. The schematic shows a graphical representation of the identified structures that are present at actin nodules. The insert on the upper left shows the punctate presence of actin nodules (identified by green arrows) in a platelet. Scale bar is 5μm. Adapted from (Poulter et al., 2015).

and β3 subunits), Fyn, moesin, cortactin, talin, vinculin, p-Tyr, WASp (Figure 1.11) (Calaminus et al., 2008, Kasirer-Friede et al., 2010, Poulter et al., 2015). Another protein that has been found to co-localise with actin nodules is an Adhesion-and Degranulation-promoting Adapter Protein (ADAP) (Kasirer-Friede et al., 2010). In the absence of ADAP, it was identified by Kasirer-Friede, that vinculin does not localise to the formed actin nodules (Kasirer-Friede et al., 2010). Another finding by Calaminus et al. (2008) has been the absence of Src co-localisation with actin nodules (Calaminus et al., 2008), but under flow conditions, Kasirer-Friede et al identified activated Src co-localisation with these nodules (Kasirer-Friede et al., 2010). These findings provided the notion that not all proteins co-localising with the nodule are required for its formation but rather it may actually be serving as a hub for various activities such as signalling and providing anchorage to platelets under shear (Calaminus et al., 2008, Kasirer-Friede et al., 2010, Poulter et al., 2015).

1.7.4 RhoA and Stress fibres

RhoA proteins comprise of three isoforms, RhoA, RhoB and RhoC. These isoforms have an 85% amino acid similarity with each other, while diverging at the C-terminus (Wheeler and Ridley, 2004). Although highly homologous, RhoA are generated from individual genes present on separate chromosomes (Cannizzaro et al., 1990). RhoA isoforms have differences in their expression profiles. These proteins have a small fraction localised in the plasma membrane with RhoA and RhoC mainly identified in the cytoplasm, while RhoB has been identified with endosomes and lysosomes (Adamson et al., 1992).

Differences in the C-termini of the RhoA proteins and minor changes in their ligand binding region points us the possibility of these isoforms to have their own specificities, such as attaching to different effectors and even having different temporal and spatial arrangements within the cell. Differential preference for binding to effecter proteins brings up the individuality possessed by these isoforms. RhoA has been found to regulate actomyosin contractility; RhoB regulates cytokine trafficking and cell survival while RhoC has been implicated in cell motility (Wheeler and Ridley, 2004).

Stress fibres are contractile structures that are formed in non-muscle cells (Buckley and Porter, 1967, Isenberg et al., 1976). As shown in the figure 1.13, they are composed of actin, actin binding proteins and myosin (Naumanen et al., 2008). Stress fibres have a complex and lengthened structure having actin bundles with 10 to 30 actin filaments

(Cramer et al., 1997). The actin filaments are arranged parallel and crosslinked by actin binding proteins, such as α-actinin, to provide structural integrity to their arrangement (Lazarides and Burridge, 1975). A filamentous form of myosin is incorporated with the actin filaments (Langanger et al., 1986), thus providing the contractile element for the formed stress fibres.

These actin bundles, stress fibres, cross the body of the cell and attach to the cell membrane at focal adhesions, which are site of communication between the intracellular actin cytoskeleton and the ECM (Figure 1.13) (Geiger et al., 2009, Parsons et al., 2010, Pellegrin and Mellor, 2007). The maturity of the stress fibres is dependent on the presence of mechanical stress experienced by the cell and myosin IIa mediated contractility (Bershadsky et al., 2006, Smith et al., 2010). Thus, their presence provides stability and structural integrity to the cell (Pellegrin and Mellor, 2007, Naumanen et al., 2008). As with other cell types, platelets also possess these similar characteristics of stress fibres (Langanger et al., 1986).

RhoA directs the formation of stress fibres. RhoA has been the most studied of the Rho isoforms. Structurally RhoA has an effector domain, 4 GTP/GDP binding regions which are present individually through the whole protein, a hypervariable region and a CAAX box motif at the C-terminal (Lartey and Lopez Bernal, 2009). The effector domain modulates the guanosine phosphate domain binding for the GTP or GDP. The hypervariable region provides diversity to the protein and may have sites for membrane association of the protein. The CAAX box motif dictates post-translational modifications, where ‘C’ is the Cysteine, ‘A’ are aliphatic residues and ‘X’ determines the type of prenylation (Lartey and Lopez Bernal, 2009).

Effectors of RhoA for the formation of stress fibres include Rho-associated coiled-coil kinase (ROCK) and mDiaphanous 1 (Figure 1.13) (Leung et al., 1996, Watanabe et al., 1997). ROCK activates LIM kinase which inhibits cofilin-induced depolymerisation of actin filament (Maekawa et al., 1999), while mDia1 enables polymerization of actin filaments into long parallel bundles (Hotulainen and Lappalainen, 2006, Tominaga et al., 2000). The formed stress fibres on contraction lead to an attainment of mature focal adhesions owing to an increase in mechanical stress in the cell (Colombelli et al., 2009).

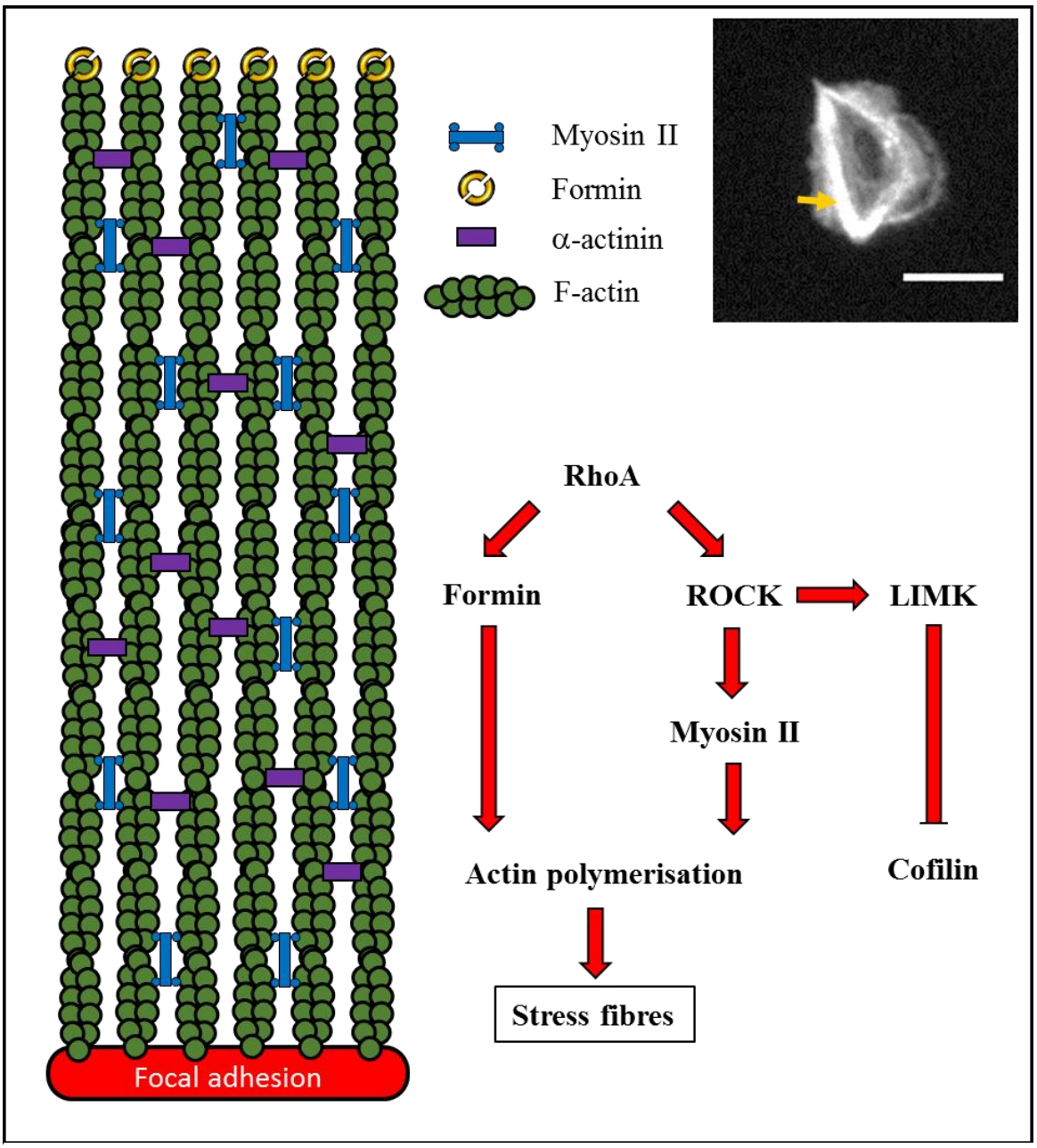

Figure 1. 13: Structure of stress fibre. A stress fibre is a filamentous actin structure which is present in a fully spread platelet. The schematic shows a graphical representation of the stress fibre along with the signalling involved for its formation. The insert on the upper right shows the cord like structure of stress fibres (identified by yellow arrow) in a platelet. Scale bar is 5μm. Adapted from (Pellegrin and Mellor, 2007).

The stress fibres with its contractions are linked downstream to an increase in phosphorylation of the myosin light chain (MLC) (Somlyo and Somlyo, 2000). Increases in the level of phosphorylated MLC leads to Myosin II activation, and hence the formation of stress fibres. Phosphorylation of MLC has been identified to be controlled by two distinct mechanisms, a Rho-dependent pathway and a Ca^{2+}/Calmodulin-dependent pathway (Amano et al., 1996, Katoh et al., 2001). The Ca^{2+}/Calmodulin-dependent pathway, phosphorylates MLC by activating the myosin light chain kinase (MLCK), while the RhoA-ROCK pathway, inhibits the myosin light chain phosphatase (MLCP) (which would have converted phosphorylated MLC to its non-phosphorylated form) and also directly phosphorylates MLC (Amano et al., 1996, Kimura et al., 1996, Totsukawa et al., 2000). Dephosphorylation of MLC is regulated by the disinhibition of MLCP activity.

Inactivation of RhoA prevents the activation of ROCK, increases MLCP activity and therefore decreases myosin light chain phosphorylation and myosin II activation. This causes a reduction in stress fibre formation, and also can cause stress fibre dissolution.

One signalling pathway which has been implicated in the control of the activation status of RhoA is the PKA signalling pathway (Qiao et al., 2003). RhoA is a substrate for phosphorylation by PKA. If RhoA is phosphorylated by PKA it interacts with Guanine-nucleotide Dissociation Inhibitor (GDI) and becomes unavailable to be bound to ROCK reducing the activity of RhoA (Aburima et al., 2013).

1.8 Aims of this study:

PGI_2 and NO, are derived from vascular endothelium and have been known to inhibit platelets from being activated. PGI_2 is more potent at inhibiting platelets (Ehrman and Jaffe, 1980), and has been found at suboptimal concentration in the circulation (FitzGerald et al., 1981). Platelet inhibition by PGI_2 and NO allows a smooth flow of blood, without the formation of unwanted thrombi in circulation. The inhibition is overcome by the activatory stimulus perceived by the platelets from the microenvironment of the vascular lesion. On activation, platelets change their shape and attain a spread profile by reorganising their actin cytoskeleton.

The changes in actin cytoskeleton provide a means to monitor the level of platelet activation. From having a discoid presence in non-activated state in the circulation they form filopodia, lamellipodia, actin nodules and on completion of their spreading they attain stress fibres. Activated platelets forming a thrombus along with the damaged endothelium tend to generate thrombin which is known to increase PGI_2 production by the endothelium. The release of PGI_2 in the vicinity of the thrombus had not been investigated before for the effects it could generate on the thrombus itself.

My study was designed to understand if platelet activation within thrombi could be reversed by the presence of PGI_2. To conduct this research following aims were recognised:

1) Identify the effect of PGI_2 on spreading of platelets, monitoring via changes to the actin cytoskeleton.
2) Determine the signalling dynamics of the changes observed in spread platelets upon treatment with PGI_2.
3) Identify the significance of the changes observed in the actin dynamics on treatment of thrombi with PGI_2, under flow.

The impact of the outcomes of this research could have far reaching benefits, whether it be for mere understanding the concept of the effect of PGI_2 on thrombus formation or helping to formulate new therapies and develop newer strategies to target thrombosis.

CHAPTER 2:

Materials and Methods

2.1 Materials and Instruments:

PGI_2 (Cayman Chemical, Michigan, USA), Forskolin (Sigma-Aldrich, UK), Fibrinogen (Enzyme Research, Swansea, UK), Collagen (Nycomed, Linz, Austria), Y-27632 (Abcam, Cambridge, UK), RP-8cpt-cAMPS (Biolog, Bremen, Germany), KT5720 (Abcam, Cambridge, UK), Rhosin (EMD Millipore Calbiochem, Billerics, MA USA), $pRhoA^{Ser188}$ (Santa-Cruz Biotechnology, Heidelberg, Germany), $pMLC^{Ser19}$ and $pVASP^{Ser157}$ (New England Biolabs, Hitchin, UK), GAPDH and Arp2/3 (Millipore, Watford, Hertfordshire, UK), PKA RI (Cell Signalling Technology, Leiden, Netherlands), PKA RII (BD Biosciences, Oxford, UK), pPKA substrate (Cell Signalling Technology, Leiden, Netherlands), WASp (Santa-Cruz Biotechnology, Heidelberg, Germany), Anti-Phosphotyrosine (Millipore, Watford, Hertfordshire, UK), RhoA pulldown kit (Cytoskeleton, Denver, UK), cAMP assay (GE Healthcare) and ProLong Diamond Antifade Mountant (GE healthcare, Little Chalfont, Buckinghamshire, UK), Flourescent secondary IRDye 800CW anti-mouse and IRDye 680RD anti-rabbit antibodies (LI-COR Biotechnology, Cambridge, UK). All other chemicals stated below were from Sigma Ltd (Poole, UK) unless otherwise stated. FITC-phalloidin, PBS, Indomethacin, Apyrase, Paraformaldehyde, Glucose, Tris-Na Citrate, NaCl, Citric acid, EDTA, KCl, HEPES, NaH_2PO_4, $NaHCO_3$, $MgCl_2$, Triton X-100, KH_2PO_4, PIPES, EGTA, Acrylamide 30%, methanol, PVDF, BSA, Milk, TEMED, APS, Tris base, SDS, Glycine, Glycerol, Bromophenol blue, Dithiothreitol, Tween-20, 24-well plate, 6-well plate, 10 cm dish, Haemocytometer, coverslips, glass slides, plate reader, licor_Odyssey, Latrunculin A, phosphatase and protease inhibitors.

2.2 Platelet preparation:

Whole blood from the vein of healthy volunteers was obtained into 1:5 ratio of acid-citrate dextrose (ACD) (114mM Glucose, 30mM Tris-Na Citrate, 72.6mM NaCl and 3.0mM Citric acid pH 6.4). Care was taken in maintaining a standardized phlebotomy technique along with safe transfer of blood from the phlebotomy room to the laboratory. The blood was put in 10ml bijou tubes. These tubes were initially centrifuged using, Thermo Scientific Megafuge 16, at 700rpm, 20°C for 10 minutes. Platelet rich plasma (PRP) was transferred into separate bijou tubes, while 1ml of the plasma was left in the blood tubes. These tubes with the blood were re-centrifuged at 900rpm, 20°C for additional 10 minutes. The remaining PRP was collected using a Pasteur pipette into the tubes with previously

PRIMARY ANTIBODY	**DILUTION** **WB:** Western blotting **CM:** Confocal microscopy	**SECONDARY ANTIBODY**
VASP^{Ser157} New England Biolab (#3111)	1:1000 (**WB**)	IRDye 680RD anti-Rabbit (P/N 925-68071) (1:10000)
pRhoA^{Ser188} Santa Cruz Biotechnology (sc-32954)	1:1000 (**WB**) 1:200 (**CM**)	IRDye 680RD anti-Rabbit (P/N 925-68071) (1:10000)
pMLC^{Ser19} New England Biolab (#3671)	1:1000 (**WB**)	IRDye 800CW anti-Mouse (P/N 925-32280) (1:10000)
GAPDH Millipore (AB2302)	1:6000 (**WB**)	IRDye 800CW anti-Mouse (P/N 925-32280) (1:10000)
Anti-PKA-RIα/β Cell Signaling Technology (#3927)	1:200 (**CM**)	Thermo Fisher Scientific AlexaFluor647 anti-Mouse (1:200)
Anti-PKA-RIIβ BD Biosciences (pS114)	1:200 (**CM**)	Thermo Fisher Scientific AlexaFluor488 anti-Mouse (1:200)
Anti-Phosphotyrosine (4G10) Millipore (05-321)	1:1000 (**CM**)	Thermo Fisher Scientific AlexaFluor647 anti-Mouse (1:200)
Arp2/3 Millipore (MABT95)	1:200 (**CM**)	Thermo Fisher Scientific AlexaFluor647 anti-Rabbit (1:200)

Table 2. 1: List of antibodies. The list of primary and secondary antibodies with reference to their dilutions and their use in the experiments as for western blotting (WB) and confocal microscopy (CM).

acquired PRP. The pH of the PRP was adjusted to 6.4 by adding 20µl/ml of 0.3M citric acid. The PRP containing citric acid was centrifuged at 1800rpm, 20°C for 10 minutes. The supernatant containing the platelet poor plasma (PPP) was discarded, while the attained pellet was re-suspended in 3ml of wash buffer (36mM Citric acid, 10mM EDTA, 5mM Glucose, 5mM KCl and 90mM NaCl) (pH 7.4). The re-suspended pellets were centrifuged for additional 10minutes at 20°C at 2200rpm. The supernatant was drained while the inside of the tube is wiped using a tissue, care is taken not to disturb the pellet. The pellet is re-suspended in 2ml of Modified Tyrode's buffer (150mM NaCl, 5mM HEPES, 0.55mM NaH_2PO_4, 7mM $NaHCO_3$, 2.7mM KCl, 0.5mM $MgCl_2$ and 5.6mM Glucose) (pH 7.4). Platelets were then incubated for 30minutes to rest before using them for experimentation.

2.3 Platelet counting:

During platelet resting a platelet count was obtained. This was done either using a Beckman Coulter counter (Z^{TM} Series Coulter – Cell and Particle Counter) or a haemocytometer. The electrode was washed with isotonic fluid (Isoton II diluent). In a cuvette (Accuvette ST) 5µl of platelet suspension was added to 10ml of isotonic fluid and platelet number was analyzed. The count was taken thrice, and an average count was obtained.

To obtain a platelet count using a haemocytometer, the apparatus was initially cleaned thoroughly with ethanol. A coverslip was placed on top of haemocytometer, and the pattern on the haemocytometer is focused using the x10 objective. Platelets were then diluted using modified Tyrodes' buffer (1:100) (5µl in 495µl). After mixing, 20µl of platelets were added to the slide. To visualize the platelets, 20x or 40x objectives were used. Platelets were counted in 10 of the 25 small squares, remembering to count the platelets on two of the outer margins but excluding those lying on the other two outside edges. Platelets in the same area on both sides of the counting chamber were counted. The two counts were averaged and the number of platelets per milliliter was calculated using the formula:

Platelet count = Average count of platelets * 25000 * 100

2.4 Microscopy:

I have used epifluorescence and confocal microscopy during my research. Both of them are classified as fluorescence microscope. The working principle for these microscopes involves a light source, dichroic mirror(s) and excitation and emission filters (Figure 2.1).

Before visualising samples under the fluorescence microscopes they were stained either by fluorophores such as FITC/TRITC phalloidin targeted against filamentous actin or the samples were stained by using antibodies with fluorophores directed against the molecule to be detected. Once stained, the samples were exposed to specific wavelength of energy, such as UV light, that excites the fluorophores in the sample. Excitation of the fluorophores causes them to emit the attained energy in longer wavelengths. This allows the dichroic mirror to transmit the longer wavelength emission waves towards the ocular apparatus while reflecting the shorter wavelength excitation waves. To avoid unwanted fluorescence to distort the image, excitation and emission filters are used that channels the correct wavelength of energy to be received by the sample and be visualised by the user.

The confocal microscopy uses a LED light or LASER to excite the fluorophore in the sample. Using excitation and emission confocal pinhole apertures, it allows for sharper images with improved resolution due to less crosstalk and automated detection of the colours and their intensities. It allows optical sectioning of objects by scanning a single point in an X-Y manner, thereby enabling a three-dimensional reconstruction of specimen.

2.5 Platelet spreading:

Coverslips (0.13mm in thickness) were put in a 24 well plate and incubated with 300µl of fibrinogen (100µg/ml) or collagen (100µg/ml) for 1 hour at room temperature or overnight at 4^0C. The wells were washed twice with PBS using a Pasteur pipette, taking care to add to the walls of the well so as not to disturb the laid down matrix. In the meantime, 5mg/ml of fatty acid free BSA was prepared. The BSA was boiled for 10 minutes so as to denature the proteins. Once cooled the BSA was filtered using 0.45µm filter. The washed coverslips were incubated with 200µl of BSA to block any of the glass not covered by the matrix proteins so as to reduce non-specific binding of platelets. After incubation with BSA for 1 hour at room temperature, the wells are washed twice with PBS. The next steps were dependent upon the experimental plan, however if the experiments required apyrase

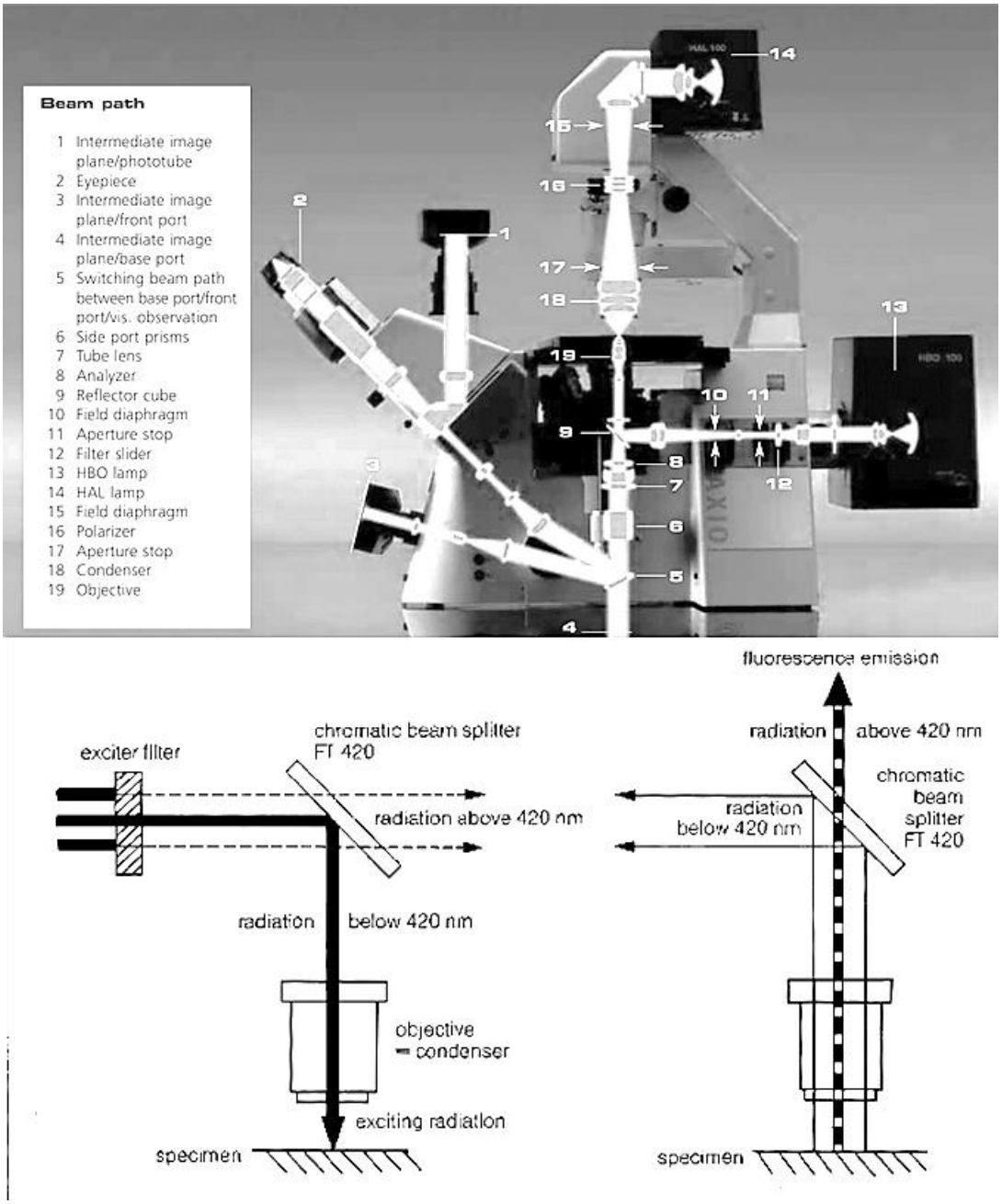

Figure 2. 1**: Principle of fluorescence microscopy.** An inverted fluorescence microscope (**top image**) identifies the sources of light, its passage through different lenses and filters and an image being observed by the observer through oculars or cameras. The principle of fluorescence microscope (**bottom image**) highlights the core concept of chromatic beam splitter (dichroic mirror) and the excitation and emission wavelengths. For fluorescence microscopy, light source (13) passes through the excitation filters (10, 11, 12) and gets reflected from the dichroic mirror (9) and is projected through the objective (19) onto the specimen. The specimen takes the energy and generates it back which passes through the dichroic mirror (9) and after passing through the emission filters (8, 7, 6) is reflected to the eyepiece (2) or the camera (1, 3).

(2U/ml) and indomethacin (10μM), these were added to the platelets 2 minutes prior to incubation on the matrix proteins.

2.5.1 Spreading profile of platelet

This was completed on fibrinogen. Adding 200μl of platelets ($2.0x10^7$) to the wells labelled for individual timepoints at 5, 10, 25, 35 and 45 minutes. These experiments were performed both in the presence and absence of apyrase (2U/ml) and indomethacin (10μM).

2.5.2 Prior incubation of platelets with PGI_2, Fsk, Y27632 and Rhosin

This was completed on both collagen and fibrinogen matrix proteins. Dose response effect of prior incubation of PGI_2 (1, 10, 100 and 1000nM), Forskolin (0.1, 1, 10 and 100μM), Y27632 (1, 10, 30 and 50μM) and Rhosin (1, 10, 30 and 50μM) were observed with platelets. For 2 minutes, platelets ($2.0x10^7$) were treated with respective agents prior to them being spread for 45 minutes at 37^0C.

2.5.3 Post incubation of spread platelets with PGI_2 and Fsk

This was completed on both collagen and fibrinogen matrix proteins. 200μl of platelets ($2.0 x10^7$) were allowed to spread for 25 minutes. The wells were washed twice with PBS so to remove cells which had not adhered. Initially different concentrations of PGI_2 (1, 10, 30, 100 and 1000nM) and Fsk (0.1, 1, 10 and 100μM) were prepared in modified Tyrodes' buffer. The platelets were treated with these doses of PGI_2 and Fsk (200μl/well) for 10 minutes. The platelets were then fixed. Additionally, after identifying 10nM for PGI_2 and 1μM for Fsk, as the optimum doses for the experiment, platelets were stimulated with PGI_2 or Fsk for 0, 2, 5, 10, 25, 40 and 60 minutes. This experiment was repeated for the 10 minute timepoint, optimum duration identified for the effects to be observed, in the presence and absence of apyrase (2U/ml) and indomethacin (10μM). Finally, to confirm that this was mediated by PKA, $2.0x10^7$/ml platelets were spread on fibrinogen for 25 minutes in the presence and absence of PKA inhibitors [RP-8cpt-cAMPS (500μM) and KT5720 (10μM) used in combination]. The wells were washed twice with PBS. The platelets were then stimulated with PGI_2 (10nM) and Fsk (1μM) for further 10 minutes, both in the presence and absence of RP and KT before fixation.

After being washed twice by PBS, the spread cells were fixed with 4% paraformaldehyde (PFA) for 10 minutes. The fixed platelets were then washed twice with PBS and lysed with

200µl of 0.1% Triton X-100 for 5 minutes. The cells were then washed twice with PBS and 200µl of 2mM FITC-phalloidin solution was added. The wells were incubated for 1 hour at room temperature under dark conditions. After incubation the wells were washed twice with PBS and the coverslips were placed inverted (the side with platelets facing towards the glass) on a labeled glass slide using a histamount. The slides were stored under dark at 4^0C.

For cases of co-immunolocalisation, the spread platelets that had been treated with PGI_2 (10nM) and Fsk (1µM) were fixed, permeabilized and were incubated for 30 minutes with the primary antibodies; Arp2/3, p-Tyr, pRhoA, PKA RI or RII. After 30 minutes of incubation, the secondary antibody, AF647 (anti-mouse and/or anti rabbit) (1:200), was prepared in PBS containing FITC-phalloidin (1:1000). An exception was PKA RII staining which was performed with AF488 (anti-mouse) (1:200) secondary antibody in conjunction with TRITC. The wells with the stain were then incubated for 1 hour at room temperature under dark conditions. After incubation the wells were washed twice with PBS and the coverslips were placed on its head on a labelled glass slide having histamount. The slides were stored under dark at 4^0C.

2.5.4 Platelet visualization

The spread platelets were visualized using the fluorescence and confocal microscope.

2.5.4.1 Conventional Fluorescence microscopy

The slides were visualized using a Zeiss Axio Observer (Zeiss, Cambridge, UK) with x63 oil immersion objective (1.4 NA) and Zen Pro software (Carl Zeiss, Cambridge, UK). There were 5 images of each condition that the spread platelets had been treated and were analysed using ImageJ software (NIH, Bethesda, USA). The images were selected in a randomised manner taking care to obtain an image each from the upper right, upper left, lower right, lower left and centre of the slide for each condition. Approximately 200-250 platelets per condition were analysed for the numbers of platelets containing either actin nodules or stress fibres, and platelet adhesion. Surface area was also analysed by manually circling 100 randomly selected platelets for each condition.

2.5.4.2 Confocal microscopy

The slides were visualized using a Zeiss Axio Observer (Zeiss, Cambridge, UK) with x100 oil immersion objective (1.4 NA) and Zen Pro software (Carl Zeiss, Cambridge, UK).

2.6 Western blotting:

For immunoblotting platelet concentration of $2.0x10^8$/ml was used. Platelet volumes of 300µl, 1000µl and 3000µl were used in 24-well plate, 6-well plate and/or 10cm dish, respectively, depending upon the needs of the experiment. Platelets were spread for 25 minutes on fibrinogen.

2.6.1 Dose response of PGI_2 and Fsk on spread platelets

The wells were washed twice with PBS to remove cells, which had not adhered. Different concentrations of PGI_2 (1, 10, 30, 100 and 1000nM) and Fsk (0.1, 1, 10 and 100µM) were prepared in modified Tyrodes' buffer and platelets were treated with these doses for 10 minutes.

2.6.2 Time course of PGI_2 and Fsk on spread platelets

The wells were washed twice with PBS. Choosing 10nM for PGI_2 and 1µM for Fsk, a time course was performed. The chosen timepoints were 0, 2, 5, 10, 25, 40 and 60 minutes of PGI_2 (or Fsk) stimulation.

2.6.3 Response of signalling components at 10 minute treatment of spread platelets

For the signalling experiments, 10 cm dishes were used to spread platelets. After their specific experimental design, the spread platelets were collected using a cell scraper and were then lysed with 50-100µl of 2x lysis buffer [100mM Tris pH6.8, 4% SDS, 10% Glycerol, 2% 2-Mercaptoethanol, 10mM EDTA pH8.0, Protease inhibitor cocktail (1:100), Phosphatase inhibitor (1:100)]. Protein estimation was performed using Bradford assay (explained in the section 2.9). The samples were treated with 1:6 ratios of 6x Laemmli buffer [10ml (pH6.8): 1.2g SDS, 4.7ml Glycerol, 1.2ml Tris 0.5M (pH6.8), 6mg Bromophenol blue and 0.93g Dithiothreitol (DTT)] and were boiled by keeping them on the heat block for 10 minutes. The prepared samples were to be analysed for the signalling pattern for $pVASP^{Ser157}$, $pRhoA^{Ser188}$, $pMLC^{Ser19}$ and GAPDH, whilst treatment of spread platelets with PGI_2 (or Fsk). An exception to the above protocol for sample preparation had been $pMLC^{Ser19}$, as it is incompatible with lysis buffer; the samples were directly lysed by 1x Laemmli buffer.

After preparing the samples, they were then run on SDS-PAGE (fixed-10%) for 90-120 minutes at a constant 110V using 1mm thick gels. Using a custom made transfer sandwich, the proteins from the gel were shifted onto a PVDF membrane by the BioRad Trans-Blot Turbo (25V, 1.3A and 10 minutes). The membranes were blocked with 5% milk or 10% BSA for 60 minutes at room temperature. These membranes were blotted overnight in the primary antibody (listed in the material section) at 4^{o}C on a rocker. After retrieval from the antibody the membranes were washed twice for 10 minutes each with TBS-tween (0.1%). Secondary antibodies (anti-rabbit and/or anti-mouse) (listed in the material section) were prepared in TBS-tween (0.1%) in a 1:10000 dilution and membranes were incubated with it under dark for 60 minutes at room temperature. The membranes were washed three times with TBS-tween (0.1%) for 5 minutes each. The blots were imaged by Licor (Odyssey CLx).

The images were analyzed by (Image studio Ver. 5.2). Densitometries for the blots were measured by making equal sized rectangles to the bands on the images. These values were converted into ratio by dividing them with the densitometry for GAPDH as it had been used as the loading control.

2.7 F-actin:

Filamentous actin in platelets was assessed by F-actin assay (modified method of Machesky et al, 1997). I had used this assay to identify any changes in the level of filamentous actin in suspended and spread platelets.

For analysis of F-actin content of platelets in suspension (200µl) ($1.0x10^8$ to $8.0x10^8$) were aliquoted in duplicates. One group served as the basal while the other was activated with 0.1U/ml of thrombin (for 1min). For each of the aliquots 200µl of fixative buffer (20mM KH_2PO_4, 10mM PIPES, 5mM EGTA, 2mM $MgCl_2$, 2% Triton X-100, 2µM FITC-phalloidin, 3.7% paraformaldehyde) was added. The samples were rotated for 60 minutes in the dark. The cells were pelleted by microcentrifugation for 2 minutes at 13000x. The supernatant was removed and the cells were washed with saponin buffer (20mM KH_2PO_4, 10mM PIPES, 5mM EGTA, 2mM $MgCl_2$, 2% Triton X-100, 0.1% (v/v) saponin) by re-suspension of the pellets. The samples were again microcentrifuged for 2 minutes at 13000x. Supernatant was discarded while the pellets were resuspended in 200µl of methanol. The samples were rotated in the dark for 60 minutes. The cells were microcentrifuged for 2 minutes at 13000x. The supernatant was measured using the Tecan

plate reader (excitation=488 and emission=520). An aliquot of platelets (50µl) ($1.0x10^8$ to $8.0x10^8$) was used to calculate proteins (refer to section 2.10) at these ranges of platelet concentration by lysing the cells with 50µl of 2x lysis buffer. Measuring the OD of the F-actin at the range of platelets used ($1.0x10^8$ to $8.0x10^8$) and measuring the amount of proteins for the same range of platelet concentration; provided the means to link the OD of the platelets to the concentration of protein. Thus, a graph was plotted for the fluorescence versus protein concentration.

For analysis of F-actin concentration in spread cells, 6 well plates were coated with 1ml fibrinogen (100µg/ml) for overnight incubation. After washing the excess fibrinogen with PBS the wells were blocked with 1ml of BSA (5mg/ml). 1ml of $2.0x10^8$ platelets were allowed to spread for 25 minutes. The wells were washed twice with PBS and the spread platelets were treated with 10nM PGI_2 or 1µM Fsk for 10 minutes. The conditions were run in duplicates; one set was used for protein estimation by lysing them with 2x lysis buffer (50µl) (refer to section 2.10) while the other set was fixed by fixative buffer (50µl). Further steps for F-actin assay followed the same protocol as of the suspended platelets. As a positive and negative control to filamentous actin levels the fluorescence for basal platelets ($2.0x10^8$), stimulated platelets ($2.0x10^8$) with 0.1U/ml of thrombin and platelets ($2.0x10^8$) treated with Latrunculin A (at 3µM) were used.

2.8 cAMP assay:

Six well plates were coated with fibrinogen (100µg/ml) for an overnight incubation at 4°C washed with PBS to remove unbound matrix protein and blocked with denatured fatty acid free BSA (5mg/ml) for 1 hour at room temperature. Washed platelets ($2x10^8$/ml) were adhered for 25 minutes. The non-adherent platelets were removed and adherent platelets were treated with Tyrodes' buffer with or without PGI_2 (10nM) for 2 minutes. To calculate the cAMP levels of these spread platelets, cAMP assay kit (GE Healthcare – Amersham cAMP Biotrak EIA system – RPN 225) was used. Platelets were scrapped and lysed using the lysis reagent provided in the commercial kit. Transfer 100µl of sample and standards to their labelled wells in duplicates in a 96-well plate. Another 100µl of antiserum was added to the wells, gently mixed and incubated at 4^oC for 2 hours. After the incubation finished 50µl cAMP-peroxidase conjugate was added to the wells. Again mix it gently and incubate it at 4^oC for 1 hour. After completion, the wells were aspirated and washed four times with wash buffer. Immediately 150µl of enzyme substrate was dispensed in the wells and

incubated at room temperature on the shaker for 1 hour. The reaction was stopped by adding 100µl of 1.0M sulphuric acid and the plate was read using the Tecan plate reader at 450nm. As it had been done in duplicate, an average was obtained. Using the standards, a standard curve was obtained to determine the cAMP levels in the samples.

2.9 RhoA Pull-down assay:

The 10cm plates were coated with fibrinogen (100µg/ml) for an overnight incubation at 4°C. They were washed with PBS to remove unbound matrix protein and blocked with denatured fatty acid free BSA (5mg/ml) for 1 hour at room temperature. Washed platelets ($2x10^8$/ml) were adhered for 25 minutes. The non-adherent platelets were removed and adherent platelets were treated with Tyrodes buffer with or without PGI_2 (10nM) or Fsk (1µM) for 10 minutes. From the samples the spread platelets were harvested using a cell scraper and were lysed. From individual lysates, 50µl of samples was used for protein estimation (refer to section 2.10) and for western blotting for total RhoA protein. Using RhoA pulldown kit (Cytoskeleton Inc.; Cat # BK036-S), the remaining lysates (200µg) were incubated for 90 minutes at 4°C with Rhotekin-RBD-beads (50µg). Bead pellets were washed once and Laemmli buffer was added. After boiling the samples with Laemmli buffer they were immunoblotted.

For immunoblotting, the samples were run a 10% fixed gel 90 minutes at a constant 110V using 1.5mm thick gels. Using a custom made transfer sandwich, the proteins from the gel were shifted onto a PVDF membrane by the BioRad Trans-Blot Turbo (25V, 1.3A and 10 minutes). The membranes were blocked with 5% milk for 60 minutes at room temperature. These membranes were blotted overnight in the RhoA primary antibody at 4^oC on a rocker. After retrieval from the antibody the membranes were washed twice for 10 minutes each with TBS-tween (0.1%). Secondary antibodies (anti-mouse) were prepared in TBS-tween (0.1%) in a 1:10000 dilution and membranes were incubated with it under dark for 60 minutes at room temperature. The membranes were washed three times with TBS-tween (0.1%) for 5 minutes each. The blots were imaged by Licor (Odyssey CLx).

The images were analyzed by (Image studio Ver. 5.2). Densitometries for the active and total RhoA were measured by making equal sized rectangles to the bands on the blots obtained. These values were converted into ratio by dividing the respective active RhoA to its total RhoA counterpart.

2.10 Protein estimation:

Protein estimation was performed using Precision Red Advanced Protein Assay by Cytoskeleton. For protein estimation, 3µl of the sample was mixed with the Precision Red reagent (ADV02) in a 96 well plate to make a final volume of 300µl. These wells were prepared in duplicates so as to ascertain for the accuracy of the results obtained. The wells were incubated for 1 minute and read at an absorbance of 600nm on a Tecan plate reader. The obtained duplicate values were averaged. Using the conversion factor of 1 OD_{600nm} = 125µg; protein concentration were obtained by using the formula below.

Protein concentration (µg/ml) =Average value * 125 * 100

2.11 Flow studies:

Flow studies were performed with multichannel biochips (Cellix, Dublin Ireland). Biochips were coated with fibrinogen (100µg/ml, 300µg/ml and 1000µg/ml) and collagen (25µg/ml) for an overnight incubation at 4°C and blocked with denatured BSA (5mg/ml) for 1 hour at room temperature. The blood was collected with 100µM PPACK (Phenylalanyl-Prolyl-Arginyl Chloromethyl Ketone - an irreversible inhibitor of thrombin). Depending on the conditions of the experiment:

- Whole blood was stained with $DIOC_6$ (10µM) and flowed through the biochips for 2 minutes at a shear rate of $1000s^{-1}$ at 37°C. Biochips then underwent a post-flow with Tyrode's buffer supplemented with or without PGI_2 (1-100nM) for 10 minutes.

- Whole blood was stained with $DIOC_6$ (10µM). 100µl per condition was incubated for 2 minutes with PGI_2 in a dose response manner (1-100nM). It was then flowed through the biochips for 2 minutes at a shear rate of $1000s^{-1}$ at 37°C.

- Whole blood, incubated either in the presence or absence of RP-8cpt-cAMPS (500µM) and KT5720 (10µM) was stained with $DIOC_6$ (10µM) and flowed through the biochips for 2 minutes at a shear rate of $1000s^{-1}$ at 37°C. Biochips then underwent a post-flow with Tyrode's buffer supplemented with or without PGI_2 (100nM) for 10 min.

Real-time videos for the whole duration of the flow experiment were made using the Olympus IX71 lens 60x/0.70. The thrombi were then fixed with 4% paraformaldehyde for 30 minutes, stained overnight at 4°C with $DiOC_6$ (10µM) and imaged using an Apotome.2 confocal unit on a Zeiss Axio Observer (Zeiss, Cambridge, UK) with a x63 oil immersion

objective (1.4 NA) and Zen Pro software (Carl Zeiss, Cambridge, UK). Analysis was performed for the effect on thrombus height (by doing z-stack analysis) and surface area (snaps at specific time points analyzed by imageJ). Analysis of thrombus height and the surface area coverage for the different conditions were performed using ImageJ software (NIH, Bethesda, USA). The videos were edited to a speed of 16x by the use of the software Movie maker (ver. 2012).

2.12 Statistical analysis:

Platelets having stress fibres and/or actin nodules were counted on ImageJ software and their percentages calculated. Some platelets were not classified as they were bright spot stains. Arcsine transformation was applied to the percentage data and One-way Analysis of Variance (One-way ANOVA) was applied with a P value of < 0.05. The data was then back transformed into percentage to be presented in the figures as mean ± standard error of mean (SEM). Using the ImageJ software the adhesion and surface area of platelets were calculated. Results for the surface area and adhesion of platelets were shown as mean ± standard error of mean. The data was statistically analysed directly using one-way ANOVA with a P value of < 0.05.

Surface area coverage of thrombi from flow data was measured by Otsu threshold method in ImageJ and presented as a percentage. Arcsine transformation was applied to the percentage data and One-way Analysis of Variance (One-way ANOVA) was applied with a P value of < 0.05. The data was then back transformed into percentage to be presented in the figures as mean ± standard error of mean. Zen lite from Ziess (Blue edition) software was used to analyse z-stack images of the thrombi. The images were taken at 0.5μm thickness. For each condition 5 images were taken for each experiment. The height and the number of thrombi were measured. A thrombus was defined as a height greater than 3μm. Results for the height and number of thrombi per image were shown as mean ± standard error of mean (SEM). The data was statistically analysed directly using one-way ANOVA with a P value of < 0.05.

The means of oneway ANOVA were compared between different groups by using the Tukey HSD post-hoc test.

CHAPTER 3:

The role of PGI_2 within platelet spreading

3.1 Introduction:

Platelets circulate close to the endothelial layer within the circulation. This situation is maintained as red blood cells in circulation push the platelets nearer to the endothelial lining where they bathe continuously in endothelial released PGI_2 and NO (Moncada et al., 1976, Radomski et al., 1987b). Defective PGI_2 signaling results in hyper-activation of platelets that induces a prothrombotic phenotype (Van Geet et al., 2009), whilst animal models lacking NO, when induced with NO-related compounds showed a reduction in thrombus formation (Stasch et al., 2011). These studies signify that PGI_2 and NO provide an effective means to significantly inhibit thrombus formation and platelet adhesion on ECM proteins (Higgs et al., 1978). In the case of PGI_2 this is achieved via increasing intracellular cAMP levels, activating PKA and therefore causing the phosphorylation of substrates that affects downstream signaling regulation and also modulates the actin cytoskeletal dynamics in platelets (Smolenski, 2012, Beck et al., 2014). By targeting these substrates PGI_2 can therefore inhibit platelet cytoskeletal changes, required to resist the shear forces within the circulation and therefore allow thrombus formation to occur.

During thrombus formation, exposed ECM proteins allow the platelets to undergo a spreading response. This spreading response is critical to allowing the thrombus to withstand the high shear environment of the vasculature. The spreading response causes the platelets to modulate their form from a discoid to a flattened shape. During this process the platelet cytoskeleton remodels itself, forming multiple different actin structures. Initially fingerlike projections called filopodia are formed (Hartwig, 1992). The gaps between these are then filled in by lamellipodia (Hartwig, 1992, McCarty et al., 2006), and then finally stress fibres are formed, ensuring that the shape of the fully spread platelet is maintained (Calaminus et al., 2007). The modulation of this cytoskeleton is matrix specific, as the actin nodule is not present on collagen and yet is present on fibrinogen indicating a matrix specific role for this structure (Calaminus et al., 2008). However these cytoskeletal changes are active processes and as such as liable to both positive and negative signals. PGI_2 has been shown in other cell types to play a significant role in the actin cytoskeleton dynamics. It disassembles filamentous actin, thereby inhibiting smooth muscle cell proliferation and migration in human aorta (Bulin et al., 2005). In vascular endothelial cells, PGI_2 remodels actin cytoskeleton to enhance a peripheral filamentous actin rim; thereby reinforcing the endothelial cell integrity (Birukova et al., 2007). However within platelets, although PGI_2 is well known to prevent activation of the actin cytoskeleton, there is no

evidence to indicate that it can play a role in remodulating a fully activated and spread platelet. This is an important idea, if PGI_2 can help to reverse platelet spreading, it places PGI_2 as an important player in the prevention of excessive thrombus formation, and therefore preventing occlusion of the blood vessel. This certainly agrees with the evidence that indicates that thrombin, which is induced by thrombus formation, causes the upregulation of PGI_2 production (Weksler et al., 1978), and so is acting to try to prevent excessive thrombus formation. Therefore it is necessary to identify the role of PGI_2 in the modulation of the actin cytoskeleton to identify if it could play a role in reversing platelet activation.

3.2 Aims of the chapter:

The aim of this chapter was to identify the profile of platelet spreading, in terms of actin cytoskeletal changes, on treating them with cAMP elevating agents (PGI_2 and Forskolin).

- Identify the effect(s) on actin cytoskeleton caused by increasing the intracellular cAMP levels in spread platelets
- Recognize changes in the actin cytoskeleton of spread platelets by elevation of cAMP in the absence of platelet secretion.
- Measure changes in the level of filamentous actin on increasing intracellular cAMP of spread platelets.

3.3: Platelet spreading profile on Fibrinogen

In order to understand how platelet rearrange their actin cytoskeleton in response to matrix proteins, a spreading profile of platelets exposed to fibrinogen was completed. Platelets ($2.0x10^7$/ml) were allowed to spread on fibrinogen (100μg/ml) coated coverslips for 45 minutes. At 5, 10, 25, 35 and 45 minutes of spreading, the platelets were fixed, stained and then visualized using fluorescence microscopy. For each condition analysis of actin structures was performed. The number of platelets having actin nodules and stress fibres were counted manually and tabulated as percentage of total number of platelets per condition per image. The adhesion of platelets to the matrix protein (fibrinogen) was also counted and expressed as total number of platelets. Surface area of the platelets was analyzed using ImageJ software.

The percentage of platelets having stress fibres (Figure 3.1A and B) increased from 27.38±2.38% at 5 minutes to 54.51±15.37% at 10 minutes, reaching a peak of 70.52±4.65% at 25 minutes. After 25 minutes the percentage of platelets having stress fibres stabilized with 71.31±7.33% at 35 minutes and 68.18±8.36% at 45 minutes of spreading. The percentage of platelets having actin nodules (Figure 3.1A and C) decreased from 64.82±2.84% at 5 minutes to 40.22±16.74% at 10 minutes, reaching to a minimum of 25.16±4.26% at 25 minutes. Similar to the stress fibres, the number of platelets having actin nodules were also maintained after 25 minutes of spreading. Directly proportional to platelets acquiring stress fibres, with the passage of time, an increase in the surface area was observed (Figure 3.1A and D), with 17.72±1.96μm^2 at 5 minutes, 23.85±4.47μm^2 at 10 minutes and reaching an plateau of 32.13±2.34μm^2 at 25 minutes, which was maintained at 35 minutes (34.80±3.10μm^2) and 45 minutes of spreading (36.56±5.44μm^2). The experiment reveals that 25 minutes of platelet spreading attains a maximal spreading profile.

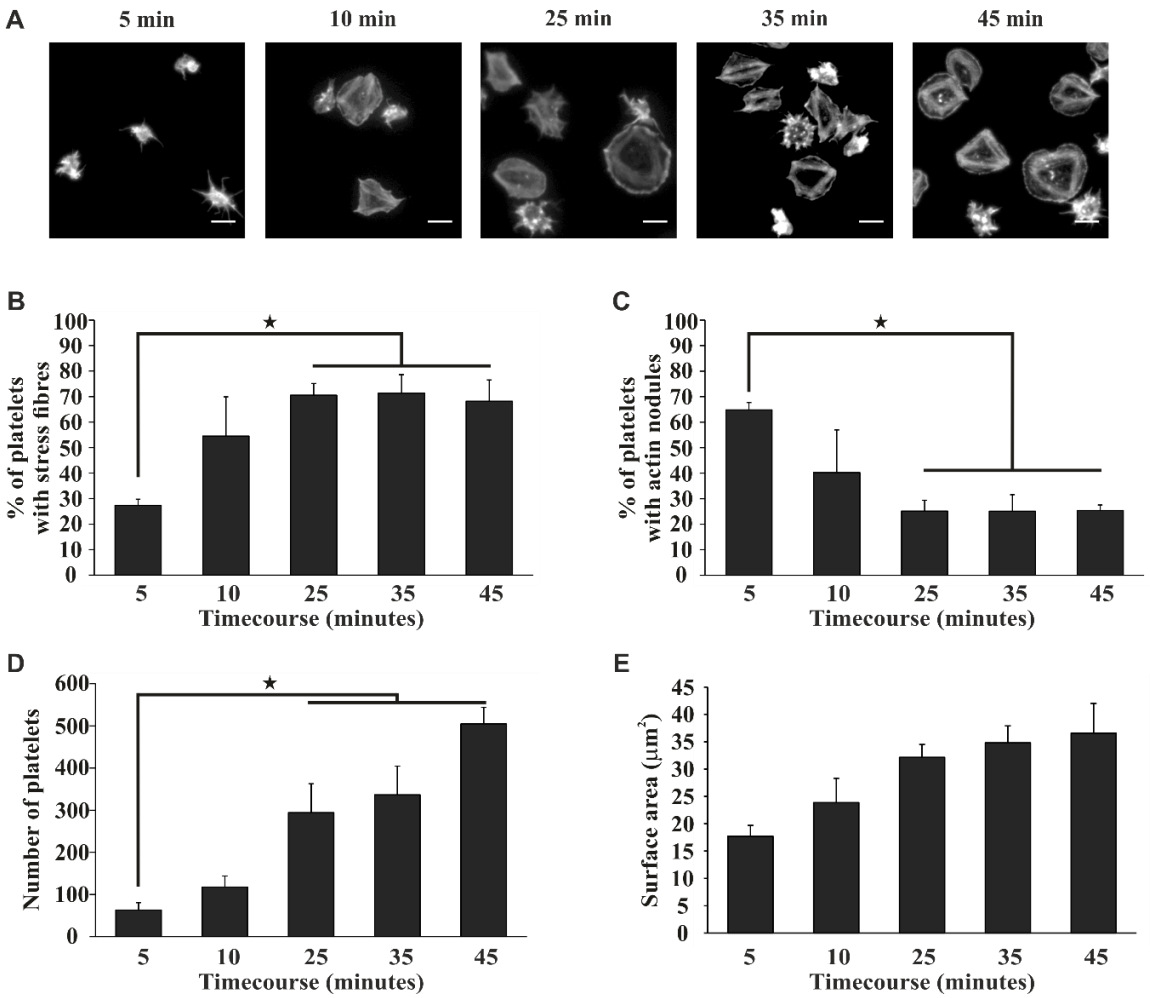

Figure 3. 1: Spreading profile of platelets. Platelets ($2x10^7$/ml) were spread on 100μg/ml fibrinogen for a duration of 5 - 45 minutes. After their respective time points of spreading, the platelets were washed with PBS and were then fixed. These fixed platelets were then stained with FITC-phalloidin before being imaged on conventional microscope. **A)** Images are representative of three separate experiments. Scale bar is 5μm. **B)** The percentage of platelets containing stress fibres at different time points of spreading. **C)** The percentage of platelets containing actin nodules at different time points of spreading. **D)** The total number of platelets adhered for these time points. **E)** The average surface area of the spread platelets was calculated for these time points. The data was presented as average±SEM of n=3. $p<0.05$.

In order to understand the role of the secondary mediators (ADP and TXA_2) within this spreading process the platelets were treated prior to spreading with apyrase and indomethacin, to curb the effect of ADP and TXA_2 respectively. Analysis was performed as per figure 3.1 to identify the number of platelet adhered, the average platelet surface area, and the percentage of platelets containing stress fibres and actin nodules for each timepoints of spreading profile.

The analysis indicated that the percentage of platelets having stress fibres (Figure 3.2A and B) increased from 7.13±0.88% at 5 minutes to 24.46±0.07% at 10 minutes, reaching a maximum of 67.06±7.69% at 25 minutes. Onwards from 25 minutes the number of platelets having stress fibres stabilized with 64.46±3.64% at 35 minutes and 68.17±14.54% at 45 minutes of spreading. Again as the number of stress fibres increased the number of platelet containing actin nodules decreased, from 89.75±2.25% at 5 minutes to 64.67±2.40% at 10 minutes, reaching to a minimum of 25.33±11.18% at 25 minutes. The percentage of platelets having actin nodules were maintained after 25 minutes to 29.78±4.57% at 35 minutes and 28.41±13.49% at 45 minutes of spreading. Once again as the time increased, the number of platelets adhering increased in a time dependent manner. Furthermore, the average surface area of the platelet increased from 16.92±3.20μm^2 at 5 minutes, to 17.83±2.17μm^2 at 10 minutes and reaching a maximum of 30.0±3.0μm^2 at 25 minutes. This surface area was maintained over time with 27.20±2.50μm^2 at 35 minutes and 29.90±4.10μm^2 at 45 minutes of spreading (Figure 3.2A and E). It was identified that platelets achieved a maximal spreading response by 25 minutes even in the absence of secretion (figure 3.2).

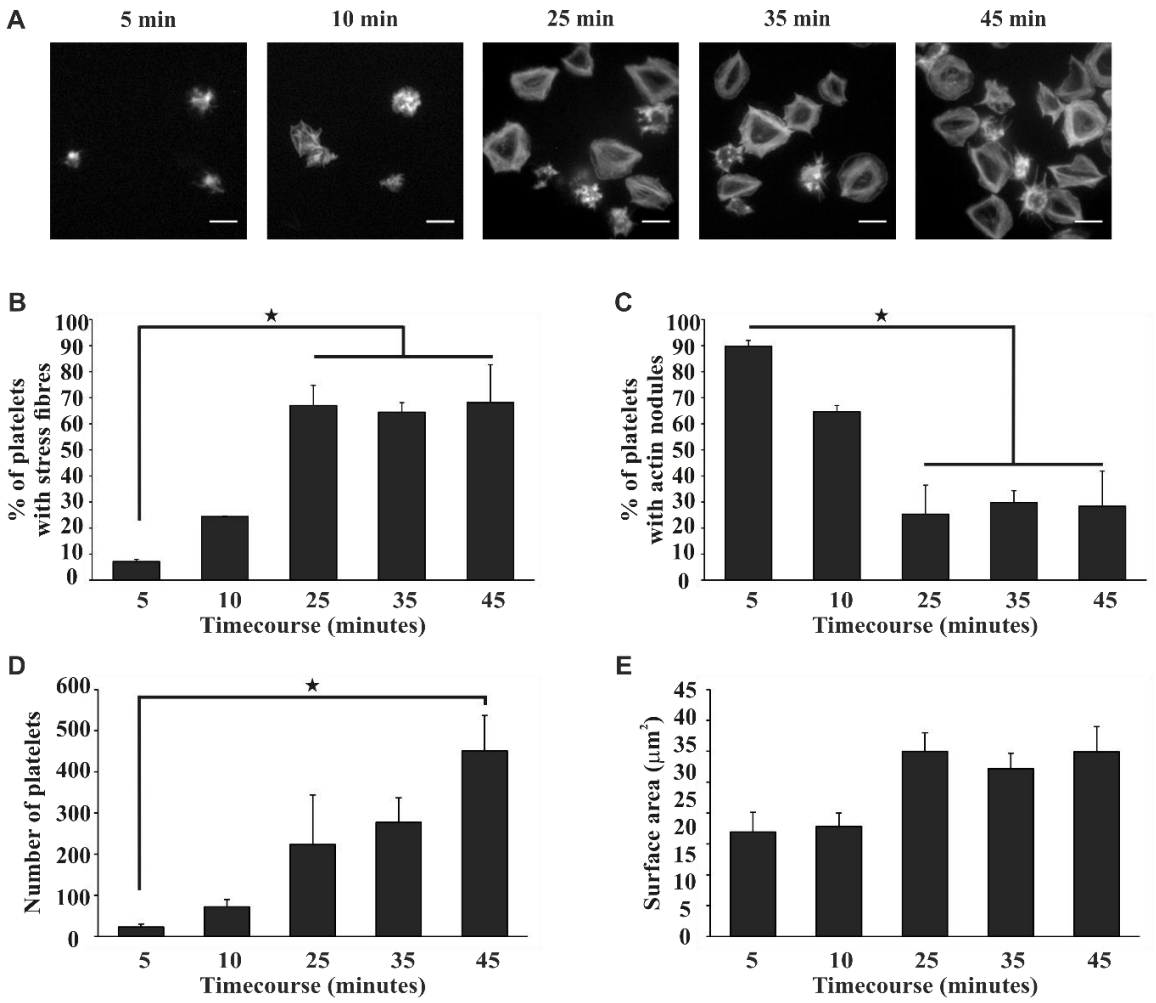

Figure 3. 2: Spreading profile of platelets in the absence of ADP and TXA_2. Platelets ($2x10^7$/ml) were treated for 2 minutes with apyrase and indomethacin prior to spreading on 100μg/ml fibrinogen for a duration of 5 - 45 minutes. After their respective time points of spreading, the platelets were washed with PBS and were then fixed. These fixed platelets were then stained with FITC-phalloidin before being imaged on conventional microscope. **A)** Images are representative of three separate experiments. Scale bar is 5μm. **B)** The number of platelets containing stress fibres at different time points of spreading. **C)** The number of platelets containing actin nodules at different time points of spreading. **D)** The total number of platelets adhered for these time points. **E)** The average surface area of the spread platelets was identified for these time points. The data was presented as average±SEM of n=3. $p<0.05$.

3.4: The effect of prior incubation of PGI_2 and Fsk on platelet spreading

In order to understand the effect of PKA signaling on spreading, the human platelets were preincubated for 2 minutes with increasing doses of cAMP elevating agents; PGI_2 and Forskolin (Fsk); before spreading on fibrinogen for 45 minutes as shown in the schematic in Figure 3.3A

Preincubation with PGI_2 had only significantly affected the percentage of platelets containing stress fibres at 1μM (Figure 3.3B and C). The control sample had 76.24±5.61% of platelets containing stress fibres, which upon treatment with 1nM PGI_2 dropped to 57.82±12.99%, 10nM PGI_2 dropped to 53.30±14.50%, 100nM PGI_2 dropped to 47.51±9.16% and 1000nM PGI_2 dropped to 20.10±13.05%. Similarly, there was not a significant effect on the percentage of platelets having actin nodules in comparison to the control unless a high concentration of PGI_2 was used (Figure 3.3B and D). The basal platelets have 19.08±4.64%; which upon treatment with 1nM PGI_2 was 39.13±12.52%, 10nM PGI_2 was 43.81±14.64%, 100nM PGI_2 was 48.78±8.99% and 1000nM PGI_2 was 77.18±12.60%. No significant change in adhesion was observed (figure 3.3E). In agreement with the changes in the actin nodules and stress fibres, only the highest dose of PGI_2 induced a significant reduction in surface area, with the control level of 34.32±1.35μm^2 dropping to 28.38±4.85μm^2 at 1nM, 25.98±4.81μm^2 at 10nM, 22.90±1.67μm^2 at 100nM and 19.16±2.46μm^2 at 1000nM PGI_2 (Figure 3.3F).

The results show that preincubation with PGI_2 had little effect on platelet spreading in terms of the number of platelets containing actin nodules, stress fibres, surface area analysis or adhesion of platelets to the matrix, unless used at high concentrations (Figure 3.3).

In agreement with preincubation with PGI_2, preincubation of platelets prior to spreading with Fsk had reduced the percentage of platelet having stress fibres in comparison to the control (figure 3.4A and B). However here the effect was significant at all doses with the control containing 69.12±8.46% of platelets containing stress fibres, which upon treatment with 0.1μM Fsk dropped to 30.14±15.23%, 1μM Fsk dropped to 19.03±11.97%, 10μM

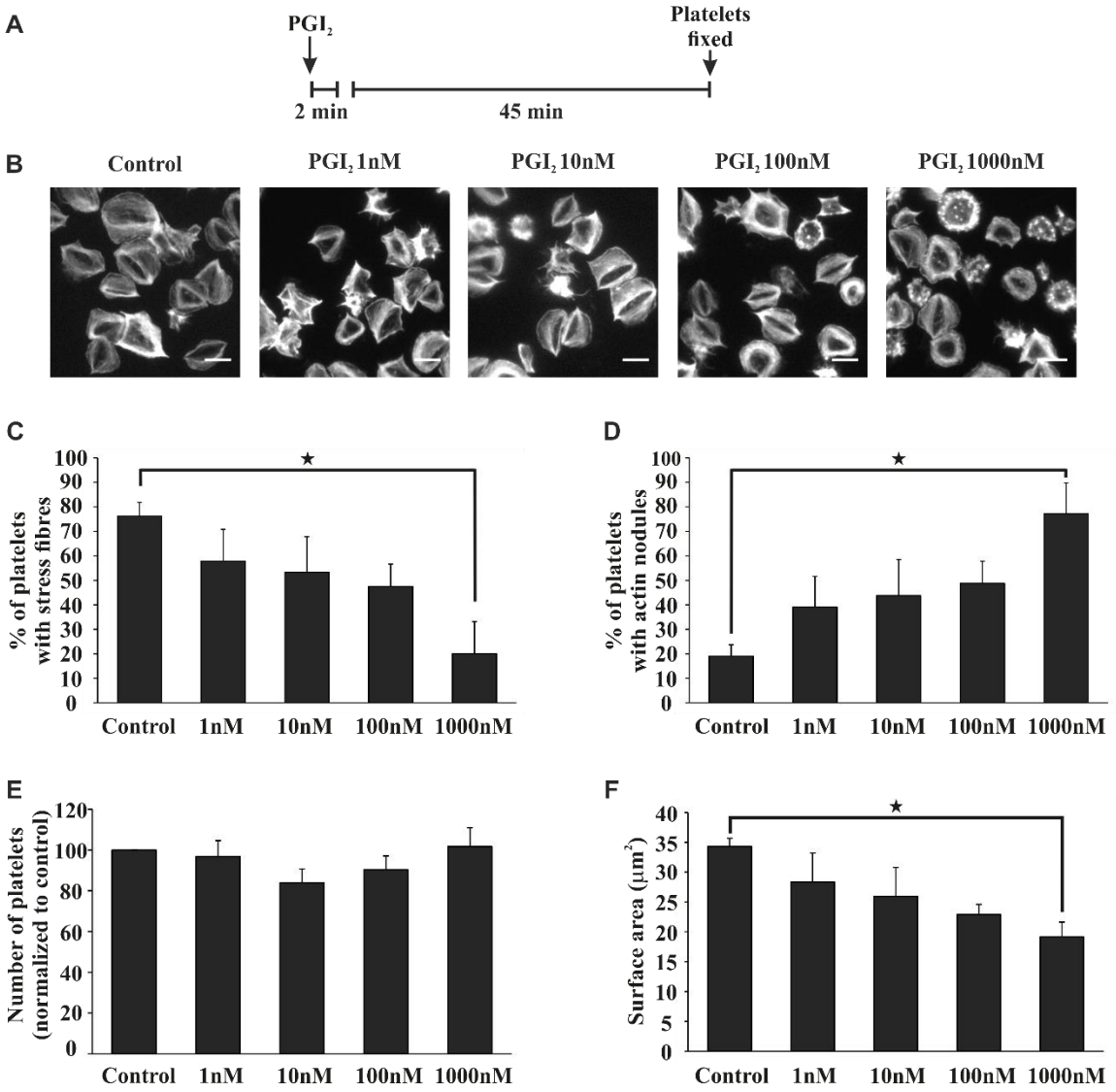

Figure 3. 3: Prior treatment with PGI_2 inhibits platelet spreading in a dose response. Platelets ($2x10^7$/ml) were treated for 2 minutes with 1-1000nM PGI_2. They were then allowed to spread on 100μg/ml fibrinogen for 45 minutes, shown in **(A)** as a schematic; before washing, fixation and staining with FITC-phalloidin before being imaged on conventional microscope. **B)** Images are representative of three experiments. Scale bar is 5μm. **C)** The number of platelets containing stress fibres was identified in control and PGI_2 treated samples. **D)** The number of platelets containing actin nodules was calculated in control and PGI_2 treated samples. **E)** The total number of platelets adhered, was calculated in control and PGI_2 treated samples. **F)** The average surface area of the spread platelets was identified in control and PGI_2 treated samples. The data was presented as average±SEM of n=3. $p<0.05$

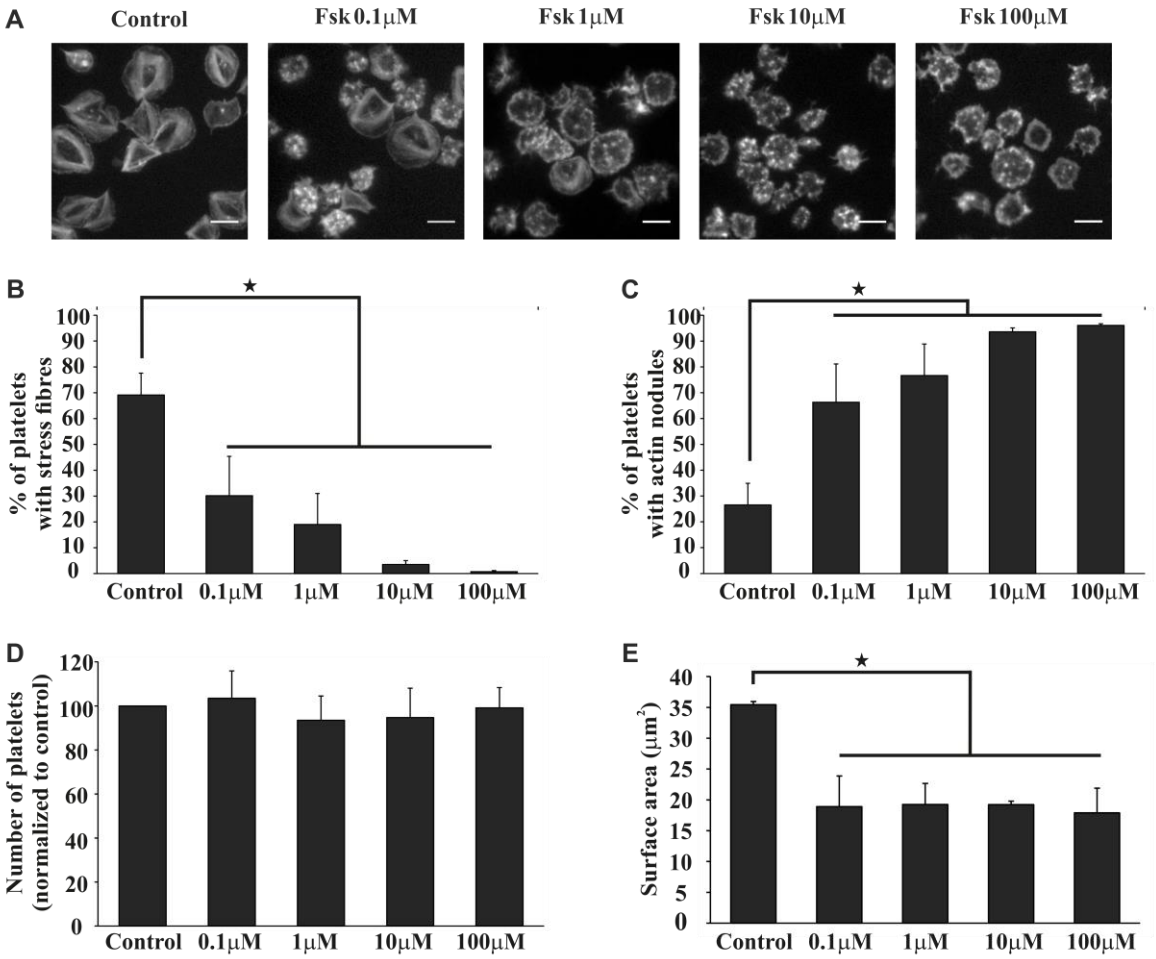

Figure 3. 4: Prior treatment with Fsk has an inhibitory effect on platelet spreading. Platelets ($2x10^7$/ml) were treated for 2 minutes with 0.1-100μM Fsk. They were then allowed to spread on 100μg/ml fibrinogen for 45 minutes, before washing, fixation and staining with FITC-phalloidin before being imaged on conventional microscope. **A)** Images are representative of three experiments. Scale bar is 5μm. **B)** The number of platelets containing stress fibres was calculated in control and Fsk treated samples. **C)** The number of platelets containing actin nodules was calculated in control and Fsk treated samples. **D)** The total number of platelets adhered, was calculated in control and Fsk treated samples. **E)** The average surface area of the spread platelets was identified in control and Fsk treated samples. The data was presented as average±SEM of n=3. $p<0.05$.

Fsk dropped to 3.50±1.50% and 100μM Fsk dropped to 0.76±0.43% of platelets. Similarly, a significant effect on the percentage of platelets containing actin nodules in comparison to the control was observed (Figure 3.4A and C). In the control 26.55±8.37% platelets contained actin nodules, which upon treatment with 0.1μM Fsk increased to 66.32±14.81%, 1μM Fsk increased to 76.65±12.24%, 10μM Fsk increased to 93.62±1.49% and 100μM Fsk increased to 96.08±0.65%. In agreement, the surface area reduced significantly from the control level of 35.43±0.54μm^2 to 18.90±4.97μm^2 at 0.1μM Fsk, 19.26±3.41μm^2 at 1μM Fsk, 19.22±0.58μm^2 at 10μM Fsk and 17.90±4.0μm^2 at 100μM Fsk (Figure 3.4E). No significant change in adhesion was observed (Figure 3.4D)

The difference between the effects of prior treatment of platelets with PGI_2 (Figure 3.3) and Fsk (Figure 3.4) is due to the stability of the molecule. PGI_2 has a short half-life and therefore over a 45 minute period its effect would have been reduced, whereas Fsk, which involves direct and continued activation of adenylyl cyclase, can cause a sustained inhibition of platelet spreading.

3.5: The effect of post incubation of PGI_2/Fsk on platelet spreading

My aim had been to try and observe the effects of PGI_2 on platelet spreading. However prior incubation of platelets did not identify clearly the effect of cAMP elevating agents on the cytoskeleton. Therefore, as Figure 3.1 identified that platelets were fully spread at 25 minutes post spreading, a series of experiments were designed to allow platelets to spread for 25 minutes, before the addition of PGI_2/Fsk at different doses and incubated for different time points. This would then allow for analysis of the actin structures in the presence of PGI_2. The slides were mounted and imaged on fluorescence microscope.

Platelets that had been allowed to spread for 25 minutes were treated with different doses of PGI_2 for 10 minutes, prior to fixation, staining and imaging (Figure 3.5A). Analysis of these images identified that increasing doses of PGI_2 caused a significant reduction in the percentage of platelets containing stress fibres, with the control containing 64.86±7.85% platelets with stress fibres. This was reduced to 33.54±14.3% with 1nM PGI_2. It continued to decrease and reach significance with 10nM PGI_2 to 2.55±1.20%, with 100nM PGI_2 to 1.75±0.52% and with 1000nM PGI_2 to 0.85±0.23% of platelets containing stress fibres (Figure 3.5B and C). A reciprocal increase in actin nodules was observed with increasing

dose of PGI_2. Starting at 30.76±6.66% platelets to have actin nodules at control conditions; that increased to 61.15±12.37% with 1nM PGI_2 and reached significance of 91.49±1.05% with 10nM PGI_2. This was maintained with 100nM PGI_2 (94.85±0.55%) and 1000nM PGI_2 (96.38±0.49%) (Figure 3.5B and D). Adhesion of platelets remained similar with treatment with different doses of PGI_2 (Figure 3.5E). However, the average surface area of the platelets reduced from 38.59±3.29μm^2 in the control to 24.86±5.33μm^2 at 1nM PGI_2, reached significance by 22.98±1.11μm^2 at 10nM PGI_2 and plateaued for 100nM PGI_2 (22.90±3.06μm^2) and 1000nM PGI_2 (21.83±0.55μm^2) (Figure 3.5B and F).

Using the schematic as shown in Figure 3.5A, spread platelets were treated with increasing concentrations of Fsk. Fsk being a positive control to the effects of PGI_2, acting via direct stimulation of adenylyl cyclase resulted in a similar response to that observed with PGI_2. There was a reduction from a control level of 64.86±7.85% of platelets containing stress fibres to reach significance of 26.66±14.74% at 0.1μM Fsk. This effect was strengthened at higher doses of Fsk with only 3.88±1.49% platelets containing stress fibres at 1μM Fsk, 2.29±1.33% at 10μM Fsk and 1.24±0.19% at 100μM of Fsk (Figure 3.6A and B). Similarly, a reciprocal increase was observed in actin nodules with a control level of 30.76±6.66% of platelets having actin nodules to 67.65±16.23% with 0.1μM Fsk. Again this effect was stronger with elevated levels of Fsk, with 91.31±2.12% platelets containing actin nodules with 1mM Fsk, 92.76±2.55% with 10μM Fsk and 96.51±1.29% platelets with actin nodules with 10μM Fsk (Figure 3.6A and C). Adhesion was not affected (Figure 3.6 D). However, in agreement with PGI_2 treatment, Fsk treatment induced a significant reduction in the average surface area from 43.32±2.81μm^2 in the control to 26.83±5.35μm^2 at 0.1μM, 22.53±3.39μm^2 at 1μM, 22.90±3.06μm^2 at 10μM and 22.20±4.98μm^2 at 100 μM of Fsk (Figure 3.6A and E).

Using the results from Figures 3.5 and 3.6, the dose of PGI_2 confirmed for further experiments was chosen to be 10nM PGI_2, and 1μM Fsk. In order to understand the longevity of the effect upon the actin cytoskeleton by PGI_2 and Fsk a timecourse (Figures 3.7 and 3.8) was now completed.

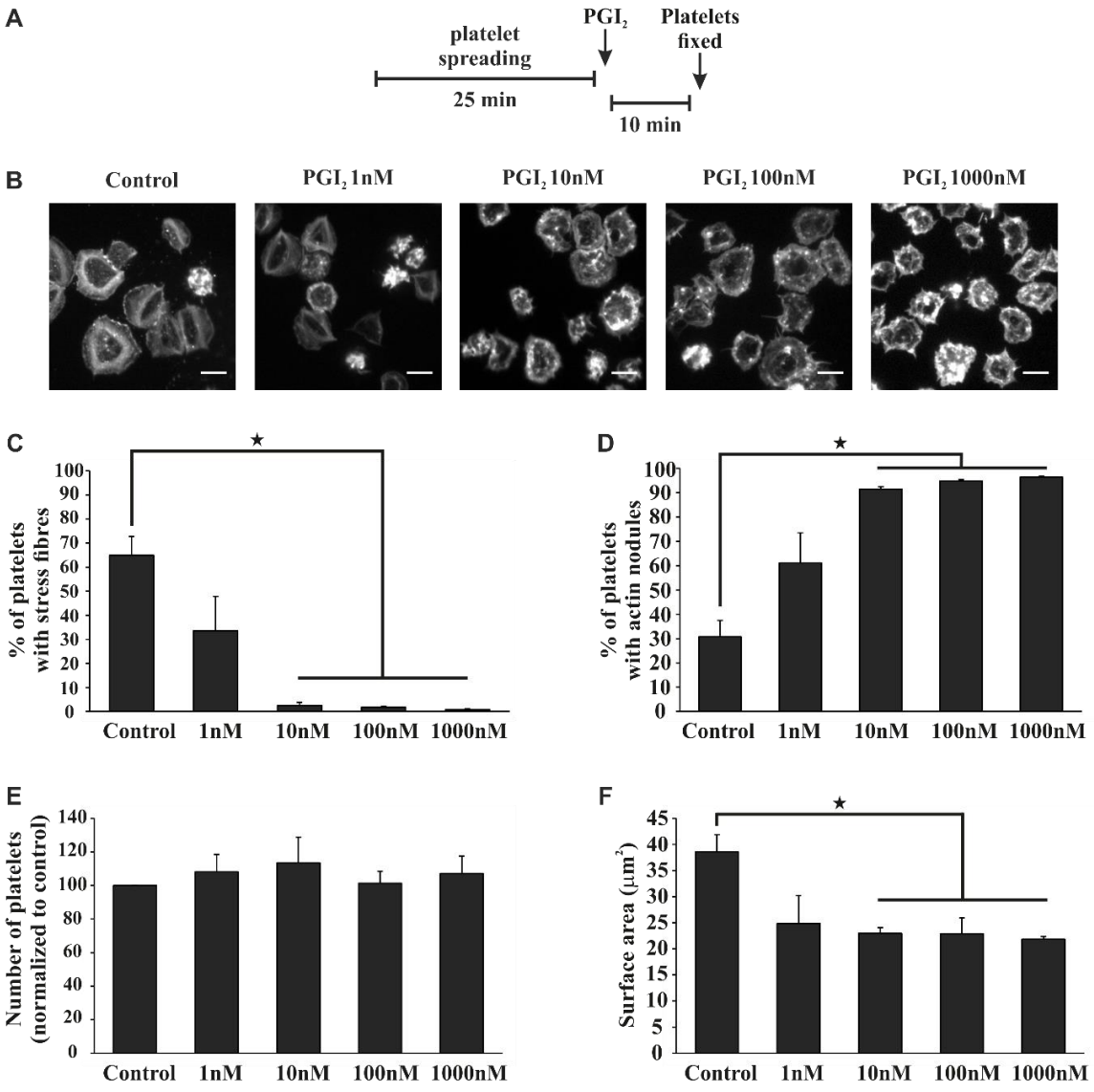

Figure 3. 5: Dose response of PGI_2 with spread platelets on fibrinogen. Platelets ($2x10^7$/ml) were spread on 100μg/ml fibrinogen for 25 minutes. The wells were washed with PBS, and 1-1000nM PGI_2 was added for a further 10 minutes, schematic shown in (**A)**. The platelets were then fixed and stained with FITC-phalloidin before being imaged on conventional microscope. **B)** Images are representative of three experiments. Scale bar is 5μm. **C)** The number of platelets containing stress fibres under different doses of PGI_2. **D)** The number of platelets containing actin nodules under different doses of PGI_2. **E)** The total number of platelets adhered, and **F)** the average surface area of the spread platelets was analysed for each dose. The data was presented as average±SEM of n=3. $p<0.05$.

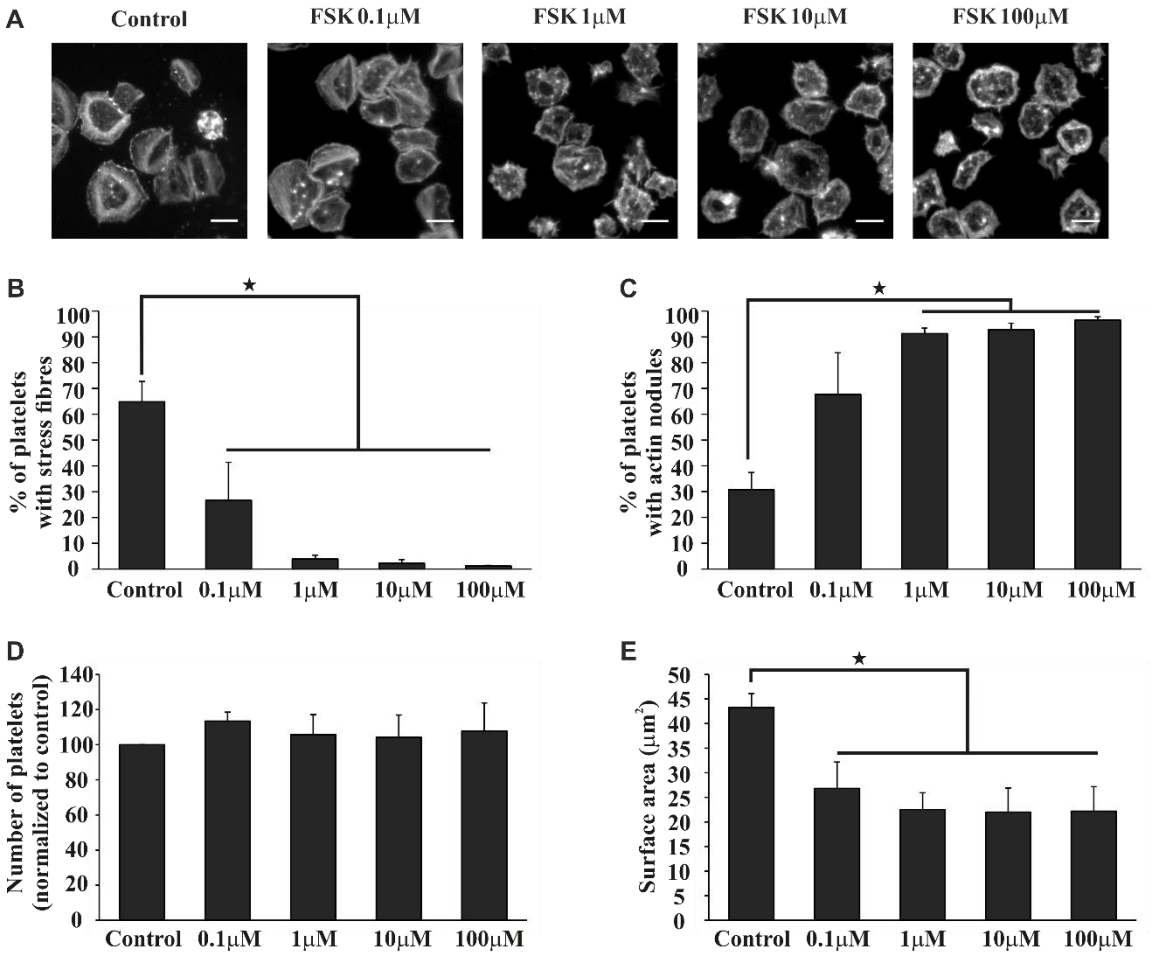

Figure 3. 6: Dose response of Fsk with spread platelets on fibrinogen. Platelets ($2x10^7$/ml) were spread on 100μg/ml fibrinogen for 25 minutes, before washing with PBS, and addition of 1-100μM Fsk, for a further 10 minutes. The platelets were then fixed and stained with FITC-phalloidin before being imaged on conventional microscope. **A)** Images are representative of three experiments. Scale bar is 5μm. **B)** The number of platelets containing stress fibres under different doses of Fsk. **C)** The number of platelets containing actin nodules under different doses of Fsk. **D)** The total number of platelets adhered, and **E)** the average surface area of the spread platelets was analysed for each dose. The data was presented as average±SEM of n=3. $p<0.05$.

Platelets ($2x10^7$/ml) were spread on 100μg/ml fibrinogen for 25 minutes prior to incubation with 10nM PGI_2 for duration of 2-60 minutes, as shown in the schematic in Figure 3.7A. The spread platelets were fixed at their respective time points, stained and visualized under Zeiss fluorescence microscope. For the time course with PGI_2, an individual control for each time point was also prepared for comparison. The bold bars in Figure 3.7C, D, E and F represent control samples at individual time points of the experiment, while the white bars represent treatment of spread platelets with PGI_2. It was identified that in a fully spread phenotype 69.16±8.22% spread platelets had stress fibres which were maintained across the control samples. However within platelet samples treated with PGI_2 the percentage of platelets containing stress fibres was reduced on treatment with PGI_2 at 2 minutes (29.5±13.34%), reaching a significant reduction at 5 minutes (8.37±4.58%). This significant reduction was maintained over 10 and 25 minutes (0% and 2.80±2.36%, respectively). However by 40 minutes the effect of PGI_2 was reducing allowing recovery of stress fibre formation with 27.2±10.41% of platelet containing stress fibres, which recovered to 49.27±1.24% at 60 minutes of PGI_2 stimulation (Figure 3.7B and C). The percentage of platelets having actin nodules increased from 18.52±4.94% in fully spread form to 38.3±14.50% at 2 minutes and continued to rise to a significant level of 83.4±0.85% at 10 minutes, after that it started reducing to 57.87±8.27% at 40 minutes and reached insignificance 39.27±3.26% by 60 minutes (Figure 3.7B and D).

Interestingly there is also an effect upon the surface area of the spread platelet that reduced from 32.34±2.13μm^2 to 24.65±0.83μm^2 at 2 minutes, reaching significance by 24.18±1.14μm^2 at 10 minutes of PGI_2 treatment. The decrease in the surface area reached its minimum of 18.17±0.74μm^2 at 25 minutes and started easing back up to 22.23±0.72μm^2 at 40 minutes and returned to a comparable level as the control of 34.02±0.69μm^2 at 60 minutes post PGI_2 stimulation. This indicated that the loss of stress fibres is also associated with a subsequent reduction in surface area (Figure 3.7B and F). However, at all time points there was no change in adhesion of the platelets (Figure 3.7E).

This effect of maximal stress fibre inhibition with maximal attainment of actin nodules by 10 minutes of PGI_2 treatment with a reversal achieved by 60 minutes of stimulation, demonstrate the reversibility of the effect of PGI_2 on the platelet actin cytoskeleton.

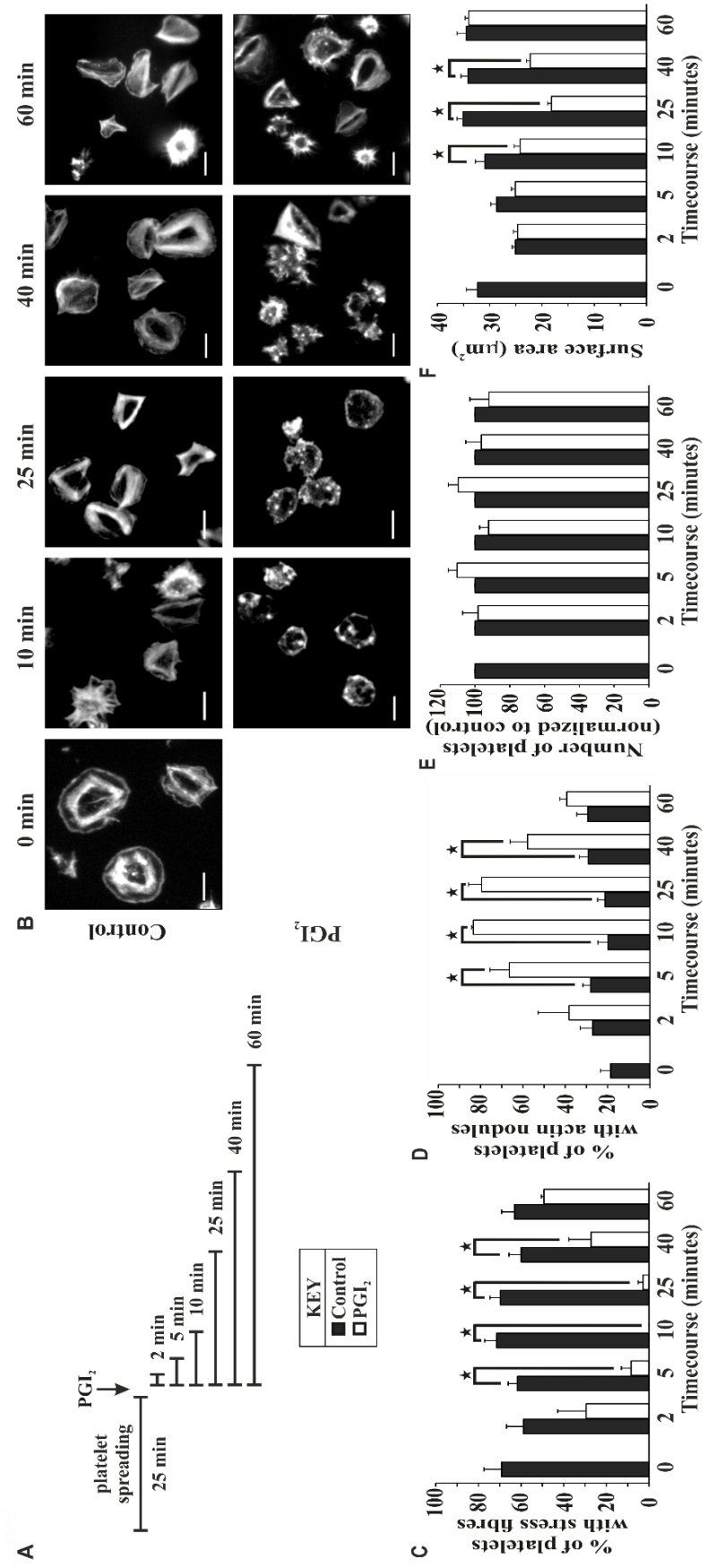

Figure 3. 7: Post treatment of PGI_2 induces stress fibre reversal and actin nodule formation in platelets spread on fibrinogen in a time dependent manner. Platelets ($2x10^7$/ml) were spread on 100μg/ml fibrinogen for 25 minutes, washed with PBS, and then 10nM of PGI_2 was added, for a further 2-60 minutes. The platelets were then fixed, stained and imaged on conventional microscope. **A)** Representative images of each condition of the experiment. **B)** The number of spread platelets containing stress fibres in control and PGI_2 treated samples. **C)** The number of spread platelets containing actin nodules in control and PGI_2 treated samples. **D)** The total number of spread platelets in control and PGI_2 treated samples, normalised to their individual controls. **E)** The average surface area of the spread platelets was analysed for each timepoint in control and PGI_2 treated samples. Analysis was performed using Image J. The data was presented as average±SEM of n=5. $p<0.05$. Scale-bar 5μm.

Using the schematic in Figure 3.7A, the spread platelets were fixed at their respective time points, stained and visualized under Zeiss fluorescence microscope. Controls for individual time points during the time course with Fsk were prepared for comparison. Similarly the bold bars in Figure 3.8 represent control samples at individual time points of the experiment which remained steady, while the white bars represent treatment of spread platelets with Fsk.

In a control sample, 69.16±8.22% spread platelets had stress fibres, after 25 minutes of spreading. This was reduced on treatment with Fsk to 60.25±14.09% at 5 minutes, reaching significance at 10 minutes of 21.24±5.03%, which continued to reduce to 15.84±5.9% at 25 minutes and reached a minimum level of 3.08±1.01% at 40 minutes (Figure 3.8A and B). The percentage of platelets having actin nodules steadily increased from 18.52±4.94% in the control sample to 34.22±12.49% at 5 minutes to a significant level of 72.65±4.98% at 10 minutes, 81.26±5.31% at 25 minutes, 93.47±0.97% at 40 minutes and 95.64±0.86% by 60 minutes (Figure 3.8A and C). In agreement with these actin cytoskeletal changes, Fsk significantly reducing the surface area of the spread platelets from 35.40±1.92μm^2 to 29.92±1.49μm^2 at 10 minutes, 27.49±1.04μm^2 at 25 minutes, 30.09±1.28μm^2 at 40 minutes and 30.55±1.77μm^2 at 60 minutes of treatment (Figure 3.8A and E). Interestingly at 25 and 40 minutes of Fsk stimulation the adhesion was significantly affected. However, this effect reversed back at 60 minutes of treatment (Figure 3.8D).

In order to understand if this effect was mediated by PGI_2 modulating the secretion of ADP or TXA_2, platelets ($2x10^7$/ml) were incubated in the presence of apyrase and indomethacin for 2 minutes prior to spreading them on 100μg/ml fibrinogen for 25 minutes. The spread platelets were then treated with 10nM PGI_2 for a duration of 10 minutes, similar to the schematic in Figure 3.5A. The spread platelets were fixed, stained and visualized under Zeiss fluorescence microscope. A separate control for each of the respective conditions with PGI_2 was prepared for comparison. Similar to Figure 3.7, the bold bars in Figure 3.9 represent control samples at individual time points of the experiment while the white bars represent treatment of spread platelets with PGI_2. It was identified that the control samples without apyrase and indomethacin had 71.52±5.52% of platelets containing stress fibres, which in the presence of apyrase and indomethacin had reduced to 59.05±1.76% platelets with stress fibres at 10 minutes post spreading (Figure 3.9A and B). Treatment of spread

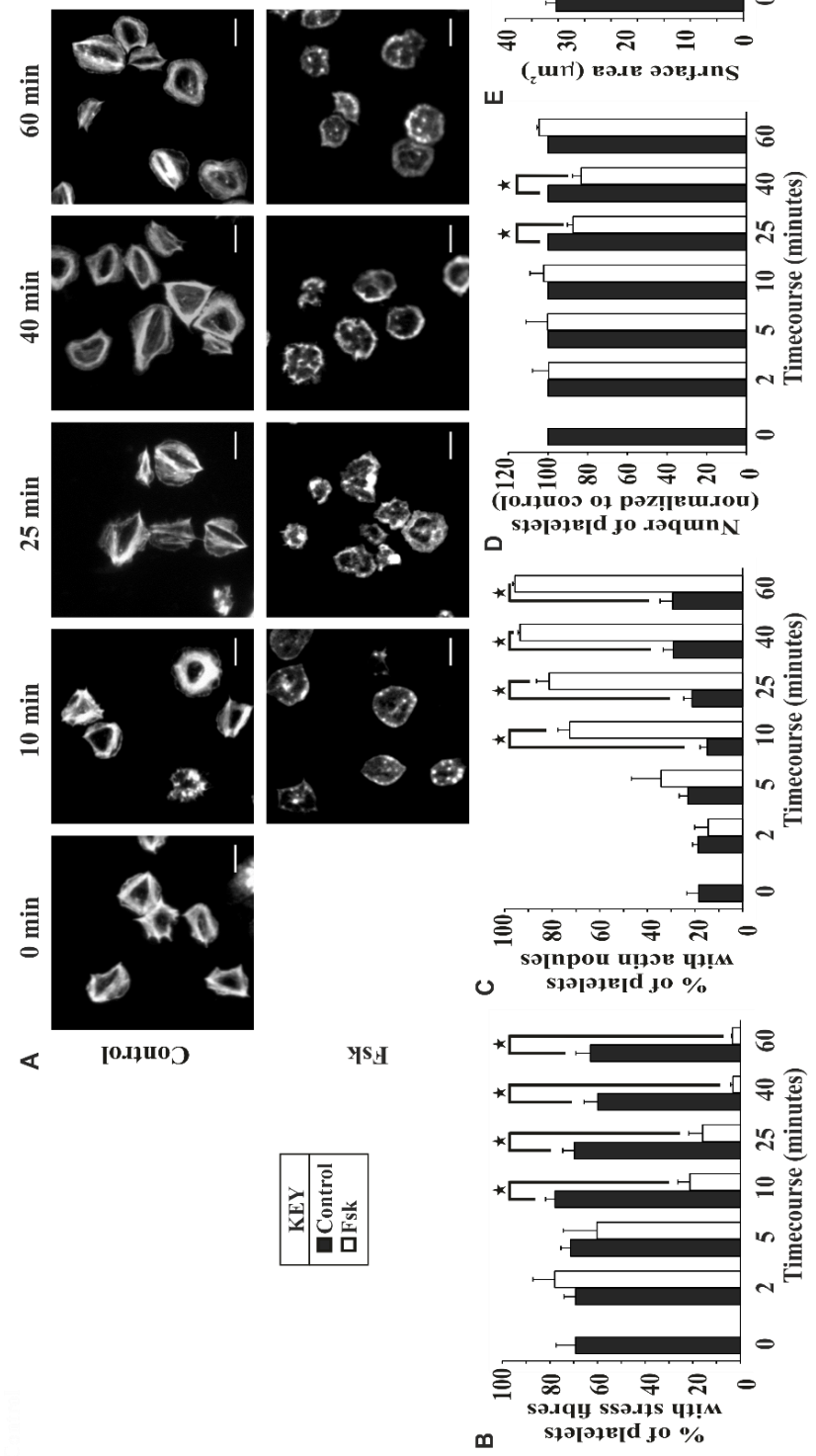

Figure 3. 8: Post treatment of Fsk induces stress fibre reversal in platelets spread on fibrinogen in a time dependent manner. Platelets ($2x10^7$/ml) were spread on 100μg/ml fibrinogen for 25 minutes, before being washed with PBS, and then 1μM Fsk was added, for a further 2-60 minutes. The platelets were then fixed and stained with FITC-phalloidin before being imaged on conventional microscope. **A)** Representative images from three separate experiments. Scale-bar 5μm. **B)** The number of spread platelets containing stress fibres was identified in control and Fsk treated samples. **C)** The number of spread platelets containing actin nodules was identified in control and Fsk treated samples. **D)** The average surface area of the spread platelets was analyzed for each timepoint in control and Fsk treated samples using Image J. The data was presented as average±SEM of n=3. $p<0.05$.

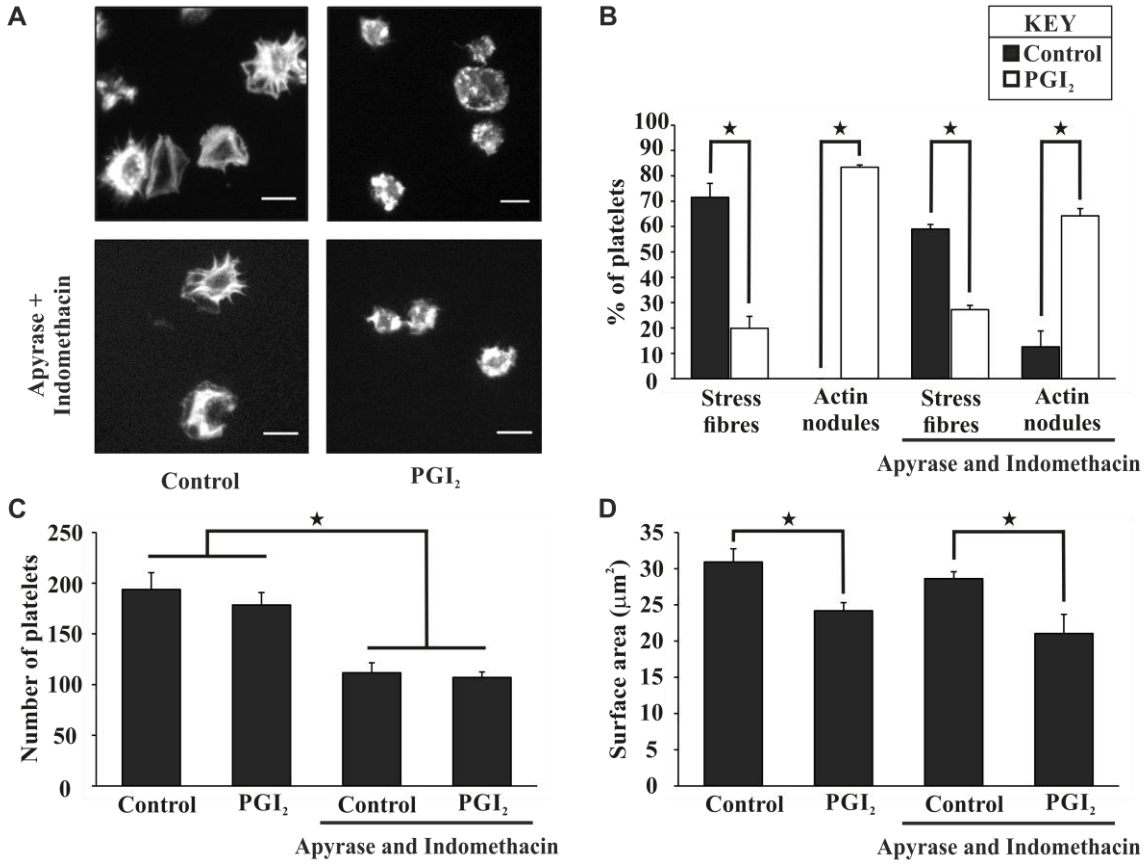

Figure 3. 9: Post treatment of PGI_2 induces stress fibre reversal and actin nodule formation in platelets spread on fibrinogen in the presence of apyrase and indomethacin. Platelets ($2x10^7$/ml) were spread on 100μg/ml fibrinogen for 25 minutes in the presence of apyrase and indomethacin, washed with PBS, and then 10nM of PGI_2 was added with apyrase and indomethacin, for a further 10 minutes. The platelets were then fixed and stained with FITC-phalloidin before being imaged on conventional microscope. **A)** Representative images from three separate experiments. Scale-bar 5μm. **B)** The number of spread platelets containing stress fibres was identified in control and PGI_2 treated samples, in the presence or absence of apyrase and indomethacin. **C)** The number of spread platelets containing actin nodules was identified in control and PGI_2 treated samples, in the presence or absence of apyrase and indomethacin. **D)** The average surface area of the spread platelets was analysed in control and PGI_2 treated samples, in the presence or absence of apyrase and indomethacin. Analysed using Image J. The data was presented as average±SEM of n=5. $p<0.05$.

platelets with PGI_2 revealed that no platelets had stress fibres. However in the presence of apyrase and indomethacin the PGI_2 reduced the percentage of platelets containing stress fibres to 12.6±6.21%. In agreement there was a strong increase of platelets containing actin nodules from 19.88±4.71% in the control to 83.4±0.85% upon treatment of spread platelets with PGI_2. However, in the presence of apyrase and indomethacin this increase in the percentage of platelets with actin nodules was less pronounced from 27.25±1.67% to 64.2±2.86% on treatment with PGI_2 (figure 3.9A and B).

A similar reduction in surface area was observed with control from 30.92±1.82μm^2 to 24.18±1.14μm^2 on treatment with PGI_2 (figure 3.9D). In the presence of apyrase and indomethacin the surface area in the control sample reduced from 28.62±0.96μm^2 to 21.04±2.66μm^2 on treatment with PGI_2 (figure 3.9D).

Further to this although, the effect of treating platelets with apyrase and indomethacin reduced the number of platelets adhering on fibrinogen, the addition of PGI_2 did not affect platelet adhesion in the presence or absence of apyrase and indomethacin (figure 3.9C). Therefore, in the presence of apyrase and indomethacin there was no significant change in the effectiveness of PGI_2 to modulate the actin cytoskeleton.

3.6: Does PGI_2 and Fsk stimulation induce the actin nodule?

Both PGI_2 and Fsk stimulation of spread platelets induced an increase in punctate areas of actin staining. This was presumed to be the actin structure, the actin nodule. The actin nodule is a filamentous actin structure that has been characterized by Calaminus (2008), to appear during an early phase of platelet spreading on fibrinogen. These nodules localise multiple proteins such as Arp2/3, beta-integrins, Fyn, moesin, cortactin, talin, p-Tyr, Rac, WASp (Calaminus et al., 2008, Poulter et al., 2015), and have been implicated in thrombus formation. However the mechanisms by which they are formed and dissolved are not well understood.

Therefore in order to prove that the punctate actin structures induced by PGI_2 and Fsk were indeed actin nodules, platelets were allowed to spread, before stimulation with PGI_2 and Fsk for 10 minutes, before fixation, and staining with the actin nodule markers, WASp, Arp2/3 and pTyr. Analysis of the images clearly indicates that the areas of punctate actin

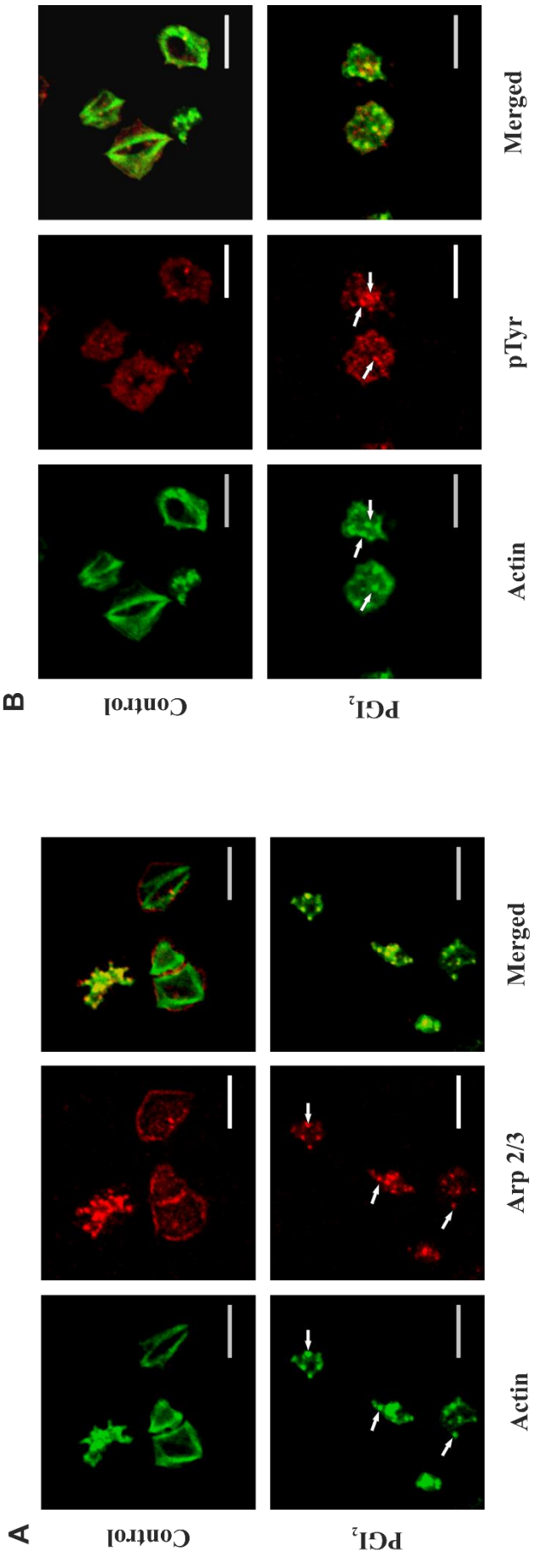

Figure 3. 10: Confirmation of the presence of Actin nodules. Platelets ($2x10^7$/ml) were spread on 100µg/ml fibrinogen for 25 minutes before being washed with PBS. The platelets were then treated with Tyrodes with or without 10nM PGI_2 for a further 10 minutes. The platelets were then fixed, lysed and stained for either **A)** Arp2/3 (1:1000) or **B)** pTyr (1:1000); and co-stained with actin (FITC-Phalloidin) for 60 minutes, before mounting and imaging the slides on confocal microscope. Images are representative of at least 3 experiments. Scale bar is 5µm.

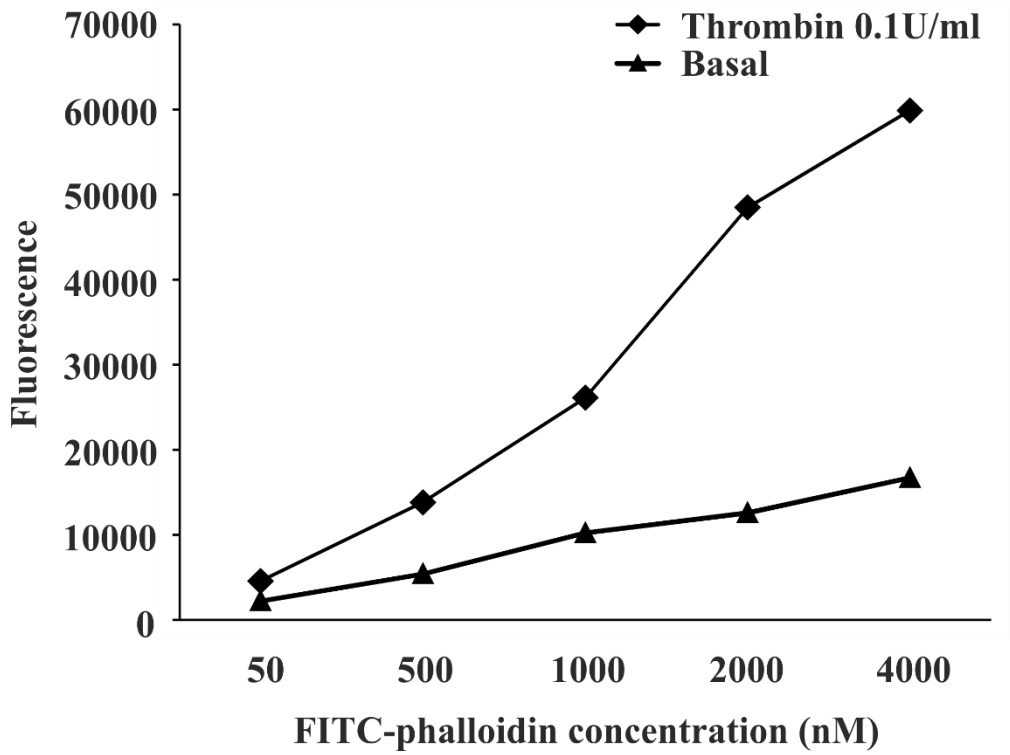

Figure 3. 11: An increase in filamentous actin detected with an increasing dose of FITC-phalloidin used on treating platelets with thrombin Using 200µl of platelets (2 $x10^8$ /ml), the amount of FITC-phalloidin was ascertained that would give an appreciable change upon stimulation of suspended platelets with 0.1U/ml of thrombin for 1 minute. A dose of 2000nM FITC-phalloidin was identified to be used for further experiments. The experiment was performed once.

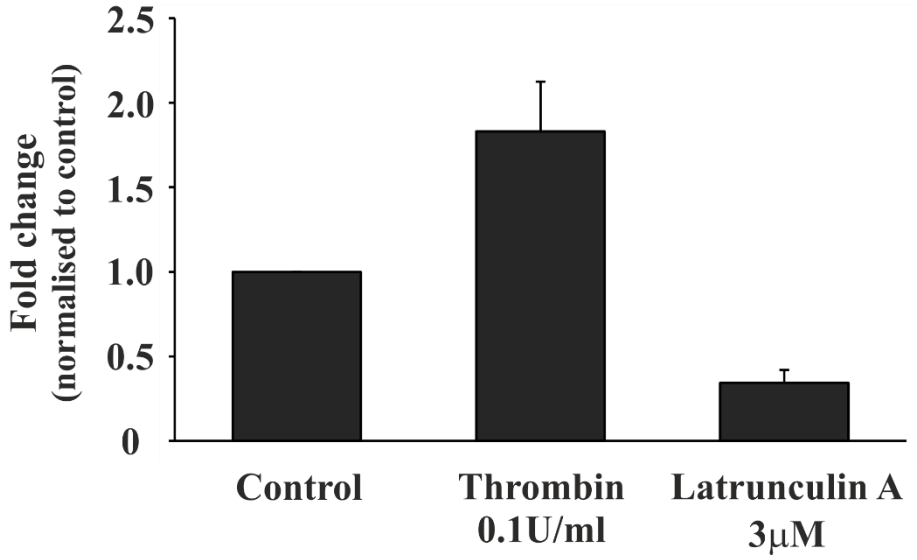

Figure 3. 12: A confirmation that the increase in fluorescence with thrombin stimulation was due to filamentous actin formation. Using 200μl of platelets (2 $x10^8$ /ml), the amount of FITC-phalloidin was assessed in suspended platelets. The suspended platelets were treated with either 0.1U/ml of thrombin (acts as a positive control) or 3μM of Latrunculin A (acts as a negative control) and assessed for the level of filamentous actin. The data was presented as average±SEM of n=3.

staining induced by PGI_2 treatment co-localised with Arp2/3 and pTyr and so are actin nodules (Figure 3.10A, B and C).

3.7: Does PGI_2 stimulation modulate actin polymerisation?

As there was a clear modulation of the actin cytoskeleton by PGI_2 and Fsk, it was necessary to understand if this modulation was due to alterations in actin polymerisation or if it was the interconversion from one form of filamentous actin to another which resulted in changes in actin structures within the platelets. Therefore to answer this question it was necessary to identify the level of F-actin within control, PGI_2 and Fsk treated samples.

Therefore initially to identify the concentration of FITC-phalloidin that provided a significant change between basal and stimulated situations, washed human platelets ($2x10^8$/ml) were treated with 0.1U/ml of thrombin for 1 minute before fixation and staining them with different concentrations of FITC-phalloidin (50 – 4000nM) (Figure 3.11). This identified that a dose of 50nM FITC-phalloidin was enough to stain the available filamentous actin in the cell at its basal level only, as no appreciable increase in the treatment with thrombin was noted. Increasing the dose of FITC-phalloidin led to an increased level of fluorescence, indicative of increased F-actin within the thrombin stimulated samples. Therefore to quantify an increase in F-actin concentration and to get an optimum response a dose of 2000nM FITC-phalloidin was selected for subsequent experiments.

To ensure the correct conditions for the assay, platelets in an unstimulated condition along with stimulation by a positive control (0.1U/ml Thrombin) or an F-actin polymerization inhibitor Latrunculin A (3μM) were prepared and assessed for their fluorescence. Figure 3.12, demonstrates that Thrombin induced a robust elevation of F-actin, whilst Latrunculin A treated samples disrupted F-actin leading to a reduction in the fluorescence.

Although the conditions were now correct in order to identify the basal levels of F-actin within spread platelets, it was necessary to link the level of F-actin fluorescence to protein level. Therefore platelets in suspension ($1.0x10^8$/ml to $8.0x10^8$/ml) were fixed, stained and analyzed for both fluorescence (Figure 3.13A) and protein concentration (Figure 3.13B). The level of protein could then be analyzed alongside the level of F-actin fluorescence (Figure 3.13C). This graph could be used to identify the basal level of fluorescence in spread platelet samples of the same protein concentration.

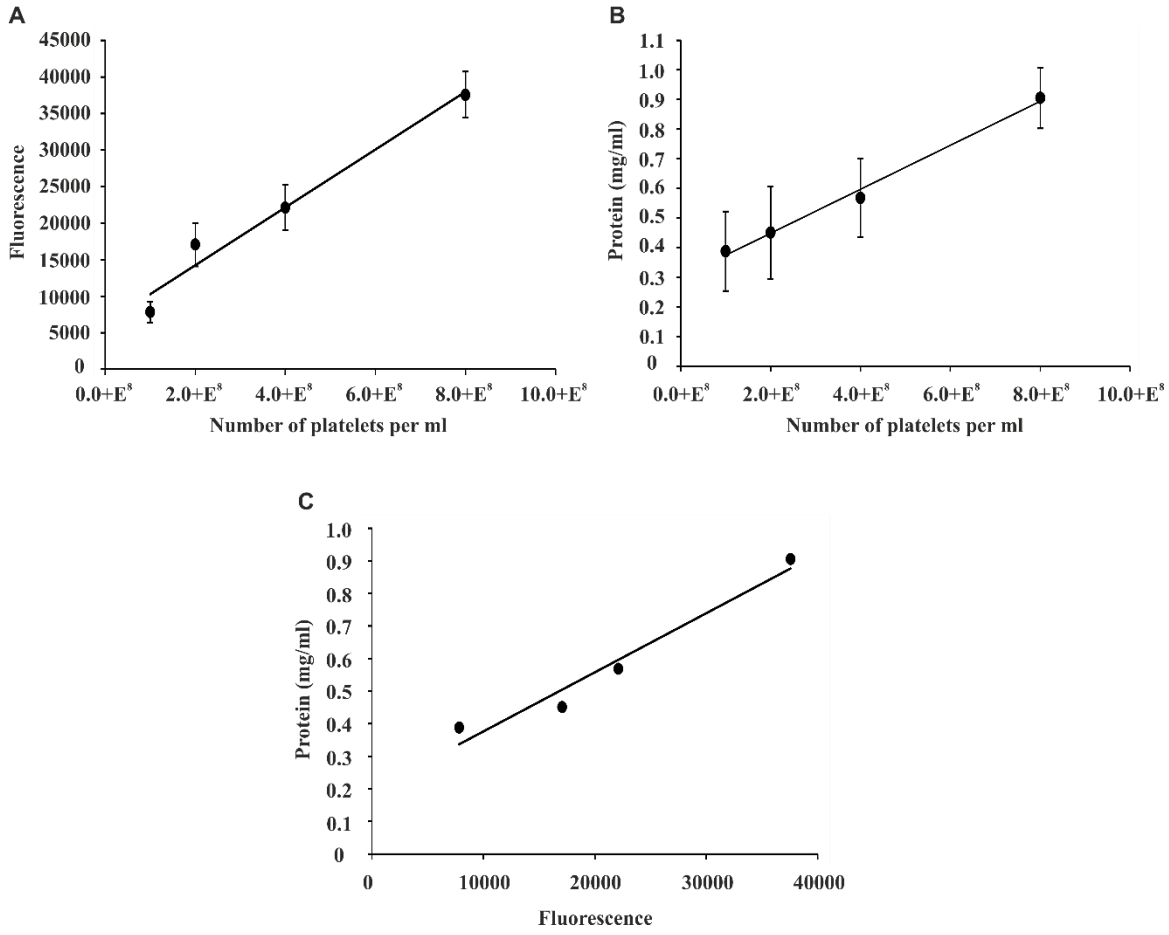

Figure 3. 13: Increase in the level of filamentous actin with increasing concentration of suspended platelets. Using 200µl of platelets ($1x10^8$ to $8x10^8$), the amount of proteins and the level of filamentous actin were analyzed using a spectrophotometer. **A)** Amount of fluorescence obtained using different concentrations of platelets in suspension. **B)** Amount of proteins obtained using different concentrations of platelets in suspension. **C)** Amount of protein was plotted against the level of fluorescence obtained using different concentrations of platelets in suspension. The data was presented as average±SEM of n=3.

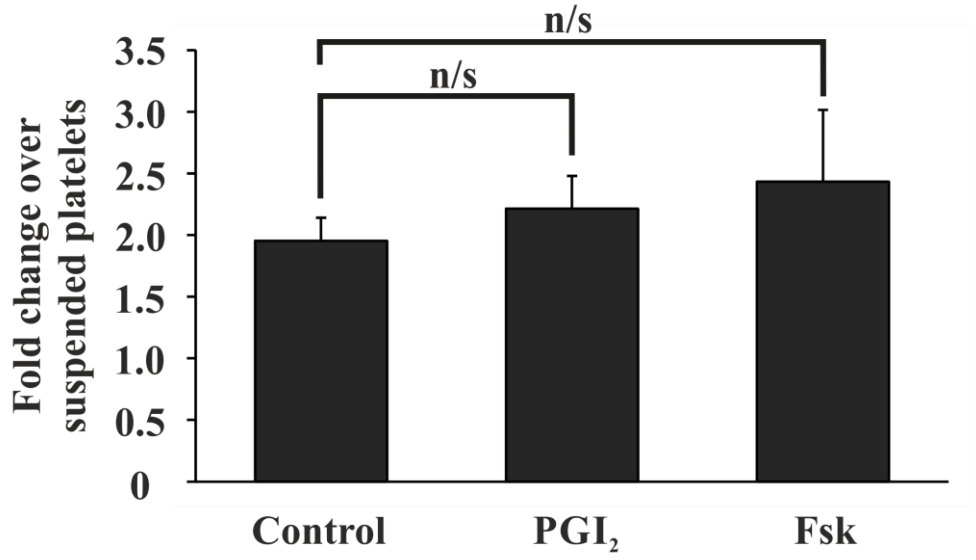

Figure 3. 14: Increased levels of filamentous actin in spread platelets. Using 3ml of 2 $x10^8$ platelets/ml, the amount of FITC-phalloidin was assessed in suspended and spread platelets. Platelets spread on fibrinogen (100μg/ml) for 25 minutes were treated with 10nM PGI_2 or 1μM Fsk for 10min and assessed for the level of filamentous actin. The results were normalized to the level of filamentous actin in basal suspended platelets. The data was presented as average±SEM of n=3. (n/s= non-significant)

Using the above conditions, washed platelets ($2.0x10^8$/ml) were spread for 25 minutes on fibrinogen coated 6 well plates, prior to stimulation for 10 minutes with either PGI_2 (10nM) or Fsk (1μM). Fluorescence and protein concentration are determined for these spread platelets. The basal level of fluorescence for these samples was calculated from using the graph in figure 3.13C, using the protein concentration value identified from spread platelets. This was then compared to the level of F-actin from the spread samples in order to obtain the fold change in F-actin production from basal to spread platelets. The analysis indicated that spread platelets had a 1.95±0.19 fold increase of F-actin when compared to their basal equivalents. Treatment of spread platelets with cAMP elevating agents had no effect on actin polymerisation with a 2.21±0.27 fold increase with PGI_2 and a 2.43±0.58, fold increase in the presence of Fsk. Therefore, PGI_2 and Fsk do not affect the actin polymerisation within the spread platelet (Figure 3.14).

3.8: Discussion:

This chapter focuses on platelet spreading and how it is modulated by the PKA activating agents, PGI_2 and Fsk. The cAMP/PKA pathway has been previously shown to modulate the actin cytoskeleton of various cell types, including neurons, fibroblasts, smooth muscle cells, epithelial and endothelial cells; both in an inhibitory and activatory manner (Birukova et al., 2007, Bulin et al., 2005, Dong et al., 1998, Ramakers and Moolenaar, 1998, Edwards et al., 1993, Whelan and Senger, 2003, Dormond and Ruegg, 2003). A study by Aburima A et al. (2013) identified the role of cAMP signaling in inhibiting shape change in suspended platelets, but the effect of PGI_2 on spread platelets had not been identified to-date.

Initially before understanding the effect of PGI_2 or Fsk on platelet spreading, the process of platelet spreading in normal conditions needed to be understood. Therefore, platelets were studied in a static system by placing them on immobilized fibrinogen and allowing them to spread. The changes in the actin cytoskeleton were observed for the time profile of platelet spreading. It was identified that 25 minutes provided enough time for human platelets to achieve a completely spread profile (i.e. maximal number of platelets to have attained stress fibres). These results agree with the findings of other groups that have used a 30 minute time point for obtaining fully spread platelets (Poulter et al., 2015, Peters et al., 2012). Although literature does suggest some people to have used much longer time points (upto 2 hours) for observing the spreading of platelets, our data suggests that above 30 minutes there are no significant changes in platelet morphology across the whole population (Naik and Naik, 2003, O'Brien et al., 2012).

In order to identify the role of PGI_2 and Fsk on platelet spreading, platelets were initially pretreated with PGI_2 or Fsk and were allowed to spread on immobilized fibrinogen for 45 minutes, as suggested by the literature (Borgognone et al., 2014). My findings reveal a negligible effect on platelet cytoskeletal changes and surface area, unless PGI_2 was used at a high concentration (1000nM). This finding is in agreement with Borgognone et al. (2014) who similarly identified that a high dose of 1000nM PGI_2 inhibited aggregation and similarly pretreatment of platelets with this dose of PGI_2 reduced thrombin stimulated platelet spreading without any change to platelet adhesion. Furthermore, Siess W. et al (1989) identified PGI_2 at a dose of 500ng/ml (1418.6nM) inhibited platelet aggregation in suspension, whilst Higgs et al using an *in-vivo* model identified greater than 1000nM PGI_2, reduced platelet adhesion stimulated with ADP (Higgs et al., 1978). The negligible effect

of PGI_2 on platelet spreading was linked to it being quickly hydrolysed in aqueous solutions within 3 minutes (Horton et al., 2005).

Therefore, it was conceptualised to track the effect of PGI_2 on already spread platelets. The platelets were allowed to spread on fibrinogen for 25 minutes and then treated with PGI_2 in a dose dependent manner. It was identified that a 10 minute treatment of these spread platelets with 10nM PGI_2 significantly altered the actin cytoskeleton, reversing stress fibre formation and initiating actin nodule formation in spread platelets. This dose is in agreement with similar doses that affect platelet function, for example 2nM of PGI_2 inhibits aggregation and shape change in platelets induced via ADP or TXA_2 (Ehrman and Jaffe, 1980), whilst 6nM PGI_2 caused disaggregation of collagen stimulated platelets in suspension (Radomski et al., 1987a). Interestingly, FitzGerald G.A. et al. published an estimated concentration of PGI_2 in the human circulation to be 3.4pg/ml (10pM) (FitzGerald et al., 1981). Furthermore FitzGerald G.A. et al identified for platelets to be inhibited from aggregation, the threshold PGI_2 concentration required in the body was 36pg/ml (0.1nM) (FitzGerald et al., 1981).

Identifying that a low dose of PGI_2 could reorganize the actin cytoskeleton of spread platelets, a timecourse study was employed to identify the sustained nature of this effect. This timecourse analysis identified that 10 minutes after treatment with 10nM PGI_2 there was a maximal effect on the reversal of stress fibres and the formation of the punctuate actin structure, the actin nodules. Interestingly, this effect of PGI_2 was reversed by 60 minutes post stimulation. Although PGI_2 has a short half-life of 3 minutes, even after its degradation its effects on spreading lasted until 40 minutes post stimulation. This long time course of PGI_2 is due to the effect of the second messenger used by the IP receptor. The IP receptor is linked to the heterotrimeric G-protein coupled receptor complex, $G\alpha$ and $\beta\gamma$. The type of $G\alpha$ identifies if it should increase or decrease an effect. The $G\alpha$ linked with PGI_2 stimulates production of cAMP in a spatial and temporal manner. Therefore, although PGI_2 would have had already been degraded, until cAMP would not have been degraded and PKA substrates dephosphorylated, PGI_2's effect would continue.

The cAMP signaling network is a complex arrangement, due to the variety in the available isoforms of adenylyl cyclase, PKA, and PDEs in platelets (Raslan et al., 2015a). The relative activities of the adenylyl cyclases and the PDEs determine the amount of cAMP in a platelet which thereby modulates the level of PKA and hence the amount of downstream

phosphorylation of proteins. Reflective of these variations and their spatial locations within the platelet, the level of phosphorylation of the PKA substrates differ. Some proteins such as $VASP^{Ser157}$ gets phosphorylated quickly and returns back to its non-phosphorylated form in a matter of minutes while $RhoA^{Ser188}$ had been identified to have a slow increase in the phosphorylation but this phosphorylated state continues for more than an hour, as had been shown in suspended platelets by Aburima A. *et al* (2013).

PGI_2 mediates its effects via a cAMP dependent mechanism, as already identified by Moncada et al (1976). To confirm the findings obtained by the timecourse of PGI_2 on spread platelets, a similar treatment was employed with Fsk, a direct activator of adenylyl cyclase. It resulted in a sustained inhibition of platelet spreading, observed with a significant shift from the removal of platelet stress fibres and the major presence of platelets with actin nodules. As both, PGI_2 and Fsk, work via the same downstream mechanism of elevating cAMP, it confirmed that the reversal of stress fibre formation was a cAMP dependent process.

In order to identify if secretion affected the response of the spread platelets to cAMP elevating agents, platelets were spread and stimulated with PGI_2 in the presence of apyrase and indomethacin, to inhibit ADP and TXA_2 respectively. The presence of apyrase and indomethacin slowed the spreading response. This identified that although ADP and TXA_2 do not affect the spreading of platelets directly, rather the reduction in cAMP caused by them had helped platelets to spread better; as had been identified in Chapter 4 figure 4.4.

It was identified that spread platelets do respond to PGI_2, both in the presence and absence of apyrase and indomethacin. The attained response was similarly significant for the changes in actin structures caused by PGI_2 in either of the two conditions. This signifies that secretion possibly does not impact on the effects caused by PGI_2 on the actin cytoskeleton. A possible difference arises during agonist-mediated platelet activation that leads to an inside-out integrin signaling. This tier of platelet activation is closely followed by α-granule secretion which further amplifies platelet activation and integrin outside-in signaling that culminates in the spreading of platelets. This would imply that secretion does have a role to play in spreading of platelets depending upon the type of integrin activation.

Platelet spreading involves the reorganization of the actin cytoskeleton which forms the scaffolding for the observed effects seen during the shape change of the platelets. The actin

structures formed during platelet shape change included filopodia, lamellipodia, actin nodules and stress fibres. Actin nodules appear at the initial phase of platelet spreading while stress fibres are the final actin rearrangement usually associated with the end stage of platelet spreading. The actin nodules tend to have an inversely proportional relationship to the presence of stress fibres. They are both filamentous actin structures as they are stained by phalloidin (Buchwalow and Bocker, 2010). It was necessary to make sure that the punctate area of filamentous actin, appearing regularly with PGI_2 and Fsk treatment, which were stained by phalloidin was actually the actin nodule identified by Calaminus et al (2008). After staining them for the Arp2/3 complex, pTyr and WASp (data not shown), it was confirmed that these punctuate areas were actin nodules.

As PGI_2 was inducing a significant effect on the actin cytoskeleton of the spread platelet, it was necessary to identify if this was due to an effect by PGI_2 on the ability of the platelet to maintain the correct level of actin polymerisation to maintain its fully formed actin structures. Therefore, F-actin assay was undertaken, which identified the effect of PGI_2 and Fsk on the F-actin polymerisation was not significant. The interpretation of this data alongside the rearrangement of actin induced by PGI_2, indicated that PGI_2 was targeting the actin cytoskeleton in a specific manner that caused reversal of stress fibre formation via mechanism other than alteration of the level of actin polymerisation.

Therefore, this chapter identified that platelets respond to immobilized fibrinogen by an outside-in activation of integrins, leading to the formation of various actin structures that reorganises into the formation of stress fibres in a fully spread platelet. Furthermore, PGI_2 treatment of a fully spread platelet interconverts the stress fibres to form another actin structure present in the initial stages of platelet spreading, the actin nodule, independent of secretion or any effect on the level of actin polymerization. This identified that PGI_2 can not only inhibit platelet activation in suspension prior to activation, but that once platelets are activated they are still able to respond to PGI_2, resulting in the alteration of actin cytoskeletal structures.

CHAPTER 4:

The role of PKA in the control of RhoA and stress fibre formation

4.1 Introduction:

PGI_2 induces cellular responses via its prostanoid IP-Receptor. IP-R is associated with a $G\alpha_s$ intracellular component, which upon stimulation leads to triggering of adenylyl cyclase, causing an increase in conversion of ATP to cAMP (Gorman et al., 1977, Tateson et al., 1977). The rise in the levels of cAMP promotes the activation of Protein Kinase A (PKA). The activation of PKA in the cell causes phosphorylation of a multitude of downstream proteins such as Rap1B, Rap1GAP, RhoA, $G\alpha_{13}$, IP_3-R, PDE3A, GPIbβ, GSK3α/β, VASP, Lim and SH_3 domain proteins (LASP), Heat shock protein 27 (HSP27), FilaminA and Caldesmon (Lang et al., 1996, Smolenski, 2012, Beck et al., 2014, Aburima et al., 2013).

The phosphorylation of these identified PKA substrates causes an inhibition of platelet function, and also antagonises agonist induced platelet activation (Walter et al., 1993). They could be classified as inhibitors of G-proteins (Rap1B, Rap1GAP, $G\alpha_{13}$ and possibly direct inactivation of RhoA), regulators of negative feedback control of cAMP (PDE3A) and modulators of actin dynamics in platelets (VASP, LASP, HSP27, FilaminA and Caldesmon) (Aburima et al., 2013, Beck et al., 2014, Smolenski, 2012, Lang et al., 1996).

For this study, VASP and RhoA were chosen as key targets for PKA phosphorylation that are associated with the actin cytoskeleton (Thomson et al., 2011, Zhang et al., 2014). VASP serves as a downstream effector of PKA activity (Walter et al., 1993). It is an actin regulatory protein which binds to the barbed end of the filamentous actin and facilitates its elongation (Bear and Gertler, 2009, Thomson et al., 2011). It correlates well, in its phosphorylated form, with the inhibitory status of the platelet (Walter et al., 1993, Zhang et al., 2014). RhoA is also a downstream effector of PKA activity (Chardin et al., 1989). It is implicated in stress fibre formation. It has previously been shown, both in platelets and other cell types that the inhibition of RhoA via C3 exoenzyme derived from *Clostridium botulinum* affects cell spreading by inhibiting stress fibre formation (Aburima et al., 2013, Chardin et al., 1989, Gorman et al., 1977). PGI_2 has been shown to cause phosphorylation of RhoA in a sustained manner (Aburima et al., 2013). However not only is this data in suspended platelets without stimulation by any other agonist; but also there is no understanding of the effect on the actin cytoskeleton on this phosphorylation event. Therefore the effect of PGI_2 mediated phosphorylation of RhoA in spread or stimulated

platelets is not at present clear. Furthermore it is not clear what this phosphorylation of RhoA means, and if it directly correlates to RhoA activity in platelets.

In chapter 3 it was identified that the treatment of spread platelets with PGI_2 reversed the stress fibre formation. Therefore, it was hypothesized that PGI_2 induced this reversal of stress fibre formation in a cAMP/PKA dependent manner through phosphorylation of RhoA, leading to a reversal of RhoA activity, a decrease in MLC-p and therefore a reversal of stress fibre formation.

4.2 Aims of the chapter

The aim of this chapter was to identify the mechanism by which PGI_2 induced the reversal of stress fibre formation in spread platelets.

- To identify if PGI_2 treatment induces cAMP production in platelets spread on fibrinogen.
- To identify the timecourse of PGI_2 signalling in spread platelets using the phosphorylation of VASP and RhoA as markers.
- To identify if stress fibre reversal is mediated via a PKA dependent mechanism.
- Assess the ability of PGI_2 to modulate the activity of RhoA, and if this correlates with RhoA phosphorylation.

4.3: PGI_2 induces cAMP and PKA mediated phosphorylation in suspended platelets.

It has been previously reported that stimulation of platelets with PGI_2 induces elevation in cAMP (Tateson et al., 1977). Therefore to confirm this result, suspended platelets ($2.0x10^8$/ml) were stimulated with 10nM PGI_2 for 1 minute prior to lysis. The samples were then analysed using a cAMP kit (GE healthcare) and measured for fluorescence on a spectrophotometer. Figure 4.1, demonstrates that under basal conditions platelets contained 396.40±37.15 fmol/μg of cAMP. However upon stimulation with 10nM PGI_2, the cAMP concentration dramatically increased to 779.26±196.93 fmol/μg. This demonstrated that platelets in suspension stimulated with PGI_2 induced an elevation in cAMP concentration.

To identify if elevation of cAMP correlated with increases in PKA signaling, platelets ($2.0x10^8$/ml) in suspension were treated for 1 minute with different doses of PGI_2 (1, 10, 100 and 1000nM) under non-aggregating conditions. These platelets were then lysed, western blotted and probed for $pVASP^{Ser157}$ and GAPDH. PGI_2 induced a dose dependent elevation in phosphorylation of $VASP^{Ser157}$ (Figure 4.2A). Densitometry revealed that $pVASP^{Ser157}$ levels (Figure 4.2B) in basal conditions were 0.01±0.004, which increased to 0.26±0.14 at 1nM, 0.42±0.11 at 10nM, 0.49±0.05 at 100nM and 0.62±0.16 at 1000nM of PGI_2.

Further to this, to understand the timecourse of PKA signaling, suspended platelets ($2.0x10^8$/ml) were stimulated with 100nM PGI_2 under non-aggregating conditions and were lysed at 1, 5, 10, 15, 30 and 60 minutes. The samples were western blotted and probed for $pVASP^{Ser157}$ and GAPDH.

Figure 4.3A and B, shows the phosphorylation of $VASP^{Ser157}$ was significantly elevated after 1 minute stimulation from a basal level of 0.012±0.005 to 0.31±0.04. The level of phosphorylation was then reduced to 0.092±0.05 by 5 minutes and significantly reduced at 0.042±0.02 by 10 minutes which continued onwards to 0.030±0.01 by 15 minutes, and 0.024±0.01 by 30 minutes. By 60 minutes, the level of phosphorylation reduced to 0.012±0.005, becoming equivalent to the basal level of VASP phosphorylation.

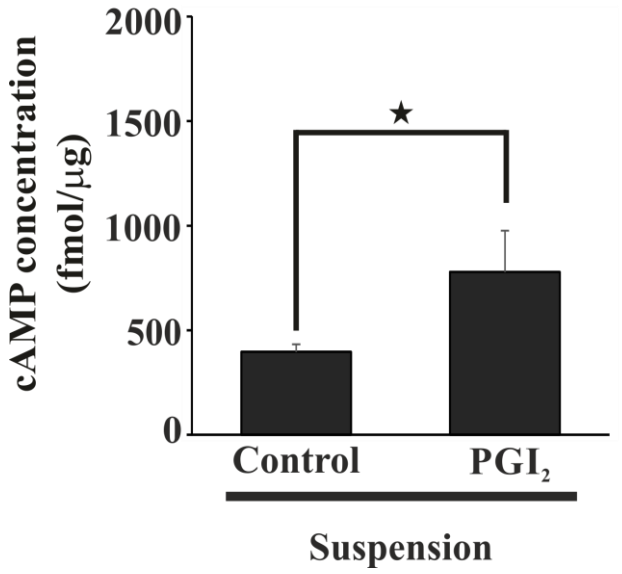

Figure 4. 1: Increase in cAMP levels of suspended platelets on treating them with PGI_2. Suspended platelets ($2x10^8$/ml) were stimulated with 10nM PGI_2 for 1minute. Using a cAMP commercial kit, the platelets were lysed and their levels of cAMP assessed. The bar chart represents the level of fluorescence in femtomoles per microgram of protein. The data was presented as average±SEM of n=3.$p<0.05$.

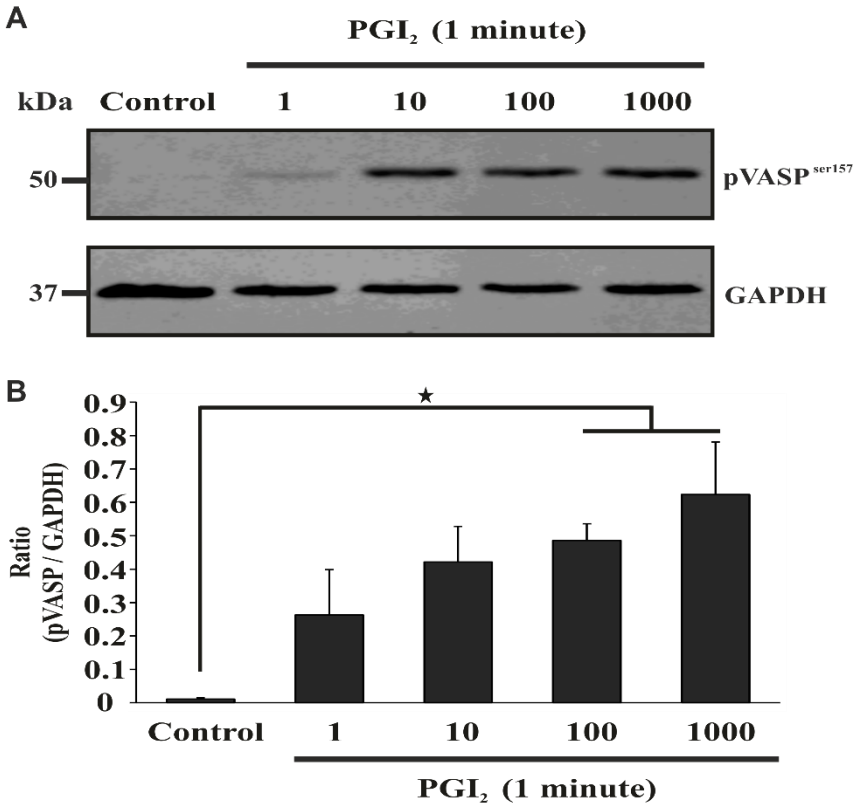

Figure 4. 2: PGI_2 induces VASP phosphorylation in a dose dependent manner in suspended platelets. Platelets ($2x10^8$/ml) were stimulated with PGI_2 (1-1000nM) for 1 minute. They were lysed with Laemmli buffer and western blotted. On transferring the proteins to the membrane it was blotted for $pVASP^{Ser157}$ and GAPDH. **A)** Western blots for pVASP and GAPDH. **B)** Densitometry for pVASP. The data was presented as average±SEM of n=3. $p<0.05$.

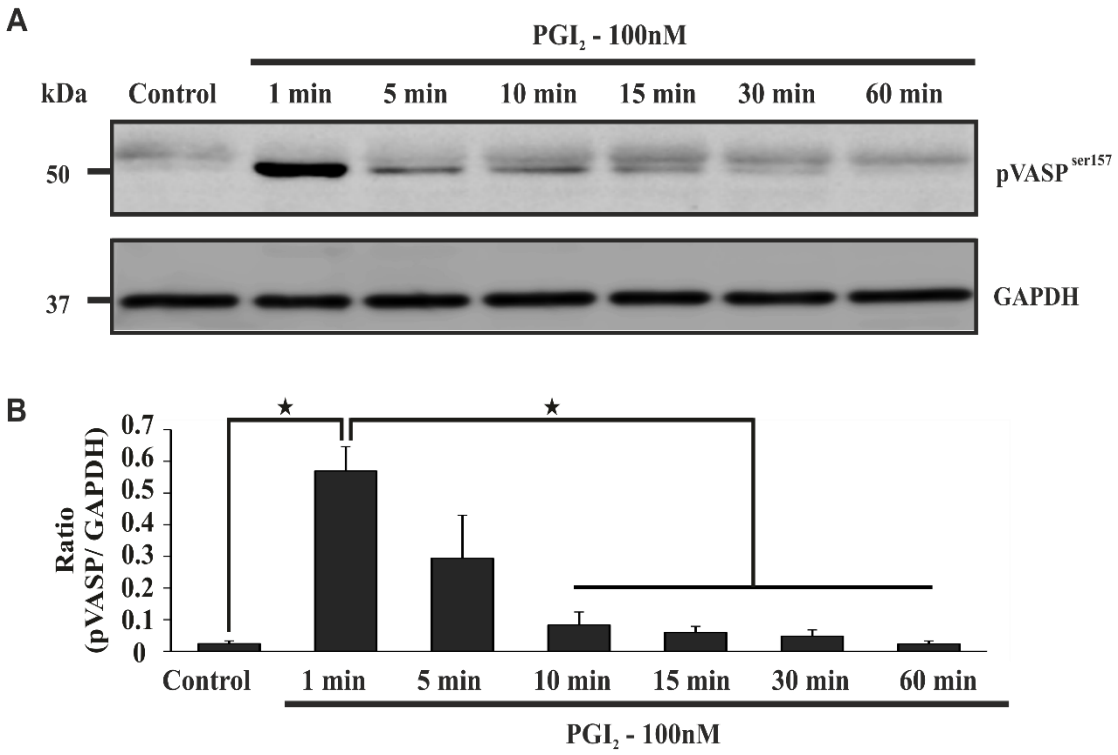

Figure 4. 3: PGI_2 induces VASP phosphorylation in a time dependent manner in suspended platelets. Platelets ($2x10^8$/ml) were stimulated with PGI_2 (100nM) for 1-60 minutes. They were lysed with Laemmli buffer and western blotted. On transferring the proteins to the membrane it was blotted for $pVASP^{Ser157}$ and GAPDH. **A)** Western blots for $pVASP^{Ser157}$ and GAPDH. **B)** Densitometry for $pVASP^{Ser157}$. The data was presented as average±SEM of n=3. $p<0.05$.

Therefore, platelets in suspension, stimulated with PGI_2 induce both, an elevation in intracellular cAMP levels and an increase in phosphorylation of the PKA target, $VASP^{Ser157}$.

4.4: PGI_2 induced elevation of cAMP in spread platelets and phosphorylation of PKA target proteins.

Chapter 3 demonstrated that PGI_2 induced a significant change in spread platelets. However at present there is no data to identify if cAMP is elevated in spread platelets upon stimulation with PGI_2. Therefore platelets ($2.0x10^8$/ml) were spread on fibrinogen for 25 minutes and then treated with 10nM PGI_2 (dose selected from Figure 3.5) for 2 minutes. The samples were lysed by analysis via the cAMP kit used within Figure 4.1.

Figure 4.4 demonstrates that platelets spread on fibrinogen had a slightly, but not significantly reduced level of intracellular cAMP (152.15±51.96 fmol/μg) as compared to the unstimulated platelets in suspension (396.40±37.15 fmol/μg) (Figure 4.4). Furthermore upon stimulation of spread platelets with 10nM PGI_2 for 2 minutes, a significant elevation in cAMP levels to 1575.82±293.17 fmol/μg was observed (Figure 4.4).

In order to identify if ADP and TXA_2 play a role in cAMP production by PGI_2, analysis was performed on platelets that had been treated with apyrase and indomethacin prior to spreading them on fibrinogen for 25 minutes. The platelets were then stimulated with 10nM PGI_2 for 2 minutes prior to lysis by cAMP lysis buffer and analysing for the changes observed. Interestingly, treatment with apyrase and indomethacin increased the level of basal cAMP in platelets from 152.15±51.96 fmol/μg to 717.62±192.33 fmol/μg, when compared to basal spread platelets without incubation with apyrase and indomethacin. However, treatment with PGI_2 in the presence of apyrase and indomethacin induced a similar level of cAMP in spread platelets as to that seen without apyrase and indomethacin, 1713.78±63.05 fmol/μg in comparison to 1575.82±293.17 fmol/μg, respectively (Figure 4.4).

Having confirmed that PGI_2 can induce an increase in cAMP concentration within spread platelets, it was then determined if PGI_2 can also induce an elevation in the phosphorylation of $pVASP^{Ser157}$.

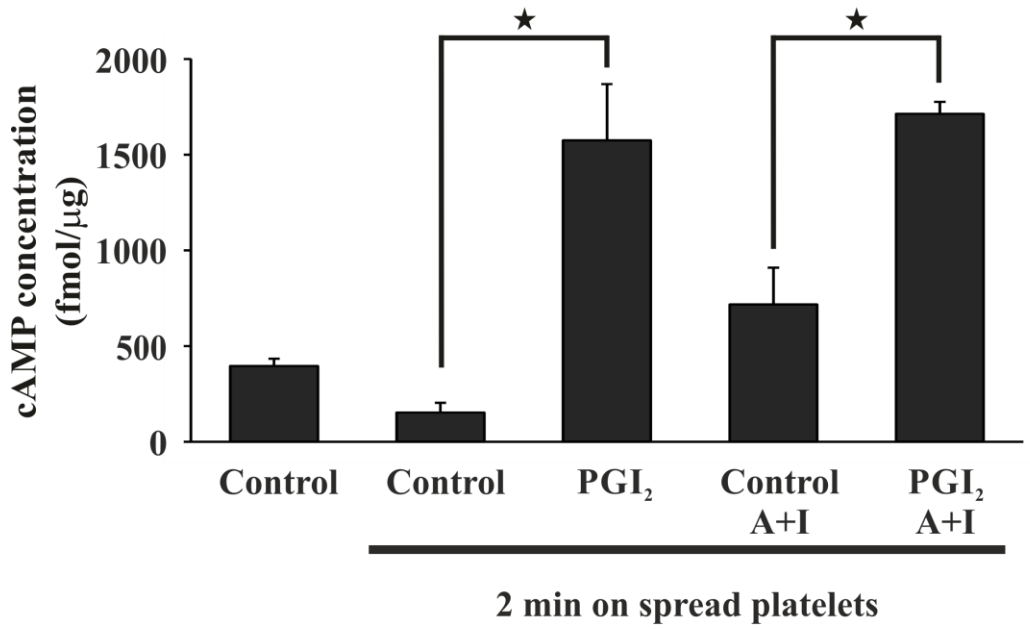

Figure 4. 4: Increase in cAMP levels of spread platelets on treating them with PGI_2 in the presence and absence of apyrase (A) and indomethacin (I). Platelets ($2x10^8$/ml) were spread on 100μg/ml fibrinogen, in the presence or absence of apyrase (A) and indomethacin (I), for 25 minutes before being washed with PBS. These spread platelets were stimulated with PGI_2 (10nM) for 2 minutes, in the presence or absence of apyrase (A) and indomethacin (I). Using the lysis buffer, provided in the cAMP commercial kit, the platelets were lysed at 2 minutes of stimulation and their levels of cAMP assessed. The bar chart represents the level of fluorescence in femtomoles per microgram (fmol/μg) of protein. The data was presented as average±SEM of n=3. $p<0.05$.

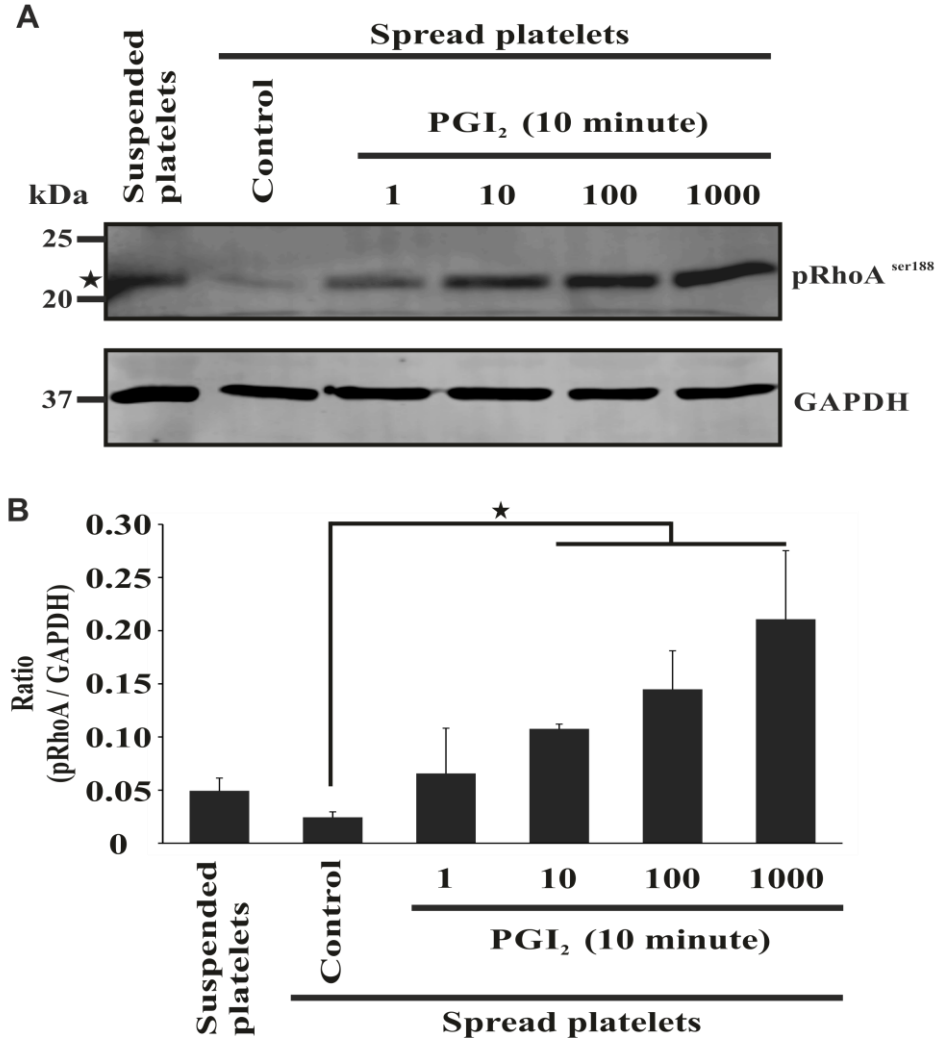

Figure 4. 5: PGI_2 induces VASP phosphorylation in a dose dependent manner in spread platelets. Platelets ($2x10^8$/ml) were spread on 100μg/ml fibrinogen for 25 minutes before being washed with PBS. These spread platelets were stimulated with PGI_2 (1-1000nM) for 10 minutes. They were lysed with Laemmli buffer and western blotted. On transferring the proteins to the membrane it was blotted for $pVASP^{Ser157}$ and GAPDH. **A)** Western blots for $pVASP^{Ser157}$ and GAPDH. **B)** Densitometry for pVASP. The data was presented as average±SEM of n=3. $p<0.05$.

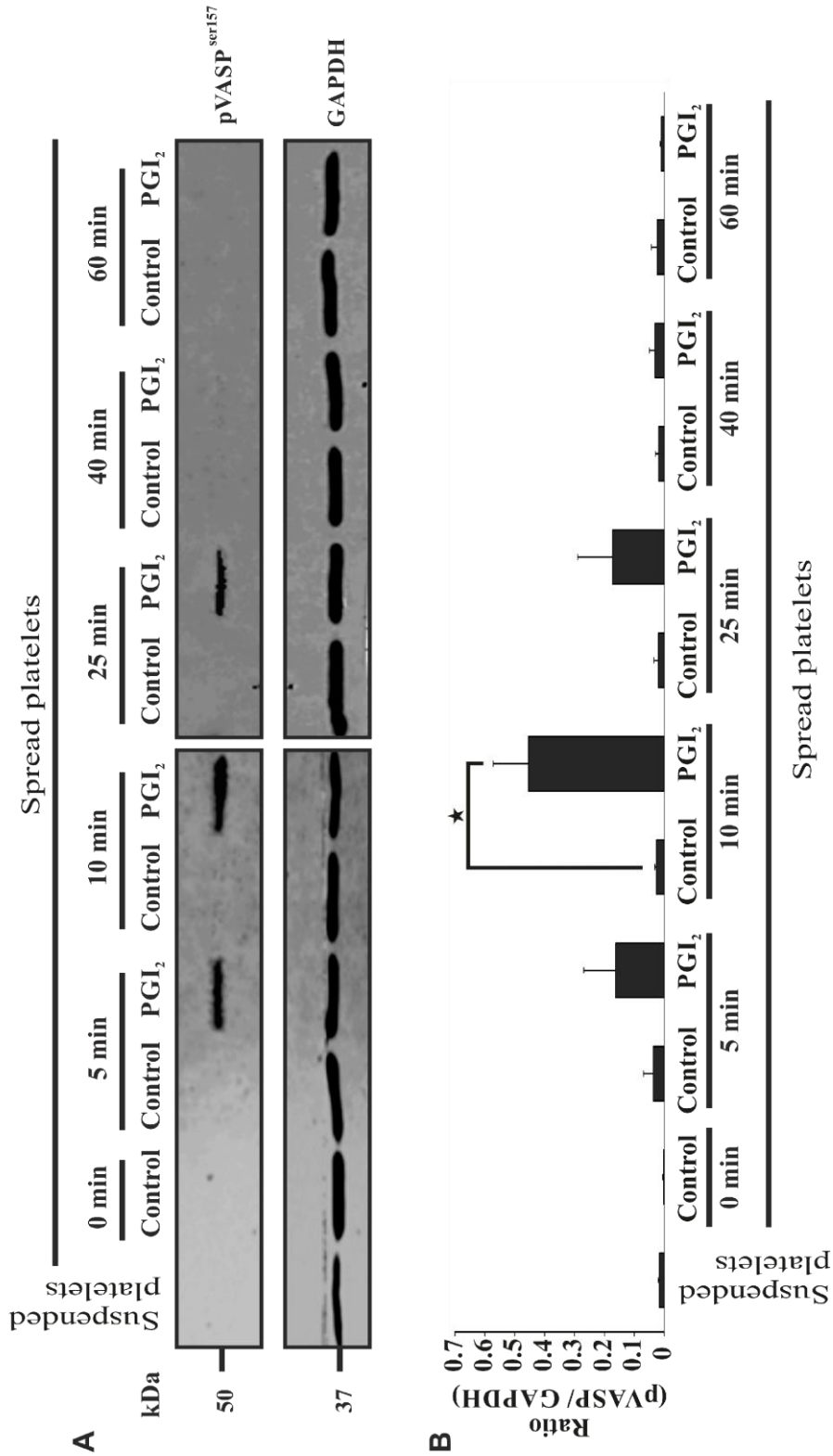

Figure 4. 6: PGI_2 induces VASP phosphorylation in a time dependent manner in spread platelets. Platelets ($2x10^8$/ml) were spread on 100µg/ml fibrinogen for 25 minutes before being washed with PBS. These spread platelets were stimulated with PGI_2 (10nM) for upto 60 minutes. They were lysed with Laemmli buffer at each individual timepoints along with their controls and were run on the gel for separating out the proteins. On transferring these proteins to the membrane it was blotted for $pVASP^{Ser157}$ and GAPDH. **A)** Western blots for $pVASP^{Ser157}$ and GAPDH. **B)** Densitometry for $pVASP^{Ser157}$. The data was presented as average±SEM of n=3. $p<0.05$.

Platelets ($2.0x10^8$/ml) were spread on fibrinogen for 25 minutes, prior to stimulating them with different doses of PGI_2 (1, 10, 100 and 1000nM) for 10 minutes. The samples were lysed, western blotted and probed for $pVASP^{Ser157}$ and GAPDH. The $pVASP^{Ser157}$ was elevated in a dose dependent manner in response to stimulation with PGI_2 (Figure 4.5A). Densitometry revealed that $pVASP^{Ser157}$ levels (Figure 4.5B) in spread platelets under basal conditions were 0.02±0.005, which increased to 0.31±0.17 at 1nM, 0.51±0.16 at 10nM, 0.49±0.09 at 100nM and 0.48±0.10 at 1000nM of PGI_2, respectively. Therefore the maximal level of PKA signaling, as observed using $pVASP^{Ser157}$ as a marker, was induced by 10nM PGI_2, which correlated with the maximal dose of PGI_2 that caused reversal of stress fibre formation in spread platelets (Figure 3.5).

To understand the timecourse of PGI_2 signaling within spread platelets, platelets ($2.0x10^8$/ml) were spread on fibrinogen for 25 minutes prior to stimulation with 10nM PGI_2 for duration of 1–60 minutes. At each time point there was a control sample taken in addition to the sample stimulated with PGI_2. The cells were lysed, western blotted and probed for $pVASP^{Ser157}$ and GAPDH (figure 4.6A).

It was observed that the phosphorylation of $VASP^{Ser157}$ (Figure 4.6A and B) increased steadily from basal levels of 0.004±0.003 to 0.163±0.106 at 5 minutes and peaked significantly at 0.454±0.118 at 10 minute after PGI_2 stimulation. The levels of $pVASP^{Ser157}$ reduced to 0.173±0.117 by 25 minutes and levelled to basal level of phosphorylation by 40 minutes.

4.5: PGI_2 induced stress fibre reversal is PKA dependent.

Although the previous data had shown that PGI_2 caused both an elevation in cAMP and phosphorylation of proteins, it was necessary to confirm that the phosphorylation of VASP in spread platelets was mediated by PKA. Therefore, platelets ($2x10^7$/ml) were allowed to spread on fibrinogen for 25 minutes in the presence or absence of the PKA inhibitors Rp-8-cpt-cAMP (RP) and KT5720 (KT). The two inhibitors work via different mechanisms with RP competitively attaching to the cAMP binding sites on the regulatory domain of PKA while KT binds to the phosphorylation site on the catalytic domain of the PKA subunit, providing a robust inhibition of PKA. The spread platelets were then stimulated with PGI_2

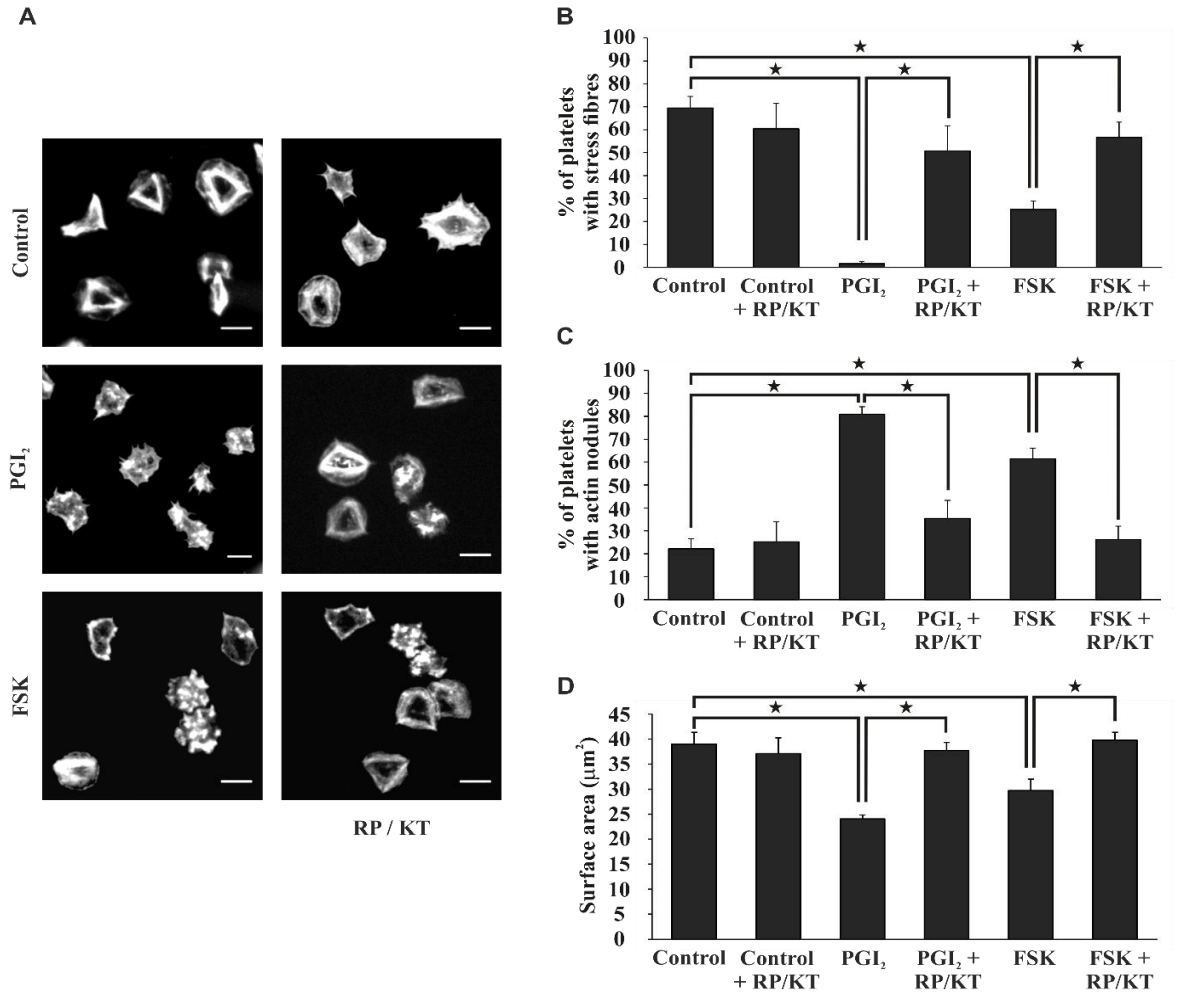

Figure 4. 7: Reversal of platelet stress fibre formation and induction of actin nodule formation is dependent on PKA activation. Platelets ($2x10^7$/ml) were spread on 100μg/ml fibrinogen for 25 minutes in the presence or absence of PKA inhibitors; 500μM RP-8-CPT-cAMP (RP) and 10μM KT5720 (KT), before being washed with PBS. The platelets were then treated with Tyrodes containing 10nM PGI_2 or 1μM Fsk with or without PKA inhibitors 500μM RP-8-CPT-cAMP and 10μM KT5720, for a further 10 minutes. The platelets were then fixed, stained with FITC-phalloidin and imaged. **A)** The levels of cAMP were assessed in basal suspended platelets and basal and 10nM PGI_2 treated spread platelets. **B)** Representative images of spread platelets under different experimental conditions. Scale bar is 5μm. **C)** The number of spread platelets containing stress fibres were calculated for each condition in control and treated samples. **D)** The number of spread platelets containing actin nodules were calculated for each condition in control and treated samples. **E)** The average surface area of the spread platelets was analysed for each condition in control and treated samples using ImageJ. The data was presented as average±SEM of n=3. $p<0.05$.

(10nM) or Fsk (1μM) for 10 minutes, in the presence or absence of RP and KT inhibitors. After treatment, the platelets were fixed, stained and visualized under a fluorescence microscope.

Control platelets spread on fibrinogen had 69.52±5.0% of platelets containing stress fibres. However on treatment with 10nM PGI_2, a significant drop to 1.62±0.95% was observed in the percentage of platelets having stress fibres (shown previously in Figure 3.7B). However the use of the PKA inhibitors, RP and KT, inhibited the reversal of stress fibres, with 50.78±10.93% of platelets having stress fibres after PGI_2 stimulation (Figure 4.7A and B). In agreement with these changes in stress fibres, there was also a significant change in the percentage of platelets containing actin nodules, with control having 22.18±4.31% which significantly increased to 80.91±3.30% in their PGI_2 treated samples. Again this increase was inhibited after the use of the PKA inhibitors RP and KT, with just 35.42±7.88% of platelets containing actin nodules in the presence of PGI_2 (10nM) (Figure 4.7A and C). These changes in actin cytoskeletal structures were also mirrored by the change in the surface area of the spread cells with a significant reduction from 39.02±2.31μm^2 to 24.06±0.77μm^2 in PGI_2 treated samples. Again this change in surface area was reversed to 37.73±1.61μm^2 after using the PKA inhibitors RP and KT in the presence of PGI_2 (Figure 4.7A and D).

To show the requirement of PKA to other cAMP elevating agents, platelets were spread in the presence of 1μM Fsk in the presence and absence of RP and KT. In control cells

69.52±5.0% contained stress fibres, which was significantly reduced to 25.27±3.64% in the presence of 1μM Fsk. However, upon the use of RP and KT in the presence of 1μM Fsk it reversed to 56.70±6.60% (Figure 4.7A and B). In agreement, in the control 22.18±4.31% of platelets contained actin nodules, with a significant rise to 61.46±4.67% in the Fsk treated samples. This increase was reversed in the presence of RP and KT, with 26.21±5.83% of platelets containing actin nodules. The changes in actin cytoskeletal structures were also mirrored by the change in the surface area of the spread cells from control 39.02±2.31μm^2 to 29.71±2.27μm^2 in Fsk treated samples, which reversed to 39.78±1.57μm^2 on using RP and KT inhibitors in the presence of Fsk (Figure 4.7A and D).

4.6: PGI_2 modulates the activity of RhoA in spread platelets.

Reversal of the effect of PGI_2 and Fsk on actin dynamics of spread platelets, by RP and KT, confirmed the involvement of PKA in the downstream signaling. However, to fully understand how PKA could mediate a reversal of stress fibre formation, it was necessary to understand how stress fibres are formed within platelets. Stress fibres are formed through the activation of the GTPase RhoA. Therefore to confirm the critical nature of RhoA to the process of stress fibre formation, platelets ($2.0x10^7$/ml) were spread in the presence of increasing doses of Rhosin (RhoA inhibitor) and the inhibitor of Rho kinase-ROCK (the downstream activator of RhoA) by Y27632 for 2 minutes prior to spreading them on fibrinogen for 45 minutes. The small molecules Y27632 inhibit ROCK, association with Rho-GTP while Rhosin acts further upstream by inhibiting the conversion of Rho-GDP to its active Rho-GTP bound form; this helped to delineate the Rho-ROCK association pathway in the formation of stress fibres.

In Figure 4.8A, pretreating platelets with Y27632 significantly reduced the number of platelets having stress fibres from 59.11±3.40% in the control to 22.43±5.45% at 1μM, 10.84±0.77% at 10μM, 4.67±1.72% at 30μM and 3.48±0.11% at 50μM Y27632 respectively (Figure 4.8B). In agreement with this, a reciprocal increase was observed in platelets containing actin nodules from 33.50±4.36% in the control to 72.04±5.85% at 1μM, 85.09±1.02% at 10μM, 92.06±2.62% at 30μM and 95.05±0.45% at 50μM Y27632 respectively (Figure 4.8C). No significant change in adhesion was appreciated using different doses of Y27632 (Figure 4.8D). The surface area from a basal level of 35.21±0.35μm^2 reduced significantly with increasing doses of Y27632 to 22.95±2.71μm^2 at 1μM, 23.84±2.50μm^2 at 10μM, 24.63±2.36μm^2 at 30μM and 22.21±2.03μm^2 at 50μM Y27632 respectively (Figure 4.8E).

Similarly, pretreating platelets with Rhosin (Figure 4.9A) also reduced the number of platelets having stress fibres from 59.55±3.40% in the control to 45.68±4.71% at 1μM, 16.53±0.17% at 10μM, 13.28±5.02% at 30μM and 6.71±1.44% at 50μM Rhosin respectively (Figure 4.9B). In agreement the percentage of platelets containing actin nodules increased from a control level of 33.50±4.36% to 48.93±3.70% at 1μM, 81.07±1.69% at 10μM, 82.81±4.10% at 30μM and 89.08±1.46% at 50μM Rhosin respectively (Figure 4.9C). Although there was no significant change in adhesion (Figure

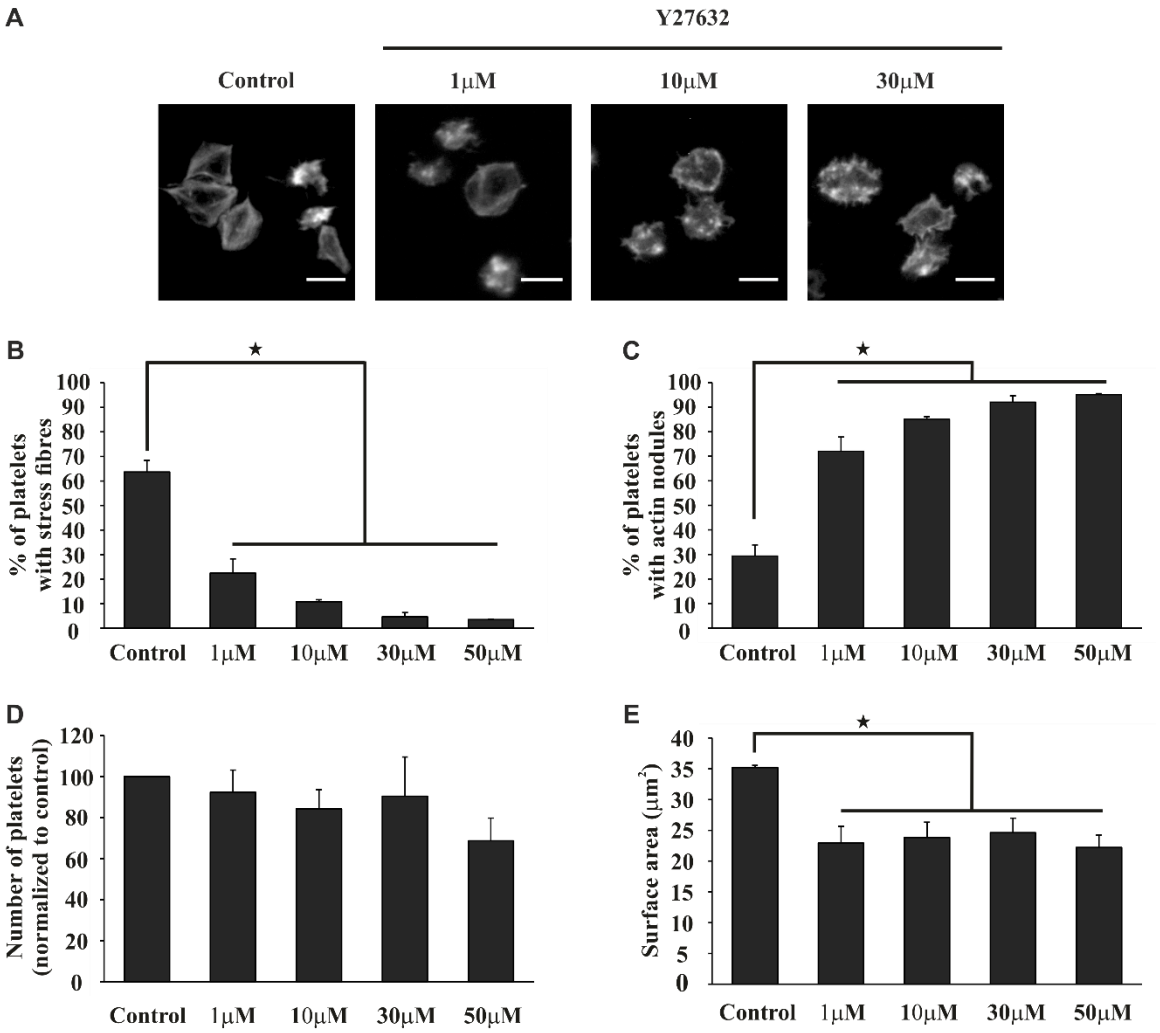

Figure 4. 8: A reduction in stress fibres with a reciprocal increase in actin nodules by treating platelets with Y27632 in a dose dependent manner prior to spreading them on fibrinogen. Platelets ($2x10^7$/ml) were treated with ROCK inhibitor, Y27632 (1, 10, 30 and 50μM), prior to spreading them on 100μg/ml fibrinogen for 45 minutes. The platelets were then fixed and stained with FITC-phalloidin before being imaged. **A)** Images are representative of three experiments. Scale bar is 5μm. **B)** The number of platelets containing stress fibres whilst their treatment with Y27632. **C)** The number of platelets containing actin nodules whilst their treatment with Y27632. **D)** The number of platelets adhered to fibrinogen after their treatment with Y27632. **E)** The average surface area of the spread platelets after their treatment with Y27632. The data was presented as average±SEM of n=3. $p<0.05$.

4.9D) there was a significant reduction in the surface area from a basal level of 35.21±0.35μm^2 with increasing doses of Rhosin to 28.02±2.65μm^2 at 1μM, 22.93±2.80μm^2 at 10μM, 20.60±3.82μm^2 at 30μM and 18.00±1.85μm^2 at 50μM (Figure 4.9E).

Use of both Y27632 and Rhosin caused a significant reduction in stress fibres with a concomitant significant increase in actin nodules identifying the critical importance of RhoA activity to stress fibre formation. Given this critical role, it was therefore identified if PKA could target RhoA. Initially the level of phosphorylation at Ser188 on RhoA was identified as a proxy for the activity of RhoA.

Therefore platelets (2.0x10^8/ml) were spread on fibrinogen for 25 minutes, prior to stimulating them with different doses of PGI_2 (1, 10, 100 and 1000nM) for 10 minutes. The samples were lysed, western blotted and probed for pRhoA^{Ser188} and GAPDH. In agreement with pVASP^{Ser157} in figure 4.5B, the level of pRhoA^{Ser188} was also elevated in a dose dependent manner in response to stimulation with PGI_2. Densitometry of pRhoA^{Ser188} (Figure 4.10A and B) showed an increase in phosphorylation status in spread platelets with the basal levels at 0.02±0.01, increasing to 0.07±0.04 at 1nM, which becomes significant onwards from 0.11±0.004 at 10nM, 0.14±0.04 at 100nM and 0.21±0.06 at 1000nM of PGI_2 respectively.

To understand the effect of RhoA phosphorylation in a timecourse of PGI_2 treatment on spread platelets, platelets (2.0x10^8/ml) were similarly spread on fibrinogen for 25 minutes prior to stimulation with 10nM PGI_2 for duration of 1–60 minutes. At each time point a control sample was taken in addition to the sample stimulated with PGI_2. The cells were lysed, western blotted and probed for pRhoA^{Ser188} and GAPDH. Phosphorylation of RhoA^{Ser188} (figure 4.11A and C) increased steadily from a basal level of 0.019±0.002 at 0 minute stimulation to reach a significant level of 0.076±0.014 by 10 minutes. The level of phosphorylation remained significantly elevated at 0.190±0.11 after 40 minutes and started coming down to 0.174±0.072 at 60 minutes post stimulation by 10nM PGI_2.

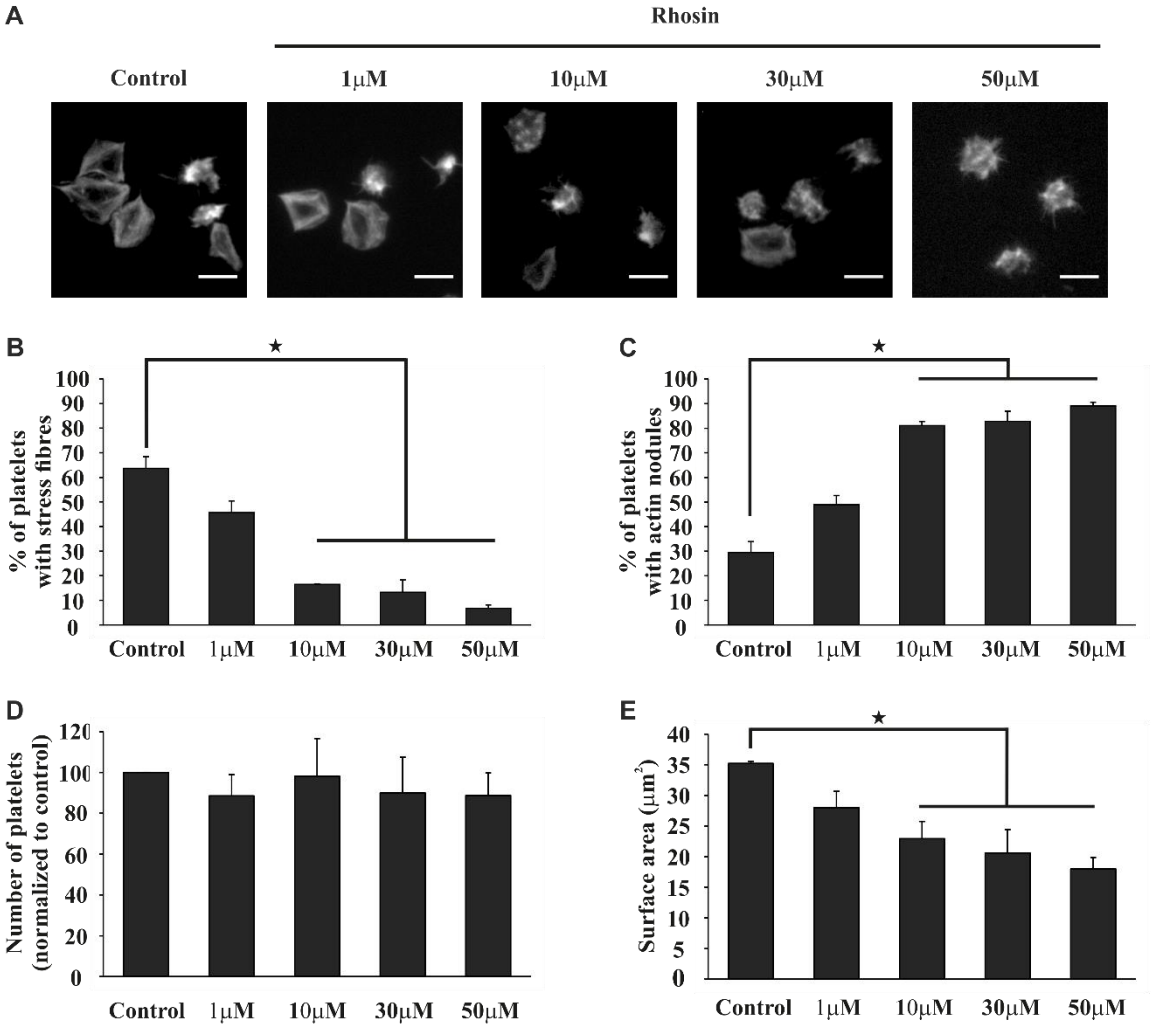

Figure 4. 9: A reduction in stress fibres with a reciprocal increase in actin nodules by treating platelets with Rhosin in a dose dependent manner prior to spreading them on fibrinogen. Platelets ($2x10^7$/ml) were treated with RhoA inhibitor, Rhosin (1, 10, 30 and 50μM), prior to spreading them on 100μg/ml fibrinogen for 45 minutes. The platelets were then fixed and stained with FITC-phalloidin before being imaged. **A)** Images are representative of three experiments. Scale bar is 5μm. **B)** The number of platelets containing stress fibres whilst their treatment with Rhosin. **C)** The number of platelets containing actin nodules whilst their treatment with Rhosin. **D)** The number of platelets adhered to fibrinogen after their treatment with Rhosin. **E)** The average surface area of the spread platelets after their treatment with Rhosin. The data was presented as average±SEM of n=3. $p<0.05$.

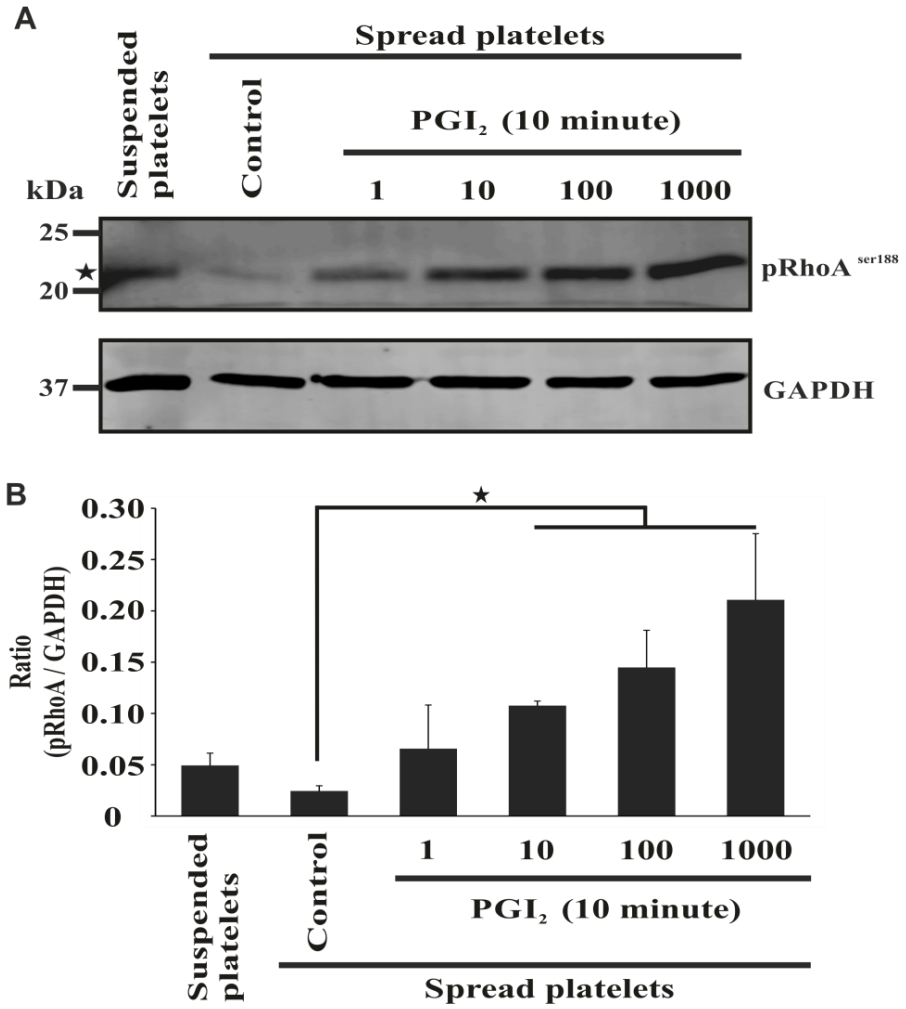

Figure 4. 10: PGI_2 induces RhoA phosphorylation in a dose dependent manner in spread platelets. Platelets ($2x10^8$/ml) were spread on 100μg/ml fibrinogen for 25 minutes before being washed with PBS. These spread platelets were stimulated with PGI_2 (1-1000nM) for 10 minutes. They were lysed with Laemmli buffer and western blotted. On transferring the proteins to the membrane it was blotted for $pRhoA^{Ser188}$ and GAPDH. **A)** Western blots for pRhoA (identified by an asterisk) and GAPDH. **B)** Densitometry for pRhoA. The data was presented as average±SEM of n=3. $p<0.05$.

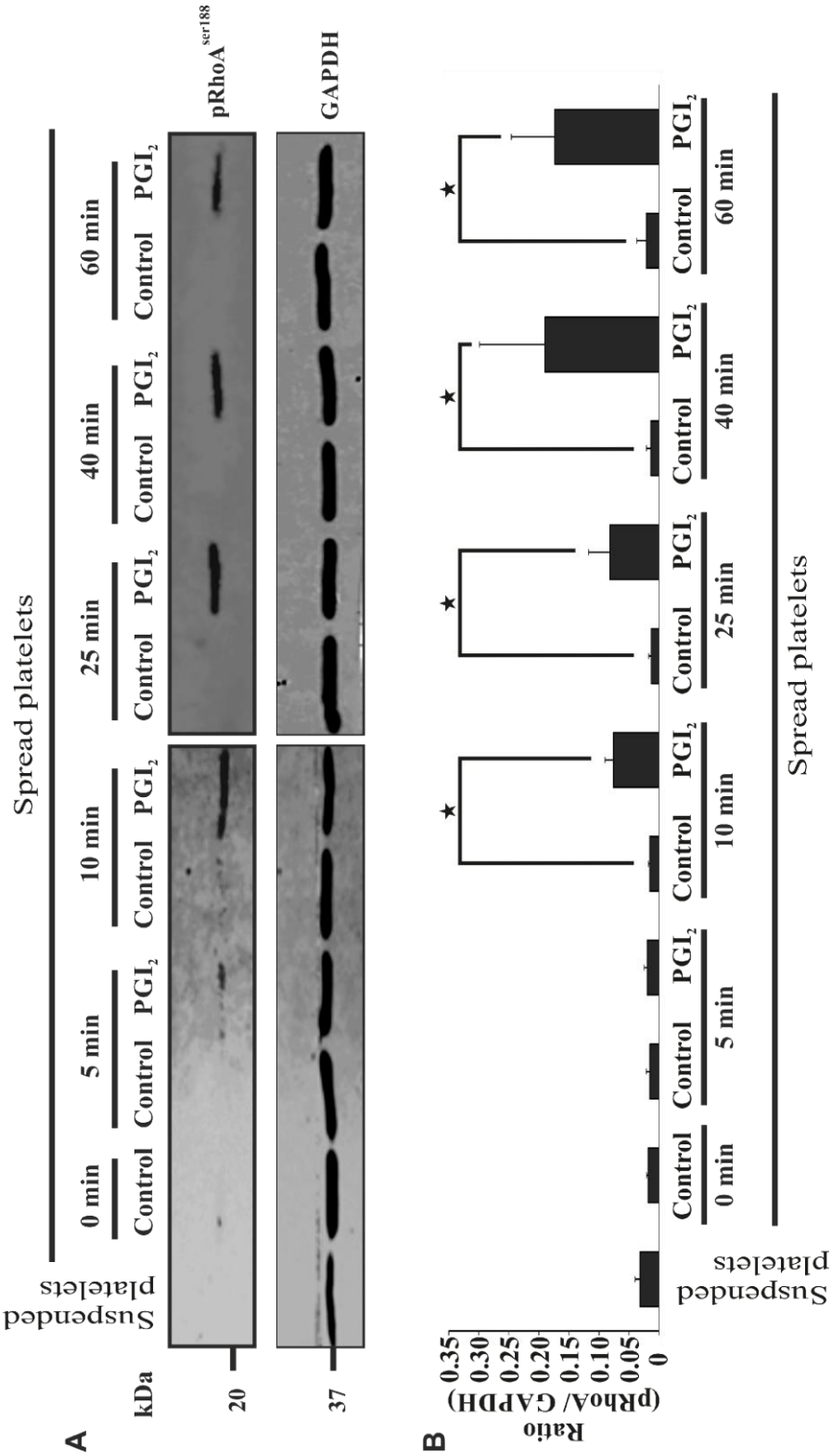

Figure 4. 11: PGI_2 induces RhoA phosphorylation in a timecourse manner in spread platelets. Platelets ($2x10^8$/ml) were spread on 100µg/ml fibrinogen for 25 minutes before being washed with PBS. These spread platelets were stimulated with PGI_2 (10nM) for upto 60 minutes. They were lysed with Laemmli buffer at each individual timepoints along with their controls and were run on the gel for separating out the proteins. On transferring these proteins to the membrane it was blotted for $pRhoA^{Ser188}$ and GAPDH. **A)** Western blots for pRhoA (identified by an asterisk) and GAPDH. **B)** Densitometry for $pRhoA^{Ser188}$. The experiments are an average of n=3. $p<0.05$.

Although PGI_2 induced the phosphorylation of $VASP^{Ser157}$ and $RhoA^{Ser188}$ in a time dependent manner, they both seemed to have a different profile of phosphorylation in spread platelets (figure 4.6A and 4.11A). The levels of $pVASP^{Ser157}$ rapidly peaked and came down quickly while the levels of $pRhoA^{Ser188}$ continued to increase up to 40 minutes and then started declining. This identified that while PGI_2 would have been degraded in the first few minutes, however the downstream effectors, still continued to modulate the functioning of the platelet by upto an hour.

As it was now shown that PGI_2 could induce phosphorylation of $RhoA^{Ser188}$ in spread platelets, it was now necessary to further explore the phosphorylation status of other proteins with stress fibre signaling. Therefore, platelets ($2.0x10^8$/ml) were treated with inhibitors (RP/KT and Y27632) for 2 minutes prior to allowing them to spread on fibrinogen for 25 minutes in the presence or absence of these inhibitors. The spread platelets were then stimulated with PGI_2 (10nM) or Fsk (1μM) for 10 minutes. The samples were lysed, western blotted and probed with $pVASP^{Ser157}$, $pRhoA^{Ser188}$; $pMLC^{Ser19}$ and GAPDH. Elevated levels of $pMLC^{Ser19}$ correlate with stress fibre formation, but should not be directly targeted by PKA activity.

In spread platelets, treatment with PGI_2 caused a significant increase, 4.067±0.36 fold, in phosphorylation of $VASP^{Ser157}$ over control, as previously identified (Fig.4.6A and B). This effect was reduced to a 2.017±0.64 fold increase in the presence of RP and KT (figure 4.12A and B). As previously shown in Fig 4.11, $RhoA^{Ser188}$ was significantly phosphorylated by PGI_2 with a 5.142±0.30 fold increase that significantly reduced to 1.946±0.487 in the presence of the PKA inhibitors, RP and KT (figure 4.12A and C). Further to the effect on $RhoA^{Ser188}$ phosphorylation, analysis of MLC^{Ser19} phosphorylation determined that MLC^{Ser19} was phosphorylated heavily in spread platelets, in an antagonistic manner to $pRhoA^{Ser188}$, and in correlation to the heavy percentage of platelets with stress fibres. Stimulation with PGI_2 induced a significant reduction of $pMLC^{Ser19}$ to 0.210±0.04 in comparison to the normalized control conditions. This reduction in phosphorylation was reversed to 0.820±0.03 of control samples in the presence of RP and KT (figure 4.12A and D).

In agreement with PGI_2, treatment of spread platelets with 1μM Fsk, mirrored the activity of PGI_2. Fsk caused a significant increase in the level of $pVASP^{Ser157}$ to 2.737±0.05 over

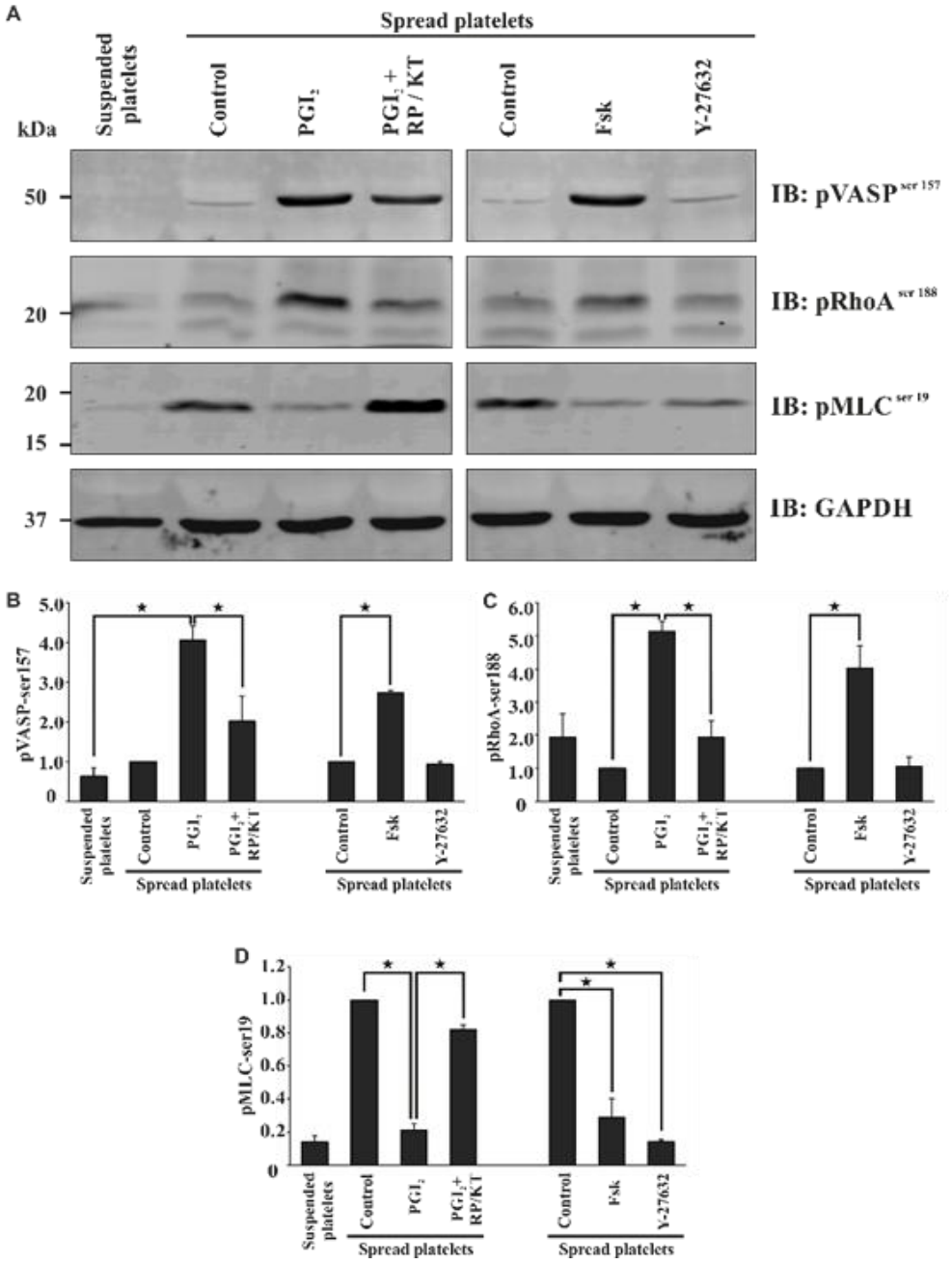

Figure 4. 12: PGI_2 induces a PKA signaling response in spread platelets. Platelets ($2x10^8$/ml) were spread on 100μg/ml fibrinogen for 25 minutes in the presence or absence of PKA inhibitors 100μM RP-8CPT-cAMPS (RP) and 2μM KT5720 (KT), before being washed with PBS. **A)** The platelets were then treated with Tyrodes containing 10nM PGI_2 with or without PKA inhibitors (100μM RP-8CPT-cAMPS and 2μM KT5720), or 1μM Fsk, or Y27632 (10μM), for a further 10 minutes. The samples were then lysed with Laemmli buffer before being western blotted for $pVASP^{Ser157}$, $pMLC^{Ser19}$, $pRhoA^{Ser188}$, and GAPDH. Images are representative of atleast three experiments. Densitometry for the western blots; **B)** $pVASP^{Ser159}$, **C)** $pRhoA^{Ser188}$ **D)** $pMLC^{Ser19}$; using GAPDH as the loading control. The ratios were standardised to the control. Analysis is an average of at least n=3 experiments. $p<0.05$.

the control (figure 4.12A and B), a significant increase in the level of pRhoA^{Ser188} to 4.027±0.69 over the control (figure 4.12A and C) and a significant decrease in the level of pMLC^{Ser19} to 0.290±0.11 (figure 4.12A and D), when compared with the control.

The use of Y27632 did not cause changes in the levels of pVASP^{Ser157} (0.933±0.08) (figure 4.12A and B) or pRhoA^{Ser188} (1.059±0.27) as expected when compared with the normalized control (figure 4.12A and C). However Y27632, did cause a significant decrease in the level of pMLC^{Ser19} (0.143±0.01) when standardized to its control (figure 4.12A and D). Reduction in the level of pMLC^{Ser19} referred to a reduction in stress fibres which is in agreement with the spreading data suggesting decrease in the number of platelets having stress fibres on treatment with Y27632 (figure 4.8).

The spreading data and western blotting, both, in the presence of inhibitors had confirmed that an increase in intracellular PKA activity phosphorylates RhoA (figure 4.11A and C). However there is no data to identify where pRhoA^{Ser188}, or the PKA subunits RI and RII localize within spread platelets. Therefore, platelets ($2.0x10^7$/ml) were spread on fibrinogen for 25 minutes, prior to stimulating them with 10nM PGI_2 for 10 minutes. The spread platelets were fixed, stained with FITC-phalloidin along with either pRhoA, PKA RI or PKA RII antibodies. The coverslips were mounted on a slide and visualized under confocal microscope.

It was noted, in figure 4.13, that pRhoA^{Ser188} localized to actin nodules upon treatment with PGI_2. Interestingly, PKA RII and not PKA RI, colocalised with the actin nodules (figure 4.14A and B). This identified that pRhoA and PKA RII were present in actin nodules after treatment with PGI_2.

All this data demonstrated that PKA mediates phosphorylation of RhoA, and that both phosphorylated form of RhoA and PKA regulatory subunit PKA RII are present in actin nodules. It was necessary to ascertain if this proximity then correlates to a change in RhoA activity. Phosphorylation of RhoA has been correlated inversely to RhoA activity in other cell types (Dong et al., 1998). Therefore analysis of RhoA activity was measured with a RhoA specific pull down assay.

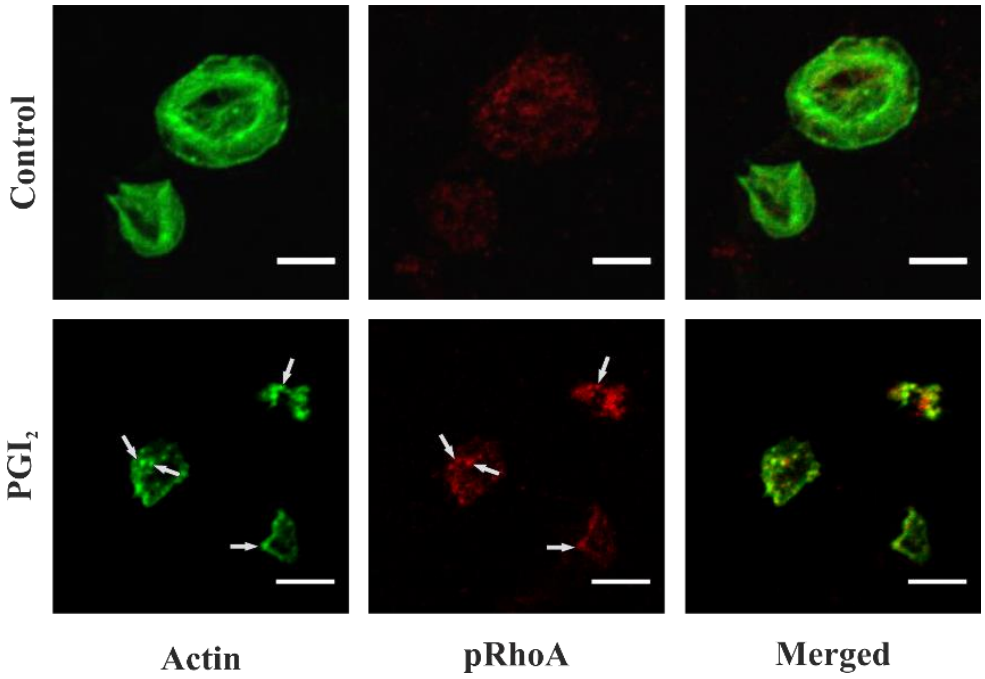

Figure 4. 13: Actin nodules contain phospho-RhoA. Platelets ($2x10^7$/ml) were spread on 100μg/ml fibrinogen for 25 minutes before being washed with PBS. The platelets were then treated with Tyrodes with or without 10nM PGI_2 for a further 10 minutes. The platelets were then fixed, lysed and stained for pRhoA (1:1000) and co-stained with actin (FITC-Phalloidin) for 60 minutes, before mounting and imaging the slides on confocal microscope. Images are representative of at least 3 experiments. Scale bar is 5μm.

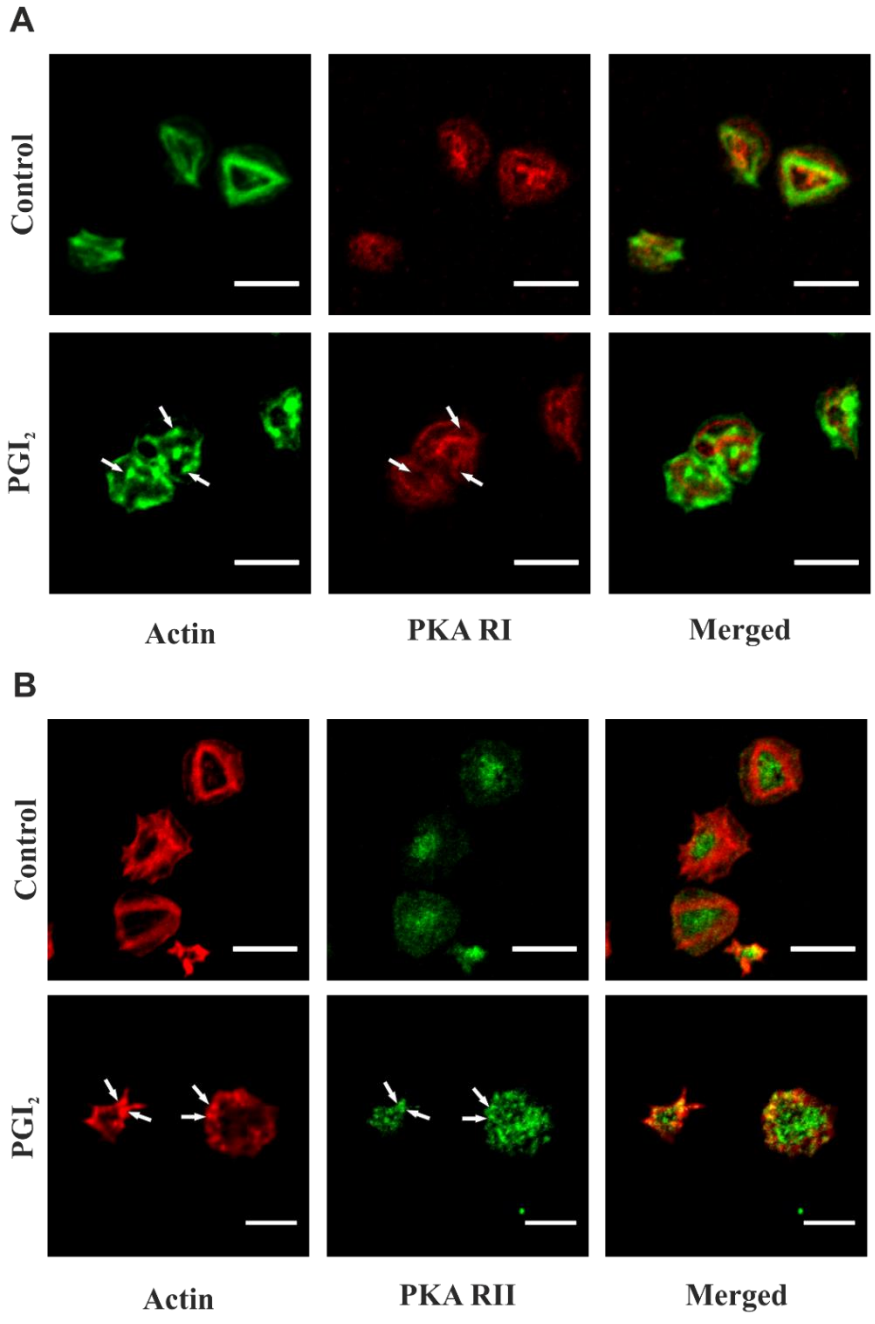

Figure 4. 14: Actin nodules contain PKA signaling proteins. Platelets ($2x10^7$/ml) were spread on 100μg/ml fibrinogen for 25 minutes before being washed with PBS. The platelets were then treated with Tyrodes with or without 10nM PGI_2 for a further 10 minutes. The platelets were then fixed, lysed and stained for either **A)** PKA RI (1:100) or **B)** PKA RII (1:100); and co-stained with actin (FITC-Phalloidin) for 60 minutes, before mounting and imaging the slides on confocal microscope. Images are representative of at least 3 experiments. Scale bar is 5μm.

Prior to understanding if PGI_2 modulates RhoA activity, it was necessary to optimise the number of beads, and protein levels required to complete the assay effectively. Therefore, platelets ($2x10^8$/ml) in suspension were stimulated with different doses of thrombin using 50μg beads. The use of thrombin increased the active form of RhoA. This increase was maximal with the use of 0.1U/ml as compared to the 1.0U/ml of thrombin. This confirmed that 50μg beads could effectively pick up the increase in the level of RhoA-GTP bound form when compared with the basal suspended platelets (Figure 4.15A).

As 50μg showed a good response in suspended platelets, it was now necessary to understand how the beads would work using spread platelets. Therefore spread platelets were lysed and incubated with either 25μg or 50μg beads (Figure 4.15 B). The suspension samples were used as a positive control. The result showed that in spread platelets there was a good band for RhoA-GTP with either 25 or 50μg of beads. However the total RhoA bands for 25μg were weak, whilst at 50μg showed a good response. This indicated that 50μg beads were required to effectively complete the assay for further analysis.

After optimizing the conditions for the RhoA specific pull down assay, the experimental conditions were setup to check the levels of RhoA-GTP on stimulation with PGI_2. Platelets ($2.0x10^8$/ml) were allowed to spread on fibrinogen for 25 minutes in the presence or absence of PKA inhibitors, RP and KT. The spread platelets were then stimulated with PGI_2 (10nM) for 10 minutes, in the presence or absence of RP and KT. The samples were lysed, western blotted and probed for RhoA (Figure 4.16A). Densitometry revealed that suspended platelets had 0.028±0.01 active RhoA that increases significantly to 0.451±0.07 upon spreading of platelets on fibrinogen (Figure 4.16A and B). Treatment with PGI_2 significantly reduces the level of RhoA-GTP to 0.062±0.03 that was reversed to 0.314±0.07 on using PKA inhibitors RP and KT (Figure 4.16A and B). This confirmed that not only does PGI_2 cause phosphorylation of RhoA, but this correlates with a reduction in RhoA activity which is mediated by PKA.

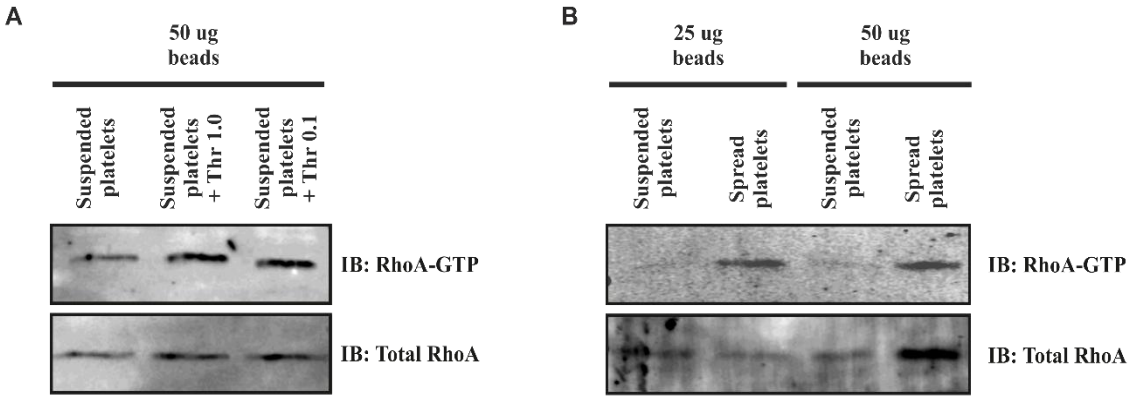

Figure 4. 15: Optimizing the concentration of RhoA pull down beads in both suspended and spread platelets. Platelets ($2x10^8$/ml) were spread on 100μg/ml fibrinogen for 25 minutes before being washed with PBS. The platelets were then incubated with Tyrodes for a further 10 minutes and were then lysed. Suspended samples were prepared by lysing platelets ($2x10^8$/ml). Lysis was performed using the lysis buffer in the commercial kit, before the addition of RhoA GTP beads. Samples were then western blotted for active RhoA and total RhoA. **A)** Using 50μg beads, the level of activation response in suspended platelets was assessed using 1.0 and 0.1IU/ml of Thrombin concentration. Representative images of n=3 of the blots for active and total RhoA is shown. **B)** 25μg and 50μg of beads were tested on both suspended and spread platelet lysates to pick the signal for active RhoA (RhoA-GTP). Representative images of the blots for active and total RhoA is shown.

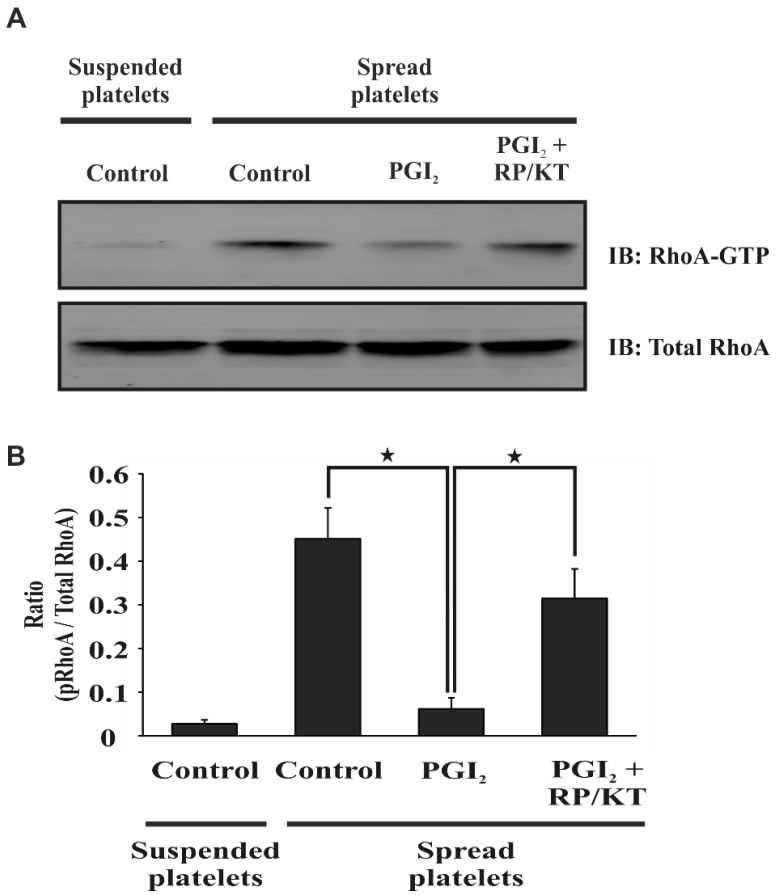

Figure 4. 16: Reversal of active RhoA concentration during treatment of spread platelets with PGI_2 in the presence of PKA inhibitors. Platelets ($2x10^8$/ml) were spread on 100µg/ml fibrinogen for 25 minutes in the presence or absence of PKA inhibitors 100µM RP-8CPT-cAMPS (RP) and 2µM KT5720 (KT), before being washed with PBS. The platelets were then treated with Tyrodes containing 10nM PGI_2, with or without PKA inhibitors (100µM RP-8CPT-cAMPS and 2µM KT5720), for a further 10 minutes. The samples were then lysed, using the lysis buffer in the commercial kit, before the addition of RhoA GTP beads (50µg). Samples were then western blotted for active RhoA and total RhoA. **A)** Representative images of the blots for active and total RhoA. **B)** Densitometry analysis for the RhoA pull down. The data was presented as average±SEM of n=3.

4.7: Discussion:

The previous chapter identified the effects of PGI_2 on the reversal of activation of spread platelets. This results section is based on identifying how PGI_2 co-ordinates this change to the platelet actin cytoskeleton. Is the reversal of platelet spreading a PKA mediated effect? What are the downstream components involved with PKA mediation of the effects on the platelet actin cytoskeleton?

PGI_2 is known to inhibit platelets in circulation, mediating via an increase in cAMP levels (Tateson et al., 1977, Aszodi et al., 1999). This rise could result from either an increased intracellular production such as by encountering a cAMP elevating agent in circulation or a potential reduction in its breakdown due to decreased activity of PDEs. Furthermore, an increase in platelet intracellular cAMP results in phosphorylation of downstream substrates via PKA. VASP is one of the established downstream proteins associated with PKA activation in platelets (Aszodi et al., 1999). My results identified that treatment of suspended platelets with PGI_2 led to both an elevation of cAMP and phosphorylation of $VASP^{Ser157}$ in a dose-dependent and time specified manner in agreement with Aburima *et al.*(2013).

In chapter 3, it was demonstrated that treatment with PGI_2 led to changes in the actin cytoskeleton of spread platelets. In this chapter therefore it was necessary to identify if PGI_2 induces these actin cytoskeletal modulations via altering the levels of cAMP in spread platelets. Furthermore, would this elevation in cAMP lead to phosphorylation of VASP in spread cells, as that identified in suspended platelets (Aszodi et al., 1999). Interestingly it was found that upon platelet spreading, platelets decrease their levels of cAMP. This effect could be explained by the activity of PDE in the cell. When platelets are activated by interaction between integrin $\alpha_{IIb}\beta_3$ and fibrinogen, possibly the PDE3 (a cAMP-targeting enzyme), would have been activated. This would have reduced the levels of cAMP in the platelet and would have helped in its' spreading. These assumptions have been based on the findings that the activity of PDE3 increases in suspended platelets upon stimulation by thrombin (Zhang and Colman, 2007) and an increase in cAMP levels inhibits cellular spreading (Hertz and Beavo, 2011), thus providing a plausible explanation to the observed effects in spread platelets.

However on treating these spread platelets with PGI_2 an approximate 3-fold increase in the intracellular level of cAMP was observed when compared with basal suspended platelets.

This clearly identifies that PGI_2 can cause an increase in the cAMP levels of spread platelets as had been experienced with suspended platelets. Similarly an elevation of $pVASP^{Ser157}$ was recognized in a dose-dependent and time specified manner in spread platelets in response to PGI_2, identifying that the spread platelets are capable of responding to PKA activity.

Further to this analysis of cAMP levels, platelets were spread in the presence of apyrase and indomethacin that inhibit the secondary mediators ADP and TXA_2, respectively. Interestingly platelets that had been spread in the presence of apyrase and indomethacin, had an increased level of cAMP in comparison to those spread without apyrase and indomethacin. This elevation of cAMP levels with the use of apyrase and indomethacin was most likely due to the absence of secretion from the platelets. The activation of platelet via spreading would have induced the release of ADP (even via stimulation by TXA_2) (Paul et al., 1999, Woulfe et al., 2001). The released ADP binds to P2Y1 and P2Y12 that function downstream via activation of the $G\alpha_i$ and $G\alpha_q$ subunits. The $G\alpha_i$ decreases the activity of adenylyl cyclase while $G\alpha_q$ activates the PI3K/Akt 1/2 pathway to activate PDE3 and thus decrease the level of cAMP in the platelet. In comparison, lack of secretion could not counter the increased cAMP under basal condition. This in addition correlates with the delay in spreading observed in platelets that had been treated with apyrase and indomethacin.

However, stimulation of spread platelets with PGI_2 in the presence of apyrase and indomethacin revealed a similar peak as to that had been achieved without treatment with apyrase and indomethacin. This correlated to a similar level of reversal of platelet activation observed in Figure 3.9, in the presence or absence of apyrase and indomethacin, with regards to removal of stress fibres and appearance of actin nodules.

Having identified the elevation of cAMP in spread platelets, it was now necessary to identify if the effect of PGI_2 on spread platelets was mediated downstream via PKA. To answer this question the PKA inhibitors, RP-8CPT-cAMPS (RP) and KT5720 (KT) were employed which targeted the regulatory and catalytic domains of PKA, respectively. It was observed that the platelets that had been spread in the presence of RP/KT did not produce the actin structural changes, of a decrease in stress fibres and an increase in actin nodules,

on treatment with PGI_2. This finding confirmed the actin structural changes associated with PGI_2 treatment to be PKA mediated.

Having identified that PGI_2 induced the actin cytoskeletal changes in a cAMP and PKA dependent manner, it was now necessary to identify the downstream targets of PKA that could be mediating the cytoskeletal effects. Previously, RhoA had been identified as a modulator for shape change in suspended platelets in a PKA dependent manner (Aburima et al., 2013). Furthermore Ren X.D. et al (1999) identified high levels of RhoA to be associated with a greater number of stress fibres in spread fibroblasts. To identify if RhoA acts as a potential candidate that links the PKA mediated actin cytoskeletal changes in spread platelets, the platelets were treated with Y27632 and Rhosin before allowing them to spread on fibrinogen. Both of these inhibitors target the Rho mediated pathway; Y27632 selectively inhibits Rho kinase (ROCK) by competing with ATP for binding to the kinase (Ishizaki et al., 2000), while Rhosin inhibits the GEF catalyzes RhoA activation by binding to RhoA on two adjacent groves which are required for interacting with GEF (Shang et al., 2012). The findings, using the inhibitors, revealed that inhibition of RhoA decreased stress fibres with a reciprocal increase in actin nodules in a dose dependent manner. This data is in agreement with the findings by Calaminus S.D.J. *et al.* (2008) that actin nodules are correlated with low RhoA-ROCK activity. In addition, a reduction in the surface area was observed. These findings suggested RhoA as a strong candidate for PKA mediated actin cytoskeletal rearrangement.

RhoA phosphorylation by PKA has been linked to its inactivation in platelets and other cell types (Chardin et al., 1989, Gorman et al., 1977, Aburima et al., 2013). Interestingly there was an increase in the level of $pRhoA^{Ser188}$, whilst there was a reciprocal reduction in the level of active GTP-bound form of RhoA after 10 minutes of treatment of spread platelets with PGI_2. Phosphorylation of RhoA has been postulated to tag it for binding to GDI, which makes RhoA less available from being converted back to its active GTP-form by a GEF (Faure and Dagher, 2001). This therefore has the effect of reducing the level of active RhoA in the cell, and therefore at the same time causes a reduction in stress fibre formation.

Interestingly studying the dynamics of $RhoA^{Ser188}$ phosphorylation, in a time course manner identified that upon treatment with PGI_2, maximal phosphorylation of $RhoA^{Ser188}$ (40mins) was preceded by the maximal removal of stress fibres (10mins).

A probable explanation for this prolonged phosphorylation event of RhoA in the platelet could be the lack of the protein to bind to platelet membrane and to remain in the cytosol, thus disabling the interaction with RhoGDI as it involves binding to the platelet membrane (Aburima A. et al 2013), or it may involve interaction with an A Kinase Anchoring Protein (AKAP). An AKAP plays an important role in the spatial and temporal regulation of the levels of cAMP in the cell. It compartmentalizes cAMP into restricted microdomains thereby providing a better control to the activities that cAMP could ensue in a cell (Raslan et al., 2015a). Formation of the microdomains relies on the activity of the adenylyl cyclase forming cAMP and the bounding limit and activity of the PDEs that cleave the cAMP to AMP. The AKAP binds to the substrate and brings it closer to interact with the anchored 'Kinase'; while keeping it within the bounding limits of the microdomain. The discrepancy in the signaling of RhoA and actin cytoskeletal changes possibly suggest that an AKAP could retain a phosphorylated RhoA and hold it in a spatial manner that prevents its dephosphorylation due to the spatial localization of cAMP and PDEs.

Although it is clear that PGI_2 is inactivating RhoA, and this removes stress fibre formation, does PKA also play a role in the formation of actin nodules, or is the reversal of stress fibres formation always going to form actin nodules independent of PKA? The actin nodule is a filamentous actin structure which is composed of a core which is made by Arp2/3, WASp, filamentous actin, and a ring-like assembly of integrins which is linked to the actin cytoskeleton of the core via multiple proteins. One of the postulated roles for the actin nodule is to act as a signaling hub (Calaminus et al., 2008). The actin nodules have been identified to contain AKAPs, moesin and Rac. The phospho-PKA substrates antibody hinted the presence of PKA phosphorylated proteins to be present at the actin nodules. Interestingly, Figures 4.13 and 4.14, identified phosphorylated $RhoA^{Ser188}$ and PKA regulatory component RII to be co-localized to these actin nodules. Therefore, this identified the possibility that inactivation of RhoA by PKA leads to the localization of $pRhoA^{Ser188}$ to the actin nodule. As Rac has also been shown to be identified at the nodule, this brings forward the possibility that the interaction between active Rac and active RhoA is critical in the formation and dissolution of the actin nodules.

Based on the results thus far along with findings from the literature, a schematic shown in figure 4.17, was developed to understand the mechanism by which PGI_2 mediates it effects upon the actin cytoskeleton. Spreading of platelets on fibrinogen involved activation of the

integrin receptor, αIIbβ3, via outside-in signaling (Salsmann et al., 2005). This recruits Src to the β3 subunits of αIIbβ3. The Src regulates RhoGEF that helps to convert RhoA to its active GTP-bound form. Active RhoA binds to ROCK that leads to inhibition of MLCP. The inhibition of MLCP leads to increased levels of phosphorylated MLC that corresponds to an increased stress fibre formation. Therefore interaction of RhoA-ROCK leads to an increase in stress fibres as seen in spread platelets. PGI_2 triggers an increase in cAMP, activating PKA causing the phosphorylation of RhoA and leads to the disinhibition of MLCP. This results in dephosphorylation of MLC, thereby removing stress fibres and causing the formation of actin nodules. Although there is an alternative pathway leading to MLC phosphorylation via activation of MLCK by Ca^{2+} mobilization, the data at present indicates this pathway does not play a major role in modulation of stress fibres in spread platelets by PGI_2.

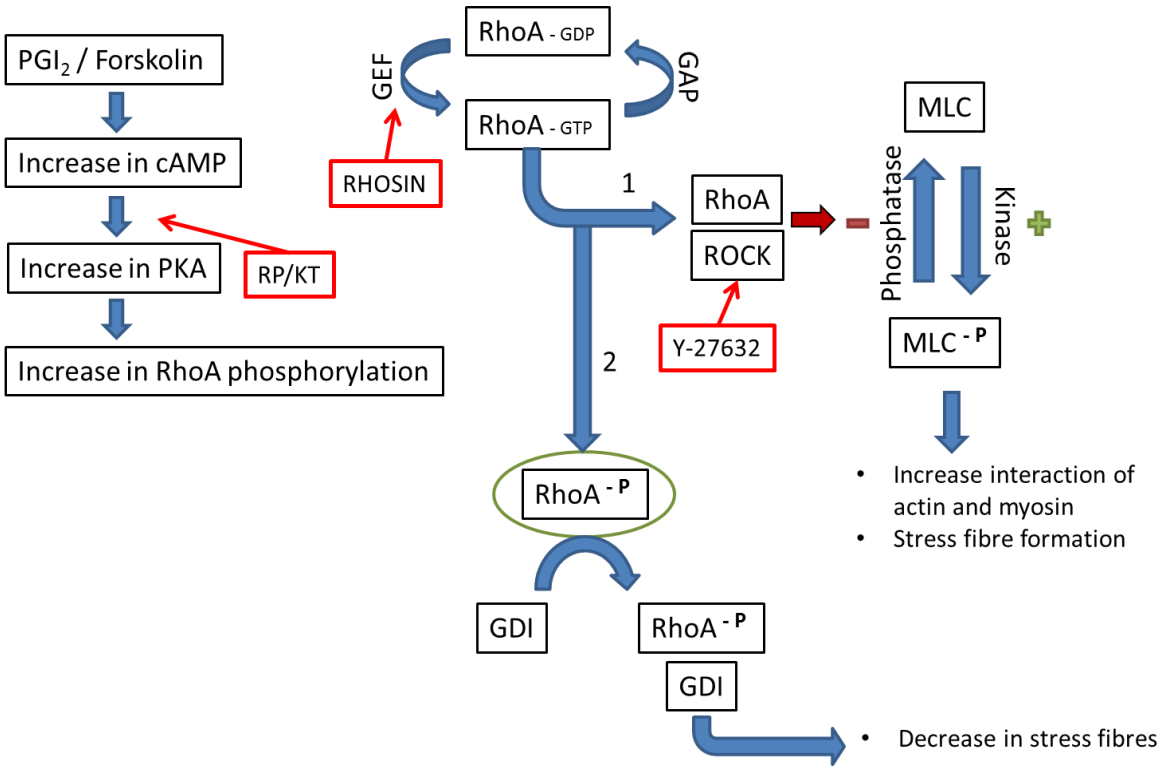

Figure 4. 17: Schematic of the effect of PGI_2 on RhoA-ROCK pathway. (1) Activation of RhoA via GEF enables the interaction of active RhoA to incorporate with Rho kinase (ROCK). This interaction inhibits the myosin light chain phosphatase that converts phosphorylated MLC to a non-phosphorylated form. This inhibition of conversion increases the phosphorylated form of RhoA which culminates in an increased interaction among actin and myosin and hence stress fibre formation. **(2)** PGI_2 via binding to its receptor (direct activation via Fsk) increases cAMP that stimulates production of PKA. An increased activity of PKA phosphorylates RhoA and tags it to be bound to GDI. Interaction with GDI channels the active RhoA away from interaction with ROCK and hence disinhibits myosin light chain phosphatase, reduces phosphorylated form of MLC and thus decreases stress fibres.

CHAPTER 5:

PGI_2 modulates thrombus formation under high shear

5.1 Introduction:

Haemostatic plug formation is a multifaceted dynamic process that requires many factors to be coordinated effectively in order for its eftective completion. The co-ordination is required as aberrations in the co-ordination can lead to either too little thrombus formation and excessive bleeding, or too much thrombus formation and the formation of occlusive thrombi that hinder the flow of blood in the vessel.

Platelets are a key part of this process of haemostasis. They circulate through the body in the vasculature. Within this environment, the red blood cells push the platelets to the periphery of the vessel, near to the endothelial lining of the vessel wall. The endothelium plays a pivotal role in mediating a swift but a controlled response of the platelets. In its undamaged and non-inflamed state the endothelium provides a non-adherent site for the platelets and moreover, it releases PGI_2 and NO into the circulation that act as vasodilators and powerful inhibitors of platelet activation (Bergmeier and Hynes, 2012, Moncada et al., 1976).

An increase in the formation of a thrombus results in a greater shear of the flowing blood and an enhanced generation of thrombin. Both of these factors have been linked with an increase in the release of PGI_2 in the circulation (Bouaziz et al., 1998, Weksler et al., 1978).

In addition, the endothelium is also known to deposit, towards its basal surface, ECM proteins onto the basement membrane (Bergmeier and Hynes, 2012). Upon injury to the vessel wall the underlying ECM proteins are exposed, which leads to activation of platelets. Collagen has been considered the most abundant component of the matrix protein (Halper and Kjaer, 2014) and has been classed as a strong activator of platelets (Bergmeier and Hynes, 2012). As reviewed by Brass L.F. *et al. (2011*), the exposed matrix proteins are initially decorated by the vWF that interacts with its receptor (GP-Ib-IX-V) along with integrin ($\alpha_{IIb}\beta_3$) present on the surface of the platelets (Hantgan et al., 1990a, Hantgan et al., 1990b). These interactions provide enough time for the collagen to induce clustering of its receptors (GPVI and $\alpha_2\beta_1$) (Chen et al., 2002, Clemetson et al., 1999). This helps in the formation of a monolayer of platelets to which additional platelets, using their activated integrin ($\alpha_{IIb}\beta_3$) interact with available fibrinogen either from the plasma or secreted by platelets, build upon developing a thrombus. Therefore the basal layer of platelets is

mediated by collagen interaction while successive layers in a thrombus are regulated by fibrinogen.

The depth of the injury determines the amount and the type of matrix protein encountered by the platelets and thereby the response that they would generate. Collagen type IV is present closer to the vascular endothelial layer, being in the basement membrane while collagen types I, III and V are found in deeper layer of the vascular ECM. Although these and other subtypes of collagen act via activation of GPVI receptor, still collagen types I, III, V are more potent agonists than collagen type IV to GPVI receptor activation (Bergmeier and Hynes, 2012). A deeper injury would generate an increased response; while a superficial injury ensues a weaker response. Therefore, a level of control exists that interplays to the comparable response generated to the depth of the injury.

It has recently been identified that thrombi have a core and shell region. Within these regions there are differing levels of platelet activation, due to differing concentrations of agonists. Within the core region thrombin dominates. This causes full platelet activation allowing for the formation of tightly packed platelet core and a complete spreading response. In contrast in the shell region thrombin is not present. Instead ADP and TXA_2 are present from those platelets that have been activated by thrombin, which allow for partial platelet activation. Due to the partial platelet activation there is increased porosity and a looser arrangement of platelets within the shell, theoretically allowing access for PGI_2 into the shell region. (Stalker et al., 2013, Stalker et al., 2014, Welsh et al., 2014).

5.2 Aims of the chapter

The aim of this chapter was to identify if the cytoskeletal changes induced within a spread platelet by PGI_2, would cause an effect upon thrombus formation, its' stability or its' dissolution.

- To identify if PGI_2 treatment under flow induces morphological changes to platelets spread on fibrinogen
- To identify if PGI_2 treatment has any effect on the actin cytoskeleton of platelets that have been spread on collagen.
- To identify if PGI_2 treatment under flow induces morphological changes to platelets spread on collagen and if the effect is reversed by inhibition of PKA.

5.3 Thrombus formation on Fibrinogen

Since Chapters 3 and 4 identified the significant effect of PGI_2 on the actin cytoskeleton of spreading of platelets and the molecular mechanism underlying the effect of PGI_2, it was necessary to understand how these cytoskeletal changes induced by PGI_2 might affect platelet function in the more physiological relevant assay, in vitro flow.

5.3.1 Thrombus formation under flow using different dose of Fibrinogen

In order to identify a possible effect of PGI_2 on thrombus formation on fibrinogen, it was first necessary to identify the appropriate concentration of the matrix protein for further experiments. Fibrinogen concentrations of 100, 300 and 1000µg/ml were used to coat cellix biochips (vena endothelial+ specialized for whole blood flow assays), for an overnight incubation at 4^oC in a humid chamber. The next day human blood mixed with PPACK (100µM) as an anticoagulant was stained with $DIOC_6$ (10µM) for 20 minutes before flowing through the biochip chamber at a shear rate of 1000/sec (45.0 dynes/cm^2) for 2 minutes. Thrombus formation was followed via video microscopy. After 2 minutes the thrombi were fixed with 4% paraformaldehyde for 30 minutes. The biochip was restained using $DIOC_6$ (10µM) with an overnight incubation and subsequently z-stack images were taken using Zeiss Apotome microscope. The images were analyzed for the number of thrombi per image, the percentage of average surface area coverage by the thrombi and the height attained by these thrombi.

It was found that the surface area coverage by the platelets in the whole blood increased with an increasing concentration of fibrinogen. The 100µg/ml attained 32.21±15.78% coverage that increased to 38.24±8.29% at 300µg/ml and finally reached 56.45±24.84% coverage at 1000µg/ml of fibrinogen concentration (Figure 5.1A and B). Interestingly however, there was no change in the height of the thrombus with 4.05±0.07µm at 100µg/ml, 4.11±0.001µm at 300µg/ml and 4.39±0.002µm at 1000µg/ml of fibrinogen concentration (Figure 5.1C). However, the number of thrombi increased with increased fibrinogen concentration with 2.46±0.58 thrombi per image at 100µg/ml, 3.89±0.49 thrombi per image at 300µg/ml and 8.14±2.86 thrombi per image at 1000µg/ml of fibrinogen concentration (Figure 5.1D).

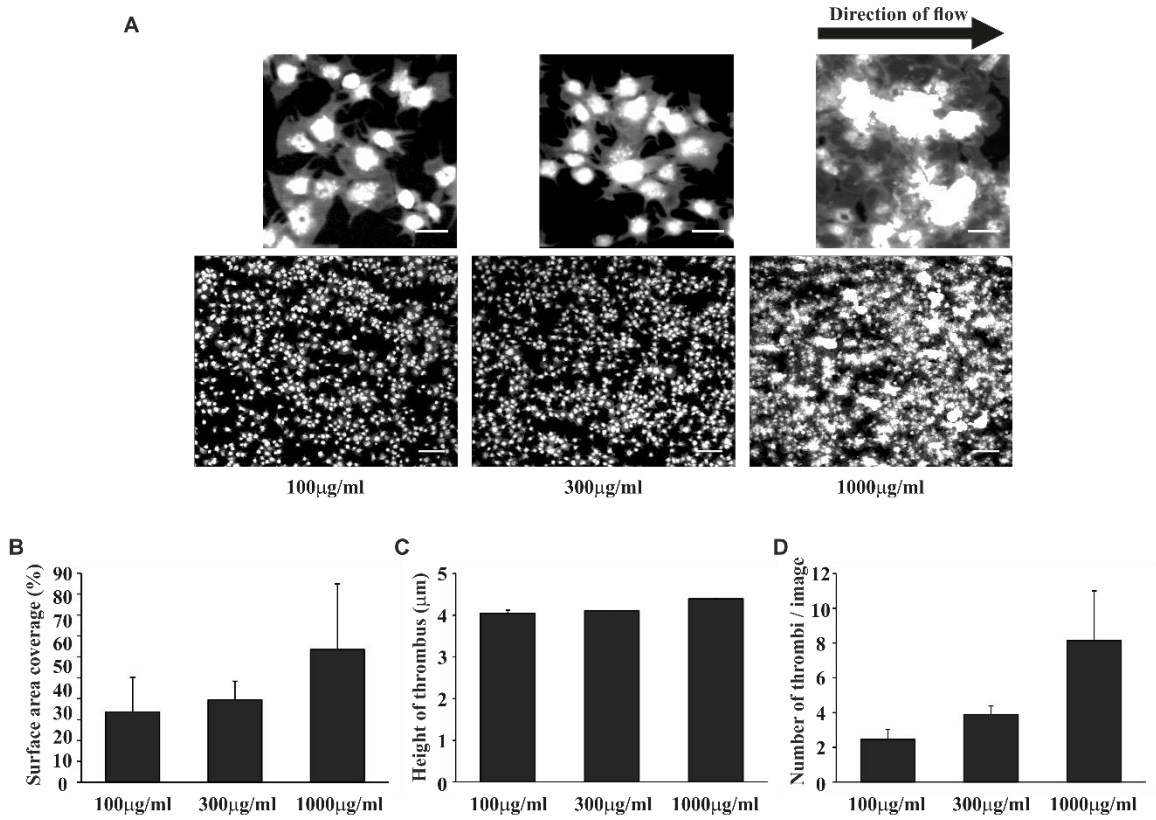

Figure 5. 1: Increase in thrombus formation on increasing concentration of fibrinogen. Human whole blood (with PPACK) was stained with $DIOC_6$ and flown over biochips that had been coated overnight with different concentrations of fibrinogen at 100, 300 and 1000µg/ml. The blood was flown for 2 minutes prior to fixation and restained with $DIOC_6$. Using a fluorescence microscope z-stack images were obtained. **A)** Representative images for the different concentrations of fibrinogen. Scale bar is 20µm. The insert shows an enlarged image of their respective images with a scale bar of 5µm. **B)** Analysis of percentage of the surface area coverage at 100, 300 and 1000µg/ml of fibrinogen. **C)** Analysis of height of the thrombus at 100, 300 and 1000µg/ml of fibrinogen. **D)** Analysis of number of thrombi per image at 100, 300 and 1000µg/ml of fibrinogen. The data was presented as average±SEM of n=2-3.

The data identified that 100μg/ml fibrinogen showed fewer number of platelet accumulations while 1000μg/ml showed a more accumulation of platelets which had indistinct overlapping margins of the spread platelets. Therefore, for further experiments, 300μg/ml of fibrinogen attained a fine balance to observe the effects of PGI_2 treatment on platelet spreading and any changes that may follow to the formed thrombi.

5.3.2 Effect of pretreating blood with PGI_2 and allowing thrombus formation on Fibrinogen

The next step was to observe the effect of prior PGI_2 treatment on thrombus formation. The human whole blood with PPACK was stained with $DIOC_6$ for a minimum of 20 minutes. The blood was treated with different concentrations of PGI_2 for 2 minutes in suspension, shown in the schematic figure 5.2A, prior to flowing it on the already prepared cellix biochips that had been coated with 300μg/ml of fibrinogen for an overnight incubation. The flow lasted for 2 minutes after which the thrombi were fixed. Analysis of the surface area coverage indicated that in control conditions there was 35.29±5.63% coverage, with 1nM of PGI_2 was 41.50±0.02% at 10nM was 23.93±7.52% and at 100nM was 21.64±2.84% (Figure 5.2B and C). However, the height of the thrombus remained stable with the use of different concentrations of PGI_2 for pretreatment of platelets, with the control level at 3.92±0.11μm 3.52±0.52μm at 1nM, 3.85±0.37μm at 10nM and 3.67±0.14μm at 100nM PGI_2 (Figure 5.2D). The analysis in figure 5.2E indicated that pretreatment of platelets with an increasing dose of PGI_2 possibly increased the number of thrombi. The control had 4.50±0.67 thrombi per image, which decreased to 2.75±1.25 thrombi per image at 1nM, while it increased to 6.42±0.42 thrombi per image at 10nM and 6.96±1.21 thrombi per image at 100nM PGI_2.

After establishing that pre-treated platelets with PGI_2 inhibits platelet adhesion under high shear on fibrinogen, it was now necessary to identify if PGI_2 would have an effect on platelets that have already been adhered, and started to form thrombi on fibrinogen.

5.3.3 PGI_2 treatment of thrombi formed on Fibrinogen

As completed previously, human whole blood mixed with PPACK was stained with $DIOC_6$ and flown over 300μg/ml fibrinogen for 2 minutes (Supplementary Video 1). At

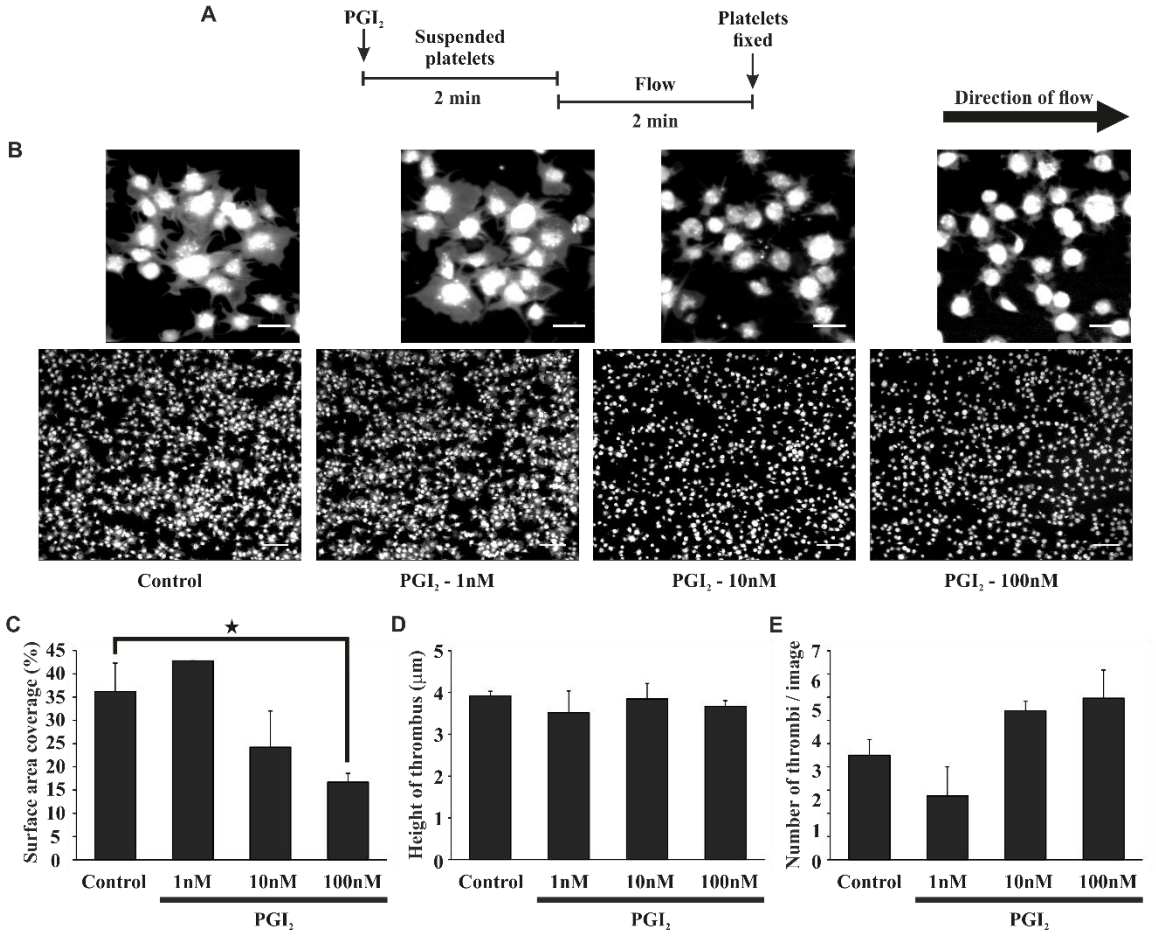

Figure 5. 2: Pretreating platelets with PGI_2 induces a dose dependent reduction in surface area coverage under flow on fibrinogen. Human whole blood (with PPACK) was stained with $DIOC_6$ and pretreated for 2 minutes with 1nM, 10nM and 100nM of PGI_2 prior to flowing them over biochips for 2 minutes that had been coated overnight with 300µg/ml of fibrinogen. The biochip was fixed and restained with $DIOC_6$. Using a fluorescence microscope, z-stack images were obtained. A) A schematic for the experimental plan. B) Representative images for the pretreatment with different concentrations of PGI_2. Scale bar is 20µm. The insert shows an enlarged image of their respective images with a scale bar of 5µm. C) Analysis of percentage of the surface area coverage at pretreatment of platelets with 1nM, 10nM and 100nM of PGI_2. D) Analysis of height of the thrombus at pretreatment of platelets with 1nM, 10nM and 100nM of PGI_2. E) Analysis of number of thrombi per image at pretreatment of platelets with 1nM, 10nM and 100nM of PGI_2. $p<0.05$. The data was presented as average±SEM of n=2-3.

this point the samples were treated for another 10 minutes with PBS in the presence or absence of PGI_2 (100nM) (Figure 5.3A) (Supplementary Videos 2 and 3). The results revealed that the surface area coverage attained at 2 minutes of flowing blood was 38.24±6.77% that increased to 43.46±6.80% at 10 minutes flow without PGI_2. On treatment with PGI_2 (100nM) for 10 minutes the surface area coverage reduced significantly to 24.39±2.94% (Figure 5.3B and C).

The data demonstrate that PGI_2 reduces platelet adhesion under flow. As had been identified that in accordance with the effect on surface area coverage of thrombi, events of embolisation were also observed on treatment with 100nM PGI_2 (Supplementary Video 2), while these events were absent on flow with PBS (Supplementary Video 3). Therefore, to confirm that this effect of PGI_2 was mediated via PKA, the PKA inhibitors – RP-8CPT-cAMPS and KT-5720 were used with human whole blood under flow on fibrinogen.

5.3.4 PGI_2 mediates its effect on formed thrombi (on fibrinogen) via PKA activity

Human whole blood mixed with PPACK was stained with $DIOC_6$ for a minimum of 20 minutes. As shown in the schematic in figure 5.4A, whole blood was incubated for 20 minutes in the presence and absence of RPKT inhibitors prior to flowing it on 300μg/ml of fibrinogen for 2 minutes (Supplementary Video 4) and continuing for another 10 minutes with the presence or absence of RPKT inhibitors in the presence or absence of PGI_2 (100nM) (Supplementary Videos 5 and 6).

The results identified that the average surface area coverage (standardized with individual control) under basal conditions reduced significantly to 57.55±8.05% on treatment with 100nM of PGI_2 (Figure 5.4B and C). In the presence of the PKA inhibitors, RP-8CPT-cAMPS (500μM) and KT-5720 (10μM), PGI_2 treatment did not alter the average surface area coverage (100.4±11.72% of control) (Figure 5.4B and C). In agreement the embolisation events observed with PGI_2 treatment of formed thrombi on fibrinogen, as seen in the Supplementary Video 2, were not identifed on treatment of RP/KT inhibitors in the presence of PGI_2 (Supplementary Video 5).

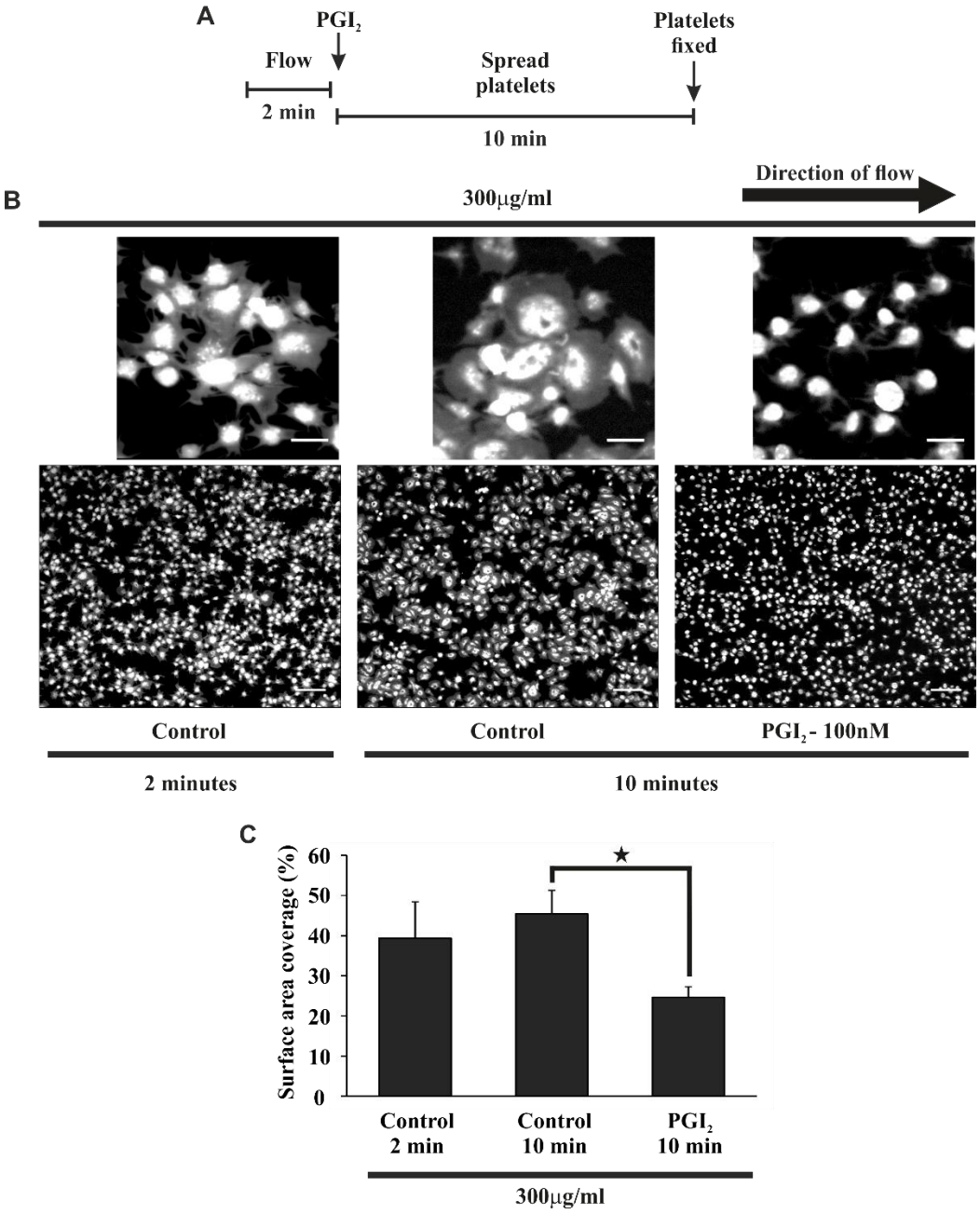

Figure 5. 3: Platelets spread on fibrinogen have reduced surface area coverage on treatment with PGI_2 under flow. Human whole blood (with PPACK) was stained with $DIOC_6$ and allowed to flow over fibrinogen coated (300µg/ml) biochips for 2 minutes. The flow with PBS, in the presence or absence of 100nM PGI_2, was continued over formed thrombi for 10 minutes before fixation and restaining with $DIOC_6$. Using a fluorescence microscope, z-stack images were obtained. A) A schematic for the experimental plan. B) Representative images for the experiment with a scale bar of 20µm. The insert shows an enlarged image of their respective images with a scale bar of 5µm. C) Analysis of percentage of the surface area coverage at treatment of thrombi with 100nM PGI_2. $p<0.05$. The data was presented as average±SEM of n=3.

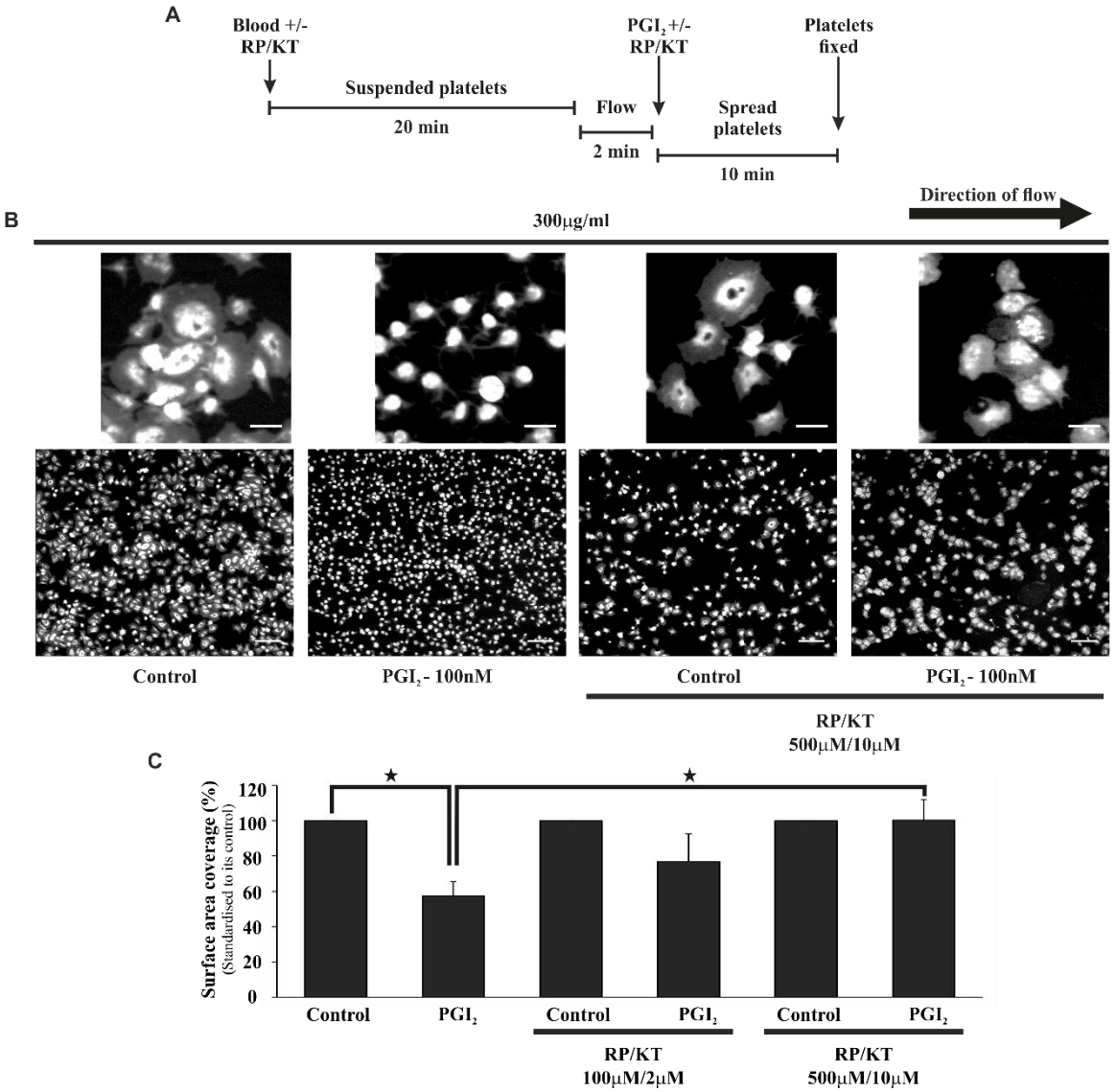

Figure 5. 4: Post perfusion of 100nM PGI_2 on platelets spread on fibrinogen reduces surface area coverage, under flow, which in inhibited in the presence of PKA inhibitors. Human whole blood (with PPACK) was stained with $DIOC_6$. It was incubated with RP-8CPT-cAMPS (RP) and KT-5720 (KT) for 20 minutes prior to flowing over fibrinogen coated (300µg/ml) biochips for 2 minutes. The flow was continued with PBS containing RP/KT in the presence or absence of 100nM PGI_2, over formed thrombi, for 10 minutes before fixation and restaining with $DIOC_6$. Using a fluorescence microscope, z-stack images were obtained. **A)** A schematic for the experimental plan. **B)** Representative images for the experiment with a scale bar of 20µm. The insert shows an enlarged image of their respective images with a scale bar of 5µm. **C)** Analysis of percentage of the surface area coverage, standardized to its control, on treatment of thrombi with 100nM PGI_2 in the presence or absence of RP/KT. $p<0.05$. The data was presented as average±SEM of n=2-5.

5.4 Thrombus formation on Collagen

Although PGI_2 caused a clear reduction in platelet surface area coverage under flow on fibrinogen, it was necessary to identify if this effect was present on the main ECM component involved within the thrombus formation process, collagen.

5.4.1 PGI_2 treatment of thrombi formed on Collagen

As the previous data had suggested that post treatment of PGI_2 induced a reduction in surface area on fibrinogen, it was necessary to identify if this also occurred on the more relevant thrombogenic ECM protein collagen. A 25μg/ml of collagen concentration was used within the assay as it provides robust thrombus formation (Ollivier et al., 2014). Therefore, human whole blood mixed with PPACK, as an anticoagulant, was stained with $DIOC_6$ and flown over collagen coated biochips for 2 minutes (Supplementary Video 7) and continued for another 10 minutes with PBS in the presence or absence of PGI_2 (100nM), similar to the schematic in figure 5.3A (Supplementary Videos 8 and 9). The results revealed that the surface area coverage attained by the control was 15.01±3.07% which reduced to 2.33±0.66% at 100nM post flow with PGI_2 (Figure 5.5A and B). On treating already formed thrombi with PGI_2 for 10 minutes the height of the thrombus in the control was 7.26±0.68μm which reduced to 4.38±0.12μm at 100nM (Figure 5.5A and C). Measuring the number of thrombi per image, it was found that the control attained 15.52±1.61 thrombi which reduced to 7.24±1.15 thrombi with 100nM PGI_2 post flow (Figure 5.5A and D). In comparison to the control, PGI_2 treatment of preformed thrombi led to embolisation events as identified in the Supplementary Videos 8 and 9.

5.4.2 PGI_2 mediates its effect on formed thrombi (on collagen) via PKA activity

This data identified that PGI_2 mediated a significant reduction in thrombi after they had been formed on collagen. However to demonstrate that PGI_2 was mediating this in a PKA dependent manner human whole blood mixed with PPACK, was stained with $DIOC_6$ for a minimum of 20 minutes. In addition, it was incubated in the presence or absence of PKA inhibitors (100μM RP-8CPT-cAMPS / 2μM KT5720) for 20 minutes and flown over collagen coated biochips for 2 minutes (Supplementary Video 10). The flow was continued for another 10 minutes with PBS in the presence or absence of PGI_2 (100nM) and the PKA

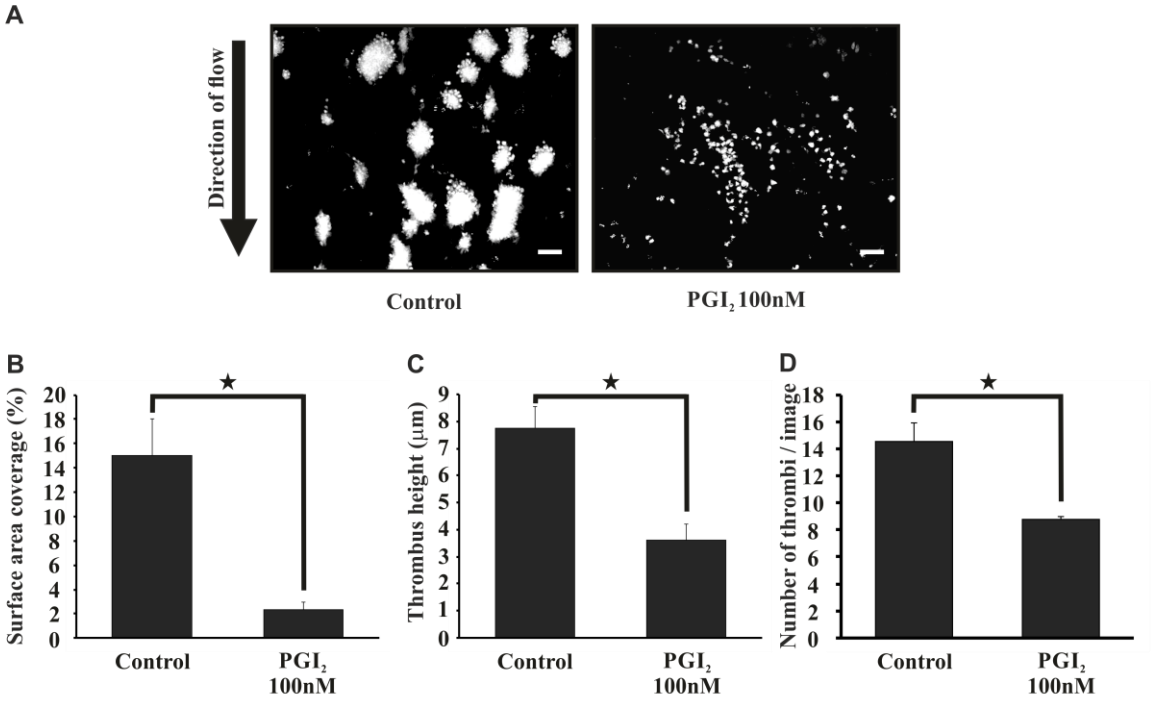

Figure 5. 5: Effect of post perfusion of PGI_2 in a dose response manner. Whole blood, stained with $DiOC_6$ was flown over collagen (25μg/ml) coated slides for 2 minutes at a shear rate of $1000s^{-1}$. After 2 minutes, PBS in the presence or absence of PGI_2 (10 and 100nM) were perfused over the preformed thrombi for 10 minutes at $1000s^{-1}$. **A)** Representative images of the thrombi observed under these different experimental conditions. **B)** The surface area coverage of the thrombi after 10 minutes of perfusion with or without 100nM PGI_2. **C)** Changes in the height of the thrombus after post perfusion with 100nM PGI_2. **D)** Effect on the number of thrombi per image with 100nM PGI_2. The thrombi were fixed, restained and imaged (z-stack=0.5μm). The data was presented as average±SEM of n=3. $p<0.05$. Scale bar is 20μm.

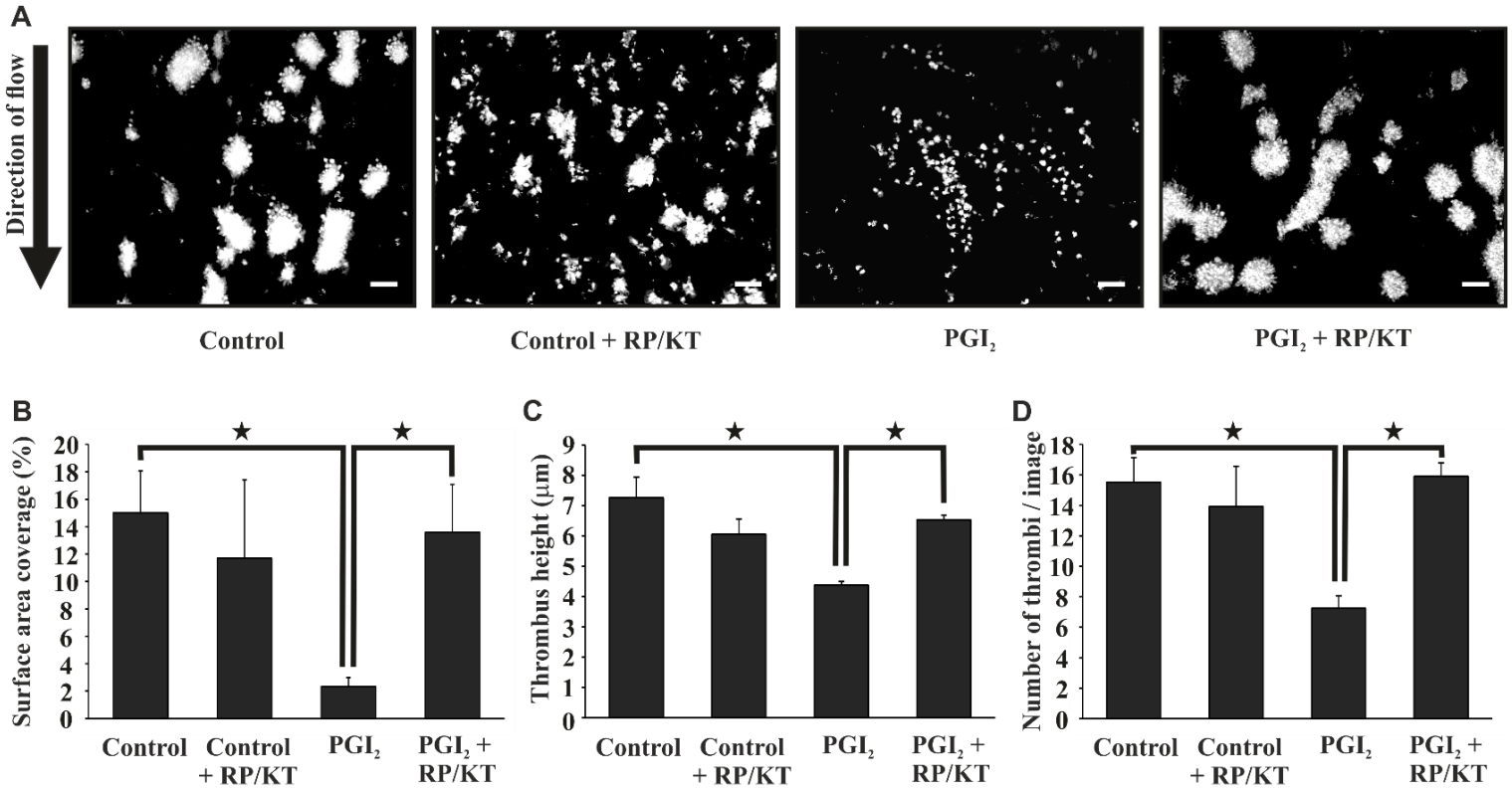

Figure 5. 6: Post perfusion of 100nM PGI_2 induces embolization of performed thrombi. Whole blood, stained with $DiOC_6$ was flown over collagen (25μg/ml) coated slides for 2 minutes at a shear rate of $1000s^{-1}$. After 2 minutes, PBS in the presence or absence of 100nM PGI_2 [in the presence or absence of PKA inhibitors (100μM RP-8CPT-cAMPS / 2μM KT5720)] were perfused over the preformed thrombi for 10 minutes at $1000s^{-1}$. **A)** Representative images of the thrombi observed under these different experimental conditions. Scale bar is 20μm. **B)** The surface area coverage of the thrombi after 10 minutes of perfusion with 100nM PGI_2, with or without PKA inhibitors (100μM RP-8CPT-cAMPS / 2μM KT5720). **C)** Changes in the height of the thrombus with 100nM PGI_2, with or without PKA inhibitors. **D)** Effect on the number of thrombi per image with 100nM PGI_2, with or without PKA inhibitors. The thrombi were fixed, restained and imaged (z-stack=0.5μm). $p<0.05$. n=3.

inhibitors (100μM RP-8CPT-cAMPS / 2μM KT5720), similar to the schematic in figure 5.4A (Supplementary Videos 11 and 12). The results in figure 5.6B revealed that the surface area coverage attained by the control was 15.01±3.07% which reduced significantly to 2.33±0.66% at 100nM PGI_2 post flow. In the presence of RPKT the control attained 11.7±5.71% surface area coverage which was unaffected with the addition of 100nM PGI_2 at 13.59±3.48% (Figure 5.6A and B). In agreement, the thrombus height was also significantly reduced from 7.26±0.68μm in control to 4.38±0.12μm at 100nM PGI_2 with PKA inhibition blocking this reduction in thrombus height. Similarly, the embolisation observed with preformed thrombi on collagen, on treatment with PGI_2 was not observed in the presence of RPKT inhibitors with PGI_2 (Supplementary Videos 8 and 11).

Analysis of the number of thrombi per image identified 15.52±1.61 thrombi (13.92±2.65 for control treated with RPKT) in the control that reduced significantly to 7.24±0.81 thrombi with 100nM PGI_2 and reverted to significant levels at 15.9±0.90 thrombi with 100nM PGI_2 post flow in the presence of RPKT (Figure 5.6B and D). This confirmed that

the effects observed in terms of surface area coverage, height of thrombus and number of thrombi formed on collagen is mediated by PGI_2 via a PKA dependent mechanism.

5.4.3 Effect of PGI_2 on platelets spread on collagen

As there was a strong inhibition of thrombus formation on collagen, it was necessary to try to identify the effect of PGI_2 on spread platelets on collagen, to identify if PGI_2 was modulating the actin cytoskeleton on platelets spread only fibrinogen or also collagen. Therefore ($2x10^7$/ml) platelets were spread on collagen as per the schematic in Figure 5.8A. The platelets were then fixed, stained with FITC-phalloidin and imaged using a fluorescence microscope.

Analysis of the platelets identified that the adhesion of the platelets spread on collagen, standardized to the control, remained steady (Figure 5.7B and C). The surface area of these spread platelets just before addition of 10nM PGI_2 was 30.24±4.01μm^2 which increased to 32.96±1.37μm^2 for a further 10 minutes spreading in the absence of PGI_2 but on treatment with PGI_2 for 10 minutes the surface area was 34.02±2.13μm^2 (Figure 5.7B and D). Analysis of actin nodule formation was not possible as actin nodules do not form on collagen (Calaminus et al., 2008).

Using the same schematic in figure 5.7A, platelets ($2x10^7$/ml) were spread on 100μg/ml of collagen for 25 minutes in the presence of apyrase (2U/ml) and indomethacin (10μM). The platelets were then washed before the addition of 10nM PGI_2, in the presence of apyrase (2U/ml) and indomethacin (10μM), for 10 minutes. The platelets were then fixed, stained with FITC-phalloidin and imaged using a fluorescence microscope. The addition of apyrase (2U/ml) and indomethacin (10μM) reduced platelet adhesion in comparison to the control without apyrase (2U/ml) and indomethacin (10μM) (Figure 5.8A and B). However the addition of PGI_2 in the presence of apyrase and indomethacin had no effect on the actin cytoskeleton of the spread platelet. Furthermore, surface area analysis of the apyrase and indomethacin treated spread platelets, in the absence or presence of 10nM PGI_2 identified surface area coverage of 32.92±0.96μm^2 in the control whilst PGI_2 treated samples treated had a surface area of and 33.88±2.10μm^2, respectively (figure 5.8A and C).

Therefore PGI_2 had no effect on the actin cytoskeleton of platelets spread on collagen, as stress fibres could not be reversed in these spread platelets. This effect on the actin cytoskeleton was maintained even in the absence of platelet secretion.

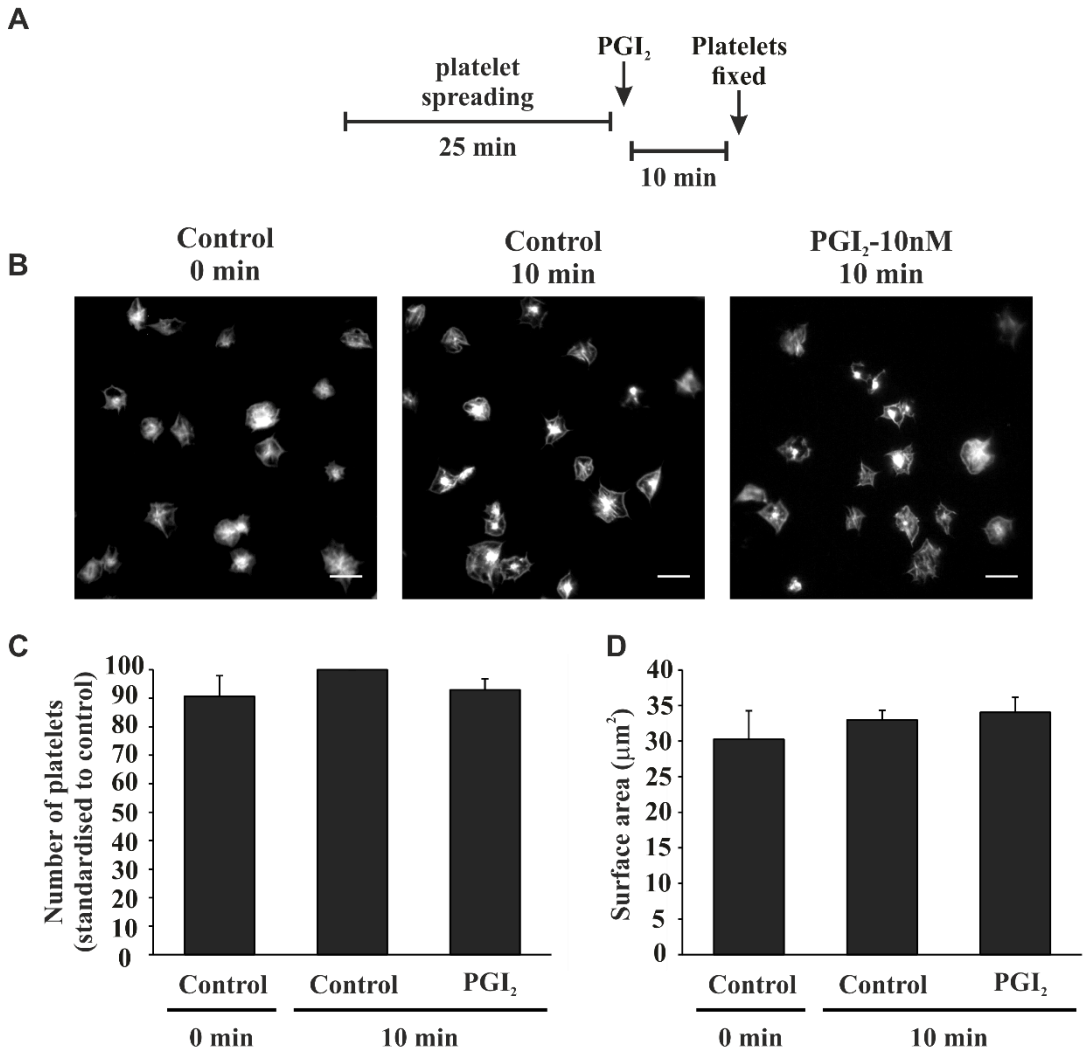

Figure 5. 7: PGI_2 does not affect stress fibre formation in prespread platelets on collagen. Platelets ($2x10^7$/ml) were spread on 100μg/ml collagen for 25 minutes. The platelets were then washed, before the addition of 10nM PGI_2 for 10 minutes. The platelets were then fixed, stained with FITC-phalloidin and imaged. **A)** Experimental design and **B)** representative images of experimental conditions. Scale bar is 5μm. **C)** The number of platelets adhered, and **D)** the average surface area of the platelets were analyzed using ImageJ. The data was presented as average±SEM of n=3.

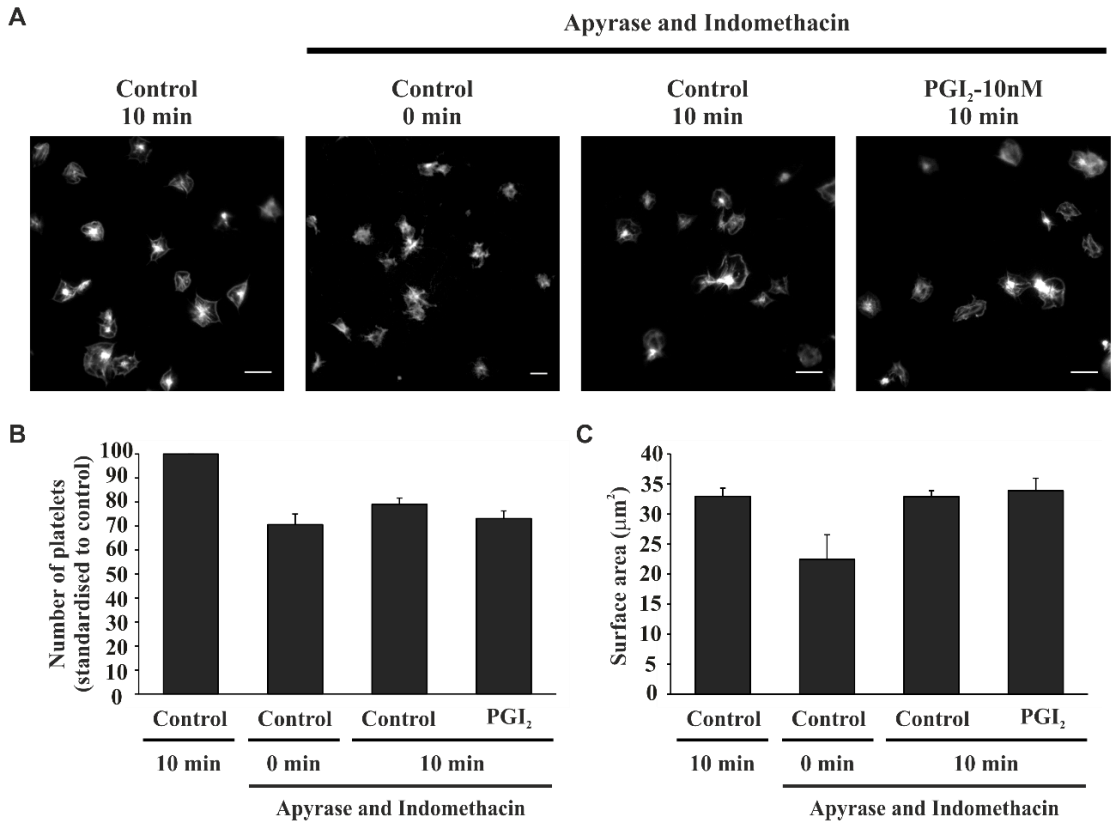

Figure 5. 8: PGI_2 does not affect stress fibre formation in prespread platelets on collagen in the absence of ADP and TXA_2. Platelets ($2x10^7$/ml) were spread on 100μg/ml collagen for 25 minutes with apyrase (2U/ml) and indomethacin (10μM). After 25 minutes, the platelets were then washed with Tyrodes, before the addition of 10nM PGI_2 for 10 minutes in the presence of apyrase (2U/ml) and indomethacin (10μM). The platelets were then fixed, stained with FITC-phalloidin and imaged. A) Representative images of three individual experiments. Scale bar is 5μm. B) The number of platelets adhered, and C) the average surface area of the platelets were analyzed using ImageJ. The data was presented as average±SEM of n=3.

5.5 Discussion

The main role postulated for the endothelial derived factor, PGI_2, is that it ensures the inhibition of platelets within the vasculature. This prevents the platelet from aberrantly activating and causing thrombus formation in unwanted locations. However on endothelial damage platelet activation ensues. This activation process can override the inhibitory signals induced by PGI_2, leading to platelet activation and thrombus formation. Therefore, key to the platelet is the balance between the activatory and inhibitory signals within the vasculature environment. However it has been difficult to identify if PGI_2 is released prior to injury. One school of thought indicates PGI_2 is present at all times within the vasculature. This therefore indicates that platelets are exposed to the inhibition by PGI_2 at all times. A publication by FitzGerald et al. (1981), measured levels of PGI_2 in the human circulation. According to the article 10pM PGI_2 was identified to be present in the circulation, while 0.1nM was required to inhibit platelets (FitzGerald et al., 1981). The other school of thought indicates that PGI_2 is not released continually, but that NO can maintain platelets in an inhibited state within the normal vasculature. PGI_2 production by the endothelial cells is then induced after thrombus formation is initiated by the presence of thrombin as shown by Weksler *et al.* (1978). This therefore opens up the possibility that PGI_2 could be important in controlling thrombus formation, as elevation of PGI_2 concentration induced by Thrombin could then limit the activatory signals from Thrombin, ADP and fibrinogen within the thrombus. However at present there is little data to support this theory.

5.5.1 The role of PGI_2 in thrombus formation on fibrinogen

Within this thesis I have already identified that PGI_2 can reverse the activatory state of spread platelets by removal of stress fibers and the appearance of actin nodules. This effect of stress fibre reversal was PKA mediated. The question that has been targeted in this results section had been to identify if the reversal of stress fibers by the addition of PGI_2 would have physiological relevance under flowing conditions over preformed thrombi.

Analysis of the flow experiments indicated that there was a decrease in platelets spreading and a reduction in the surface area coverage on fibrinogen with the pre-treatment of blood with PGI_2. This is in agreement with the findings of Weiss H.J. and Turitto V.T. (1979) that pretreatment of blood with PGI_2, flowing on rabbit de-endothelialised matrix at arterial shear rate inhibited thrombus formation.

Interestingly, fibrinogen could not support the formation of a thrombus, rather platelets tends to form aggregates. This is due to the fact that platelets on exposure to fibrinogen spreads on the matrix without the generation of thrombin nor a detectable Ca^{2+} level within the platelet (Heemskerk et al., 1997). Both of these factors enhance platelet activation that leads to a robust thrombus formation. Absence of this enhanced activation while spreading on fibrinogen platelets accumulates to form small aggregates rather than thrombi. Further analysis of preattached platelets on fibrinogen under high shear in the presence of PGI_2 showed a significant reduction in the surface area coverage. Interesting again, this was likely to be associated both with the embolisation of platelets from the surface, but also the reduction in platelet surface area in the presence of PGI_2. This finding under flow corroborated the effect that had been observed under a static system, however, due to the paucity of thrombus formation on fibrinogen, no change in the height of the thrombus (platelet aggregate) was appreciated either in control or with PGI_2 treatment. This data identifies that PGI_2 release does have a physiological relevance to regulate thrombus formation.

As part of this analysis thrombus height and number was analysed. However, this induced a curious result with an elevation in the number of thrombi in the PGI_2 pretreated platelets. However, PGI_2 induces the rounding up of the platelet, as the platelet withdraws its lamellipodia (Figure 5.2C). Therefore, as no a height difference was appreciated between a flattened spread platelet and a more rounded PGI_2 treated platelet, thereby affecting the analysis of thrombus height. This is most pertinent here as there is not a true thrombus formation, but really a monolayer of platelets, with some platelet aggregates formation. Therefore, it is likely that the analysis of thrombus height and thrombus number on treatment with PGI_2 were misleading.

5.5.2 The role of PGI_2 on thrombus formation on collagen

Collagen forms the key matrix that is exposed on an injury to the vascular endothelium. Formation of thrombi on collagen involves the basal platelets to be adhered onto collagen with fibrinogen becoming the major mediator for the thrombus. So it was of interest to identify if the effects observed with PGI_2 on fibrinogen could be replicated with collagen. A reduction in thrombus surface area was observed, on treatment with PGI_2, but this effect could not be ascertained if this had been due to collagen or fibrinogen. A static collagen spreading assay, revealed that PGI_2 does not cause removal of stress fibers or a reduction

in the surface area in platelets spread on collagen. Thereby, it confirms that the drop in surface area and the height of the thrombus was mediated by the effect of PGI_2 on fibrinogen. Therefore the level of PGI_2 release in the circulation could well be controlling the height of the thrombus without hampering the clot formation to stop the bleeding.

According to Stalker T.J. et al (2014), the thrombus could roughly be categorized into having a 'core' with compactly arranged platelets and an outer 'shell' with loosely organized platelets. Intermediary to the extremes is the 'transition' area where varying characteristics of the two zones exists. The difference between these regions is the potent ability of thrombin, ADP and TXA_2 to mediate their effects in a gradient pattern. Thrombin acting mainly on platelets in the core while ADP and TXA_2 act on loosely arranged platelets present in the shell of the thrombus. Could PGI_2 be the cause of the shell to be a shell and the core to remain as a core? As an increase in thrombin generation and an increase in shear of the flowing blood facilities PGI_2 production, hints that it does have a role to play in thrombus formation.

CHAPTER 6:

Discussion and Future directions

6.1 General discussion

Thrombus formation is a critical response to vascular damage in order to prevent excessive blood loss. The control of this response is critical, as too little thrombus formation leads to bleeding, whilst too much thrombus formation could lead to cardiovascular disease (CVD) mainly acute conditions such as heart attack and stroke. According to the World Health Organization (WHO), it has been estimated that 17.5 million people died of CVD in 2012, which could exceed to 23.6 million deaths per year by 2030 (approximately 30% of all global deaths) (World_Health_Organization, 2016, Mozaffarian D et al., 2015). Of these deaths, the majority (80%) were linked to heart attack and stroke (World_Health_Organization, 2016).

There is significant understanding of how thrombi are formed. It is a highly intricate and coordinated approach used by the body to help stem the loss of blood from the circulation. Platelets are the major respondents to this coordinated approach. They freely circulate in the blood and are kept in a docile state by factors secreted by the vascular endothelium. An injury to the blood vessel that exposes the platelets to the ECM activates them and culminates in thrombus formation. Recently, thrombus formation has been reimagined by the group led by Lawrence F. Brass. They identified that a thrombus is not merely an accumulation of activated platelets that are held together by fibrin meshwork, but that structurally a thrombus has a central core composed of closely packed and highly activated platelets that are surrounded by a peripheral shell that has loosely arranged and less activated platelets (Stalker et al., 2014, Tomaiuolo et al., 2014, Welsh et al., 2016, Welsh et al., 2014). There is an intermediate zone between the core and the shell that contains platelets with varying characteristics of the two zones (Stalker et al., 2014, Tomaiuolo et al., 2014, Welsh et al., 2016, Welsh et al., 2014). However there are some key areas of thrombus formation which are poorly understood. One of these areas is the role of the actin cytoskeleton, and how it responds to different agonists, or platelet inhibitors in different parts of the thrombus. Furthermore there is no clear understanding of how actin arranges itself within the 3D environment of the thrombus.

The main aim of this thesis was to understand how PGI_2 via PKA could modulate the actin cytoskeleton of spread platelets. The research on PGI_2 has largely been focused on its potent effect on inhibition of circulating platelets that limits the formation of unwanted thrombi in the circulation (Moncada et al., 1976), while the impact of PGI_2 on platelets that have become activated and have formed a thrombus have not been explored. Exploring the

effects of PGI_2 on the actin cytoskeleton of spread platelets would enable us to identify the effects it could have on thrombus formation.

Key to this understanding is when platelets are exposed to PGI_2. Within researchers there seems to be two schools of thought regarding this query. One believes that it is secreted continuously in the circulation to cause inhibition of the platelets, as had been seen in the case of NO (another endothelial derived factor) that inhibits platelets. The other school of thought believes that NO is being continuously released in order to inhibit the platelets in circulation while PGI_2 is released only after initiation of thrombus formation, due to stimulation via thrombin. Part of the reason why there is a lack of understanding here is that it is difficult to accurately identify the levels of PGI_2 in circulation. It is unstable and is hydrolyzed quickly, that makes it difficult for an accurate analysis of its level. However researchers have tried to identify the levels of PGI_2 in circulation via measuring its degraded metabolite in the urine (FitzGerald et al., 1981). They identified a very low level of PGI_2 (10pM) in human circulation which was noted to be 10-fold lower than that needed for countering the effect of platelet agonists (0.1nM) (FitzGerald et al., 1981). I consider that PGI_2 is secreted in the circulation continuously at a suboptimal concentration, as identified by FitzGerald et al. (1981). This release of PGI_2 would then synergize the effect of NO in inhibiting platelet activation, as shown by Radomski *et al.* (1987b) that under aggregation PGI_2 potentiates the effects of NO. On initiation of a thrombus, thrombin is generated by activated platelets that increase PGI_2 release from the endothelium (Weksler et al., 1978). With an increased formation of a thrombus, the flow of blood is hindered that thereby induces shear on the vascular endothelial cells which results in increased amount of PGI_2 being secreted in the circulation

If PGI_2 is elevated during thrombus formation this argues that PGI_2 is likely to be playing a role in the control of thrombus formation, above that of inhibiting platelets prior to their activation. Therefore, the basis of this thesis was to understand if PGI_2 could reverse the activation of the platelet and so provide a mechanism by which thrombus formation could be reduced, via increased embolization and thrombus instability.

6.2 Effects of PGI_2 on spread platelets

The actin cytoskeleton forms an essential component to orient a functional response to a stimulus perceived by a cell. The integrins are critical to this response as these link the

ECM to the intracellular actin cytoskeleton (Schwartz, 2010). Within a platelet a controlled and effective actin cytoskeletal response is key to maintaining the ability to withstand the high shear associated with thrombus formation. Therefore alterations in the signals received by cells, for instance addition of PGI_2 could therefore play an important role in the actin cytoskeletal response.

Interestingly the effect of cAMP elevation on the actin cytoskeleton is dependent on the cell type involved. For instance an increase in cAMP can encourage stress fibre formation, or lead to stability of stress fibres (Tamma et al., 2003, Banan et al., 2000). Alternatively, cAMP elevation can induce disassembly of stress fibres and also a reduction in actin polymerization (Birukova et al., 2007, Bulin et al., 2005, Duggirala et al., 2015, Peppelenbosch et al., 1993). In platelets, little is known about how PGI_2 alters stress fibre formation.

Treatment of spread platelets with PGI_2 resulted in dissolution of stress fibers which is in agreement with a similar stress fibers dissolution in human vascular smooth muscle cells, rat cerebeller astrocytes and fibroblasts (Bulin et al., 2005, Pelletier et al., 2005, Perez et al., 2005). In the case of many cell types, including platelets, there are two main mediators of PGI_2, Epac and PKA (Schmidt et al., 2013, Herfindal et al., 2013, Cheng et al., 2008). However the dissolution of stress fibers in spread platelets was inhibited by using PKA inhibitors which confirmed that this change by PGI_2 was PKA mediated.

Stress fibre formation is linked with the small RhoGTPase, RhoA, activity (Paterson et al., 1990). On treatment with PGI_2, the GTP-bound form of RhoA was reduced and thereby dissolution of stress fibers is observed. Further to a change in stress fibres there was also a reduction in surface area. At present it is not clear if this change is mediated by the inhibition of RhoA, or due to alteration of the activity of Rac leading to a reduction in lamellipodial extensions. This is an area for future experimentation but in other cell types such as endothelial cells Rac1 activity was seen to be increased by an increase in cAMP levels and this thereby affected the actin dynamics of the cell (Baumer et al., 2008).

6.2.1 Is RhoA the central signaling component for spreading?

Literature has identified that cAMP relays its effects on actin cytoskeleton while directing the activity of small Rho GTPases such as Cdc42, Rac1 and RhoA (Nobes and Hall, 1995).

The small GTPases cycle between, an active GTP-bound and an inactive GDP-bound forms. This conversion from GTP-bound form to its GDP counterpart is regulated by GAPs. The GDP-bound form is converted back to its GTP-bound form via GEFs. This replacement of GDP by GTP via GEF is inhibited by GDIs as it hinders the dislodging of the GDP molecule.

RhoA has been identified in multiple cell types to be the central signaling molecule for mediating effects on the actin cytoskeleton (Busca et al., 1998, Dong et al., 1998, Lang et al., 1996). The activity of RhoA-ROCK directs the shape change in suspended platelets (Aburima et al., 2013). During my thesis work, signaling revealed a basal level of active GTP-bound form of RhoA to be present in suspended platelets which was increased when a platelet was fully spread. It has been shown that direct interaction occurs between the β_3 subunit of the integrin with the heterotrimeric GPCR subunit - $G\alpha_{13}$ (Gong et al., 2010). The $G\alpha_{13}$ has been shown to interact with p115RhoGEF as well, that converts RhoA to its active GTP-bound form (Huveneers and Danen, 2009). Both, β3 subunit and the p115RhoGEF, share the same binding region on $G\alpha_{13}$. Therefore on integrin activation a competitive shift occurs with the $G\alpha_{13}$ binding away from p115RhoGEF to β_3 subunit of the integrins, thereby reducing the conversion to active RhoA (Huveneers and Danen, 2009).

Interaction of $G\alpha_{13}$ also led to activation of Src (via tyrosine phosphorylation) that directly activates p190RhoGAP thus inhibiting active RhoA. Activation of downstream Src also stimulated the conversion of Rac1 to its active GTP-bound form. Both Rac1 and RhoA play opposing roles in integrin mediated cell spreading (Harburger and Calderwood, 2009, Huveneers and Danen, 2009). The active form of Rac1 reduced active RhoA either directly (via activation of p190RhoGAP) or indirectly (via inhibiting p115RhoGEF). Thereby a multilevel reduction in the activity level of RhoA was identified in the initial phase of platelet spreading (Ridley, 2000). Continued activation of Rac1 led to increased spreading of the platelet. This created an augmented stress in the platelet that induced Fyn-dependent RhoGEF activation, thereby increasing the RhoA GTP-bound form in the later stage of spreading while inhibiting the active Rac1. This was marked by the appearance of stress fibres in a fully spread platelet (Paterson et al., 1990).

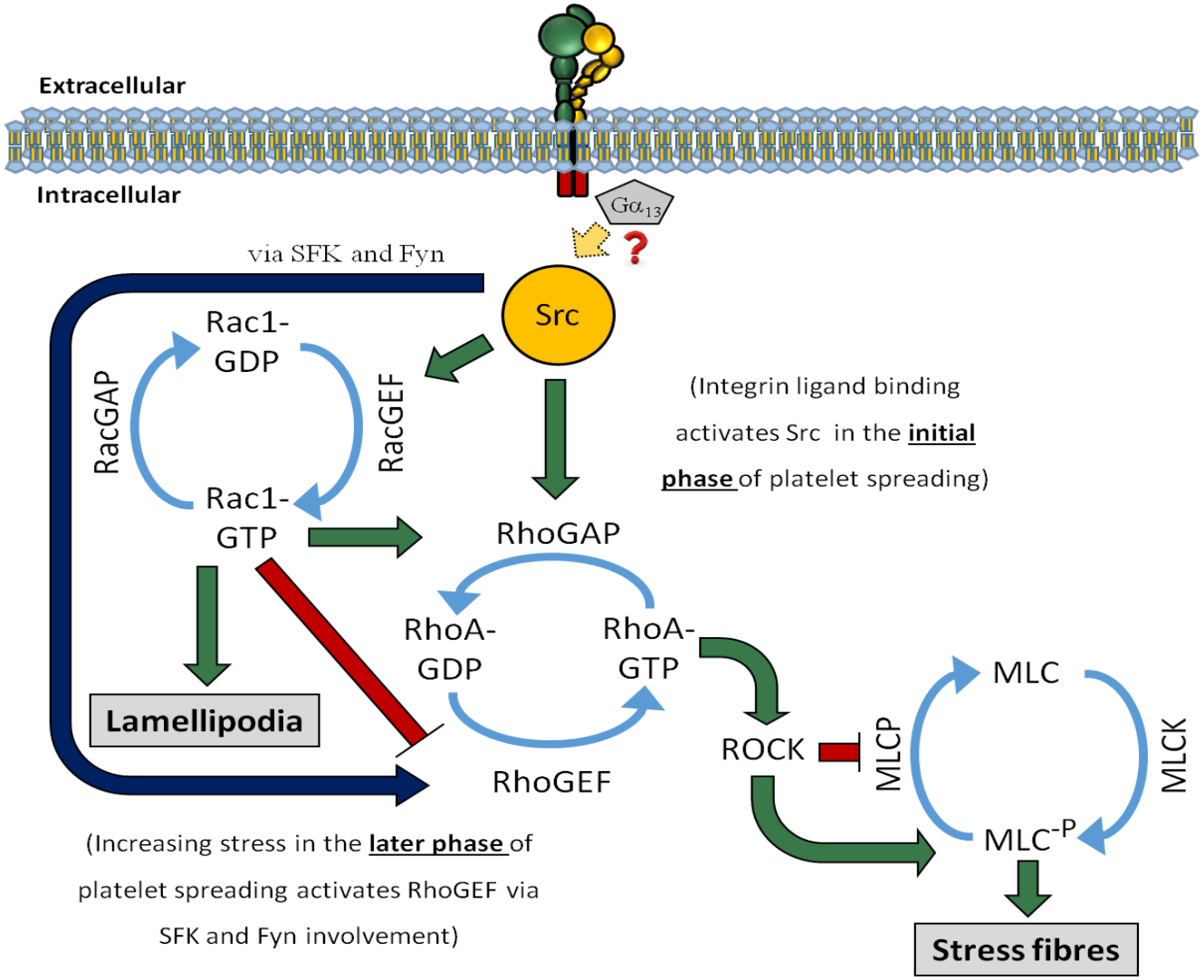

Figure 6. 1 Downstream regulation of RhoA activity leading to stress fibre formation. On outside-in activation of the integrin receptor, Src plays an important role in inhibiting the formation of active RhoA (RhoA-GTP) during the initial phase of platelet spreading. It does so by activating RhoGAP and RacGEF. Activation of RacGEF stimulates Rac1 activity that further inhibits the formation of RhoA-GTP form, via inhibiting RhoGEF. Therefore reduced RhoA association with Rho Kinase (ROCK) leads to reduced inhibition of phosphatase that converts the phosphorylated MLC to its non-phosphorylated form, hence reduced stress fibres. During the later phase of spreading RhoGEF gets activated via SFK and Fyn, thereby an increased formation of stress fibres occur.

Formation of stress fibers required an increase in the GTP-bound active RhoA. The active RhoA itself binds to ROCK (a complex of Rho Kinase) that inhibits the dephosphorylation of myosin light chain (MLC) and thereby increases stress fibre formation. PGI_2 via cAMP-PKA pathway phosphorylates RhoA. This phosphorylation of RhoA at ser188, tags it for binding to GDI. Interaction with GDI precludes RhoA from causing further downstream effects unless it is taken out of the inhibition caused by GDI. On taken out of the Rho-ROCK association by GDI, the inhibition on the phosphatase to MLC is removed, which thereby decreases stress fibres and hence the appearance of actin nodules.

6.2.2 Actin nodule formation

The story so far…!

Actin nodules are filamentous actin structures which were identified by Calaminus *et al*. (2008). These were noted to be punctate areas of F-actin that appeared during platelet spreading on fibrinogen. Using a mouse with a transgene for GFP-actin, these nodules were studied in real-time and were identified as early spreading structures. These actin nodules had an inverse relationship with stress fibres; as the appearance of one leads to the disappearance of the other. Interestingly, stress fibres were formed, as had been found, in the presence of higher levels of active GTP-bound RhoA while actin nodules had been associated with low activity of RhoA (Calaminus et al., 2008).

I have identified that treatment of spread platelets with PGI_2, via cAMP-PKA pathway, leads to dissolution of stress fibres with a reciprocal increase in actin nodules. This change was not associated with any change in the levels of filamentous actin in the platelets. Interestingly in other cell types this alteration of stress fibres did not lead to the formation of an actin nodule like actin structure.

- Vascular smooth muscle cells form stress fibres which disappear on treatment with cAMP elevating agents and form long dendritic processes. The cells also tend to roundup and form a stellate structure with small actin ring like structures. These ring-like structures were bigger than actin nodules as they had an average diameter of 1.3μm. Interestingly, these ring-like structures were not associated with RhoA activity rather they were formed by a reduced Rac1 activity (Pelletier et al., 2005).

- Human aortic smooth muscle cells upon elevation of cAMP, lose stress fibres and focal adhesions, and form a rounded morphology leaving behind thin branched extensions. No nodular structures were identified to be formed (Bulin et al., 2005).

- Rat cerebellar astrocytes form stress fibres which are replaced by another filamentous actin structure, which morphologically has dot-like appearance and has been termed as 'stellate', on treatment with cAMP elevating agents (Perez et al., 2005). The paper identified that this change in the actin structures was mediated by factors working upstream of RhoA and was independent of PKA activity (Perez et al., 2005).

- Lung vascular endothelial cells, on treatment with a cAMP elevating agent, leads to an increase in filamentous actin formation at the peripheral rim near the cellular membrane, thereby providing greater ability to withstand shear (Birukova et al., 2007). This increase in filamneotus actin is dependent on PKA and Epac mediated activation of Rac1 (Birukova et al., 2007).

In all these examples, quoted above, it could be identified that the response generated by an increase in cAMP, has cell-type specific effects on the actin cytoskeletal rearrangement. This is most likely due to the proteins expressed within these cells, for instance the type of PKA subunits, and if Epac is also produced. Furthermore given that only the platelet does not have a nucleus, gene expression changes induced by PKA could also play an important role in how the cell responds to PGI_2.

6.2.3 Actin nodule as a signaling hub

The actin nodules were postulated to act as a hub to the presence of multiple proteins. The identified proteins involved with actin nodules, as shown in table 6.1, included Fyn, Rac1, Arp2/3, WASp and phosphotyrosines (Calaminus et al., 2008, Poulter et al., 2015). Src had been identified not to associate with actin nodules on platelets spreading on immobilized fibrinogen; interestingly, under flow, the nodules did colocalise with activated Src (Kasirer-Friede et al., 2010, Calaminus et al., 2008).

I was able to colocalize PKA RII and pRhoA to these nodular actin structures. The PKA RI was present independently of these actin nodules in a pattern that was speculated for it to be associated with microtubules. This identification further strengthens the notion for actin nodules to act as a signaling hub; as they are actin cytoskeletal structures, linked to

Table 6. 1: Properties of actin nodules. The properties of actin nodules have been summarised here; classifying it by the components found to colocalise with the nodules, dependence on the matrices, characteristics in terms of presence, their diameter and their lifetime and lastly the identified functions are identified. Adapted from (Calaminus et al., 2008, Kasirer-Friede et al., 2010, Poulter et al., 2015).

		Actin nodules
Components		Arp2/3, WASp, Fyn, cortactin, integrins, talin, vinculin, PKA subs, Rac1, RhoA, PKA RII, pTyr, ±Src (absent on spreading while present under flow)
Matrix	Fibrinogen	Yes
	Collagen	No
Characteristics	Presence	Platelets
	Diameter	0.5±0.12μm (0.25-0.62)
	Lifetime	22.1sec (13.5 – 36.3)
Functions		An intermediary actin structure involved with platelet spreading. It has been postulated to act as a signaling hub.

sites of adhesion in a platelet, are associated with PKARII and the phosphorylated form of RhoA. Similarly, literature has identified that PKA RII, in neuronal and non-neuronal cells, are associated with actin cytoskeleton (Li et al., 1996). All linking to the possibility of cAMP to mediate its effect on the formation of actin nodules by phosphorylating RhoA at the nodules via PKA RII subunit present in the same vicinity.

6.2.4 Platelet AKAPs at the actin nodule

The intracellular increase in cAMP is not a generalized effect, rather it is compartmentalized by means of PDE activity and the role played by AKAPs in anchoring the cAMP-effector proteins to a distinct subcellular location (Beene and Scott, 2007, Gloerich and Bos, 2010). Limiting cAMP spreading from a limited space would proportionately limit the effects produced by the cAMP-effectors on the actin cytoskeleton. The data identified that the phosphorylation of RhoA, presumed marker for actin cytoskeletal changes, showed a different timeprofile to the cytoskeletal effects observed. This hints at a possible presence of AKAPs in controlling the phosphorylation of RhoA. The presence of AKAPs, potentially identifies localized areas within the platelet to have continued presence of cAMP/PKA, although PGI_2 would have long been degraded by then.

Identifying the presence of PKA RII at the nodules also points in the same direction of the involvement of AKAP in the system. The AKAP would help explain the involvement of cAMP/PKA signaling in a spatiotemporal manner. AKAP 75 protein has been identified to bind to PKA RII and associate it with actin cytoskeleton (Abe et al., 2003). RhoA has also been identified in the literature to be associated with AKAP13 (Diviani et al., 2001). It could be these identified AKAPs or any other molecule that could potentially serve as an AKAP to PKA RII and would have generated this effect on the actin cytoskeletal remodeling.

6.3 Impact of PGI_2 on thrombus formation

After confirming that platelet activation is a reversible phenomenon and this change to be brought about by PGI_2, led to further queries. The presence of stress fibres helped the platelets in the thrombus to remain spread and bear the shear force of the flowing blood. On encountering PGI_2, loss of stress fibres with a replacement by actin nodules, destabilized the platelets that culminated in their embolization under shear flow of the blood. Would it not lead to resumption of bleeding from the injury again? Platelets forming

a thrombus are encountered with collagen for the first layer while successive layers of the platelets in the thrombus interact with each other via fibrinogen. To answer our first query regarding rebleeding, we needed to identify if actin nodules formed on other matrices. Similar to Calaminus et al (2008), I was also able to demonstrate that the formation of actin nodules in a spreading platelet was a matrix dependent effect, as they do form on fibrinogen but do not appear on collagen, upon their treatment with PGI_2. Absence of actin nodules on collagen, on treatment with PGI_2, highlighted the significance that the basal layer of platelets in a thrombus, would be spared of the actin cytoskeletal effects of PGI_2. Hence the release of PGI_2 would not destabilize the basal layer of platelet spreading and thus the issue of re-bleeding was clarified. Why would still the actin nodules be needed on treating platelets spread on fibrinogen with PGI_2? Logically they could be providing a negative feedback control to the extent of thrombus. The thrombi formed either on fibrinogen or collagen, on treatment with PGI_2, showed a reduction in the surface area coverage and increased embolization. These results, along with the absence of actin nodules on collagen identifies that PGI_2 could possibly be playing a role in controlling the extent of the thrombus formed.

6.3.1 Porosity of a thrombus

It has recently been identified by Brass *et al.* (2011), using computational studies, that a thrombus is composed of platelets with graded activation. In a thrombus, there is presence of an inside core of platelets which are compactly arranged, are less porous for intra-thrombus solute movement and is mediated by thrombin (Brass et al., 2011, Stalker et al., 2013, Stalker et al., 2014, Tomaiuolo et al., 2014, Welsh et al., 2016, Welsh et al., 2014). The contained thrombin maintains platelet activity, enabling a fully spread phenotype, by dropping their cAMP levels, and therefore enhancing platelet spreading and controlling the compact arrangement of platelets in this zone (Stalker et al., 2014, Tomaiuolo et al., 2014, Welsh et al., 2016, Welsh et al., 2014). The shell covers the core and is composed of loosely arranged platelets make this zone more porous and hence ADP and TXA_2, released from the thrombin activated platelets from the core, can penetrate the shell to continue activation (Brass et al., 2011, Stalker et al., 2013). I consider the release of PGI_2 from endothelium inhibits spreading of platelets in the shell and thereby making it more porous. The porosity reduces with an increasing depth of the thrombus as platelets towards the core would be less exposed to the concentration of released PGI_2.

6.3.2 Embolisation events

Flowing PGI_2, at an arterial shear, on already formed thrombi on either fibrinogen or collagen revealed occurrence of embolization events. This occurrence challenged the finding obtained on immobilized fibrinogen as integrin inactivation, measured via platelet adhesion, was not affected at a similar dose used under flow conditions. A logical possibility for embolization under flow could be an interplay that exists between the exposure to PGI_2 and the shear flow of the blood. On embolization, would the platelets go back into circulation? Would they be functional again? Would the released emboli clog any other smaller vessel? Although PGI_2 caused platelet embolization from already formed thrombi but whether these platelets would be functional again was not tested. Similarly in the absence of endothelial PGI_2, what would be the effect on platelet activity? What would be the effect on thrombus formation and its propagation?

6.4 Clinical outlook

Endothelial dysfunction has been established to play critical roles in the pathogenesis of CVD, stroke, diabetes mellitus, insulin resistance, venous thrombosis, chronic kidney failure and tumour growth (Hadi et al., 2005, Libby, 2001, Rajendran et al., 2013). A dysfunction of the vascular endothelium relates to an altered production of PGI_2 and NO in the circulation. Presence of both, PGI_2 and NO, is important in inhibiting the activation of platelets.

6.4.1 Cardiovascular disorders (CVD)

Platelets in circulation are kept in an inhibited state majorly by NO as it is being produced continuously; while PGI_2 has been found to be at suboptimal level in the circulation. One of the possibility could be that NO be the major player in inhibiting platelets from getting activated while PGI_2 takes its role of platelet inhibition when activated by thrombin or by an increased shear of flowing blood. Another possibility could be that PGI_2 and NO could synergize in their functioning and therefore individually, reduced concentrations of them would be needed to produce the desired effects of inhibiting platelet activity and on formation of a thrombus. As identified in my thesis that PGI_2 takes an important role once the thrombus formation occurs. It does so by checking for the height and the extent of the thrombus formed; in a person with dysfunctional vascular endothelium, an increase in the formation of unwanted thrombi would be expected. This observation corelates the clinical findings of higher degrees of endothelial dysfunction in CVD patients. Similarly

endothelial dysfunction would also impact on the initial activity status of platelets, due to reduced levels of NO and PGI_2 in the circulation, which is confirmed by the clinical findings of hyperactivity of platelets in the circulation of CVD patient.

6.4.2 Diabetes Mellitus (DM)

Diabetes mellitus is a multifactorial disease. It is characterized by the dysregulation of glucose and lipid metabolisms along with some developing resistance to the formed insulin within their body. Interestingly, the morbidity of DM patients relies majorly on their vascular complications of endothelial dysfunction. The endothelial dysfunction is compounded by the hyperglycemic state of the blood that shares an equal contribution to the hyperactivity of the platelets (Schafer and Bauersachs, 2008, Beckman et al., 2002). A badly controlled gylcaemic index stratifies DM patients at a risk of developing a thrombotic complication.

Identifying, during my thesis, that PGI_2 does have a major effect on restricting the extent of thrombus formation; it would imply that if a longer acting PGI_2 be used to treat patients with these disorders, it would provide a better life expectancy to people with CVD or DM.

6.5 Future directions

6.5.1 Is there a synergy between PGI_2 and NO in thrombus modulation?

Synergy between NO and PGI_2 had been identified to play a role in regulating the haemostasis, for the flow of blood (Moreau et al., 2003). As I had identified that PGI_2 does have an inhibitory role for activated platelets that form a thrombus. I wanted to explore the role played by NO, being secreted continuously from the endothelium, what role would it play on the formation of a thrombus? Would it continue inhibiting the spreading of platelets, similar to PGI_2 or would it target some other aspect of thrombus formation, possibly affecting the adhesion of platelets to the thrombus. I would want to employ similar methodology as had been used for PGI_2 alone, to identify the working with NO in the presence or absence of PGI_2.

I would want to identify the working doses for both NO and PGI_2, individually and in combination. I would want to explore this concept via spreading of platelets on both collagen and fibrinogen and analyzing them for actin structures (stress fibres and actin nodules), adhesion and surface area of platelets, the levels of active RhoGTPases, western blotting for the downstream signaling and the use of fluorescence and confocal

microscopy. I might be able to discover, whether NO and PGI_2 synergize to produce their effect on the thrombus, hence controlling the extremes of thrombus formation.

6.5.2 PGI_2 in circulation: role of the two doses!

PGI_2 has been known for its inhibition of platelets in circulation. My work identified that PGI_2 could negatively regulate the formation of thrombus. Could PGI_2 actually cause an increase in platelet spreading? This seemed to be in stark contrast to the roles of inhibition that had been identified for PGI_2. This query arose while performing a dose response analysis of pretreatment of blood with PGI_2 that was then flown over fibrinogen matrix. It was noted that platelets that were pretreated with low dose of PGI_2 provided an increase in the surface area coverage, signifying better spreading, when compared with platelets from untreated blood or pretreatment of blood with increased doses of PGI_2. On the same notion, the use of PKA inhibitors, RP-8CPT-cAMPS and KT-5720, would have reduced the effect of cAMP in the presence or absence of PGI_2, revealed a reduction in the adhesion of platelets on reducing levels of cAMP. These observations signified a possibility that during circulation and while initiation of adhesion, an increase in cAMP is needed by the platelets that would help them to adhere better on an injury in the vasculature. This increase in cAMP in the platelets could either be mediated by a reduction in the activity of PDEs or a basal presence of PGI_2 in the circulation that enhances the cAMP levels in these platelets. An interesting finding, with flowing PGI_2 over already formed thrombi on collagen, noted a reduction in the height of thrombus along with reduced surface area coverage of the thrombus.

Although it may be quite early to deduce anything from these observations I speculate that the basal dose of PGI_2 released by the endothelium, is at a suboptimal level. Increase in the thrombus formation would increase activation of thrombin and the shear of the blood flow, surmounting to the extent of the thrombus. The greater the thrombus size, enhanced is the production of PGI_2 by the endothelial cells. Therefore production of increased amount of PGI_2 leads to a reduction in the height of the thrombus.

6.5.3 What is the downstream regulation of the actin nodules?

During my thesis I had identified that PGI_2 mediated dissolution of stress fibres in spread platelets is a PKA dependent mechanism controlled by the active form of RhoA. This dissolution of stress fibres led to the replacement by another filamentous actin structure, actin nodules, in the platelet. PGI_2 treatment would have led to an increase in intracellular

cAMP. Could the formation of actin nodules be a PKA-mediated mechanism also? Could the actin nodules be formed via other cAMP mediated mechanism such as Epac? It has been identified that on treating spread platelets with PGI_2 have led to an increase in cAMP and the formation of actin nodules. This effect was terminated by applying PKA inhibition, suggesting that cAMP via PKA has an effect on actin nodule formation rather than the Epac mechanism. In order to rule out a double stimulation via both PKA and Epac, an Epac specific agonist (8-pCPT-2'-o-Me-cAMP) (Rehmann et al., 2003) could be used in the presence of PKA inhibition and could be followed for the formation of actin nodules in platelets spread on fibrinogen. If actin nodules still form, then it could be inferred to be under control to both PKA and Epac mediation. If the actin nodules do not form then it would be confirmed that Epac does not have any control to the formation of actin nodules.

Another possibility to the control of actin nodules is by PGI_2 to mediate Ca^{2+} signaling aspect in platelets via controlling the activity of the IP_3 receptor directly. Could it not be a possibility that formation of actin nodules is an independent mechanism to stress fibres dissolution? The Ca^{2+} signaling could be playing its part in the formation of actin nodules parallel to the activity of inhibition of RhoA that affects stress fibre formation in the platelet. Therefore both the activities correlate, with stress fibre dissolution occurring at the same time of the appearance of actin nodules and resumption of stress fibres leads to disappearance of actin nodules.

Downstream effectors controlling the formation of actin nodules have not been identified till now. As the formation of stress fibres is emulated by an increase in active RhoA it was postulated that reduced activity of RhoA would direct actin nodule formation. I had identified that the phosphorylation of RhoA had mirrored the appearance of actin nodules but there was a delay in the phosphorylation status and the physical presence of the actin nodules. Could an increase in phosphorylation of RhoA be implied as an increase in inactive form of RhoA? Could some unknown mediator be at interplay that could be targeted by PGI_2 and could provide the missing link for the control of actin nodule formation?

Of the known Rho GTPase, I had only checked the activity of RhoA. I would still need to identify the activity levels of Cdc42 and Rac1 alongside RhoA activity. As the active RhoA levels are reduced on treatment of spread platelets with PGI_2, would a reciprocal increase in the activity of Rac1 and Cdc42 be identified? This involved using Cdc42 and

Rac1 pull-down commercial kits for assessing their respective activatory levels at the point of stress fibre reversal with an increase in the formation of actin nodules. In aortic endothelial cell the formation of podosomes is linked downstream to the activity of Cdc42 and RhoA (Moreau et al., 2003). In platelets, the active form of Rac1 is inversely proportional to the active form of RhoA. Incidentally, Rac1 is involved with lamellipodium formation, possibly PGI_2 affects Rac1 in platelets which would explain the reduction in the spread surface area of platelets. Rac1 had also been identified to colocalize with actin nodules. These observations make Rac1 as the prime target to be analyzed for understanding the probable downstream role for regulating actin nodule formation.

6.5.4 Are podosomes progenitors to actin nodules as megakaryocyte are to platelets?

Researchers have tried to identify if these nodules are specific to platelets only. Although other cell types had been look for it but megakaryocytes which are progenitor to platelets, form the closest for comparison to structures resembling actin nodules (Poulter et al., 2015). The megakaryocytes are known to form podosomes, which are also punctate actin structures having a core and a peripheral ring, similar to actin nodules. Similar proteins have been identified in the actin nodules and podosomes; the list includes integrins, talin, vinculin, paxillin, cortactin, Src family kinases (SFK), Arp2/3 and WASp (Poulter et al., 2015).

Functionally podosomes have been identified to use their ring-like presence of integrins to encircle an area on surrounding matrix and releases their enzymes – matrix metalloproteins (MMPs) within this enclosed region. The MMPs degrade the matrix proteins and thereby enable the megakaryocyte to extend its' proplatelet through it. On extension of the proplatelet, platelets are pinched off directly in the circulation. Podosomes have not been found in platelets, similarly actin nodules have not been identified in megakaryocytes.

I would want to extend my findings for the actin nodules on to podosomes. Do megakaryocytes gets exposed to agents that would increase their levels of cAMP? Experimentally to work with megakaryocytes I would need to either approach a megakaryocytic cell line, MEG-01 or primary megakaryocytes isolated from mice. It has

been published that podosomes form on both collagen and fibrinogen, so I could expand on spreading megakaryocytes on both these matrices for comparison. Stromal cell derived

PGE_2 had been identified in the bone marrow (Li et al., 2012). This identifies a possible source of cAMP elevating agent that megakaryocytes could be exposed to, in the body. Would the effect of an increase in cAMP in megakaryocytes, be PKA or Epac-mediated? Does this increase in cAMP causes an increase in podosome formation, similar to an increase in actin nodules observed in cAMP elevation in platelets? Lasp-1 protein has been identified in podosome formation in human macrophages and rat smooth muscle cells, and it contains phosphorylation sites for PKA/PKC activity (Stolting et al., 2012). Possibly podosome formation in a megakaryocyte too would be cAMP/PKA mediated mechanism. Is the formation of podosomes, organized by the Rho/ROCK pathway? This would involve using pharmacological inhibitors such as Rhosin and Y-27632 to inhibit the RhoA-ROCK pathway. What would be the functional defect on inhibition of RhoA-ROCK pathway in megakaryocytes? Using confocal staining or proximity ligation assay, I would want to identify the involvement and localization of the PKA regulatory subunit along with RhoA and Rac1 in the podosome formation.

6.5.5 Clinical implication of actin nodules

Wiskott Aldrich Syndrome (WAS) is an X-linked recessive disorder characterised by eczema, thrombocytopenia (petechiae and bruising) and immunodeficiency (recurrent infection) in an individual. Genetically this syndrome is characterized by mutation in the WAS gene located on the X chromosome.

The WAS protein (WASp) in a normal individual is involved with Arp2/3 to activate actin polymerisation. The WASp has been identified to form the core during the formation of both, the podosomes and actin nodules, which are filamentous actin structures present in the megakaryocytes and platelets, respectively. Podosomes are required by the megakaryocytes to allow extension of the proplatelets that thereby help in the formation of platelets. An absence of WASp in WAS patients would entail deranged podosome formation and altered number and functioning of platelets (Poulter et al., 2015). Similar to podosomes, actin nodules would also be affected by the mutated WASp. It has been identified that absence of actin nodules would affect platelet adhesion and aggregation (Poulter et al., 2015).

As had been shown in my thesis that treating spread platelets with PGI_2 leads to a conversion of stress fibres to actin nodules. What would happen to platelets from WAS patient, when exposed to PGI_2? Which actin structure would form? As actin nodules have

been postulated to be the precursor to the formation of lamelliopodia and stress fibres, would platelets from WAS patient form these actin structures? What would be the downstream signalling events?

6.5.6 Pharmacological possibilities

PGI_2 has been in clinical use from 1995 for the treatment of pulmonary arterial hypertension (PAH). It had been in use in an intravenous form of Epoprostenol (Flolan), which was continuously infused to these patients due to its short half-life of 6 minutes. Similarly another drug Treprostinil was introduced which could be given in i/v or subcutaneous (s/c) (Remodulin), inhaled (Tyvaso) or oral (Orenitram) form. Another synthetic analogue of PGI_2, Iloprost, is also available as inhaled form for treating PAH.

Currently all these drugs are FDA approved and are used as vasodilators for treatment of PAH and Raynaud's phenomenon. I believe these drugs would have definite role in CVD and DM patients. Currently drugs targeting ADP receptor such as Clopidogrel and Ticagrelor are being used to inhibit the level of PDE3 activity and increase the level of cAMP in the circulating platelets so as to avoid formation of unwanted thrombi. As PGI_2 acts through an increase in cAMP, I predict that using synthetic analogues of PGI_2 would provide a new level of pharmacological control in patients with vascular dysfunction.

6.6: Project conclusions

During my thesis I have worked on identifying the effect of PGI_2 on the actin cytoskeleton of spread platelets. I have identified that platelet activation, assessed by actin cytoskeletal changes, is a reversible phenomenon. Secondly PGI_2 is able to reverse the spreading of platelets by removing stress fibres through PKA dependent modulation of RhoA activity. The stage being set with generation of thrombin and an increase in the shear of blood exerted on the surrounding endothelium, PGI_2 is released that causes dissolution of preformed platelet rich thrombi. Endothelial dysfunction hampers the control of thrombus formation, therefore implementing PGI_2 at this stage would provide a novel approach to target unwanted thrombus formation, with reduced complications for the patient, hence a better life for the individual. Similarly, the state benefits monetarily due to a reduction in the spending for complications developing with the progression of disease for the patients.

CHAPTER 7:

References

Abe, T., Kato, M., Miki, H., Takenawa, T. & Endo, T. 2003. Small Gtpase Tc10 And Its Homologue Rhot Induce N-Wasp-Mediated Long Process Formation And Neurite Outgrowth. *J Cell Sci,* 116**,** 155-68.

Aburima, A., Wraith, K. S., Raslan, Z., Law, R., Magwenzi, S. & Naseem, K. M. 2013. Camp Signaling Regulates Platelet Myosin Light Chain (Mlc) Phosphorylation And Shape Change Through Targeting The Rhoa-Rho Kinase-Mlc Phosphatase Signaling Pathway. *Blood,* 122**,** 3533-45.

Adair, B. D. & Yeager, M. 2002. Three-Dimensional Model Of The Human Platelet Integrin Alpha Iibbeta 3 Based On Electron Cryomicroscopy And X-Ray Crystallography. *Proc Natl Acad Sci U S A,* 99**,** 14059-64.

Adamson, P., Paterson, H. F. & Hall, A. 1992. Intracellular Localization Of The P21rho Proteins. *J Cell Biol,* 119**,** 617-27.

Akbar, H., Shang, X., Perveen, R., Berryman, M., Funk, K., Johnson, J. F., Tandon, N. N. & Zheng, Y. 2011. Gene Targeting Implicates Cdc42 Gtpase In Gpvi And Non-Gpvi Mediated Platelet Filopodia Formation, Secretion And Aggregation. *Plos One,* 6**,** E22117.

Amano, M., Ito, M., Kimura, K., Fukata, Y., Chihara, K., Nakano, T., Matsuura, Y. & Kaibuchi, K. 1996. Phosphorylation And Activation Of Myosin By Rho-Associated Kinase (Rho-Kinase). *J Biol Chem,* 271**,** 20246-9.

Aslan, J. E., Baker, S. M., Loren, C. P., Haley, K. M., Itakura, A., Pang, J., Greenberg, D. L., David, L. L., Manser, E., Chernoff, J. & Mccarty, O. J. 2013. The Pak System Links Rho Gtpase Signaling To Thrombin-Mediated Platelet Activation. *Am J Physiol Cell Physiol,* 305**,** C519-28.

Aslan, J. E. & Mccarty, O. J. 2013. Rho Gtpases In Platelet Function. *J Thromb Haemost,* 11**,** 35-46.

Aspenstrom, P., Fransson, A. & Saras, J. 2004. Rho Gtpases Have Diverse Effects On The Organization Of The Actin Filament System. *Biochem J,* 377**,** 327-37.

Aszodi, A., Pfeifer, A., Ahmad, M., Glauner, M., Zhou, X. H., Ny, L., Andersson, K. E., Kehrel, B., Offermanns, S. & Fassler, R. 1999. The Vasodilator-Stimulated Phosphoprotein (Vasp) Is Involved In Cgmp- And Camp-Mediated Inhibition Of Agonist-Induced Platelet Aggregation, But Is Dispensable For Smooth Muscle Function. *Embo J,* 18**,** 37-48.

Azzarelli, R., Kerloch, T. & Pacary, E. 2014. Regulation Of Cerebral Cortex Development By Rho Gtpases: Insights From In Vivo Studies. *Front Cell Neurosci,* 8**,** 445.

Banan, A., Smith, G. S., Kokoska, E. R. & Miller, T. A. 2000. Role Of Actin Cytoskeleton In Prostaglandin-Induced Protection Against Ethanol In An Intestinal Epithelial Cell Line. *J Surg Res,* 88**,** 104-13.

Barbacid, M. 1987. Ras Genes. *Annu Rev Biochem,* 56**,** 779-827.

Barkalow, K., Witke, W., Kwiatkowski, D. J. & Hartwig, J. H. 1996. Coordinated Regulation Of Platelet Actin Filament Barbed Ends By Gelsolin And Capping Protein. *J Cell Biol,* 134**,** 389-99.

Barnes, M. J., Knight, C. G. & Farndale, R. W. 1998. The Collagen-Platelet Interaction. *Curr Opin Hematol,* 5**,** 314-20.

Bath, P. M., Hassall, D. G., Gladwin, A. M., Palmer, R. M. & Martin, J. F. 1991. Nitric Oxide And Prostacyclin. Divergence Of Inhibitory Effects On Monocyte Chemotaxis And Adhesion To Endothelium In Vitro. *Arterioscler Thromb,* 11**,** 254-60.

Baumer, Y., Drenckhahn, D. & Waschke, J. 2008. Camp Induced Rac 1-Mediated Cytoskeletal Reorganization In Microvascular Endothelium. *Histochem Cell Biol,* 129**,** 765-78.

Bear, J. E. & Gertler, F. B. 2009. Ena/Vasp: Towards Resolving A Pointed Controversy At The Barbed End. *J Cell Sci,* 122**,** 1947-53.

Bearer, E. L., Prakash, J. M. & Li, Z. 2002. Actin Dynamics In Platelets. *Int Rev Cytol,* 217**,** 137-82.

Beck, F., Geiger, J., Gambaryan, S., Veit, J., Vaudel, M., Nollau, P., Kohlbacher, O., Martens, L., Walter, U., Sickmann, A. & Zahedi, R. P. 2014. Time-Resolved Characterization Of Camp/Pka-Dependent Signaling Reveals That Platelet Inhibition Is A Concerted Process Involving Multiple Signaling Pathways. *Blood,* 123**,** E1-E10.

Beckman, J. A., Creager, M. A. & Libby, P. 2002. Diabetes And Atherosclerosis: Epidemiology, Pathophysiology, And Management. *Jama,* 287**,** 2570-81.

Beene, D. L. & Scott, J. D. 2007. A-Kinase Anchoring Proteins Take Shape. *Curr Opin Cell Biol,* 19**,** 192-8.

Bergmeier, W. & Hynes, R. O. 2012. Extracellular Matrix Proteins In Hemostasis And Thrombosis. *Cold Spring Harb Perspect Biol,* 4.

Bernard, J. & Soulier, J. P. 1948. Sur Une Nouvelle Variete De Dystrophie Thrombocytaire-Hemorragipare Congenitale. *Bull Mem Soc Med Hop Paris,* 64**,** 969-74.

Bershadsky, A. D., Ballestrem, C., Carramusa, L., Zilberman, Y., Gilquin, B., Khochbin, S., Alexandrova, A. Y., Verkhovsky, A. B., Shemesh, T. & Kozlov, M. M. 2006. Assembly And Mechanosensory Function Of Focal Adhesions: Experiments And Models. *Eur J Cell Biol,* 85**,** 165-73.

Best, L. C., Martin, T. J., Russell, R. G. & Preston, F. E. 1977. Prostacyclin Increases Cyclic Amp Levels And Adenylate Cyclase Activity In Platelets. *Nature,* 267**,** 850-2.

Birukova, A. A., Zagranichnaya, T., Fu, P., Alekseeva, E., Chen, W., Jacobson, J. R. & Birukov, K. G. 2007. Prostaglandins Pge(2) And Pgi(2) Promote Endothelial Barrier Enhancement Via Pka- And Epac1/Rap1-Dependent Rac Activation. *Exp Cell Res,* 313**,** 2504-20.

Blair, P. & Flaumenhaft, R. 2009. Platelet Alpha-Granules: Basic Biology And Clinical Correlates. *Blood Rev,* 23**,** 177-89.

Borgognone, A., Navarro-Nunez, L., Correia, J. N., Pollitt, A. Y., Thomas, S. G., Eble, J. A., Pulcinelli, F. M., Madhani, M. & Watson, S. P. 2014. Clec-2-Dependent Activation Of Mouse Platelets Is Weakly Inhibited By Camp But Not By Cgmp. *J Thromb Haemost,* 12**,** 550-9.

Bouaziz, A., De Ficquelmont-Loizos, M. M., Richert, A. & Caprani, A. 1998. Direct Physical Factors And Pgi2 And Txa2 Secretions By A Human Endothelial Cell Line: In Vitro Investigation Of Pressure And Shear Stress Applied Independently Or In Synergy. *Thromb Res,* 90**,** 279-89.

Brass, L. F., Wannemacher, K. M., Ma, P. & Stalker, T. J. 2011. Regulating Thrombus Growth And Stability To Achieve An Optimal Response To Injury. *J Thromb Haemost,* 9 Suppl 1**,** 66-75.

Buchwalow, I. B. & Bocker, W. 2010. *Immunohistochemistry: Basics And Methods* Heidelberg, Germany, Springer.

Buckley, I. K. & Porter, K. R. 1967. Cytoplasmic Fibrils In Living Cultured Cells. A Light And Electron Microscope Study. *Protoplasma,* 64**,** 349-80.

Bulin, C., Albrecht, U., Bode, J. G., Weber, A. A., Schror, K., Levkau, B. & Fischer, J. W. 2005. Differential Effects Of Vasodilatory Prostaglandins On Focal Adhesions, Cytoskeletal Architecture, And Migration In Human Aortic Smooth Muscle Cells. *Arterioscler Thromb Vasc Biol,* 25**,** 84-9.

Burkhart, J. M., Vaudel, M., Gambaryan, S., Radau, S., Walter, U., Martens, L., Geiger, J., Sickmann, A. & Zahedi, R. P. 2012. The First Comprehensive And Quantitative Analysis Of Human Platelet Protein Composition Allows The Comparative Analysis Of Structural And Functional Pathways. *Blood,* 120**,** E73-82.

Busca, R., Bertolotto, C., Abbe, P., Englaro, W., Ishizaki, T., Narumiya, S., Boquet, P., Ortonne, J. P. & Ballotti, R. 1998. Inhibition Of Rho Is Required For Camp-Induced Melanoma Cell Differentiation. *Mol Biol Cell,* 9**,** 1367-78.

Caen, J. P., Nurden, A. T., Jeanneau, C., Michel, H., Tobelem, G., Levy-Toledano, S., Sultan, Y., Valensi, F. & Bernard, J. 1976. Bernard-Soulier Syndrome: A New Platelet Glycoprotein Abnormality. Its Relationship With Platelet Adhesion To Subendothelium And With The Factor Viii Von Willebrand Protein. *J Lab Clin Med,* 87**,** 586-96.

Calaminus, S. D., Auger, J. M., Mccarty, O. J., Wakelam, M. J., Machesky, L. M. & Watson, S. P. 2007. Myosiniia Contractility Is Required For Maintenance Of Platelet Structure During Spreading On Collagen And Contributes To Thrombus Stability. *J Thromb Haemost,* 5**,** 2136-45.

Calaminus, S. D., Thomas, S., Mccarty, O. J., Machesky, L. M. & Watson, S. P. 2008. Identification Of A Novel, Actin-Rich Structure, The Actin Nodule, In The Early Stages Of Platelet Spreading. *J Thromb Haemost,* 6**,** 1944-52.

Cannizzaro, L. A., Madaule, P., Hecht, F., Axel, R., Croce, C. M. & Huebner, K. 1990. Chromosome Localization Of Human Arh Genes, A Ras-Related Gene Family. *Genomics,* 6**,** 197-203.

Carlier, M. F., Laurent, V., Santolini, J., Melki, R., Didry, D., Xia, G. X., Hong, Y., Chua, N. H. & Pantaloni, D. 1997. Actin Depolymerizing Factor (Adf/Cofilin) Enhances The Rate Of Filament Turnover: Implication In Actin-Based Motility. *J Cell Biol,* 136**,** 1307-22.

Cavallini, L., Coassin, M., Borean, A. & Alexandre, A. 1996. Prostacyclin And Sodium Nitroprusside Inhibit The Activity Of The Platelet Inositol 1,4,5-Trisphosphate Receptor And Promote Its Phosphorylation. *J Biol Chem,* 271**,** 5545-51.

Chang, J. C., Chang, H. H., Lin, C. T. & Lo, S. J. 2005a. The Integrin Alpha6beta1 Modulation Of Pi3k And Cdc42 Activities Induces Dynamic Filopodium Formation In Human Platelets. *J Biomed Sci,* 12**,** 881-98.

Chang, Y., Aurade, F., Larbret, F., Le Couedic, J. P., Momeux, L., Zhang, Y. Y., Larghero, J., Louache, F., Bertoglio, J., Cramer, E., Vainchenker, W. & Debili, N. 2005b. Proplatelet Formation Is Regulated By The Rho/Rock Pathway. *Blood,* 106**,** 880a-880a.

Chardin, P., Boquet, P., Madaule, P., Popoff, M. R., Rubin, E. J. & Gill, D. M. 1989. The Mammalian G Protein Rhoc Is Adp-Ribosylated By Clostridium Botulinum Exoenzyme C3 And Affects Actin Microfilaments In Vero Cells. *Embo J,* 8**,** 1087-92.

Chen, H. & Kahn, M. L. 2003. Reciprocal Signaling By Integrin And Nonintegrin Receptors During Collagen Activation Of Platelets. *Mol Cell Biol,* 23**,** 4764-77.

Chen, H., Locke, D., Liu, Y., Liu, C. & Kahn, M. L. 2002. The Platelet Receptor Gpvi Mediates Both Adhesion And Signaling Responses To Collagen In A Receptor Density-Dependent Fashion. *J Biol Chem,* 277**,** 3011-9.

Cheng, X., Ji, Z., Tsalkova, T. & Mei, F. 2008. Epac And Pka: A Tale Of Two Intracellular Camp Receptors. *Acta Biochim Biophys Sin (Shanghai),* 40**,** 651-62.

Clapham, D. E. & Neer, E. J. 1997. G Protein Beta Gamma Subunits. *Annu Rev Pharmacol Toxicol,* 37**,** 167-203.

Clemetson, J. M., Polgar, J., Magnenat, E., Wells, T. N. & Clemetson, K. J. 1999. The Platelet Collagen Receptor Glycoprotein Vi Is A Member Of The Immunoglobulin Superfamily Closely Related To Fcalphar And The Natural Killer Receptors. *J Biol Chem,* 274**,** 29019-24.

Clemetson, K. J. & Clemetson, J. M. 2001. Platelet Collagen Receptors. *Thromb Haemost,* 86**,** 189-97.

Colombelli, J., Besser, A., Kress, H., Reynaud, E. G., Girard, P., Caussinus, E., Haselmann, U., Small, J. V., Schwarz, U. S. & Stelzer, E. H. 2009. Mechanosensing In Actin Stress Fibers Revealed By A Close Correlation Between Force And Protein Localization. *J Cell Sci,* 122**,** 1665-79.

Cramer, L. P., Siebert, M. & Mitchison, T. J. 1997. Identification Of Novel Graded Polarity Actin Filament Bundles In Locomoting Heart Fibroblasts: Implications For The Generation Of Motile Force. *J Cell Biol,* 136**,** 1287-305.

Davidson, M. M. & Haslam, R. J. 1994. Dephosphorylation Of Cofilin In Stimulated Platelets: Roles For A Gtp-Binding Protein And Ca2+. *Biochem J,* 301 (Pt 1)**,** 41-7.

De Caterina, R., Libby, P., Peng, H. B., Thannickal, V. J., Rajavashisth, T. B., Gimbrone, M. A., Jr., Shin, W. S. & Liao, J. K. 1995. Nitric Oxide Decreases Cytokine-Induced Endothelial Activation. Nitric Oxide Selectively Reduces Endothelial Expression Of Adhesion Molecules And Proinflammatory Cytokines. *J Clin Invest,* 96**,** 60-8.

Denis, C., Methia, N., Frenette, P. S., Rayburn, H., Ullman-Cullere, M., Hynes, R. O. & Wagner, D. D. 1998. A Mouse Model Of Severe Von Willebrand Disease: Defects In Hemostasis And Thrombosis. *Proc Natl Acad Sci U S A,* 95**,** 9524-9.

Dittrich, M., Birschmann, I., Mietner, S., Sickmann, A., Walter, U. & Dandekar, T. 2008. Platelet Protein Interactions: Map, Signaling Components, And Phosphorylation Groundstate. *Arterioscler Thromb Vasc Biol,* 28**,** 1326-31.

Diviani, D., Soderling, J. & Scott, J. D. 2001. Akap-Lbc Anchors Protein Kinase A And Nucleates Galpha 12-Selective Rho-Mediated Stress Fiber Formation. *J Biol Chem,* 276**,** 44247-57.

Dohlman, H. G., Bouvier, M., Benovic, J. L., Caron, M. G. & Lefkowitz, R. J. 1987. The Multiple Membrane Spanning Topography Of The Beta 2-Adrenergic Receptor. Localization Of The Sites Of Binding, Glycosylation, And Regulatory Phosphorylation By Limited Proteolysis. *J Biol Chem,* 262**,** 14282-8.

Dong, J. M., Leung, T., Manser, E. & Lim, L. 1998. Camp-Induced Morphological Changes Are Counteracted By The Activated Rhoa Small Gtpase And The Rho Kinase Rokalpha. *J Biol Chem,* 273**,** 22554-62.

Dormond, O. & Ruegg, C. 2003. Regulation Of Endothelial Cell Integrin Function And Angiogenesis By Cox-2, Camp And Protein Kinase A. *Thromb Haemost,* 90**,** 577-85.

Dos Remedios, C. G., Chhabra, D., Kekic, M., Dedova, I. V., Tsubakihara, M., Berry, D. A. & Nosworthy, N. J. 2003. Actin Binding Proteins: Regulation Of Cytoskeletal Microfilaments. *Physiol Rev,* 83**,** 433-73.

Duggirala, A., Kimura, T. E., Sala-Newby, G. B., Johnson, J. L., Wu, Y. J., Newby, A. C. & Bond, M. 2015. Camp-Induced Actin Cytoskeleton Remodelling Inhibits Mkl1-Dependent Expression Of The Chemotactic And Pro-Proliferative Factor, Ccn1. *J Mol Cell Cardiol,* 79**,** 157-68.

Dunkern, T. R. & Hatzelmann, A. 2005. The Effect Of Sildenafil On Human Platelet Secretory Function Is Controlled By A Complex Interplay Between Phosphodiesterases 2, 3 And 5. *Cell Signal,* 17**,** 331-9.

Dutting, S., Bender, M. & Nieswandt, B. 2012. Platelet Gpvi: A Target For Antithrombotic Therapy?! *Trends Pharmacol Sci,* 33**,** 583-90.

Edwards, J. G., Campbell, G., Carr, M. & Edwards, C. C. 1993. Shapes Of Cells Spreading On Fibronectin: Measurement Of The Stellation Of Bhk21 Cells Induced By Raising Cyclic Amp, And Of Its Reversal By Serum And Lysophosphatidic Acid. *J Cell Sci,* 104 (Pt 2)**,** 399-407.

Ehrman, M. L. & Jaffe, E. A. 1980. Prostacyclin (Pgi2) Inhibits The Development In Human Platelets Of Adp And Arachidonic Acid-Induced Shape Change And Procoagulant Activity. *Prostaglandins,* 20**,** 1103-16.

Ellis, S. & Mellor, H. 2000. The Novel Rho-Family Gtpase Rif Regulates Coordinated Actin-Based Membrane Rearrangements. *Curr Biol,* 10**,** 1387-90.

Elzinga, M., Collins, J. H., Kuehl, W. M. & Adelstein, R. S. 1973. Complete Amino-Acid Sequence Of Actin Of Rabbit Skeletal Muscle. *Proc Natl Acad Sci U S A,* 70**,** 2687-91.

Emsley, J., Knight, C. G., Farndale, R. W., Barnes, M. J. & Liddington, R. C. 2000. Structural Basis Of Collagen Recognition By Integrin Alpha2beta1. *Cell,* 101**,** 47-56.

Falet, H., Hoffmeister, K. M., Neujahr, R., Italiano, J. E., Jr., Stossel, T. P., Southwick, F. S. & Hartwig, J. H. 2002. Importance Of Free Actin Filament Barbed Ends For Arp2/3 Complex Function In Platelets And Fibroblasts. *Proc Natl Acad Sci U S A,* 99**,** 16782-7.

Farrell, D. H. & Thiagarajan, P. 1994. Binding Of Recombinant Fibrinogen Mutants To Platelets. *J Biol Chem,* 269**,** 226-31.

Farrell, D. H., Thiagarajan, P., Chung, D. W. & Davie, E. W. 1992. Role Of Fibrinogen Alpha And Gamma Chain Sites In Platelet Aggregation. *Proc Natl Acad Sci U S A,* 89**,** 10729-32.

Faulstich, H., Schafer, A. J. & Weckauf, M. 1977. The Dissociation Of The Phalloidin-Actin Complex. *Hoppe Seylers Z Physiol Chem,* 358**,** 181-4.

Faure, J. & Dagher, M. C. 2001. Interactions Between Rho Gtpases And Rho Gdp Dissociation Inhibitor (Rho-Gdi). *Biochimie,* 83**,** 409-14.

Feijge, M. A., Ansink, K., Vanschoonbeek, K. & Heemskerk, J. W. 2004. Control Of Platelet Activation By Cyclic Amp Turnover And Cyclic Nucleotide Phosphodiesterase Type-3. *Biochem Pharmacol,* 67**,** 1559-67.

Feinstein, M. B. & Fraser, C. 1975. Human Platelet Secretion And Aggregation Induced By Calcium Ionophores. Inhibition By Pge1 And Dibutyryl Cyclic Amp. *J Gen Physiol,* 66**,** 561-81.

Fitzgerald, G. A., Brash, A. R., Falardeau, P. & Oates, J. A. 1981. Estimated Rate Of Prostacyclin Secretion Into The Circulation Of Normal Man. *J Clin Invest,* 68**,** 1272-6.

Forstermann, U., Schmidt, H. H., Pollock, J. S., Sheng, H., Mitchell, J. A., Warner, T. D., Nakane, M. & Murad, F. 1991. Isoforms Of Nitric Oxide Synthase. Characterization And Purification From Different Cell Types. *Biochem Pharmacol,* 42**,** 1849-57.

Fox, J. E. 1993. The Platelet Cytoskeleton. *Thromb Haemost,* 70**,** 884-93.

Fox, J. E. & Phillips, D. R. 1981. Inhibition Of Actin Polymerization In Blood Platelets By Cytochalasins. *Nature,* 292**,** 650-2.

Fox, J. E. & Phillips, D. R. 1983. Polymerization And Organization Of Actin Filaments Within Platelets. *Semin Hematol,* 20**,** 243-60.

Franke, B., Akkerman, J. W. & Bos, J. L. 1997. Rapid Ca2+-Mediated Activation Of Rap1 In Human Platelets. *Embo J,* 16**,** 252-9.

Franke, B., Van Triest, M., De Bruijn, K. M., Van Willigen, G., Nieuwenhuis, H. K., Negrier, C., Akkerman, J. W. & Bos, J. L. 2000. Sequential Regulation Of The Small Gtpase Rap1 In Human Platelets. *Mol Cell Biol,* 20**,** 779-85.

Furchgott, R. F., Cherry, P. D., Zawadzki, J. V. & Jothianandan, D. 1984. Endothelial Cells As Mediators Of Vasodilation Of Arteries. *J Cardiovasc Pharmacol,* 6 Suppl 2**,** S336-43.

Gartner, T. K., Amrani, D. L., Derrick, J. M., Kirschbaum, N. E., Matsueda, G. R. & Taylor, D. B. 1993. Characterization Of Adhesion Of "Resting" And Stimulated Platelets To Fibrinogen And Its Fragments. *Thromb Res,* 71**,** 47-60.

Gawaz, M., Langer, H. & May, A. E. 2005. Platelets In Inflammation And Atherogenesis. *J Clin Invest,* 115**,** 3378-84.

Geiger, B., Bershadsky, A., Pankov, R. & Yamada, K. M. 2001. Transmembrane Crosstalk Between The Extracellular Matrix--Cytoskeleton Crosstalk. *Nat Rev Mol Cell Biol,* 2**,** 793-805.

Geiger, B., Spatz, J. P. & Bershadsky, A. D. 2009. Environmental Sensing Through Focal Adhesions. *Nat Rev Mol Cell Biol,* 10**,** 21-33.

Ginsberg, M. H., Partridge, A. & Shattil, S. J. 2005. Integrin Regulation. *Curr Opin Cell Biol,* 17**,** 509-16.

Gloerich, M. & Bos, J. L. 2010. Epac: Defining A New Mechanism For Camp Action. *Annu Rev Pharmacol Toxicol,* 50**,** 355-75.

Goggs, R., Savage, J. S., Mellor, H. & Poole, A. W. 2013. The Small Gtpase Rif Is Dispensable For Platelet Filopodia Generation In Mice. *Plos One,* 8**,** E54663.

Goldschmidt-Clermont, P. J., Furman, M. I., Wachsstock, D., Safer, D., Nachmias, V. T. & Pollard, T. D. 1992. The Control Of Actin Nucleotide Exchange By Thymosin Beta 4 And Profilin. A Potential Regulatory Mechanism For Actin Polymerization In Cells. *Mol Biol Cell,* 3**,** 1015-24.

Gong, H., Shen, B., Flevaris, P., Chow, C., Lam, S. C., Voyno-Yasenetskaya, T. A., Kozasa, T. & Du, X. 2010. G Protein Subunit Galpha13 Binds To Integrin Alphaiibbeta3 And Mediates Integrin "Outside-In" Signaling. *Science,* 327**,** 340-3.

Gorman, R. R., Bunting, S. & Miller, O. V. 1977. Modulation Of Human Platelet Adenylate Cyclase By Prostacyclin (Pgx). *Prostaglandins,* 13**,** 377-88.

Gottschalk, K. E. 2005. A Coiled-Coil Structure Of The Alphaiibbeta3 Integrin Transmembrane And Cytoplasmic Domains In Its Resting State. *Structure,* 13**,** 703-12.

Hadi, H. A., Carr, C. S. & Al Suwaidi, J. 2005. Endothelial Dysfunction: Cardiovascular Risk Factors, Therapy, And Outcome. *Vasc Health Risk Manag,* 1**,** 183-98.

Hallmann, R., Horn, N., Selg, M., Wendler, O., Pausch, F. & Sorokin, L. M. 2005. Expression And Function Of Laminins In The Embryonic And Mature Vasculature. *Physiol Rev,* 85**,** 979-1000.

Halper, J. & Kjaer, M. 2014. Basic Components Of Connective Tissues And Extracellular Matrix: Elastin, Fibrillin, Fibulins, Fibrinogen, Fibronectin, Laminin, Tenascins And Thrombospondins. *Adv Exp Med Biol,* 802**,** 31-47.

Hanoune, J. & Defer, N. 2001. Regulation And Role Of Adenylyl Cyclase Isoforms. *Annu Rev Pharmacol Toxicol,* 41**,** 145-74.

Hantgan, R. R., Hindriks, G., Taylor, R. G., Sixma, J. J. & De Groot, P. G. 1990a. Glycoprotein Ib, Von Willebrand Factor, And Glycoprotein Iib:Iiia Are All

Involved In Platelet Adhesion To Fibrin In Flowing Whole Blood. *Blood,* 76**,** 345-53.

Hantgan, R. R., Nichols, W. L. & Ruggeri, Z. M. 1990b. Von Willebrand Factor Competes With Fibrin For Occupancy Of Gpiib:Iiia On Thrombin-Stimulated Platelets. *Blood,* 75**,** 889-94.

Harburger, D. S. & Calderwood, D. A. 2009. Integrin Signalling At A Glance. *J Cell Sci,* 122**,** 159-63.

Harker, L. A., Roskos, L. K., Marzec, U. M., Carter, R. A., Cherry, J. K., Sundell, B., Cheung, E. N., Terry, D. & Sheridan, W. 2000. Effects Of Megakaryocyte Growth And Development Factor On Platelet Production, Platelet Life Span, And Platelet Function In Healthy Human Volunteers. *Blood,* 95**,** 2514-22.

Hartwig, J. (Ed.) 1999. *Platelet Morphology,* Baltimore, Usa: Williams And Wilkins.

Hartwig, J. H. 1992. Mechanisms Of Actin Rearrangements Mediating Platelet Activation. *J Cell Biol,* 118**,** 1421-42.

Hartwig, J. H. & Desisto, M. 1991. The Cytoskeleton Of The Resting Human Blood Platelet: Structure Of The Membrane Skeleton And Its Attachment To Actin Filaments. *J Cell Biol,* 112**,** 407-25.

Haslam, R. J., Dickinson, N. T. & Jang, E. K. 1999. Cyclic Nucleotides And Phosphodiesterases In Platelets. *Thromb Haemost,* 82**,** 412-23.

Heasman, S. J. & Ridley, A. J. 2008. Mammalian Rho Gtpases: New Insights Into Their Functions From In Vivo Studies. *Nat Rev Mol Cell Biol,* 9**,** 690-701.

Heemskerk, J. W., Vuist, W. M., Feijge, M. A., Reutelingsperger, C. P. & Lindhout, T. 1997. Collagen But Not Fibrinogen Surfaces Induce Bleb Formation, Exposure Of Phosphatidylserine, And Procoagulant Activity Of Adherent Platelets: Evidence For Regulation By Protein Tyrosine Kinase-Dependent Ca2+ Responses. *Blood,* 90**,** 2615-25.

Herfindal, L., Nygaard, G., Kopperud, R., Krakstad, C., Doskeland, S. O. & Selheim, F. 2013. Off-Target Effect Of The Epac Agonist 8-Pcpt-2'-O-Me-Camp On P2y12 Receptors In Blood Platelets. *Biochem Biophys Res Commun,* 437**,** 603-8.

Hertz, A. L. & Beavo, J. A. 2011. Cyclic Nucleotides And Phosphodiesterases In Monocytic Differentiation. *Handb Exp Pharmacol***,** 365-90.

Higgs, E. A., Higgs, G. A., Moncada, S. & Vane, J. R. 1978. Prostacyclin (Pgi2) Inhibits The Formation Of Platelet Thrombi In Arterioles And Venules Of The Hamster Cheek Pouch. *Br J Pharmacol,* 63**,** 535-9.

Hodivala-Dilke, K. M., Mchugh, K. P., Tsakiris, D. A., Rayburn, H., Crowley, D., Ullman-Cullere, M., Ross, F. P., Coller, B. S., Teitelbaum, S. & Hynes, R. O. 1999. Beta3-

Integrin-Deficient Mice Are A Model For Glanzmann Thrombasthenia Showing Placental Defects And Reduced Survival. *J Clin Invest,* 103**,** 229-38.

Hoffmeister, M., Riha, P., Neumuller, O., Danielewski, O., Schultess, J. & Smolenski, A. P. 2008. Cyclic Nucleotide-Dependent Protein Kinases Inhibit Binding Of 14-3-3 To The Gtpase-Activating Protein Rap1gap2 In Platelets. *J Biol Chem,* 283**,** 2297-306.

Holmback, K., Danton, M. J., Suh, T. T., Daugherty, C. C. & Degen, J. L. 1996. Impaired Platelet Aggregation And Sustained Bleeding In Mice Lacking The Fibrinogen Motif Bound By Integrin Alpha Iib Beta 3. *Embo J,* 15**,** 5760-71.

Hong-Geller, E. & Cerione, R. A. 2000. Cdc42 And Rac Stimulate Exocytosis Of Secretory Granules By Activating The Ip(3)/Calcium Pathway In Rbl-2h3 Mast Cells. *J Cell Biol,* 148**,** 481-94.

Horii, K., Kahn, M. L. & Herr, A. B. 2006. Structural Basis For Platelet Collagen Responses By The Immune-Type Receptor Glycoprotein Vi. *Blood,* 108**,** 936-42.

Horton, J. K., Capper, S. J., Jones, M. J. P. & Hughes, K. T. 2005. Assays For Drug-Screening Applications And Research. *In:* Wild, D. (Ed.) *The Immunoassay Handbook.* Oxford, Uk: Elsevier Ltd.

Hotulainen, P. & Lappalainen, P. 2006. Stress Fibers Are Generated By Two Distinct Actin Assembly Mechanisms In Motile Cells. *J Cell Biol,* 173**,** 383-94.

Hurowitz, E. H., Melnyk, J. M., Chen, Y. J., Kouros-Mehr, H., Simon, M. I. & Shizuya, H. 2000. Genomic Characterization Of The Human Heterotrimeric G Protein Alpha, Beta, And Gamma Subunit Genes. *Dna Res,* 7**,** 111-20.

Huveneers, S. & Danen, E. H. 2009. Adhesion Signaling - Crosstalk Between Integrins, Src And Rho. *J Cell Sci,* 122**,** 1059-69.

Hynes, R. O. 2002. Integrins: Bidirectional, Allosteric Signaling Machines. *Cell,* 110**,** 673-87.

Infante, E. & Ridley, A. J. 2013. Roles Of Rho Gtpases In Leucocyte And Leukaemia Cell Transendothelial Migration. *Philos Trans R Soc Lond B Biol Sci,* 368**,** 20130013.

Inoue, O., Suzuki-Inoue, K., Dean, W. L., Frampton, J. & Watson, S. P. 2003. Integrin Alpha2beta1 Mediates Outside-In Regulation Of Platelet Spreading On Collagen Through Activation Of Src Kinases And Plcgamma2. *J Cell Biol,* 160**,** 769-80.

Isenberg, G., Rathke, P. C., Hulsmann, N., Franke, W. W. & Wohlfarth-Bottermann, K. E. 1976. Cytoplasmic Actomyosin Fibrils In Tissue Culture Cells: Direct Proof Of Contractility By Visualization Of Atp-Induced Contraction In Fibrils Isolated By Laser Micro-Beam Dissection. *Cell Tissue Res,* 166**,** 427-43.

Ishizaki, T., Uehata, M., Tamechika, I., Keel, J., Nonomura, K., Maekawa, M. & Narumiya, S. 2000. Pharmacological Properties Of Y-27632, A Specific Inhibitor Of Rho-Associated Kinases. *Mol Pharmacol,* 57**,** 976-83.

Ivanciu, L., Krishnaswamy, S. & Camire, R. M. 2014. New Insights Into The Spatiotemporal Localization Of Prothrombinase In Vivo. *Blood,* 124**,** 1705-14.

Jackson, S. P. 2007. The Growing Complexity Of Platelet Aggregation. *Blood,* 109**,** 5087-95.

Jantzen, H. M., Milstone, D. S., Gousset, L., Conley, P. B. & Mortensen, R. M. 2001. Impaired Activation Of Murine Platelets Lacking G Alpha(I2). *J Clin Invest,* 108**,** 477-83.

Joo, S. J. 2012. Mechanisms Of Platelet Activation And Integrin Alphaiibeta3. *Korean Circ J,* 42**,** 295-301.

Jung, S. M., Ohnuma, M., Watanabe, N., Sonoda, M., Handa, M. & Moroi, M. 2006. Analyzing The Mechanism Of Rap1 Activation In Platelets: Rap1 Activation Is Related To The Release Reaction Mediated Through The Collagen Receptor Gpvi. *Thromb Res,* 118**,** 509-21.

Jung, S. M., Takemura, Y., Imamura, Y., Hayashi, T., Adachi, E. & Moroi, M. 2008. Collagen-Type Specificity Of Glycoprotein Vi As A Determinant Of Platelet Adhesion. *Platelets,* 19**,** 32-42.

Kabsch, W., Mannherz, H. G., Suck, D., Pai, E. F. & Holmes, K. C. 1990. Atomic Structure Of The Actin:Dnase I Complex. *Nature,* 347**,** 37-44.

Kahr, W. H. 2009. Granules And Thrombus Formation. *Blood,* 114**,** 932-3.

Kasirer-Friede, A., Ruggeri, Z. M. & Shattil, S. J. 2010. Role For Adap In Shear Flow-Induced Platelet Mechanotransduction. *Blood,* 115**,** 2274-82.

Katoh, K., Kano, Y., Amano, M., Kaibuchi, K. & Fujiwara, K. 2001. Stress Fiber Organization Regulated By Mlck And Rho-Kinase In Cultured Human Fibroblasts. *Am J Physiol Cell Physiol,* 280**,** C1669-79.

Katsel, P. L., Tagliente, T. M., Schwarz, T. E., Craddock-Royal, B. D., Patel, N. D. & Maayani, S. 2003. Molecular And Biochemical Evidence For The Presence Of Type Iii Adenylyl Cyclase In Human Platelets. *Platelets,* 14**,** 21-33.

Kaushansky, K. 2009. Determinants Of Platelet Number And Regulation Of Thrombopoiesis. *Hematology Am Soc Hematol Educ Program***,** 147-52.

Kawata, M., Kikuchi, A., Hoshijima, M., Yamamoto, K., Hashimoto, E., Yamamura, H. & Takai, Y. 1989. Phosphorylation Of Smg P21, A Ras P21-Like Gtp-Binding Protein, By Cyclic Amp-Dependent Protein Kinase In A Cell-Free System And In Response To Prostaglandin E1 In Intact Human Platelets. *J Biol Chem,* 264**,** 15688-95.

Kehrel, B., Balleisen, L., Kokott, R., Mesters, R., Stenzinger, W., Clemetson, K. J. & Van De Loo, J. 1988. Deficiency Of Intact Thrombospondin And Membrane Glycoprotein Ia In Platelets With Defective Collagen-Induced Aggregation And Spontaneous Loss Of Disorder. *Blood,* 71**,** 1074-8.

Khaitlina, S. Y. 2001. Functional Specificity Of Actin Isoforms. *Int Rev Cytol,* 202**,** 35-98.

Kieffer, N., Fitzgerald, L. A., Wolf, D., Cheresh, D. A. & Phillips, D. R. 1991. Adhesive Properties Of The Beta 3 Integrins: Comparison Of Gp Iib-Iiia And The Vitronectin Receptor Individually Expressed In Human Melanoma Cells. *J Cell Biol,* 113**,** 451-61.

Kim, M., Carman, C. V. & Springer, T. A. 2003. Bidirectional Transmembrane Signaling By Cytoplasmic Domain Separation In Integrins. *Science,* 301**,** 1720-5.

Kimura, K., Ito, M., Amano, M., Chihara, K., Fukata, Y., Nakafuku, M., Yamamori, B., Feng, J., Nakano, T., Okawa, K., Iwamatsu, A. & Kaibuchi, K. 1996. Regulation Of Myosin Phosphatase By Rho And Rho-Associated Kinase (Rho-Kinase). *Science,* 273**,** 245-8.

Kloczewiak, M., Timmons, S., Lukas, T. J. & Hawiger, J. 1984. Platelet Receptor Recognition Site On Human Fibrinogen. Synthesis And Structure-Function Relationship Of Peptides Corresponding To The Carboxy-Terminal Segment Of The Gamma Chain. *Biochemistry,* 23**,** 1767-74.

Kobilka, B. K., Kobilka, T. S., Daniel, K., Regan, J. W., Caron, M. G. & Lefkowitz, R. J. 1988. Chimeric Alpha 2-,Beta 2-Adrenergic Receptors: Delineation Of Domains Involved In Effector Coupling And Ligand Binding Specificity. *Science,* 240**,** 1310-6.

Korn, E. D., Carlier, M. F. & Pantaloni, D. 1987. Actin Polymerization And Atp Hydrolysis. *Science,* 238**,** 638-44.

Kozma, R., Ahmed, S., Best, A. & Lim, L. 1995. The Ras-Related Protein Cdc42hs And Bradykinin Promote Formation Of Peripheral Actin Microspikes And Filopodia In Swiss 3t3 Fibroblasts. *Mol Cell Biol,* 15**,** 1942-52.

Kroeze, W. K., Sheffler, D. J. & Roth, B. L. 2003. G-Protein-Coupled Receptors At A Glance. *J Cell Sci,* 116**,** 4867-9.

Lagarde, M. & Dechavanne, M. 1977. Thrombin Decreases Platelet Cyclic Amp In The Absence Of Prostaglandin Synthesis. *Biomedicine,* 27**,** 110-2.

Lai, F. P., Szczodrak, M., Block, J., Faix, J., Breitsprecher, D., Mannherz, H. G., Stradal, T. E., Dunn, G. A., Small, J. V. & Rottner, K. 2008. Arp2/3 Complex Interactions And Actin Network Turnover In Lamellipodia. *Embo J,* 27**,** 982-92.

Lane, W. J., Dias, S., Hattori, K., Heissig, B., Choy, M., Rabbany, S. Y., Wood, J., Moore, M. A. & Rafii, S. 2000. Stromal-Derived Factor 1-Induced Megakaryocyte

Migration And Platelet Production Is Dependent On Matrix Metalloproteinases. *Blood,* 96**,** 4152-9.

Lang, P., Gesbert, F., Delespine-Carmagnat, M., Stancou, R., Pouchelet, M. & Bertoglio, J. 1996. Protein Kinase A Phosphorylation Of Rhoa Mediates The Morphological And Functional Effects Of Cyclic Amp In Cytotoxic Lymphocytes. *Embo J,* 15**,** 510-9.

Langanger, G., Moeremans, M., Daneels, G., Sobieszek, A., De Brabander, M. & De Mey, J. 1986. The Molecular Organization Of Myosin In Stress Fibers Of Cultured Cells. *J Cell Biol,* 102**,** 200-9.

Lartey, J. & Lopez Bernal, A. 2009. Rho Protein Regulation Of Contraction In The Human Uterus. *Reproduction,* 138**,** 407-24.

Lazarides, E. & Burridge, K. 1975. Alpha-Actinin: Immunofluorescent Localization Of A Muscle Structural Protein In Nonmuscle Cells. *Cell,* 6**,** 289-98.

Leisner, T. M., Yuan, W., Denofrio, J. C., Liu, J. & Parise, L. V. 2007. Tickling The Tails: Cytoplasmic Domain Proteins That Regulate Integrin Alphaiibbeta3 Activation. *Curr Opin Hematol,* 14**,** 255-61.

Leung, T., Chen, X. Q., Manser, E. & Lim, L. 1996. The P160 Rhoa-Binding Kinase Rok Alpha Is A Member Of A Kinase Family And Is Involved In The Reorganization Of The Cytoskeleton. *Mol Cell Biol,* 16**,** 5313-27.

Li, H. J., Reinhardt, F., Herschman, H. R. & Weinberg, R. A. 2012. Cancer-Stimulated Mesenchymal Stem Cells Create A Carcinoma Stem Cell Niche Via Prostaglandin E2 Signaling. *Cancer Discov,* 2**,** 840-55.

Li, Y., Ndubuka, C. & Rubin, C. S. 1996. A Kinase Anchor Protein 75 Targets Regulatory (Rii) Subunits Of Camp-Dependent Protein Kinase Ii To The Cortical Actin Cytoskeleton In Non-Neuronal Cells. *J Biol Chem,* 271**,** 16862-9.

Libby, P. 2001. Current Concepts Of The Pathogenesis Of The Acute Coronary Syndromes. *Circulation,* 104**,** 365-72.

Liddington, R. C. & Ginsberg, M. H. 2002. Integrin Activation Takes Shape. *J Cell Biol,* 158**,** 833-9.

Litvinov, R. I., Mekler, A., Shuman, H., Bennett, J. S., Barsegov, V. & Weisel, J. W. 2012. Resolving Two-Dimensional Kinetics Of The Integrin Alphaiibbeta3-Fibrinogen Interactions Using Binding-Unbinding Correlation Spectroscopy. *J Biol Chem,* 287**,** 35275-85.

Liu, S., Calderwood, D. A. & Ginsberg, M. H. 2000. Integrin Cytoplasmic Domain-Binding Proteins. *J Cell Sci,* 113 (Pt 20)**,** 3563-71.

Lodish, H., Berk, A. & Zipursky, S. 2000. The Dynamics Of Actin Assembly. *In:* Freeman, W. H. (Ed.) *Molecular Cell Biology.* 4th Ed.: Macmillan Learning.

Luo, B. H., Carman, C. V. & Springer, T. A. 2007. Structural Basis Of Integrin Regulation And Signaling. *Annu Rev Immunol,* 25**,** 619-47.

Luo, B. H. & Springer, T. A. 2006. Integrin Structures And Conformational Signaling. *Curr Opin Cell Biol,* 18**,** 579-86.

Lyman, S., Gilmore, A., Burridge, K., Gidwitz, S. & White, G. C., 2nd 1997. Integrin-Mediated Activation Of Focal Adhesion Kinase Is Independent Of Focal Adhesion Formation Or Integrin Activation. Studies With Activated And Inhibitory Beta3 Cytoplasmic Domain Mutants. *J Biol Chem,* 272**,** 22538-47.

Ma, Y. Q., Yang, J., Pesho, M. M., Vinogradova, O., Qin, J. & Plow, E. F. 2006. Regulation Of Integrin Alphaiibbeta3 Activation By Distinct Regions Of Its Cytoplasmic Tails. *Biochemistry,* 45**,** 6656-62.

Machesky, L. M. & Hall, A. 1997. Role Of Actin Polymerization And Adhesion To Extracellular Matrix In Rac- And Rho-Induced Cytoskeletal Reorganization. *J Cell Biol,* 138**,** 913-26.

Machlus, K. R. & Italiano, J. E., Jr. 2013. The Incredible Journey: From Megakaryocyte Development To Platelet Formation. *J Cell Biol,* 201**,** 785-96.

Macphee, C. H., Reifsnyder, D. H., Moore, T. A., Lerea, K. M. & Beavo, J. A. 1988. Phosphorylation Results In Activation Of A Camp Phosphodiesterase In Human Platelets. *J Biol Chem,* 263**,** 10353-8.

Maekawa, M., Ishizaki, T., Boku, S., Watanabe, N., Fujita, A., Iwamatsu, A., Obinata, T., Ohashi, K., Mizuno, K. & Narumiya, S. 1999. Signaling From Rho To The Actin Cytoskeleton Through Protein Kinases Rock And Lim-Kinase. *Science,* 285**,** 895-8.

Mccarty, O. J., Calaminus, S. D., Berndt, M. C., Machesky, L. M. & Watson, S. P. 2006. Von Willebrand Factor Mediates Platelet Spreading Through Glycoprotein Ib And Alpha(Iib)Beta3 In The Presence Of Botrocetin And Ristocetin, Respectively. *J Thromb Haemost,* 4**,** 1367-78.

Mccarty, O. J., Larson, M. K., Auger, J. M., Kalia, N., Atkinson, B. T., Pearce, A. C., Ruf, S., Henderson, R. B., Tybulewicz, V. L., Machesky, L. M. & Watson, S. P. 2005. Rac1 Is Essential For Platelet Lamellipodia Formation And Aggregate Stability Under Flow. *J Biol Chem,* 280**,** 39474-84.

Mcdowall, J. 2006. *Fibrinogen* [Online]. Available: Https://Www.Ebi.Ac.Uk/Interpro/Potm/2006_11/Page1.Htm.

Mekrache, M., Kieffer, N. & Baruch, D. 2002. Activation Of Recombinant Alphaiibbeta3 Expressed In Chinese Hamster Ovary Cells Exposes Different Binding Sites For Fibrinogen Or Von Willebrand Factor: Evidence Using Monoclonal Antibodies To Alphaiibbeta3. *Br J Haematol,* 116**,** 636-44.

Mellor, H. 2010. The Role Of Formins In Filopodia Formation. *Biochim Biophys Acta,* 1803**,** 191-200.

Moers, A., Nieswandt, B., Massberg, S., Wettschureck, N., Gruner, S., Konrad, I., Schulte, V., Aktas, B., Gratacap, M. P., Simon, M. I., Gawaz, M. & Offermanns, S. 2003. G13 Is An Essential Mediator Of Platelet Activation In Hemostasis And Thrombosis. *Nat Med,* 9**,** 1418-22.

Moncada, S., Gryglewski, R., Bunting, S. & Vane, J. R. 1976. An Enzyme Isolated From Arteries Transforms Prostaglandin Endoperoxides To An Unstable Substance That Inhibits Platelet Aggregation. *Nature,* 263**,** 663-5.

Moncada, S., Palmer, R. M. & Higgs, E. A. 1991. Nitric Oxide: Physiology, Pathophysiology, And Pharmacology. *Pharmacol Rev,* 43**,** 109-42.

Moon, S. Y. & Zheng, Y. 2003. Rho Gtpase-Activating Proteins In Cell Regulation. *Trends Cell Biol.,* 13**,** 13-22.

Moreau, V., Tatin, F., Varon, C. & Genot, E. 2003. Actin Can Reorganize Into Podosomes In Aortic Endothelial Cells, A Process Controlled By Cdc42 And Rhoa. *Mol Cell Biol,* 23**,** 6809-22.

Moroi, M., Jung, S. M., Okuma, M. & Shinmyozu, K. 1989. A Patient With Platelets Deficient In Glycoprotein Vi That Lack Both Collagen-Induced Aggregation And Adhesion. *J Clin Invest,* 84**,** 1440-5.

Mozaffarian D, Benjamin Ej, Go As, Arnett Dk, Blaha Mj, Cushman M, De Ferranti S, Després J-P, Fullerton Hj, Howard Vj, Huffman Md, Judd Se, Kissela Bm, Lackland Dt, Lichtman Jh, Lisabeth Ld, Liu S, Mackey Rh, Matchar Db, Mcguire Dk, Mohler Er , Moy Cs, Muntner P, Mussolino Me, Nasir K, Neumar Rw, Nichol G, Palaniappan L, Pandey Dk, Reeves Mj, Rodriguez Cj, Sorlie Pd, Stein J, Towfighi, A, T. T., Virani Ss, Willey Jz, Woo D, Yeh Rw & Mb, T. 2015. Heart Disease And Stroke Statistics-At-A-Glance. *Circulation,* American Heart Association.

Mullins, R. D., Heuser, J. A. & Pollard, T. D. 1998. The Interaction Of Arp2/3 Complex With Actin: Nucleation, High Affinity Pointed End Capping, And Formation Of Branching Networks Of Filaments. *Proc Natl Acad Sci U S A,* 95**,** 6181-6.

Murphy, G. A., Solski, P. A., Jillian, S. A., Perez De La Ossa, P., D'eustachio, P., Der, C. J. & Rush, M. G. 1999. Cellular Functions Of Tc10, A Rho Family Gtpase: Regulation Of Morphology, Signal Transduction And Cell Growth. *Oncogene,* 18**,** 3831-45.

Murugappan, S., Shankar, H. & Kunapuli, S. P. 2004. Platelet Receptors For Adenine Nucleotides And Thromboxane A2. *Semin Thromb Hemost,* 30**,** 411-8.

Naik, U. P. & Naik, M. U. 2003. Association Of Cib With Gpiib/Iiia During Outside-In Signaling Is Required For Platelet Spreading On Fibrinogen. *Blood,* 102**,** 1355-62.

Nakeff, A. & Maat, B. 1974. Separation Of Megakaryocytes From Mouse Bone Marrow By Velocity Sedimentation. *Blood,* 43**,** 591-5.

Nathans, J. & Hogness, D. S. 1983. Isolation, Sequence Analysis, And Intron-Exon Arrangement Of The Gene Encoding Bovine Rhodopsin. *Cell,* 34**,** 807-14.

Naumanen, P., Lappalainen, P. & Hotulainen, P. 2008. Mechanisms Of Actin Stress Fibre Assembly. *J Microsc,* 231**,** 446-54.

Nermut, M. V., Green, N. M., Eason, P., Yamada, S. S. & Yamada, K. M. 1988. Electron Microscopy And Structural Model Of Human Fibronectin Receptor. *Embo J,* 7**,** 4093-9.

Nieswandt, B., Bergmeier, W., Schulte, V., Rackebrandt, K., Gessner, J. E. & Zirngibl, H. 2000. Expression And Function Of The Mouse Collagen Receptor Glycoprotein Vi Is Strictly Dependent On Its Association With The Fcrgamma Chain. *J Biol Chem,* 275**,** 23998-4002.

Nieswandt, B., Schulte, V., Bergmeier, W., Mokhtari-Nejad, R., Rackebrandt, K., Cazenave, J. P., Ohlmann, P., Gachet, C. & Zirngibl, H. 2001. Long-Term Antithrombotic Protection By In Vivo Depletion Of Platelet Glycoprotein Vi In Mice. *J Exp Med,* 193**,** 459-69.

Nieswandt, B. & Watson, S. P. 2003. Platelet-Collagen Interaction: Is Gpvi The Central Receptor? *Blood,* 102**,** 449-61.

Nieuwenhuis, H. K., Akkerman, J. W., Houdijk, W. P. & Sixma, J. J. 1985. Human Blood Platelets Showing No Response To Collagen Fail To Express Surface Glycoprotein Ia. *Nature,* 318**,** 470-2.

Nobes, C. D. & Hall, A. 1995. Rho, Rac And Cdc42 Gtpases: Regulators Of Actin Structures, Cell Adhesion And Motility. *Biochem Soc Trans,* 23**,** 456-9.

Nurden, A. T. 1999. Inherited Abnormalities Of Platelets. *Thromb Haemost,* 82**,** 468-80.

Nuyttens, B. P., Thijs, T., Deckmyn, H. & Broos, K. 2011. Platelet Adhesion To Collagen. *Thromb Res,* 127 Suppl 2**,** S26-9.

O'brien, K. A., Gartner, T. K., Hay, N. & Du, X. 2012. Adp-Stimulated Activation Of Akt During Integrin Outside-In Signaling Promotes Platelet Spreading By Inhibiting Glycogen Synthase Kinase-3beta. *Arterioscler Thromb Vasc Biol,* 32**,** 2232-40.

Oda, T., Iwasa, M., Aihara, T., Maeda, Y. & Narita, A. 2009. The Nature Of The Globular- To Fibrous-Actin Transition. *Nature,* 457**,** 441-5.

Offermanns, S., Toombs, C. F., Hu, Y. H. & Simon, M. I. 1997. Defective Platelet Activation In G Alpha(Q)-Deficient Mice. *Nature,* 389**,** 183-6.

Ogawa, M. 1993. Differentiation And Proliferation Of Hematopoietic Stem Cells. *Blood,* 81**,** 2844-53.

Ohlmann, P., Eckly, A., Freund, M., Cazenave, J. P., Offermanns, S. & Gachet, C. 2000. Adp Induces Partial Platelet Aggregation Without Shape Change And Potentiates Collagen-Induced Aggregation In The Absence Of Galphaq. *Blood,* 96**,** 2134-9.

Ollivier, V., Syvannarath, V., Gros, A., Butt, A., Loyau, S., Jandrot-Perrus, M. & Ho-Tin-Noe, B. 2014. Collagen Can Selectively Trigger A Platelet Secretory Phenotype Via Glycoprotein Vi. *Plos One,* 9**,** E104712.

Olofsson, B. 1999. Rho Guanine Dissociation Inhibitors: Pivotal Molecules In Cellular Signalling. *Cell Signal,* 11**,** 545-54.

Owen, J., Mccarty, T., Larson, M. K., Auger, J. M., Atkinson, B. T., Pearce, A. C., Ruf, S., Henderson, R. B., Tybulewicz, V. L. J., Machesky, L. M. & Watson, S. P. 2005. Rac1 Is Essential For Platelet Lamellipodia And Aggregate Stability Under Flow. *Heart,* 91.

Palmer, R. M., Ashton, D. S. & Moncada, S. 1988. Vascular Endothelial Cells Synthesize Nitric Oxide From L-Arginine. *Nature,* 333**,** 664-6.

Pantaloni, D. & Carlier, M. F. 1993. How Profilin Promotes Actin Filament Assembly In The Presence Of Thymosin Beta 4. *Cell,* 75**,** 1007-14.

Parsons, J. T., Horwitz, A. R. & Schwartz, M. A. 2010. Cell Adhesion: Integrating Cytoskeletal Dynamics And Cellular Tension. *Nat Rev Mol Cell Biol,* 11**,** 633-43.

Paterson, H. F., Self, A. J., Garrett, M. D., Just, I., Aktories, K. & Hall, A. 1990. Microinjection Of Recombinant P21rho Induces Rapid Changes In Cell Morphology. *J Cell Biol,* 111**,** 1001-7.

Paul, B. Z., Jin, J. & Kunapuli, S. P. 1999. Molecular Mechanism Of Thromboxane A(2)-Induced Platelet Aggregation. Essential Role For P2t(Ac) And Alpha(2a) Receptors. *J Biol Chem,* 274**,** 29108-14.

Pelish, H. E., Peterson, J. R., Salvarezza, S. B., Rodriguez-Boulan, E., Chen, J. L., Stamnes, M., Macia, E., Feng, Y., Shair, M. D. & Kirchhausen, T. 2006. Secramine Inhibits Cdc42-Dependent Functions In Cells And Cdc42 Activation In Vitro. *Nat Chem Biol,* 2**,** 39-46.

Pellegrin, S. & Mellor, H. 2005. The Rho Family Gtpase Rif Induces Filopodia Through Mdia2. *Curr Biol,* 15**,** 129-33.

Pellegrin, S. & Mellor, H. 2007. Actin Stress Fibres. *J Cell Sci,* 120**,** 3491-9.

Pelletier, S., Julien, C., Popoff, M. R., Lamarche-Vane, N. & Meloche, S. 2005. Cyclic Amp Induces Morphological Changes Of Vascular Smooth Muscle Cells By Inhibiting A Rac-Dependent Signaling Pathway. *J Cell Physiol,* 204**,** 412-22.

Peppelenbosch, M. P., Tertoolen, L. G., Hage, W. J. & De Laat, S. W. 1993. Epidermal Growth Factor-Induced Actin Remodeling Is Regulated By 5-Lipoxygenase And Cyclooxygenase Products. *Cell,* 74**,** 565-75.

Peralta, E. G., Winslow, J. W., Peterson, G. L., Smith, D. H., Ashkenazi, A., Ramachandran, J., Schimerlik, M. I. & Capon, D. J. 1987. Primary Structure And Biochemical Properties Of An M2 Muscarinic Receptor. *Science,* 236**,** 600-5.

Perez, V., Bouschet, T., Fernandez, C., Bockaert, J. & Journot, L. 2005. Dynamic Reorganization Of The Astrocyte Actin Cytoskeleton Elicited By Camp And Pacap: A Role For Phosphatidylinositol 3-Kinase Inhibition. *Eur J Neurosci,* 21**,** 26-32.

Persikov, A. V., Ramshaw, J. A., Kirkpatrick, A. & Brodsky, B. 2005. Electrostatic Interactions Involving Lysine Make Major Contributions To Collagen Triple-Helix Stability. *Biochemistry,* 44**,** 1414-22.

Peters, C. G., Michelson, A. D. & Flaumenhaft, R. 2012. Granule Exocytosis Is Required For Platelet Spreading: Differential Sorting Of Alpha-Granules Expressing Vamp-7. *Blood,* 120**,** 199-206.

Petersen, L. A., Wright, S. M., Peterson, E. D. & Daley, J. 2002. Impact Of Race On Cardiac Care And Outcomes In Veterans With Acute Myocardial Infarction. *Med Care,* 40**,** I86-96.

Phillips, D. R., Conley, P. B., Sinha, U. & Andre, P. 2005. Therapeutic Approaches In Arterial Thrombosis. *J Thromb Haemost,* 3**,** 1577-89.

Pidoux, G. & Tasken, K. 2010. Specificity And Spatial Dynamics Of Protein Kinase A Signaling Organized By A-Kinase-Anchoring Proteins. *J Mol Endocrinol,* 44**,** 271-84.

Pleines, I., Eckly, A., Elvers, M., Hagedorn, I., Eliautou, S., Bender, M., Wu, X., Lanza, F., Gachet, C., Brakebusch, C. & Nieswandt, B. 2010. Multiple Alterations Of Platelet Functions Dominated By Increased Secretion In Mice Lacking Cdc42 In Platelets. *Blood,* 115**,** 3364-73.

Pollard, T. D. 2001. Genomics, The Cytoskeleton And Motility. *Nature,* 409**,** 842-3.

Poulter, N. S., Pollitt, A. Y., Davies, A., Malinova, D., Nash, G. B., Hannon, M. J., Pikramenou, Z., Rappoport, J. Z., Hartwig, J. H., Owen, D. M., Thrasher, A. J., Watson, S. P. & Thomas, S. G. 2015. Platelet Actin Nodules Are Podosome-Like Structures Dependent On Wiskott-Aldrich Syndrome Protein And Arp2/3 Complex. *Nat Commun,* 6**,** 7254.

Prevost, N., Woulfe, D. S., Tognolini, M., Tanaka, T., Jian, W., Fortna, R. R., Jiang, H. & Brass, L. F. 2004. Signaling By Ephrinb1 And Eph Kinases In Platelets Promotes Rap1 Activation, Platelet Adhesion, And Aggregation Via Effector Pathways That Do Not Require Phosphorylation Of Ephrinb1. *Blood,* 103**,** 1348-55.

Pula, G. & Poole, A. W. 2008. Critical Roles For The Actin Cytoskeleton And Cdc42 In Regulating Platelet Integrin Alpha2beta1. *Platelets,* 19**,** 199-210.

Qiao, J., Huang, F. & Lum, H. 2003. Pka Inhibits Rhoa Activation: A Protection Mechanism Against Endothelial Barrier Dysfunction. *Am J Physiol Lung Cell Mol Physiol,* 284**,** L972-80.

Quinton, T. M. & Dean, W. L. 1992. Cyclic Amp-Dependent Phosphorylation Of The Inositol-1,4,5-Trisphosphate Receptor Inhibits Ca2+ Release From Platelet Membranes. *Biochem Biophys Res Commun,* 184**,** 893-9.

Radomski, M. W., Palmer, R. M. & Moncada, S. 1987a. The Anti-Aggregating Properties Of Vascular Endothelium: Interactions Between Prostacyclin And Nitric Oxide. *Br J Pharmacol,* 92**,** 639-46.

Radomski, M. W., Palmer, R. M. & Moncada, S. 1987b. Comparative Pharmacology Of Endothelium-Derived Relaxing Factor, Nitric Oxide And Prostacyclin In Platelets. *Br J Pharmacol,* 92**,** 181-7.

Rajendran, P., Rengarajan, T., Thangavel, J., Nishigaki, Y., Sakthisekaran, D., Sethi, G. & Nishigaki, I. 2013. The Vascular Endothelium And Human Diseases. *Int J Biol Sci,* 9**,** 1057-69.

Ramakers, G. J. & Moolenaar, W. H. 1998. Regulation Of Astrocyte Morphology By Rhoa And Lysophosphatidic Acid. *Exp Cell Res,* 245**,** 252-62.

Raslan, Z., Aburima, A. & Naseem, K. M. 2015a. The Spatiotemporal Regulation Of Camp Signaling In Blood Platelets-Old Friends And New Players. *Front Pharmacol,* 6**,** 266.

Raslan, Z., Magwenzi, S., Aburima, A., Tasken, K. & Naseem, K. M. 2015b. Targeting Of Type I Protein Kinase A To Lipid Rafts Is Required For Platelet Inhibition By The 3',5'-Cyclic Adenosine Monophosphate-Signaling Pathway. *J Thromb Haemost,* 13**,** 1721-34.

Rehmann, H., Schwede, F., Doskeland, S. O., Wittinghofer, A. & Bos, J. L. 2003. Ligand-Mediated Activation Of The Camp-Responsive Guanine Nucleotide Exchange Factor Epac. *J Biol Chem,* 278**,** 38548-56.

Ren, X. D., Kiosses, W. B. & Schwartz, M. A. 1999. Regulation Of The Small Gtp-Binding Protein Rho By Cell Adhesion And The Cytoskeleton. *Embo J,* 18**,** 578-85.

Ricard-Blum, S. 2011. The Collagen Family. *Cold Spring Harb Perspect Biol,* 3**,** A004978.

Ridley, A. 2000. Rho Gtpases. Integrating Integrin Signaling. *J Cell Biol,* 150**,** F107-9.

Ridley, A. J. 1995. Microinjection Of Rho And Rac Into Quiescent Swiss 3t3 Cells. *Methods Enzymol,* 256**,** 313-20.

Ridley, A. J., Paterson, H. F., Johnston, C. L., Diekmann, D. & Hall, A. 1992. The Small Gtp-Binding Protein Rac Regulates Growth Factor-Induced Membrane Ruffling. *Cell,* 70**,** 401-10.

Rivera, J., Lozano, M. L., Navarro-Nunez, L. & Vicente, V. 2009. Platelet Receptors And Signaling In The Dynamics Of Thrombus Formation. *Haematologica,* 94**,** 700-11.

Rooney, M. M., Parise, L. V. & Lord, S. T. 1996. Dissecting Clot Retraction And Platelet Aggregation. Clot Retraction Does Not Require An Intact Fibrinogen Gamma Chain C Terminus. *J Biol Chem,* 271**,** 8553-5.

Root, W. S. & Hofmann, F. G. 1963. *Physiological Pharmacology; A Comprehensive Treatise,* New York,, Academic Press.

Ruggeri, Z. M. 2002. Platelets In Atherothrombosis. *Nat Med,* 8**,** 1227-34.

Ruoslahti, E. & Pierschbacher, M. D. 1986. Arg-Gly-Asp: A Versatile Cell Recognition Signal. *Cell,* 44**,** 517-8.

Ruusala, A. & Aspenstrom, P. 2008. The Atypical Rho Gtpase Wrch1 Collaborates With The Nonreceptor Tyrosine Kinases Pyk2 And Src In Regulating Cytoskeletal Dynamics. *Mol Cell Biol,* 28**,** 1802-14.

Salsmann, A., Schaffner-Reckinger, E., Kabile, F., Plancon, S. & Kieffer, N. 2005. A New Functional Role Of The Fibrinogen Rgd Motif As The Molecular Switch That Selectively Triggers Integrin Alphaiibbeta3-Dependent Rhoa Activation During Cell Spreading. *J Biol Chem,* 280**,** 33610-9.

Salzman, E. W., Kensler, P. C. & Levine, L. 1972. Cyclic 3',5'-Adenosine Monophosphate In Human Blood Platelets. Iv. Regulatory Role Of Cyclic Amp In Platelet Function. *Ann N Y Acad Sci,* 201**,** 61-71.

Sasaki, T. & Takai, Y. 1998. The Rho Small G Protein Family-Rho Gdi System As A Temporal And Spatial Determinant For Cytoskeletal Control. *Biochem Biophys Res Commun,* 245**,** 641-5.

Schafer, A. & Bauersachs, J. 2008. Endothelial Dysfunction, Impaired Endogenous Platelet Inhibition And Platelet Activation In Diabetes And Atherosclerosis. *Curr Vasc Pharmacol,* 6**,** 52-60.

Schirenbeck, A., Bretschneider, T., Arasada, R., Schleicher, M. & Faix, J. 2005. The Diaphanous-Related Formin Ddia2 Is Required For The Formation And Maintenance Of Filopodia. *Nat Cell Biol,* 7**,** 619-25.

Schmidt, A. & Hall, A. 2002. Guanine Nucleotide Exchange Factors For Rho Gtpases: Turning On The Switch. *Genes Dev,* 16**,** 1587-609.

Schmidt, M., Dekker, F. J. & Maarsingh, H. 2013. Exchange Protein Directly Activated By Camp (Epac): A Multidomain Camp Mediator In The Regulation Of Diverse Biological Functions. *Pharmacol Rev,* 65**,** 670-709.

Schwartz, M. A. 2010. Integrins And Extracellular Matrix In Mechanotransduction. *Cold Spring Harb Perspect Biol,* 2**,** A005066.

Semple, J. W., Italiano, J. E., Jr. & Freedman, J. 2011. Platelets And The Immune Continuum. *Nat Rev Immunol,* 11**,** 264-74.

Shang, X., Marchioni, F., Sipes, N., Evelyn, C. R., Jerabek-Willemsen, M., Duhr, S., Seibel, W., Wortman, M. & Zheng, Y. 2012. Rational Design Of Small Molecule Inhibitors Targeting Rhoa Subfamily Rho Gtpases. *Chem Biol,* 19**,** 699-710.

Shattil, S. J., Hoxie, J. A., Cunningham, M. & Brass, L. F. 1985. Changes In The Platelet Membrane Glycoprotein Iib.Iiia Complex During Platelet Activation. *J Biol Chem,* 260**,** 11107-14.

Shattil, S. J. & Newman, P. J. 2004. Integrins: Dynamic Scaffolds For Adhesion And Signaling In Platelets. *Blood,* 104**,** 1606-15.

Shields, J. M., Pruitt, K., Mcfall, A., Shaub, A. & Der, C. J. 2000. Understanding Ras: 'It Ain't Over 'Til It's Over'. *Trends Cell Biol.,* 10.

Siess, W. & Lapetina, E. G. 1988. Ca2+ Mobilization Primes Protein Kinase C In Human Platelets. Ca2+ And Phorbol Esters Stimulate Platelet Aggregation And Secretion Synergistically Through Protein Kinase C. *Biochem J,* 255**,** 309-18.

Siess, W. & Lapetina, E. G. 1989. Prostacyclin Inhibits Platelet Aggregation Induced By Phorbol Ester Or Ca2+ Ionophore At Steps Distal To Activation Of Protein Kinase C And Ca2+-Dependent Protein Kinases. *Biochem J,* 258**,** 57-65.

Siess, W. & Lapetina, E. G. 1990. Functional Relationship Between Cyclic Amp-Dependent Protein Phosphorylation And Platelet Inhibition. *Biochem J,* 271**,** 815-9.

Sim, D. S., Merrill-Skoloff, G., Furie, B. C., Furie, B. & Flaumenhaft, R. 2004. Initial Accumulation Of Platelets During Arterial Thrombus Formation In Vivo Is Inhibited By Elevation Of Basal Camp Levels. *Blood,* 103**,** 2127-34.

Skalhegg, B. S. & Tasken, K. 2000. Specificity In The Camp/Pka Signaling Pathway. Differential Expression,Regulation, And Subcellular Localization Of Subunits Of Pka. *Front Biosci,* 5**,** D678-93.

Small, J. V. 1988. The Actin Cytoskeleton. *Electron Microsc Rev,* 1**,** 155-74.

Smith, J. W., Ruggeri, Z. M., Kunicki, T. J. & Cheresh, D. A. 1990. Interaction Of Integrins Alpha V Beta 3 And Glycoprotein Iib-Iiia With Fibrinogen. Differential Peptide Recognition Accounts For Distinct Binding Sites. *J Biol Chem,* 265**,** 12267-71.

Smith, M. A., Blankman, E., Gardel, M. L., Luettjohann, L., Waterman, C. M. & Beckerle, M. C. 2010. A Zyxin-Mediated Mechanism For Actin Stress Fiber Maintenance And Repair. *Dev Cell,* 19**,** 365-76.

Smolenski, A. 2012. Novel Roles Of Camp/Cgmp-Dependent Signaling In Platelets. *J Thromb Haemost,* 10**,** 167-76.

Soderling, S. H. & Beavo, J. A. 2000. Regulation Of Camp And Cgmp Signaling: New Phosphodiesterases And New Functions. *Curr Opin Cell Biol,* 12**,** 174-9.

Somlyo, A. P. & Somlyo, A. V. 2000. Signal Transduction By G-Proteins, Rho-Kinase And Protein Phosphatase To Smooth Muscle And Non-Muscle Myosin Ii. *J Physiol,* 522 Pt 2**,** 177-85.

Stalker, T. J., Traxler, E. A., Wu, J., Wannemacher, K. M., Cermignano, S. L., Voronov, R., Diamond, S. L. & Brass, L. F. 2013. Hierarchical Organization In The Hemostatic Response And Its Relationship To The Platelet-Signaling Network. *Blood,* 121**,** 1875-85.

Stalker, T. J., Welsh, J. D., Tomaiuolo, M., Wu, J., Colace, T. V., Diamond, S. L. & Brass, L. F. 2014. A Systems Approach To Hemostasis: 3. Thrombus Consolidation Regulates Intrathrombus Solute Transport And Local Thrombin Activity. *Blood,* 124**,** 1824-31.

Stasch, J. P., Pacher, P. & Evgenov, O. V. 2011. Soluble Guanylate Cyclase As An Emerging Therapeutic Target In Cardiopulmonary Disease. *Circulation,* 123**,** 2263-73.

Stehbens, W. E. & Biscoe, T. J. 1967. The Ultrastructure Of Early Platelet Aggregation In Vivo. *Am J Pathol,* 50**,** 219-43.

Stolting, M., Wiesner, C., Van Vliet, V., Butt, E., Pavenstadt, H., Linder, S. & Kremerskothen, J. 2012. Lasp-1 Regulates Podosome Function. *Plos One,* 7**,** E35340.

Strijdom, H., Chamane, N. & Lochner, A. 2009. Nitric Oxide In The Cardiovascular System: A Simple Molecule With Complex Actions. *Cardiovasc J Afr,* 20**,** 303-10.

Sunahara, R. K., Dessauer, C. W. & Gilman, A. G. 1996. Complexity And Diversity Of Mammalian Adenylyl Cyclases. *Annu Rev Pharmacol Toxicol,* 36**,** 461-80.

Svitkina, T. M. & Borisy, G. G. 1999. Arp2/3 Complex And Actin Depolymerizing Factor/Cofilin In Dendritic Organization And Treadmilling Of Actin Filament Array In Lamellipodia. *J Cell Biol,* 145**,** 1009-26.

Takenawa, T. 2010. Phosphoinositide-Binding Interface Proteins Involved In Shaping Cell Membranes. *Proc Jpn Acad Ser B Phys Biol Sci,* 86**,** 509-23.

Tamma, G., Wiesner, B., Furkert, J., Hahm, D., Oksche, A., Schaefer, M., Valenti, G., Rosenthal, W. & Klussmann, E. 2003. The Prostaglandin E2 Analogue Sulprostone Antagonizes Vasopressin-Induced Antidiuresis Through Activation Of Rho. *J Cell Sci,* 116**,** 3285-94.

Tasken, K. & Aandahl, E. M. 2004. Localized Effects Of Camp Mediated By Distinct Routes Of Protein Kinase A. *Physiol Rev,* 84**,** 137-67.

Tasken, K., Skalhegg, B. S., Tasken, K. A., Solberg, R., Knutsen, H. K., Levy, F. O., Sandberg, M., Orstavik, S., Larsen, T., Johansen, A. K., Vang, T., Schrader, H. P., Reinton, N. T., Torgersen, K. M., Hansson, V. & Jahnsen, T. 1997. Structure,

Function, And Regulation Of Human Camp-Dependent Protein Kinases. *Adv Second Messenger Phosphoprotein Res,* 31**,** 191-204.

Tateson, J. E., Moncada, S. & Vane, J. R. 1977. Effects Of Prostacyclin (Pgx) On Cyclic Amp Concentrations In Human Platelets. *Prostaglandins,* 13**,** 389-97.

Thomson, D. M., Ascione, M. P., Grange, J., Nelson, C. & Hansen, M. D. 2011. Phosphorylation Of Vasp By Ampk Alters Actin Binding And Occurs At A Novel Site. *Biochem Biophys Res Commun,* 414**,** 215-9.

Tomaiuolo, M., Stalker, T. J., Welsh, J. D., Diamond, S. L., Sinno, T. & Brass, L. F. 2014. A Systems Approach To Hemostasis: 2. Computational Analysis Of Molecular Transport In The Thrombus Microenvironment. *Blood,* 124**,** 1816-23.

Tominaga, T., Sahai, E., Chardin, P., Mccormick, F., Courtneidge, S. A. & Alberts, A. S. 2000. Diaphanous-Related Formins Bridge Rho Gtpase And Src Tyrosine Kinase Signaling. *Mol Cell,* 5**,** 13-25.

Totsukawa, G., Yamakita, Y., Yamashiro, S., Hartshorne, D. J., Sasaki, Y. & Matsumura, F. 2000. Distinct Roles Of Rock (Rho-Kinase) And Mlck In Spatial Regulation Of Mlc Phosphorylation For Assembly Of Stress Fibers And Focal Adhesions In 3t3 Fibroblasts. *J Cell Biol,* 150**,** 797-806.

Tronik-Le Roux, D., Roullot, V., Poujol, C., Kortulewski, T., Nurden, P. & Marguerie, G. 2000. Thrombasthenic Mice Generated By Replacement Of The Integrin Alpha(Iib) Gene: Demonstration That Transcriptional Activation Of This Megakaryocytic Locus Precedes Lineage Commitment. *Blood,* 96**,** 1399-408.

Van Geet, C., Izzi, B., Labarque, V. & Freson, K. 2009. Human Platelet Pathology Related To Defects In The G-Protein Signaling Cascade. *J Thromb Haemost,* 7 Suppl 1**,** 282-6.

Villalonga, P. & Ridley, A. J. 2013. Rho Gtpases And Actin Cytoskeletal Dynamics. *In:* Lennarz, W. J. (Ed.) *Encyclopedia Of Biological Chemistry.* Second Edition Ed. Usa: Elsevier.

Vinogradova, O., Velyvis, A., Velyviene, A., Hu, B., Haas, T., Plow, E. & Qin, J. 2002. A Structural Mechanism Of Integrin Alpha(Iib)Beta(3) "Inside-Out" Activation As Regulated By Its Cytoplasmic Face. *Cell,* 110**,** 587-97.

Voss, B. & Rauterberg, J. 1986. Localization Of Collagen Types I, Iii, Iv And V, Fibronectin And Laminin In Human Arteries By The Indirect Immunofluorescence Method. *Pathol Res Pract,* 181**,** 568-75.

Wagner, C. L., Mascelli, M. A., Neblock, D. S., Weisman, H. F., Coller, B. S. & Jordan, R. E. 1996. Analysis Of Gpiib/Iiia Receptor Number By Quantification Of 7e3 Binding To Human Platelets. *Blood,* 88**,** 907-14.

Walker, T. R. & Watson, S. P. 1993. Synergy Between Ca2+ And Protein Kinase C Is The Major Factor In Determining The Level Of Secretion From Human Platelets. *Biochem J,* 289 (Pt 1)**,** 277-82.

Walter, U., Eigenthaler, M., Geiger, J. & Reinhard, M. 1993. Role Of Cyclic Nucleotide-Dependent Protein Kinases And Their Common Substrate Vasp In The Regulation Of Human Platelets. *Adv Exp Med Biol,* 344**,** 237-49.

Ware, J., Russell, S. & Ruggeri, Z. M. 2000. Generation And Rescue Of A Murine Model Of Platelet Dysfunction: The Bernard-Soulier Syndrome. *Proc Natl Acad Sci U S A,* 97**,** 2803-8.

Watanabe, N., Madaule, P., Reid, T., Ishizaki, T., Watanabe, G., Kakizuka, A., Saito, Y., Nakao, K., Jockusch, B. M. & Narumiya, S. 1997. P140mdia, A Mammalian Homolog Of Drosophila Diaphanous, Is A Target Protein For Rho Small Gtpase And Is A Ligand For Profilin. *Embo J,* 16**,** 3044-56.

Watson, S. P. 2009. Platelet Activation By Extracellular Matrix Proteins In Haemostasis And Thrombosis. *Curr Pharm Des,* 15**,** 1358-72.

Watson, S. P., Asazuma, N., Atkinson, B., Berlanga, O., Best, D., Bobe, R., Jarvis, G., Marshall, S., Snell, D., Stafford, M., Tulasne, D., Wilde, J., Wonerow, P. & Frampton, J. 2001. The Role Of Itam- And Itim-Coupled Receptors In Platelet Activation By Collagen. *Thromb Haemost,* 86**,** 276-88.

Weber, A., Nachmias, V. T., Pennise, C. R., Pring, M. & Safer, D. 1992. Interaction Of Thymosin Beta 4 With Muscle And Platelet Actin: Implications For Actin Sequestration In Resting Platelets. *Biochemistry,* 31**,** 6179-85.

Wegener, K. L., Partridge, A. W., Han, J., Pickford, A. R., Liddington, R. C., Ginsberg, M. H. & Campbell, I. D. 2007. Structural Basis Of Integrin Activation By Talin. *Cell,* 128**,** 171-82.

Wei, A. H., Schoenwaelder, S. M., Andrews, R. K. & Jackson, S. P. 2009. New Insights Into The Haemostatic Function Of Platelets. *Br J Haematol,* 147**,** 415-30.

Weksler, B. B., Ley, C. W. & Jaffe, E. A. 1978. Stimulation Of Endothelial Cell Prostacyclin Production By Thrombin, Trypsin, And The Ionophore A 23187. *J Clin Invest,* 62**,** 923-30.

Welsh, J. D., Muthard, R. W., Stalker, T. J., Taliaferro, J. P., Diamond, S. L. & Brass, L. F. 2016. A Systems Approach To Hemostasis: 4. How Hemostatic Thrombi Limit The Loss Of Plasma-Borne Molecules From The Microvasculature. *Blood,* 127**,** 1598-605.

Welsh, J. D., Stalker, T. J., Voronov, R., Muthard, R. W., Tomaiuolo, M., Diamond, S. L. & Brass, L. F. 2014. A Systems Approach To Hemostasis: 1. The Interdependence Of Thrombus Architecture And Agonist Movements In The Gaps Between Platelets. *Blood,* 124**,** 1808-15.

Wess, J., Brann, M. R. & Bonner, T. I. 1989. Identification Of A Small Intracellular Region Of The Muscarinic M3 Receptor As A Determinant Of Selective Coupling To Pi Turnover. *Febs Lett,* 258**,** 133-6.

Wheeler, A. P. & Ridley, A. J. 2004. Why Three Rho Proteins? Rhoa, Rhob, Rhoc, And Cell Motility. *Exp Cell Res,* 301**,** 43-9.

Whelan, M. C. & Senger, D. R. 2003. Collagen I Initiates Endothelial Cell Morphogenesis By Inducing Actin Polymerization Through Suppression Of Cyclic Amp And Protein Kinase A. *J Biol Chem,* 278**,** 327-34.

White, J. G. & Clawson, C. C. 1980. The Surface-Connected Canalicular System Of Blood Platelets--A Fenestrated Membrane System. *Am J Pathol,* 101**,** 353-64.

Whittaker, N., Bunting, S., Salmon, J., Moncada, S., Vane, J. R., Johnson, R. A., Morton, D. R., Kinner, J. H., Gorman, R. R., Mcguire, J. C. & Sun, F. F. 1976. The Chemical Structure Of Prostaglandin X (Prostacyclin). *Prostaglandins,* 12**,** 915-28.

Wild, D. (Ed.) 2005. *The Immunoassay Handbook,* Oxford: Elsevier.

Wong, S. K., Parker, E. M. & Ross, E. M. 1990. Chimeric Muscarinic Cholinergic: Beta-Adrenergic Receptors That Activate Gs In Response To Muscarinic Agonists. *J Biol Chem,* 265**,** 6219-24.

Wood, W. & Martin, P. 2002. Structures In Focus--Filopodia. *Int J Biochem Cell Biol,* 34**,** 726-30.

World_Health_Organization. 2016. *Cardiovascular Disease* [Online]. [Accessed 07/09/2016 2016].

Woulfe, D., Jiang, H., Mortensen, R., Yang, J. & Brass, L. F. 2002. Activation Of Rap1b By G(I) Family Members In Platelets. *J Biol Chem,* 277**,** 23382-90.

Woulfe, D., Yang, J. & Brass, L. 2001. Adp And Platelets: The End Of The Beginning. *J Clin Invest,* 107**,** 1503-5.

Yamanishi, J., Kawahara, Y. & Fukuzaki, H. 1983. Effect Of Cyclic Amp On Cytoplasmic Free Calcium In Human Platelets Stimulated By Thrombin: Direct Measurement With Quin2. *Thromb Res,* 32**,** 183-8.

Yamazaki, D., Suetsugu, S., Miki, H., Kataoka, Y., Nishikawa, S., Fujiwara, T., Yoshida, N. & Takenawa, T. 2003. Wave2 Is Required For Directed Cell Migration And Cardiovascular Development. *Nature,* 424**,** 452-6.

Yang, C., Czech, L., Gerboth, S., Kojima, S., Scita, G. & Svitkina, T. 2007. Novel Roles Of Formin Mdia2 In Lamellipodia And Filopodia Formation In Motile Cells. *Plos Biol,* 5**,** E317.

Yin, H. L., Hartwig, J. H., Maruyama, K. & Stossel, T. P. 1981. Ca2+ Control Of Actin Filament Length. Effects Of Macrophage Gelsolin On Actin Polymerization. *J Biol Chem,* 256**,** 9693-7.

Yurchenco, P. D. 2011. Basement Membranes: Cell Scaffoldings And Signaling Platforms. *Cold Spring Harb Perspect Biol,* 3.

Zaidel-Bar, R., Itzkovitz, S., Ma'ayan, A., Iyengar, R. & Geiger, B. 2007. Functional Atlas Of The Integrin Adhesome. *Nat Cell Biol,* 9**,** 858-67.

Zaidi, T. N., Mcintire, L. V., Farrell, D. H. & Thiagarajan, P. 1996. Adhesion Of Platelets To Surface-Bound Fibrinogen Under Flow. *Blood,* 88**,** 2967-72.

Zalevsky, J., Grigorova, I. & Mullins, R. D. 2001. Activation Of The Arp2/3 Complex By The Listeria Acta Protein. Acta Binds Two Actin Monomers And Three Subunits Of The Arp2/3 Complex. *J Biol Chem,* 276**,** 3468-75.

Zent, R. & Pozzi, A. (Eds.) 2010. *Cell-Extracellular Matrix Interactions In Cancer*: Springer.

Zhang, W. & Colman, R. W. 2007. Thrombin Regulates Intracellular Cyclic Amp Concentration In Human Platelets Through Phosphorylation/Activation Of Phosphodiesterase 3a. *Blood,* 110**,** 1475-82.

Zhang, X., Bi, E., Novick, P., Du, L., Kozminski, K. G., Lipschutz, J. H. & Guo, W. 2001. Cdc42 Interacts With The Exocyst And Regulates Polarized Secretion. *J Biol Chem,* 276**,** 46745-50.

Zhang, Y. T., Xu, L. H., Lu, Q., Liu, K. P., Liu, P. Y., Ji, F., Liu, X. M., Ouyang, D. Y. & He, X. H. 2014. Vasp Activation Via The Galpha13/Rhoa/Pka Pathway Mediates Cucurbitacin-B-Induced Actin Aggregation And Cofilin-Actin Rod Formation. *Plos One,* 9**,** E93547.

Zimmet, J. & Ravid, K. 2000. Polyploidy: Occurrence In Nature, Mechanisms, And Significance For The Megakaryocyte-Platelet System. *Exp Hematol,* 28**,** 3-16.

Zucker, M. B. & Masiello, N. C. 1984. Platelet Aggregation Caused By Dithiothreitol. *Thromb Haemost,* 51**,** 119-24.

Zucker, M. B. & Nachmias, V. T. 1985. Platelet Activation. *Arteriosclerosis,* 5**,** 2-18.